Targeting the purine salvage pathway in *in vitro* models of cerebral ischemia

Stephanie zur Nedden

A thesis submitted for the degree of Doctor of Philosophy

School of Life Sciences

University of Warwick

June 2011

Table of contents

List of Figures

List of Tables

Acknowledgements

Firstly, I would like to thank my supervisors, Prof. Bruno Frenguelli and Dr. Alex Doney for their unending support and encouragement during my PhD. I would also, especially like to thank Prof. Nicholas Dale for his valuable input to great parts of this thesis and the papers published.

In addition, I would like to thank the following:

Dr. Robert Eason for his continuous support and technical help with the HPLC system.

Jan Lopatar and Dr. Rajen Mistry for their help with biosensor and electrophysiological experiments.

Prof. Grahame Hardie and Dr. Simon Hawley (University of Dundee) for the analysis of brain slice protein extracts for AMP-kinase activity assays and western blots.

Holly Baum, for the establishement of the XTT assay and help with experiments of Chapter 7 and 8.

Past and present members of the Frenguelli, Moffat, Dale, Wall and Pankratov labs for support, encouragement, discussions and generally a great time!

I would also like to acknowledge the generous financial support from Research into Ageing, which enabled me to carry out my PhD.

Declaration

The work contained in this thesis is the result of original research conducted by myself under the supervision of Prof. Bruno Frenguelli and Dr. Alex Doney with the following exception:

- AMPK kinase assays and western blots of brain slices protein extracts, generated by myself, have been performed by Prof. Grahame Hardie and Dr. Simon Hawley at the University of Dundee (Chapter 4).
- Prof. Nicholas Dale developed the mathematical model to establish the effect of the dead cut edges in hippocampal brain slices on the underestimation of adenine nucleotide levels in the viable core tissue in Chapter 4.
- Sensor experiments, establishing the inhibitory effect of Allopurinol on xanthine oxidase have been performed by Holly Baum (Chapter 7).
- Holly Baum also conducted the experiments with an XTT based cell viability assay, shown in Chapter 8.

Parts of Chapter 2 and 3 have been taken or adapted from: **Zur Nedden S, Eason R, Doney AS, Frenguelli BG** (2009). An ion-pair reversed-phase HPLC method for determination of fresh tissue adenine nucleotides avoiding freeze-thaw degradation of ATP, *Anal Biochem.* **388**:108-114.

Parts of Chapter 2, 4, 5 and 6 have been taken or adapted from: **Zur Nedden S, Hawley S, Pentland N, Hardie DG, Doney AS, Frenguelli** BG (2011) Intracellular ATP Influences Synaptic Plasticity in Area CA1 of Rat Hippocampus via Metabolism to Adenosine and Activity-Dependent Activation of Adenosine A1 Receptors. *J Neurosci* **31**:6221-6234.

These two papers are attached for inspection at the end of this thesis (Publications).

None of the work contained in this thesis has been submitted for any previous degree and all sources of information have been acknowledged by means of references.

Stephanie zur Nedden

June, 2011

Summary

An interruption of the blood supply to the brain, as occurs during ischemic stroke, results in a rapid decline of ATP levels and a subsequent loss of neuronal function and viability. Under physiological conditions the brain reuses ATP degradation metabolites, such as hypoxanthine, via the *purine salvage pathway*, to restore its ATP pool. However, the massive degradation of ATP during ischemia results in the accumulation and loss of diffusible purine metabolites and thereby leads to a reduction in the post-ischemic ATP pool size, leaving the brain more vulnerable to secondary ischemic insults (recurrent strokes) and less able to deploy reparative mechanisms. The aim of this study was to improve the recovery of post-ischemic ATP levels by enhancing the *purine salvage pathway*, with substances that are already known to be tolerated in humans.

Using acute hippocampal rat brain slices, I found that 1 mM Ribose (Rib) and 50 µM Adenine (Ade), two main metabolites of the *purine salvage pathway*, significantly increased the tissue ATP levels under basal conditions. Rib/Ade pre-treatment results in accelerated decline of synaptic transmission after onset of oxygen/glucose deprivation (OGD), due to increased adenosine release. However, this intervention does not delay the onset of anoxic depolarisation, or improve the recovery of synaptic transmission after prolonged ischemic periods. Pre-treatment of brain slices with 1 mM creatine, which increases phosphocreatine levels and thereby buffers the rapid decline of ATP levels upon energy shortage, significantly delays the onset of AD and helps to improve the recovery of synaptic transmission. By using cultured cerebellar granule cells, for more protracted studies on cell viability after OGD, I show that addition of Rib/Ade after ischemia helps to improves cell viability.

Therefore my results suggest that both, delaying the decline of ATP upon onset of OGD (pre-treatment with creatine), or enhancing the post-ischemic recovery of ATP (post-treatment with Rib/Ade) are useful strategies to improve cell survival and function after *in vitro* ischemia.

Abbreviations

~P	High energy phosphate bond
5-HT	5-Hydroxytryptamine/Serotonine
8-CPT	8-cyclopentyltheophylline
ACC	Acetyl-CoA carboxylase
acetyl-coA	Acetyl-coenzyme-A
aCSF	Artificial cerebrospinal fluid
AD	Anoxic depolarisation
Ade	Adenine
Ado	Adenosine
ADP	Adenosine diphosphate
AICAR	Aminoimidazole carboxamide ribonucleotide
Allo	Allopurinol
AMP	Adenosine monophosphate
AMPA	α-amino-3-hydroxy-5-methyl-4-isoxazolepropionic acid
AMPK	AMP activated protein kinase
ANOVA	Analysis of variance
APRT	Adenine phosphoribosyl transferase
ATP	Adenosine triphosphate
BSA	Bovine serum albumine
CA	Cornu ammonis
CGC	Cerebellar granule cells
CNT	Concentrative nucleoside transporter
Co	control
CTP	Cytosine triphosphate
DG	Dentate gyrus
DIPY	dipyridamole
dwt	Dry weight
ε	Etheno
E	embryonal
EC	Energy charge

Abbreviations

ENT	Equilibrative nucleoside transporter
$FADH_2$	Flavin adenine dinucleotide
FDA	Food and drug administration
fEPSP	Field excitatory postsynaptic potential
GDP	Guanosine diphosphate
GMP	Guanosine monophosphate
GTP	Guanosine triphosphate
H/PI	Hoechst/propidium iodide
HFS	High frequency stimulation
HGPRT	Hypoxanthine guanine phosphoribosyl transferase
HPLC	High performance liquid chromatography
HX	Hypoxanthine
Hz	Hertz
IMP	Inosine monophosphate
LOD	Limit of detection
LOQ	Limit of quantification
LTP	Long term potentiation
MAP-2	Microtubulus-associated protein 2
MetOH	Methanol
N^6-CPA	N^6-Cyclopentyladenosine
NADH	Nicotin amid adenine dinucleotide
NB	Neurobasal medium
NBTI	nitrobenzylthioinosine
NMDA	*N*-methyl-D-aspartate
OGD	Oxygen/glucose deprivation
P	Postnatal
p	Statistical p-value
PACSIN 1	Protein kinase C and casein kinase substrate in neurons 1
PARP1	Poly(ADP-ribose)polymerase-1
PBS	Phosphate buffered saline
PCA	Perchloric acid
Pen/Strep	Penicillin/Streptomycin

Abbreviations

PFA	Paraformaldehyde
Pi	Orthophosphate
PID	Periinfarct depolarisation
PMS	Phenazine methosulphate
POM-1	Sodium polyoxotungstate
PPADS	Pyridoxalphosphate-6-azophenyl-2',4'-disulfonic acid tetrasodium salt
PPi	Pyrophosphate
PRPP	5-phosphoribosyl-1-pyrophosphate
Rep	Reperfusion
Rib	D-Ribose
RT	Room temperature
r-tPA	Recombinant tissue plasminogen activator
SAICAR	Phosphoribosylaminoimidazolesuccinocarboxamide
S.D.	Standard deviation
S.E.M.	Standard error of the mean
TAN	Total adenine nucleotides
TBAHS	Tetra butyl ammonium hydrogensulphate
TBS	Theta-burst stimulation
TCA cycle	Tricarbocyclic acid cycle
TIA	Transient ischemic attack
UTP	Uridine triphosphate
UV	Ultraviolet
wwt	Wet weight
X	Xanthine
XTT	2,3-bis[2-methoxy-4-nitro-5-sulfopheny]-2H-tetrazolium-5-carboxyanilide

1 Introduction

1.1 Cerebral ischemia

1.1.1 Ischemic stroke

Cerebral stroke is the consequence of a cerebrovascular accident that is caused by a rupture of a blood vessel in the brain (haemorrhagic stroke) or by an interruption of the blood supply to the brain (ischemic stroke). Haemorrhagic stroke accounts for about 15 - 20 % of all strokes and occurs when a weakened blood vessel ruptures due to aneurysms or arteriovenous malformations. Ischemic stroke, which will be the main focus of this thesis, is the more common type and accounts for about 80 - 85 % of all strokes (Feigin et al., 2003). The central event in ischemic stroke is the interruption of the blood flow to the brain due to local thrombosis or embolic particles. Globally stroke is the second leading cause of death and the most common cause of long term disabilities (Feigin et al., 2003; Flynn et al., 2008). About 8 - 12 % of ischemic strokes and ~ 38 % of haemorraghic strokes result in death within 30 days (Writing Group et al., 2010). Furthermore in patients suffering a first stroke there is an increased risk of recurrent strokes within 5 years (Flynn et al., 2008; Writing Group et al., 2010).

Since the brain relies on a constant blood supply to match its high energy demand, even brief periods of cerebral ischemia result in immediate neurological dysfunctions. If the blood flow to the affected area is restored spontaneously and neurological symptoms recover completely this event is termed transient ischemic attack (TIA). TIAs often precede a full ischemic stroke, which occurs when the blood supply is interrupted for prolonged periods and the brain tissue suffers irreversible damage resulting in persistent neurological dysfunction (Flynn et al., 2008).

Depending on the area affected by stroke, stroke survivors may suffer from paralysis, sensory impairments including pain, aphasia, cognitive impairments, seizures and epilepsy or emotional disturbances (Kelly-Hayes et al., 1998). Furthermore stroke patients have an increased risk of depression (Kelly-Hayes et al., 1998; Pascoe et al.,

2011) and dementia (Desmond et al., 2002) following the months after stroke. Fifteen to thirty percent of all stroke patients remain disabled and about 20 % require institutional care within 3 months (Writing Group et al., 2010). Furthermore, including the cost related to increasing awareness, treatment of stroke, rehabilitation as well as loss of work – 21 billion € were spent in EU healthcare systems on stroke in the year of 2003 (Flynn et al., 2008). These facts reflect the major beneficial impact new stroke therapies would have for the life quality of individual patients and relatives as well as for financial expenditures of health care systems.

1.1.1.1 Current treatments for ischemic stroke patients

After committal of a stroke patient to the hospital it is critical to determine which type of stroke the patient had suffered (e.g. by computed axial tomography) in order to provide the appropriate treatment. So far FDA (Food and Drug Administration) approved therapeutic agents for ischemic stroke patients are limited, and only target the restoration of the blood supply to the brain. This should be done as quickly as possible since "*time is brain*" and the typical stroke patient loses 1.9 million neurons/min stroke is untreated (Saver, 2006).

The blood supply can be restored upon mechanically removing the blood clot (Smith et al., 2008), or upon administration of the thrombolytic agent recombinant tissue plasminogen activator (rtPA). However, rtPA must be given within ~ 3 h after stroke and is associated with an increased risk of intracerebral haemorrhage and other potential complications (Adams et al., 2003; Adams et al., 2007). Therefore only a small percentage of acute ischemic stroke patients (~ 8%) qualify for rtPA treatment, due to the delay in assessment of patients and the stringent selection criteria for rtPA treatment (Kleindorfer et al., 2004). The antiplatelet agent aspirin is frequently administered after thrombolytic therapy (within 24 – 48 h) in an effort to reduce the event of recurrent strokes (Adams et al., 2003).

However, all these treatments aim to restore vascular function and exert their protective effect via hemodynamic mechanisms. Because of this reason research focuses on the development of neuroprotective drug therapies, which target the

actual brain tissue and aim to prevent the sequence of damaging events which would otherwise result in irreversible ischemic injury. These strategies could be used as prophylactic treatment for patients with a known risk of ischemic stroke, or as treatment for actue ischemic stroke patients to prevent the continuous loss of brain cells during ischemia as well as reperfusion (restoration of the blood supply).

1.1.2 Ischemic core and penumbra

The massive reduction of blood flow in the central area of ischemia (cerebral blood flow is < 10 ml/g/min) results in necrotic cell death and irreversible damage within minutes. Tissue in this area is termed the ischemic core and is beyond therapeutic rescue (Moustafa and Baron, 2008). Within the surrounding penumbra, where collaterals provide residual circulation, tissue is affected by ischemia, but still viable and can be potentially rescued. However, the extent of salvageable tissue decreases over time and penumbral tissue can be recruited to the ischemic core even during reperfusion so that the final degree of the ischemic infarct can enlarge over a period of hours to days (Dirnagl et al., 1999). Increased survival of penumbral tissue is associated with improved neurological recovery, and is therefore a key target for neuroprotective interventions (Mergenthaler et al., 2004; Moustafa and Baron, 2008).

The main aim of this work was to help the post-ischemic brain to restore the balance of its energy metabolism, which might be protective in the penumbra, where cells are energetically challenged by ischemia. As mentioned above the brain has a very high energy demand and exclusively depends on a constant oxygen and nutrient supply from the blood. Therefore the next sections will give a background on the brains energy metabolism as well as the damaging events during ischemia and reperfusion that contribute to the continuous loss of brain cells.

1.2 Cerebral energy metabolism

1.2.1 Cellular respiration

Mitochondrial respiration and the associated synthesis of the energy carrier adenosine triphosphate (ATP) are the two pathways forming the core of cellular metabolism. During respiration the reducing agents NADH (nicotineamide adenine dinucleotide) and $FADH_2$ (flavin adenine dinucleotide) are oxidised by molecular oxygen, through a chain of electron transfer complexes which generate a proton motive force across the inner mitochondrial membrane. The transport of protons down their gradient through ATP synthase is then coupled to the transfer of orthophosphate (Pi) to ADP (adenosine diphosphate) thereby generating ATP. This process is termed oxidative phosphorylation, and the generated ATP is exported to the cytosol in exchange for ADP. NADH and $FADH_2$ are mainly provided by the degradation of glucose[1] via glycolysis in the cytosol and the tricarboxylic acid (TCA) cycle in the mitochondria. During glycolysis glucose is degraded to 2 molecules of pyruvate, thereby yielding 2 molecules of ATP and NADH. Pyruvate can be converted to lactate by lactate dehydrogenase, with the reaction products lactate and NAD^+, the latter being used to drive anaerobic glycolysis. Alternatively, pyruvate can be decarboxylated to acetyl-coenzyme-A (acetyl-CoA), by the pyruvate dehydrogenase complex in the mitochondira, releasing NADH and CO_2. Acetyl-CoA subsequently enters the TCA cycle, where it is degraded to CO_2 and H_2O in a series of steps yielding a further 3 molecules of NADH and one molecule of $FADH_2$ per acetyl-Co-A used. Glycolysis, the TCA cycle and oxidative phosphorylation produce 30 molecules of ATP per molecule of glucose (as opposed to 2 molecules of ATP/ molecule of glucose via glycolysis alone) (Stryer et al., 1995).

[1] Alternatively NADH can be generated by degradation of other fuels such as fatty acids or amino acids. However glucose is the main substrate for brain tissue.

1.2.2 Cerebral energy consumption and stores

Although the human brain represents only 2% of the total body weight, it receives about 15% of the cardiac output and consumes 20% of total body oxygen and glucose consumption (Schurr and Rigor, 1989; Shulman et al., 2004). These values reflect the high metabolic rate and energy demand of the brain under basal conditions. As seen in Figure 1.1 ~ 80% of the brains' energy in form of ATP is used for events associated with neuronal firing (mainly ion homeostasis by Na^+/K^+ ATPase) and supporting processes (Erecinska and Silver, 1994; Ames, 2000).

Although glucose is the main energy source for the brain and the majority of the glucose consumed is converted to H_2O and CO_2 during glycolysis and the TCA cycle, lactate can maintain the function of hippocampal brain slices even in the absence of glucose (Schurr et al., 1988). The astrocyte-neuron lactate shuttle hypothesis states that astrocytes play the primary role in glycolysis and release lactate during periods of high energy demand which is taken up by neurons, converted to pyruvate and subsequently used in the TCA cycle to support their energetic demand (Pellerin and Magistretti, 1994).

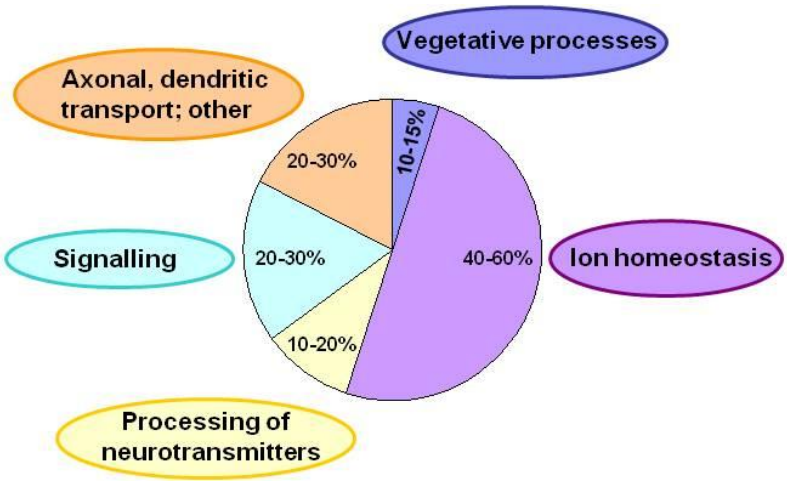

Figure 1.1: Energy consuming processes in the brain together with their relative estimates on ATP consumption.*The highest amount of energy is spent on ion homeostasis and supporting processes for neurotransmission. Values are taken from (Erecinska and Silver, 1994; Ames, 2000; Attwell and Laughlin, 2001).*

Unlike other tissues with a high energy demand, such as muscles, the brain has very little energy stores in the form of glycogen. Cerebral glycogen is mostly stored in astrocytes, and made available for neurons in the form of released lactate (Brown and Ransom, 2007). However, cerebral glycogen stores only account for ~ 0.1 % of the total brain weight (Brown, 2004), and can therefore not satisfy the brain's energy demand during periods of ischemia. It has been calculated that if the brain would continue at its normal metabolic rate, it would be completely depleted of all energy[2] within 80 seconds following cardiac arrest (Ames, 2000). It is therefore not surprising that the brain is highly vulnerable to disturbances of its nutrient and oxygen supply, as occurs during stroke.

1.3 Ischemia and Reperfusion – factors contributing to loss of cells

The decline of ATP during ischemia, due to the lack of oxygen and glucose, leads to multiple cascades of damaging cellular events that result in a loss of cells during ischemia as well as reperfusion. The main contributors to cell death are the toxic release of excitatory neurotransmitters (excitoxicity), imbalances in ion homeostasis, periinfarct depolarisations (PIDs), oxidative and nitrative stress, inflammation and apoptosis. All these processes occur on different time scales (see Figure 1.2) and contribute to the loss of neurons, glial cells as well as vascular cells over the course of minutes to days (Dirnagl et al., 1999; Heiss et al., 1999).

[2] In form of the high energy phosphate bond ~P from ATP and phosphocreatine

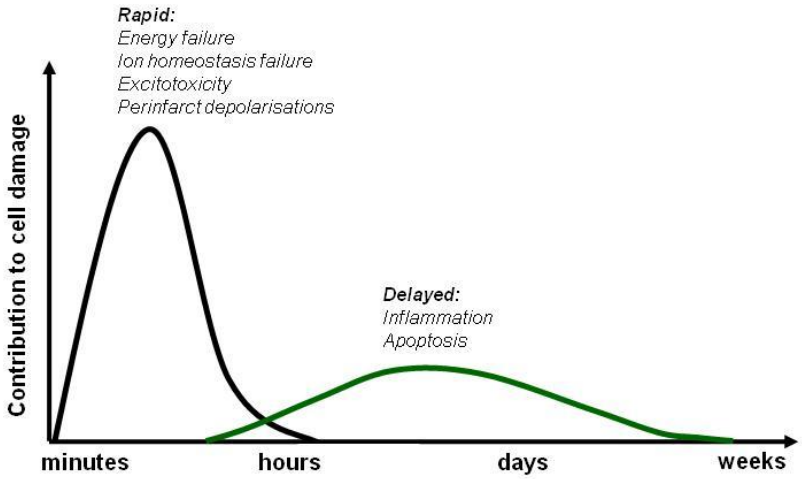

Figure 1.2: Pathophysiological processes during ischemia and reperfusion that contribute to irreversible damage of brain tissue. *Adapted from (Dirnagl et al., 1999; Heiss et al., 1999).*

1.3.1 Excitotoxicity

Due to the lack of ATP, membrane ion-transport systems, which use up to 60 % of the cellular ATP store (see Figure 1.1), fail and neurons become depolarized. The resulting influx of calcium leads to release of a number of neurotransmitters, including large quantities of the excitatory neurotransmitter glutamate. Glutamate in turn activates NMDA and AMPA receptors on postsynaptic cells, resulting in entry of calcium and sodium as well as efflux of potassium. Accordingly postsynaptic neurons become depolarized, causing further calcium influx, further glutamate release, and local amplification of the initial ischemic insult. These series of events are termed excitotoxicity, since it is caused by the toxic release of excitatory neurotransmitters (Lipton, 1999; White et al., 2000). Additionally acidosis due to anaerobic metabolism results in activation of acid sensing ion channels, which lead to a further increase of intracellular calcium levels (acidotoxicity) (Ginsberg, 2008).

High intracellular calcium levels are responsible for activation of a series of destructive enzymes such as proteases, lipases, and endonucleases, resulting in the loss of cellular integrity and necrotic cell death in the ischemic core (Siesjo, 1981; Lipton, 1999).

There are numerous studies on the neuroprotective effect of calcium antagonists or NMDA or AMPA receptor blockers. Despite these agents being beneficial in *in vivo* animal models of stroke, there was no beneficial effect in clinical trials. Indeed NMDA receptor antagonists had severe side effects (e.g. hallucinations) and were sometimes associated with increased mortatlity (Ginsberg, 2008). However, as will be discussed in Chapter 9, the negative outcomes of neuroprotective strategies in human stroke patients were potentially due to poor translation of preclinical studies into clinical trials (Ginsberg, 2008).

1.3.2 Peri-infarct depolarisations

Due to the loss of ion homeostasis neurons in the centre of the ischemic core undergo an event termed anoxic depolarisation and they never repolarise. Periinfarct depolarisations (PIDs, also called spreading depression-like depolarisations) are triggered by elevated extracellular potassium and glutamate levels and propagate from the ischemic core through the penumbra (Somjen, 2002). These waves of depolarisation, which also occur in human stroke patients (Dohmen et al., 2008), are associated with increased energy demand of already challenged neurons as well as increases in intracellular Ca^{2+} levels and therefore lead to further ischemic injury and recruitment of penumbral tissue to the ischemic core (Doyle et al., 2008).

1.3.3 Oxidative and nitrative stress

Oxygen radicals (such as superoxide anion, hydrogen peroxide and hydroxyl radical) are generated via the mitochondrial electron transfer chain and by various cytosolic enzymes (e.g. xanthine oxidase or NADH oxidase). Under physiological conditions cellular antioxidant enzymes (e.g. superoxide dismutase, glutathione peroxidase and catalase) and molecular antioxidants (e.g. glutathione, ascorbic acid and alpha-tocopherol) detoxify radicals. However, during ischemia-reperfusion radical generation is enhanced and cannot be matched by endogenous radical scavengers (Yoshida et al., 1982).

Reactive oxygen radicals directly damage lipids, proteins and nucleic acids whilst the opening of the mitochondrial transition pore (MTP) is facilitated by radical production (Chan, 2001). This in turn results in the loss of the proton gradient across the inner mitochondrial membrane and initiates a cascade of events leading to apoptosis. Upon reperfusion and re-oxygenation the loss of mitochondrial function further contributes to the generation of radical oxygen species. Additionally the generation of nitrative radicals, such as NO via activation of nitric oxide synthase contributes to a further loss of cellular integrity. NO production is linked to over activation of poly(ADP-ribose)polymerase-1 (PARP-1), a DNA repair enzyme. PARP-1 catalyzes the transformation of NAD^+ into nicotinamide and poly(ADP-ribose) and upon over-activation results in depletion of the cellular NAD^+ pool, as well as DNA damage (Ying, 2008). Oxidative tissue damage can also lead to microvascular injury and dysfunction of the blood-brain barrier and thereby contribute to the infiltration of inflammatory mediators from the blood (Lakhan et al., 2009).

Accordingly therapeutic strategies with antioxidant molecules were extensively studied in various animal models of cerebral ischemia. Several molecules with antioxidant properties, such as resveratrol had encouraging neuroprotective effects in *in vivo* animal studies (Li et al., 2010). However, the first clinical trials did not show a beneficial effect potentially due to the low blood brain permeability of the molecule (NXY-059 a radical spin trap agent) (Ginsberg, 2008). Other radical scavenging molecules such as edaravone (oxygen radical scavenger) proved more beneficial and might deserve further clinical trials (Ginsberg, 2008).

1.3.4 Ischemia/reperfusion injury – inflammation, radical generation, apoptosis

Although the restoration of the blood supply to hypoperfused brain tissue is critical after ischemia it can paradoxically result in further tissue damage, termed ischemia/reperfusion injury. Increased levels of oxygen radicals can trigger the release of pro-inflammatory mediators such as cytokines, which results in expression of adhesion molecules on endothelial cells and promote the infiltration of

neutrophiles into the peripheral areas of the infarct. Additionally, activated microglial cells, which are the mediators of the immune system in the brain, can release pro-inflammatory cytokines resulting in further tissue damage (Lakhan et al., 2009). The post-ischemic inflammation response leads to a further deterioration of the blood brain barrier, brain oedema formation and initiation of apoptosis (Lakhan et al., 2009). Apoptosis is an energy-dependent and controlled form of cell death that can be triggered via intrinsic or extrinsic mechanisms. The intrinsic pathway is activated by the opening of the mitochondrial transition pore, release of cytochrome c, activation of caspases and initiation of pro-apoptotic genes. Alternatively extracellular ligands can activate caspases via death receptor signalling. Triggers of apoptosis include protease activation via increased cellular Ca^{2+} levels, reactive oxygen and nitrogen species, death receptor ligation, DNA damage and inflammation and affects neuronal, glia and endothelial cells (Broughton et al., 2009).

Both apoptosis and inflammation contribute to brain tissue damage over the course of hours to days (see Figure 1.2) and are therefore extensively studied targets for neuroprotective interventions.

1.3.5 Recovery of cerebral energy metabolism after ischemia

In addition to the damaging events described above, the restoration of ATP is delayed during reperfusion. In *in vivo* models of stroke ATP levels are at best incompletely restored during reperfusion (Kleihues et al., 1974; Onodera et al., 1986; Hermann et al., 2001) and often undergo a secondary deterioration (Hata et al., 2000b; Lust et al., 2002). The extent of ATP recovery during early reperfusion depends on the duration of the ischemic period (Ljunggren et al., 1974; Yatsu et al., 1975; Sims and Zaidan, 1995; Lust et al., 2002) and full recovery of ATP levels may take up to 24 h (Kleihues et al., 1975; Levy and Duffy, 1977; Lipton, 1999; Hermann et al., 2001). This itself prolongs the period of energy depletion and may further contribute to a loss of challenged neurons during reperfusion (Hashimoto et al., 1992). Furthermore these compromised ATP levels leave the tissue more vulnerable to secondary ischemic insults that often occur after stroke (Phillips, 2008).

Therefore, the factors limiting ATP recovery are potentially subjects for new neuroprotective strategies.

The main aim of this thesis was to improve the recovery of ATP levels in *in vitro* models of cerebral ischemia and to evaluate the effect on synaptic transmission and viability. Therefore the following section will focus on ATP degradation and restoration and the potential basis for the reduced ATP levels after cerebral ischemia.

1.4 Purine metabolism

1.4.1 ATP as cellular energy currency

ATP was first discovered by the German biochemist Karl Lohman in 1929 (Lohmann, 1929) and in the same year independently by a group in Harvard (Fiske and Subbarow, 1929). Its chemical structure has been correctly proposed in 1935 (Makino, 1935) and established in 1945 (Lythgoe and Todd, 1945; Maruyama, 1991). ATP consists of the purine base adenine, the pentose sugar ribose and three phosphoanhydride bonds (see Figure 1.3) and usually exists in a complex with Mg^{2+}. The concept of the high energy phosphate bond (~P) was first described in 1941 by Lipmann (Lipmann, 2006) and it is now well known that the hydrolysis of the γ-phosphoanhydride bond releases free energy (~ΔG°' = -50kJ/mol) which can be used to drive thermodynamically unfavourable reactions (Stryer et al., 1995), such as ion transport against the electrochemical gradient (N^+/K^+ ATPase).

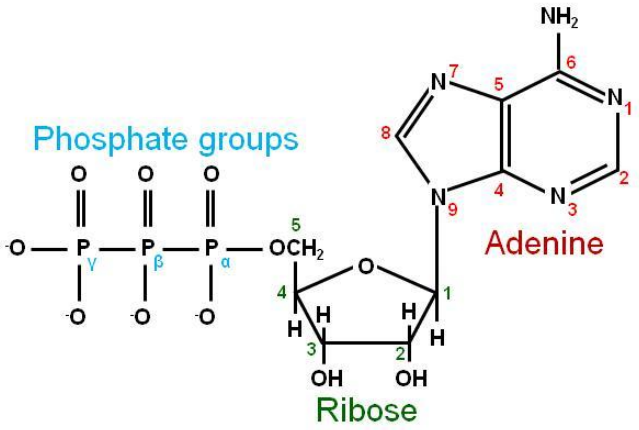

Figure 1.3: Structure of adenosine triphosphate (ATP).

Under physiological conditions ATP is the main nucleotide in the total adenine nucleotide pool (TAN), which is composed of ATP, ADP and adenosine monophosphate (AMP). Accordingly, the rate of ATP consuming and ATP generating processes is balanced, in order to maintain the ATP/ADP ratio (≥ 10) and the ATP/AMP ratio (≥ 100) many orders of magnitudes away from equilibrium (Hardie and Hawley, 2001). The capacity of ATP to drive energy requiring processes lies in this displacement from equilibrium (Nicholls and Ferguson, 1992). This is analogous to the chemicals in a fully charged battery. Hence, the cellular energy charge (EC) has been proposed as being an indicator of the metabolic available energy (in terms of phospho-anhydride bonds) in the TAN pool: [(ATP+0.5xADP)/(ATP+ADP+AMP)] (Atkinson, 1968).

Although ATP synthesis is in close proximity to the site of consumption (e.g. ATPases), and there is a close relationship between cerebral activity and the rate of oxidative phosphorylation (Du et al., 2008), simple diffusion of ATP from the side of generation (mitochondria, glycolysis) to the site of consumption would require a significant concentration gradient and would result in build up of ADP and subsequent inhibition of ATPases by ADP, Pi and H^+ (Dzeja and Terzic, 2003). Therefore it is not surprising that in addition to mitochondrial ATP synthases and glycolytic ATP production there are two more enzymes involved in maintaining high cytosolic ATP levels: adenylate kinase and creatine kinase.

Both these enzymes ensure a quick transport of ~P from the site of production to the site of consumption and they help to prevent marked changes in adenylate levels (Ames, 2000; Dzeja and Terzic, 2003) (see Figure 1.4). The functioning of this phosphoryl-transfer network requires both enzymes to be present at the site of ATP production as well as the site of ATP consumption.

1.4.1.1 Adenylate kinase

The different isoforms of adenylate kinase (1-6) are expressed in a tissue- and cell type-specific manner and in different cellular compartments. Adenylate kinase 1 and 5 are cytosolic, adenylate kinase 2, 3 and 4 are mitochondrial and adenylate kinase 6 is located in the nucleus (Noma, 2005). Adenylate kinases catalyse the reversible transfer of the γ-phosphate group from ATP (Adenylate kinases 1, 2, 5 and 6) or guanosine triphosphate (GTP, adenylate kinase 3) to AMP, yielding 2 ADP or ADP + GDP (2 ADP ↔ ATP + AMP; AMP + GTP ↔ GDP + ADP). The brain expresses adenylate kinase 1, 3, 4, and 5 (Inouye et al., 1999; Van Rompay et al., 1999; Miyoshi et al., 2009). Mitochondrial adenylate kinase 3 salvages accumulated AMP by using GTP as a phosphate donor and provides ADP for ATP synthases and GDP as a cofactor for the TCA cycle. Cytosolic adenylate kinases 1 and 5 are mainly regulated by the availability of the substrates AMP and ADP. Therefore these enzymes maintain an appropriate ATP/ADP ratio as soon as ADP levels decrease at the site of ATP generation (glycolysis) or increase at the site of consumption (e.g. ATPases, see Figure 1.4) (Noma, 2005).

1.4.1.2 Creatine kinase

Creatine kinase also exists in a mitochondrial (uMT-CK for brain tissue) and a cytosolic isoform (BB-CK for brain tissue (Andres et al., 2008)). Both isoformes contribute to the build up of a large cytosolic phosphocreatine pool (~ double the amount of ATP) by transferring the γ-phosphate group from ATP to creatine in a reversible reaction (creatine + ATP ↔ phosphocreatine + ADP) (Andres et al., 2008). Mitochondrial creatine kinases and creatine kinases in close proximity to glycolysis, provide ADP and help build up a high phosphocreatine pool. Since phosphocreatine has a higher phosphoryl-group transfer potential than ATP, cytosolic creatine kinase can buffer the decline of ATP in the proximity of ATP-using enzymes, thereby maintaining an appropriate ATP/ADP ratio (see Figure 1.4) (Dzeja and Terzic, 2003).

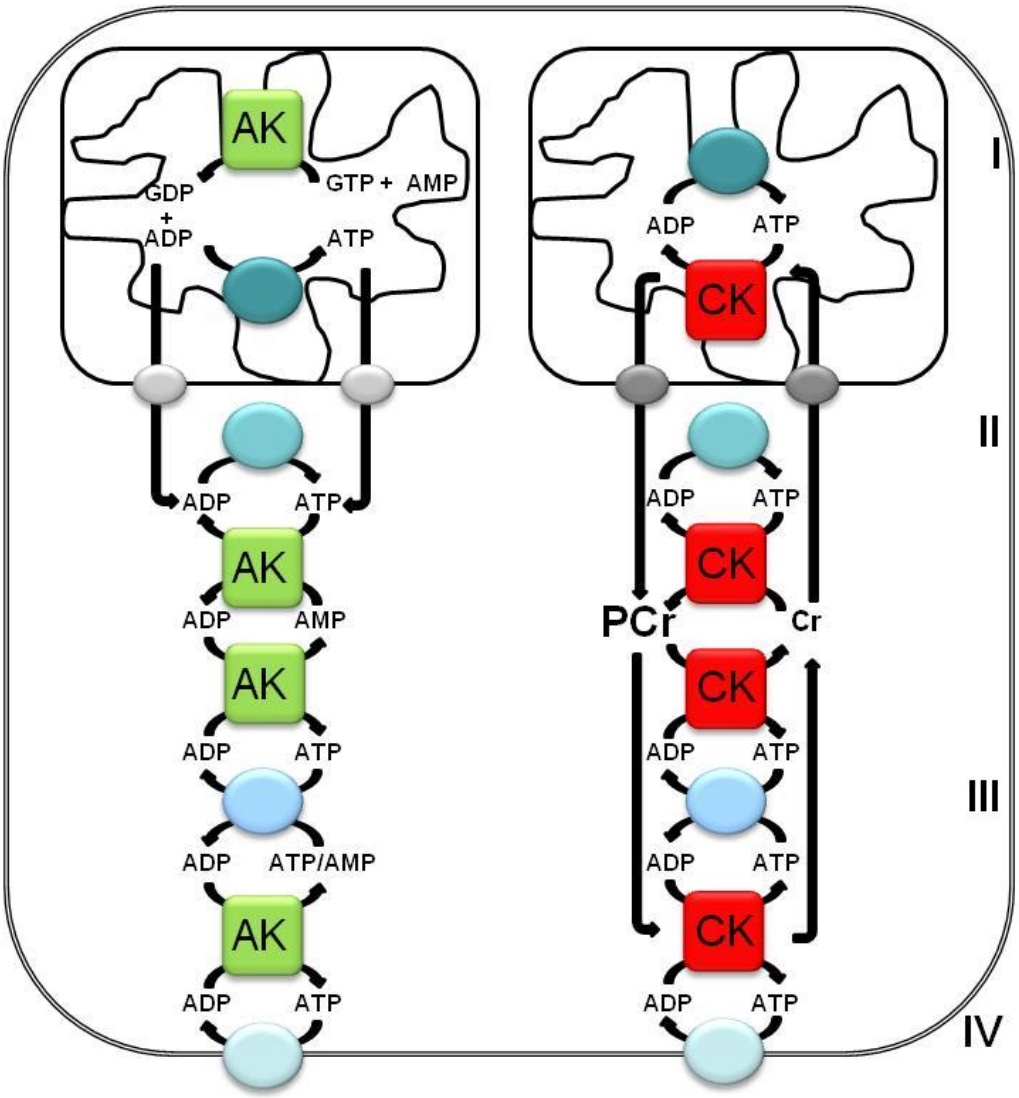

Figure 1.4: Phospho-transfer reactions catalysed by adenylate kinase (AK) and creatine kinase (CK). I *ATP is produced by mitochondrial ATP synthase. Mitochondrial AK salvages accumulated AMP by transfering the γ-phosphate group from GTP yielding ADP + GDP. Mitochondrial CK uses the accumulated ATP to generate phosphocreatine (PCr) which is transported to the cytoplasm via mitochondrial creatine transporters.* ***II*** *ATP produced by glycolysis is converted to ADP by AK and CK, the latter reaction contributing to a high intracellular PCr pool. AK and CK thereby help to ensure a continuous presence of ADP for glycolysis.* ***III*** *On the side of ATP consumption AK helps to maintain a high ATP/ADP ratio by converting ADP to ATP+AMP. Likewise CK transfers the phosphate group from PCr to ADP.* ***IV*** *The same reactions occur at membrane-bound ATPases. These phospho-transfer reactions facilitate the transport of ~P across the cell and help to maintain an appropriate ATP/ADP ratio at the site of production and consumption of ATP. Circles refer to ATP producing reactions (e.g. I ATP synthase in the mitochondria, or II phosphoglycerate kinase and pyruvate kinase during glycolysis) as well as ATP consuming reactions (e.g. III and IV ATPases). Graph was adapted from (Ames, 2000; Dzeja and Terzic, 2003; Andres et al., 2008).*

1.4.2 Intracellular degradation of ATP during metabolic stress

Despite these enzymatic systems of adenylate kinase and creatine kinase, the lack of oxygen and glucose during metabolic stress results in a rapid degradation of ATP, preceded by a fall in phosphocreatine levels with a resulting increase in ADP levels (Whittingham et al., 1984a). The accumulated ADP is converted to AMP and ATP by adenylate kinase, resulting in an increase of AMP (Figure 1.5). AMP can be deaminated to inosine monophosphate (IMP) by AMP deaminase or dephosphorylated to the purine nucleoside adenosine by 5'-nucleotidase. There are 3 cytosolic 5'nucleotidases (e-Ns, c-N-I and c-N-II) as well as an ecto-5'-nucleotidase (e-N). e-Ns and c-N-I have a preference for AMP and c-N-II has been shown to hydrolyse GMP and IMP, resulting in guanosine and inosine formation (Marques et al., 1998; Sala-Newby et al., 2000). Adenosine can also be re-phosphorylated to AMP by adenosine kinase, but it has been shown that this enzyme is downregulated during oxygen-glucose deprivation *in vitro* (Lynch et al., 1998), since adenosine kinase requires ATP as phosphate donor and is inhibited by high intracellular adenosine concentrations (Yamada et al., 1980). Therefore during metabolic stress, adenosine is either released to the extracellular space or irreversibly deaminated to inosine by adenosine deaminase. Unlike adenosine, inosine cannot be rephosphorylated to IMP, due to the lack of a specific kinase (Mascia et al., 2000). Hence inosine is either released or further degraded to the purine base hypoxanthine and the sugar moiety Ribose-1-phosphate by purine nucleoside phosphorylase, whilst hypoxanthine can be reconverted to the purine nucleotide IMP and subsequently to AMP via the purine salvage pathway, which will be discussed in the next section. Alternatively, hypoxanthine is released or converted to xanthine and subsequently uric acid and hydrogen peroxide in two reactions catalysed by xanthine oxidase. Unlike hypoxanthine, xanthine and uric acid cannot be recoverted to purine nucleotides and are therefore lost from the purine nucleotide pool. As will be discussed later, the release of upstream metabolites of hypoxanthine as well as its further degradation to xanthine contribute to the reduction of the post-ischemic TAN and ATP pool, since the brain mainly relies on the purine salvage pathway to maintain its purine nucleotide levels (Gerlach et al., 1971; Allsop and Watts, 1980).

From Figure 1.5 it is obvious that AMP degradation to inosine can follow two distinct routes (via IMP or via adenosine). AMP deaminase (AMP → IMP) and cytosolic c-N-II (IMP → inosine) are stimulated by ATP, and c-N-II is inhibited by Pi (Chapman and Atkinson, 1973; Van den Berghe et al., 1992; Ipata et al., 2011). Accodingly it has been shown that the AMP → IMP → inosine pathway is favoured in rat brain extracts upon physiological ATP concentrations (5mM) (Barsotti and Ipata, 2004). Cytosolic 5'nucleotidase c-N-I , which favours AMP as substrate, is stimulated by ADP not ATP (Itoh et al., 1986). In rat brain extracts at low ischemic ATP concentrations (< 2 mM ATP) ATP is mainly degraded via the adenosine pathway with only a little IMP formation (Barsotti and Ipata, 2004; Ipata et al., 2011). In primary neuronal cell cultures it has been shown that under physiological condition the flux through both pathways is equal, whereas upon inhibition of mitochondrial respiration adenosine production is dominant (Brosh et al., 1996). Likewise the activity of myocardial cytosolic 5'nucleotidase activity is increased by decreasing the cellular energy charge (Itoh et al., 1986), further showing that upon metabolic stress ATP degradation is shifted towards adenosine formation. Though the release of adenosine means a loss of this metabolite from the cellular nucleotide pool, it is important and protective during ischemia.

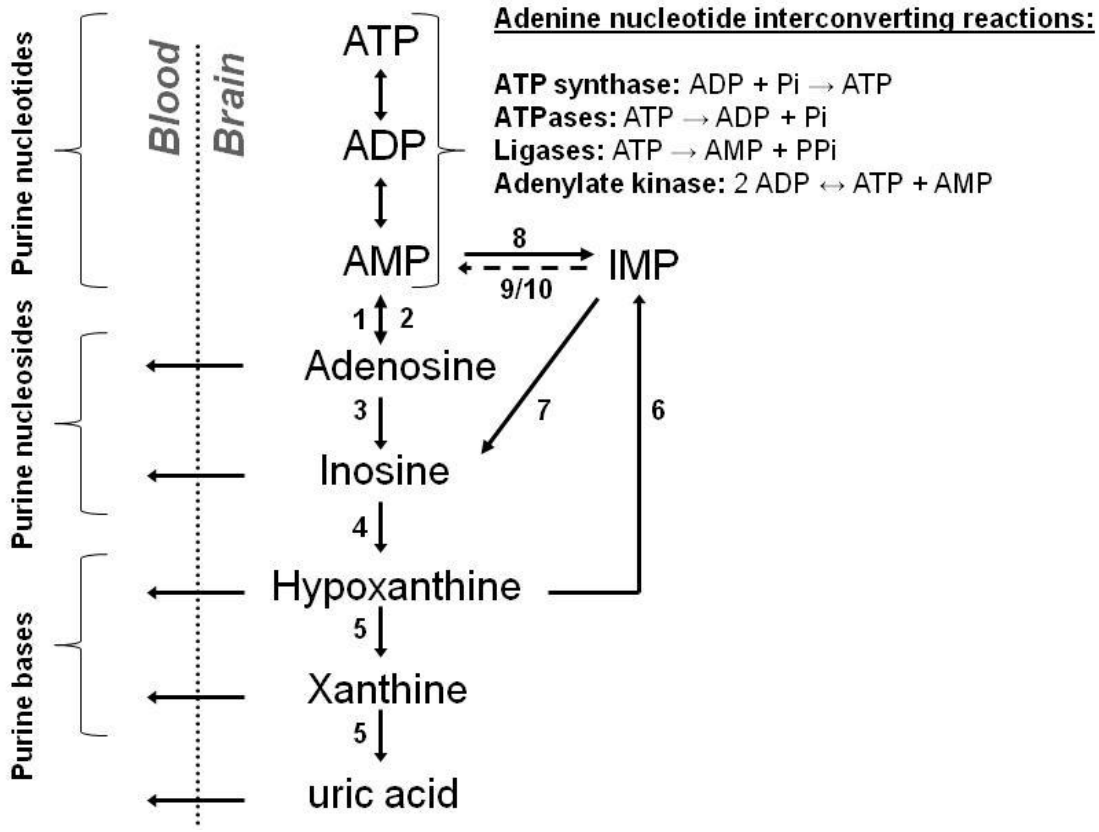

Figure 1.5: Degradation of ATP: *ATP is generated by mitochondrial ATP synthases and used by cytosolic enzymes, such as ATPases, or DNA ligases. Adenylate kinase interconverts adenine nucleotides. AMP is degraded to adenosine by 1 5'nucelotidase. Adenosine can be rephosphorylated by 2 adenosine kinase or deaminated to inosine by 3 adenosine deaminase. Inosine is degraded to the purine base hypoxanthine by 4 purine nucleoside phosphorylase and hypoxanthine can be either degraded to xanthine and uric acid by 5 xanthine oxidase or converted to IMP via the purine salvage pathway by 6 hypoxanthine guanine phosphoribosyltransferase. Inosine can also be derived from IMP via dephosphorylation by 7 5'nucleotides (c-N-II). Likewise AMP can be converted to IMP by 8 AMP deaminase and IMP can be reconverted to AMP via the intermediate adenylosuccinate catalysed by 9 adenylosuccinate synthetase and 10 adenylosuccinate lyase. All the substances indicated with an arrowhead can be released from the cell and washed out to the peripheral circulation.These substances are therefore lost from the cellular adenine nucleotide pool.*

1.4.3 Neuroprotective role of adenosine during ischemia

1.4.3.1 Purinergic signaling

Although ATP and its degradation metabolite adenosine have been traditionally viewed as having only intracellular roles, mainly as cellular energy source, precursors of RNA and DNA as well as the second messenger cAMP, about 80 years ago Drury and Szent-Gyorgyi discovered that exogenous adenosine and ATP have potent actions on the heart (Drury and Szent-Gyorgyi, 1929). About 40 years later it was proposed that ATP or a related nucleotide is a transmitter released by nerves in the gut (Burnstock et al., 1970) and the term purinergic signalling was first proposed in 1971 (Burnstock, 1971). It is now well known that both ATP and adenosine participate in a wide range of physiological responses in the central, peripheral and enteric nervous system (Burnstock, 1993; Fredholm et al., 1994; Zimmermann, 1994) and several receptors for ATP (P2 receptors) and adenosine (P1 receptors) have been identified, cloned and characterised.

1.4.3.2 Adenosine receptor subtypes

Four G protein-coupled adenosine receptors have been cloned and characterized: A_1, A_{2A}, A_{2B} and A_3. These receptors differ by their affinity for adenosine, their pharmacological specificity as well as by their distribution and abundance throughout the brain. The main intracellular signaling pathways involve the formation of cAMP by adenylate cyclase, with A_1 and A_3 receptors causing inhibition of adenylate cylcase via inhibitory G proteins Gi/o, and A_{2A} and A_{2B} receptors causing its activation via a stimulatory G protein Gs (Fredholm et al., 2001). A_1 receptors inhibit neurotransmission, by activation of K^+ channels and inhibition of Ca^{2+} channels, whereas A_{2A} and A_{2B} receptors are generally considered to have excitatory effects on neurotransmission (Dunwiddie and Masino, 2001). A_3 receptors are poorly characterized, but have been shown to desensitize A_1 receptors in the hippocampus (Dunwiddie et al., 1997). However, this is controversial (Lopes et al., 2003), and A_3 receptor activation has been shown to both, inhibit synaptic transmission (Piccinin et al., 2010) as well as facilitate long term potentiation (LTP)

(Costenla et al., 2001). All adenosine receptors are expressed in the brain with A_1 being most abundant (Dunwiddie and Masino, 2001).

Adenosine is thought to be a neuromodulator in the brain since it is not stored and released in synaptic vesicles, but is rather formed from extracellular degradation of ATP or intracellular production and subsequent release. Adenosine is involved in both normal and pathophysiological processes, such as regulation of sleep and arousal or neuroprotection (de Mendonca et al., 2000; Dunwiddie and Masino, 2001). Many different stimuli can induce adenosine release, such as increased extracellular K^+, electrical stimulation, seizure activity, and most dramatically hypoxia or ischemia (Dunwiddie and Masino, 2001; Frenguelli et al., 2007; Dale and Frenguelli, 2009).

1.4.3.3 Role of nucleoside transporters in adenosine release

There are two types of nucleoside transporters in the brain: equilibrative nucleoside tranporters (ENT 1 - 4), which mediate transport in both directions and Na^+-dependent concentrative nucleoside transporters (CNT 1 - 3) (Podgorska et al., 2005). The involvement of adenosine tranporters in adenosine release has been studied by using nitrobenzylthioinosine (NBTI), which inhibits NBTI-sensitive ENTs (*es*) and dipyridamole (DIPY), which equally affects *es* and NBTI-insensitive ENTs (*is*) in rat tissue (Latini and Pedata, 2001). Due to the lack of inhibitors the role of CNT in adenosine tranport is less clear (Latini and Pedata, 2001).

Inhibition of ENTs with NBTI/DIPY under physiological conditions results in a slow build up of extracellular adenosine, suggesting that these transporters are mainly involved in the uptake of extracellular adenosine (Frenguelli et al., 2007). Intracellular adenosine is rapidly converted to AMP by cytosolic adenosine kinase, thereby maintaining the inward concentration gradient (Boison, 2006). During ischemia, when intracellular adenosine levels increase (Latini et al., 1996), the concentration gradient is outwardly directed. However, the exact mechanism of adenosine release during ischemia/hypoxia is uncertain since administration of NBTI/DIPY has been shown to enhance adenosine release (Frenguelli et al., 2007),

suggesting that ENTs may limit its extracellular accumulation. The reversal of the Na^+ gradient during ischemia could power adenosine efflux via CNT (Gray et al., 2004). However adenosine levels increase immediately following ischemia, in advance of the loss of ion gradients (Frenguelli et al., 2007). Therefore some yet undefined mechanism, such as exocytosis or retrograde signalling may be responsible for the rapid adenosine outflow during ischemia (Dale and Frenguelli, 2009).

1.4.3.4 Neuroprotective actions of adenosine during ischemia

Extracellular adenosine concentrations of *in vivo* brain are in the nanomolar range (90 - 120 nM), sufficiently high enough to activate A_1 and A_{2A} receptors (Dunwiddie and Masino, 2001; Latini and Pedata, 2001). Release of ATP from glial cells and subsequent degradation to adenosine by ecto-nucleotidases is believed to be responsible for this adenosine tone in the CNS (Pascual et al., 2005; Wall and Dale, 2008). Adenosine may also arise from release and degradation of cAMP, by ecto-phosphodiesterase and 5'-nucleotidase, and this route may avcount for slow changes of extracellular adenosine levels (Figure 1.6) (Brundege et al., 1997; Latini and Pedata, 2001).

However, during ischemia or hypoxia adenosine levels increase rapidly in *in vitro* and *in vivo* brain, reaching levels of up to 20 -30 µM (Fredholm et al., 1984; Kobayashi et al., 1998; Dale et al., 2000; de Mendonca et al., 2000; Parkinson et al., 2002; Frenguelli et al., 2003; Frenguelli et al., 2007).

During ischemic/hypoxic conditions adenosine is mainly produced from intracellular sources, rather than extracellular degradation of ATP (Lloyd et al., 1993; Frenguelli et al., 2007). As explained above, the main pathway for intracellular adenosine formation involves AMP degradation via c-N-I, hence adenosine production is enhanced when the energy demand is greater than energy production, resulting in an increase of AMP levels and subsequent dephosphorylation (Dunwiddie and Masino, 2001). Intracellular adenosine can also be derived from S-adenosylhomocysteine in a reversible reaction catalysed by S-adenosylhomocysteine hydrolase (Figure 1.6).

This pathway is not involved in energy metabolism, but in transmethylation reactions and does not play a major role for adenosine release during ischemia (Latini et al., 1996).

Subsequent release of adenosine and activation of A_1 receptors prevents glutatmate release via combined presynaptic inhibition of Ca^{2+} channels, direct interference with the vesicle release machinery and postsynaptic activation of K^+ channels coupled with hyperpolarisation (see Figure 1.6) (Rudolphi et al., 1992; de Mendonca et al., 2000; Cunha, 2001; Ribeiro et al., 2002, 2003). All these actions reduce excitotoxic damage by reducing Ca^{2+} entry and the energy demand of cells, thereby helping to preserve ATP levels (Dunwiddie and Masino, 2001).

Accordingly, strategies that increase adenosine levels, such as inhibition of adenosine uptake (Dux et al., 1990; Gidday et al., 1995), inhibition of adenosine metabolising enzymes (Phillis and O'Regan, 1989) or administration of A_1 receptor agonists (de Mendonca et al., 2000; Ribeiro et al., 2003), have been shown to exert a neuroprotective effect during ischemia. Furthermore, adenosine released from the brain can, via activation of arterial A_{2A} receptors, vasodilate cerebral blood vessels, and therefore contribute to neuroprotection by enhancing cerebral blood flow (Phillis, 1989), whereas activation of cerebral A_{2A} receptor in the adult brain exaggerates neuronal damage, as seen in attenuated ischemic brain injury in A_{2A} knockout animals (Chen et al., 1999).

Interestingly the ischemic damage induced by global ischemia in A_1 receptor knock out mice is not different to wild type animals, allthough pre-administration of the A_1 receptor antagonist 8-CPT (8-cyclopentyltheophylline) exacerbated the neuronal damage following ischemia in wild type animals, suggesting that some effects of the A_1 receptor are compensated for in knockout animals (Olsson et al., 2004). Additionally in immature brain inhibition of A_1 receptors attenuates hypoxic/ischemic damage, by reducing white matter loss (Turner et al., 2003), whereas the hypoxic/ischemic damage is exabberated in immature A_{2A} receptor knockout mice (Aden et al., 2003). This suggests that, in contrast to adult brain, A_{2A} receptors are neuroprotective in neonates (Fredholm et al., 2005).

Like adenosine, inosine levels increase dramatically during ischemia (Dux et al., 1990; Phillis et al., 1996; Kobayashi et al., 1998; Weigand et al., 1999). On that note it is worth mentioning that exogenous inosine can preserve neuronal and glial cell viability during oxygen/glucose deprivation (Rudolphi et al., 1992; Jurkowitz et al., 1998; Litsky et al., 1999; Rathbone et al., 1999) and improve behavioural outcome after middle cerebral artery occlusion in rats (Chen et al., 2002; Shen et al., 2005). The effects of inosine are mediated by its conversion to hypoxanthine and subsequently ATP (Litsky et al., 1999; Giannecchini et al., 2005), however, inosine can also promote axonal regrowth (Chen et al., 2002; Benowitz and Carmichael, 2010) and the protective effect of inosine pre-administration during *in vivo* ischemia may also involve suppression of glutamate responses and A_3 receptor activation (Shen et al., 2005).

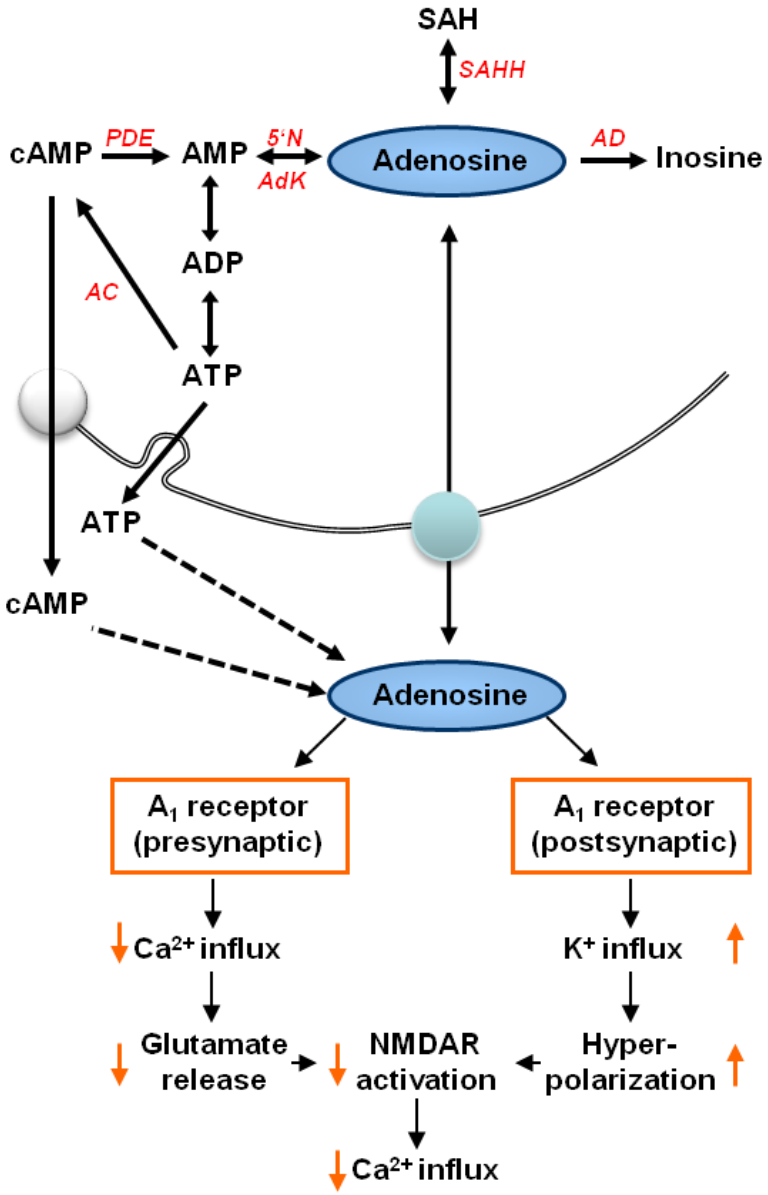

Figure 1.6: Intra and extracullar pathways for the formation of adenosine and the role of A_1 receptors in neuroprotection: *AMP, derived from ATP via adenylate kinase or cAMP via phosphodiesterase (PDE) is degraded to adenosine by 5'nucleotidase (5'N). Adenosine can be rephosphorylated to AMP by adenosine kinase (AdK) or deaminated to inosine by adenosine deaminase (AD). Adenosine can also be derived from S-adenosylhomocysteine (SAH) in a reversible rection catalysed by SAH hydrolase (SAHH). Adenosine is transported to the extracellular space where it inhibits synaptic transmission via combined activation of pre- and postsynaptic A_1 receptors. Direct release of ATP and subsequent degradation to adenosine also contributes to increased extracellular adenosine levels. Likewise cAMP can be transported to the extracellular space and subsequently degraded to adenosine. NMDAR NMDA receptor. Adapted from (de Mendonca et al., 2000; Pearson et al., 2003).*

These facts show that simply inhibiting ATP degradation during ischemia would not be a promising strategy to improve post-ischemic ATP levels, since that would also interfere with the neuroprotective release of purine nucleosides. Therefore, a more promising approach would be to enhance the re-synthesis of ATP rather than interfere with its degradation.

1.4.4 Restoration of ATP

The two main pathways for restoring and maintaining a constant TAN pool are the purine *de novo* synthesis and the purine salvage pathways. The sugar precursor to ATP is derived from the pentose phosphate pathway and is used in both pathways. Whereas the purine *de novo* synthesis is an energy-dependent process where the purine base is built from low molecular weight precursors, the purine salvage pathway re-uses preformed purine bases to restore purine nucleotides.

1.4.4.1 The synthesis of the sugar precursor

The activated sugar donor for the synthesis of purine nucleotides, 5-phosphoribosyl-1-pyrophosphate (PRPP) is derived from Ribose-5-phosphate, an intermediate of the pentose phosphate pathway (PPP, also called phosphogluconate pathway or hexose monophospahte shunt). Alternatively Ribose-1-phosphate, derived from purine nucleoside phosphorylase (see Figure 1.5, enzyme 4) can be isomerised to Ribose-5-phosphate by phosphopentomutase (Tozzi et al., 2006).

The PPP interlinks glucose, fatty acid and purine/pyrimidine metabolism and can be separated into an oxidative branch and a nonoxidative branch (Figure 1.7). In the oxidative branch glucose-6-phosphate, derived from glycolysis or glycogenolysis is converted to ribulose-5-phosphate in 3 reactions, thereby producing 2 molecules of NADPH. NADPH is used for the synthesis of free fatty acids as well as for the conversion of oxidised to reduced glutathione, a radical scavenger. In the non-oxidative branch ribulose-5-phosphate is converted to ribose-5-phosphate (by ribulose-5-phosphate isomerase) and xylulose-5-phosphate (by ribulose-5-phosphate epimerase). Both these sugars are subsequently converted to the glycolytic

intermediates fructose-6-phosphate and glycerinaldehyde-3-phosphate. Ribose-5-phosphate is however, also the substrate for PRPP synthetase, which uses ATP and transfers its pyrophosphate group to ribose-5-phosphate, yielding PRPP and AMP (Figure 1.7) (Stryer et al., 1995).

PRPP is used as a phosphoribosyl group donor in purine and pyrimidine nucleotide as well as NAD^+ synthesis (Stryer et al., 1995). Specific Phosphoribosyltransferases (PRTases) catalyse the transfer of ribose-5-phosphate from PRPP to a nitrogen-containing nucleophile (purine or pyrimidine base for salvage pathways, glutamine for purine *de novo* synthesis and quinolate for NAD^+ synthesis) producing a β-substituted ribose-5-phosphate and PPi (Sinha and Smith, 2001).

The PRPP pool is strongly regulated and maintained in the low micromolar range to avoid excessive purine and pyrimidine synthesis. PRPP synthetase is inhibited by high ATP concentrations as well as PRPP and it is strongly activated by Pi (Murray, 1971). Excessive purine synthesis, caused by abnormally high activity of PRPP synthetase or defects in purine metabolism can lead to uric acid overproduction and crystallisation and subsequently gout (Cameron et al., 1993).

In the brain only 1 - 3 % of the consumed glucose is metabolised via the PPP (Gaitonde and Evans, 1982; Gaitonde et al., 1983) and the rate limiting step in this pathway is the first reaction of the oxidative branch, catalysed by glucose-6-phosphate dehydrogenase, which converts glucose-6-phosphate to 6-phosphogluconate (Kauffman et al., 1969). In heart tissue the activity of glucose-6-phosphate dehydrogenase has been shown to be rate limiting for purine *de novo* synthesis as well as purine salvage (Zimmer, 1998).

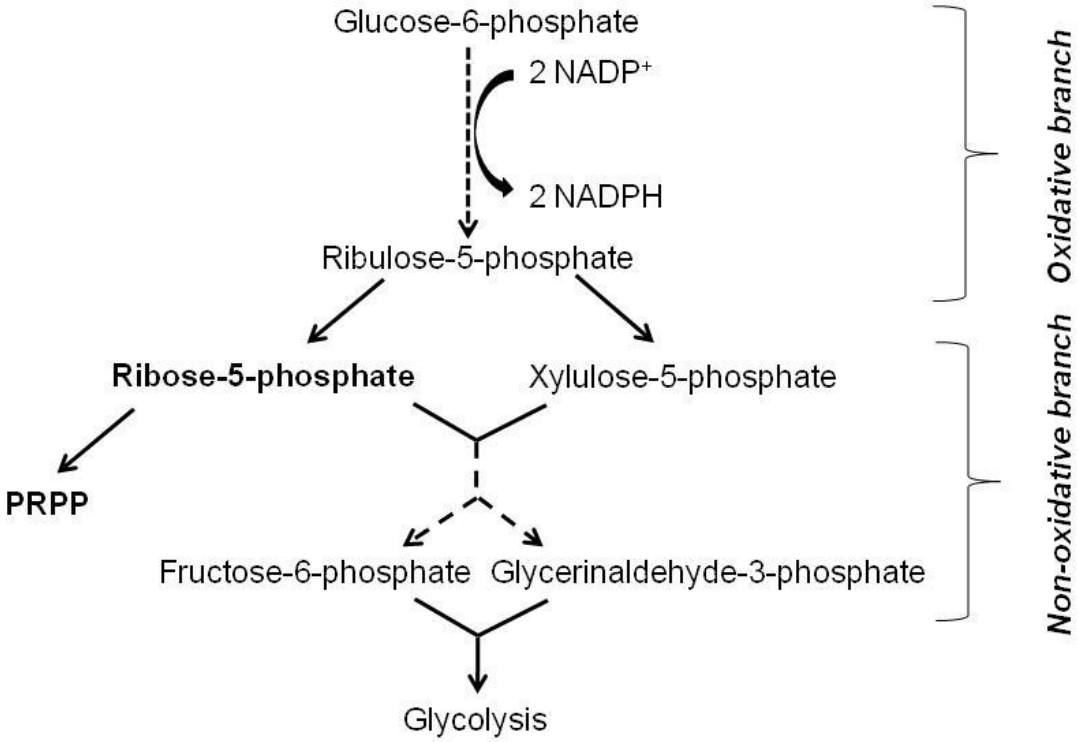

Figure 1.7: The pentose phosphate pathway: *Glucose-6-phosphate, derived from glycolysis or glycogenolysis is converted to ribulose-5-phosphate by glucose-6-phosphate dehydrogenase, gluconolactonase and 6-phosphogluconate dehydrogenase in the oxidative branch. The 2 dehydrogenases provide the reducing agent NADPH. In the non-oxidative branch ribulose-5-phosphate is converted to ribose-5-phosphate and xylulose-5-phosphate by ribulose-5-phosphate isomerase and ribulose-5-phosphate epimerase, respectively. These two pentose sugars are reconverted to the glycolytic intermediates fructose-6-phosphate and glycerinaldehyde-3-phosphate via 2 reactions catalysed by transketolase and 1 reaction catalysed by transaldolase. Ribose-5-phosphate is also the substrate for PRPP synthesases, which transfers the terminal PPi group from ATP to the C1 position of Ribose-5-phosphate, yielding AMP and 5-phosphoribosyl-1-pyrophosphate. PRPP is then subsequently used for purine salvage and de novo synthesis as an activated sugar donor.*

1.4.5 Purine *de novo* synthesis

Purine nucleotide *de novo* synthesis is an energy-dependent process, which results in formation of inosine monophosphate (IMP) from simple precursors upon expenditure of 6 molecules of ATP. This process involves 10 steps and 6 enzymes (three monofunctional, two bifunctional and one trifunctional enzyme) all of which are located in the cytosol and can form clusters in response to increased purine *de novo* synthesis (purinosome) (An et al., 2008). The purine ring is formed by amino acids, CO_2 and derivates of tetrahydrofolate, whilst the ribose phosphate moiety is derived from PRPP (Stryer et al., 1995). The origin of the various carbon and nitrogen atoms in the purine ring is shown in Figure 1.8.

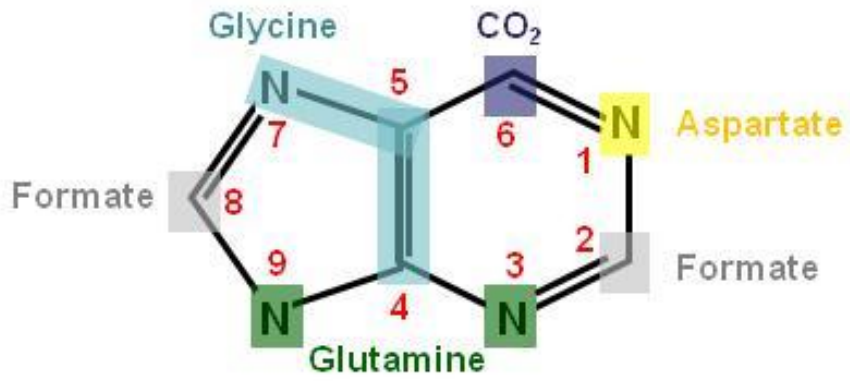

Figure 1.8: Origin of atoms in the purine ring: adapted from (Stryer et al., 1995)

The rate limiting step is the first reaction catalysed by glutamine phosphoribosyl amidotransferase, which converts glutamine and PRPP to 5-phosphoribosylamine (see Figure 1.9). The availability of PRPP, various feedback inhibitions of purine *de novo* synthesis intermediates as well as purine nucleotides are the main regulators of purine *de novo* synthesis (Watts, 1983).

The endproduct IMP acts as a common intermediate for the interconversion of adenine and guanine nucleotides. The first step of the conversion of IMP to GMP is catalysed by IMP dehydrogenase in an NAD^+-dependent reaction with ATP as energy donor. The intermediate xanthosine monophosphate (XMP) is then converted

to GMP by GMP synthase (Tozzi et al., 2006). Guanine nucleotides are involved in protein synthesis, cell signalling and GTP can serve as an energy donor in specific metabolic reactions.

The conversion of IMP to AMP is catalysed by adenylosuccinate synthetase (AS) and adenylosuccinate lyase (AL). AS is the rate limiting enzyme, which catalyses the condensation of IMP and aspartate into adenylosuccinate, using GTP as energy donor. The activity of AS is mainly regulated by the intracellular IMP concentration, and the reaction products adenylosuccinate and GDP, as well as GMP, ADP and AMP are inhibitors of the enzyme (Van den Berghe et al., 1992). AL converts adenylosuccinate to AMP and fumarate, and is also the 8th enzyme of the purine *de novo* synthesis, cleaving SAICAR (phosphoribosyl aminoimidazole succinocarboxamide) into AICAR (aminoimidazole carboxamide ribonucleotide) and fumarate. AMP, AICAR and fumarate exert a feedback inhibition on AL (Van den Berghe et al., 1992).

Purine *de novo* synthesis is dominant in the liver, which is responsible for the majority of circulating purine nucleosides and bases (Ipata et al., 2011), whereas it has been shown to be slow and weak in the brain (Gerlach et al., 1971; Allsop and Watts, 1980).

1.4.6 Purine salvage pathway

In contrast to the energy dependent-reactions of purine *de novo* synthesis, preformed purine bases can be returned to the nucleotide pool by an energy saving pathway referred to as the purine salvage pathway. This is the predominant route for the brain (Gerlach et al., 1971; Allsop and Watts, 1980; Mascia et al., 2000; Barsotti and Ipata, 2002) as well as the heart (Zimmer, 1998; Pauly et al., 2003) to restore and maintain their adenine nucleotides.

Hypoxanthine-guanosine-phosphoribosyltranserfase (HGPRT) and adenine phosphoribosyl-transferase (APRT) are the central enzymes of this pathway. HGPRT catalyzes the transfer of ribose-5-phosphate from PRPP to guanine or hypoxanthine

yielding PPi, GMP or IMP respectively (Murray, 1971). Hypoxanthine and guanine are derived from purine nucleoside phosphorylase (see Figure 1.5) and the affinity of HGPRT for both is approximately equal (Manfredi and Holmes, 1985). The reaction products IMP, GMP and PPi are inhibitors of the enzyme. However the inhibitory constants are high suggesting that under physiological conditions none of the products would be a physiological effector (Manfredi and Holmes, 1985). HGPRT is expressed in all tissues, and is very abundant in the brain, a further proof for the importance of the salvage pathway in this organ (Murray, 1966, 1971; Adams and Harkness, 1976; Allsop and Watts, 1980). Purification of HGPRT from rat brain showed that most of the enzyme is present in the cytosol, although a small but significant fraction was found in synaptosomes (Gutensohn, 1973). It is worth noting that an X-linked neurological disorder, Lesch-Nyhan syndrome, which is associated with an almost complete lack of HGPRT activity, results in mental retardation, chorea and compulsive/aggressive self injury (Nyhan, 2005).

APRT catalyses the PRPP-dependent phosphoribosylation of adenine to AMP and PPi. Like HGPRT, APRT is expressed in the brain, although its activity is lower compared to HGPRT (Allsop and Watts, 1980). The purine base adenine is derived from methylthioadenosine phosphorylase, which catalyses the cleavage of methylthioadenosine, a byproduct of polyamine synthesis, to adenine and methylthioribose-1-phosphate (Della Ragione et al., 1986; Ipata et al., 2011). Furthermore it has been shown that adenine can be derived from adenosine in primary rat neuronal cultures (Brosh et al., 1996), although it has been previously suggested that purine nucleoside phosphorylase does not react with adenosine (Murray, 1971).

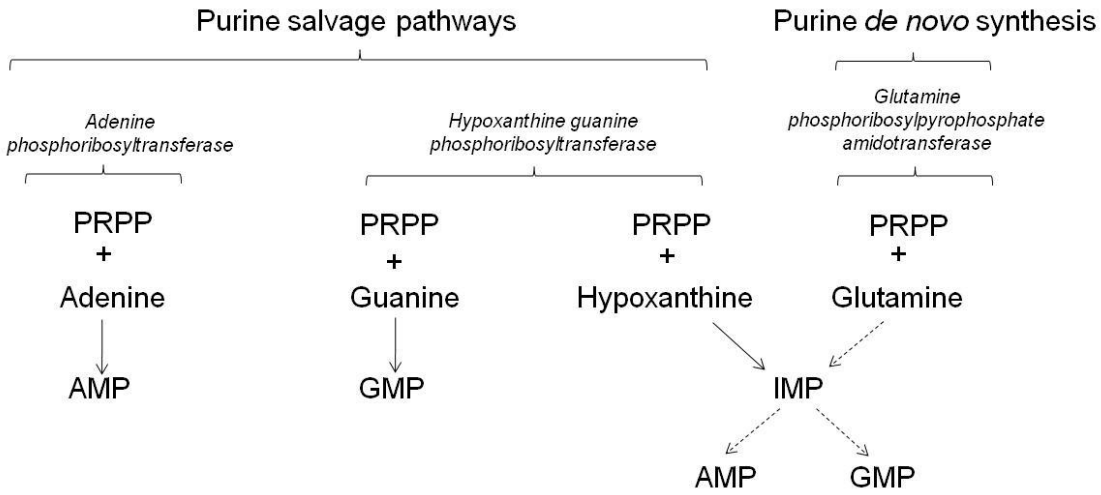

Figure 1.9: Phosphoribosyltransferases catalyse the reactions of the purine salvage pathway as well as the first step of the purine de novo synthesis. *PRPP (5-phosphoribosyl-1-pyrophosphate) is used as an activated sugar donor, to salvage accumulated purine bases to the respective nucleotides (Adenine and hypoxanthine/ guanine phosphoribosyltransferases). PRPP is also used as a sugar donor in purine de novo synthesis.*

In addition to intracellular purine base levels, circulating purine nucleosides and bases can be taken up from the blood, via specific nucleobase and nucleoside transporters (Cornford and Oldendorf, 1975; Pardridge and Oldendorf, 1977). CNT2 mediates the Na^+-dependent uptake of adenosine, inosine, guanosine and uridine across the blood brain barrier. ENTs mediate the bidirectional transport of nucleosides and are regulated by the concentration gradient (Ipata et al., 2011). Additionally nucleobase transporters, of which there are Na^+-dependent and independent types (Isakovic et al., 2008) mediate the uptake and efflux of hypoxanthine and adenine. The equilibrative nucleobase transporters are located in the blood brain barrier and are not powerful enough to mediate significant purine base uptake (Spector, 1987). The concentrative nucleobase transporters in the choroid plexus, however, have been shown to be involved in uptake of salvageable purine bases from the blood (Washington and Giacomini, 1995).

1.4.7 Basis for the reduced post-ischemic adenine nucleotide pool

Since ATP degradation during ischemia results in the accumulation and release of large quantities of adenosine, inosine and hypoxanthine these substances can be washed out of the brain to the systemic circulation via the activity of equilibrative nucleoside and nucleobase transporters (Isakovic et al., 2008; Ipata et al., 2011).

The release of purine metabolites during ischemia/hypoxia has not only been observed in *in vitro* (Fredholm et al., 1984; Kobayashi et al., 1998; Dale et al., 2000; de Mendonca et al., 2000; Parkinson et al., 2002; Frenguelli et al., 2003; Frenguelli et al., 2007) and *in vivo* animal models (Hillered et al., 1989; Dux et al., 1990; Phillis et al., 1991; Phillis et al., 1996; Kobayashi et al., 1998; Valtysson et al., 1998) but also in humans. Adenosine, hypoxanthine, xanthine and uric acid were detected in blood and cerebrospinal fluid of stroke patients (Stover et al., 1997; Laghi Pasini et al., 2000). Adenosine was also detected in human plasma during moderate hypoxia (Saito et al., 1999), in jugular venous blood of humans undergoing carotid endarterectomy with insufficient collateral blood supply of the brain (Weigand et al., 1999) and in transient ischemic attack as well as stroke patients (Laghi Pasini et al., 2000). These observations show that large quantities of purine metabolites are washed out from the brain and subsequently lost from the adenine nucleotide pool.

Additionally it has been shown that repeated episodes of hypoxia and ischemia result in a reduced release of adenosine *in vitro* (Pearson et al., 2001; Pearson et al., 2003) and *in vivo* (Dux et al., 1990; DiGeronimo et al., 1998; Valtysson et al., 1998), suggesting that the brain cannot replenish the released adenosine at a sufficiently fast rate to support non-depleting adenosine release. Since adenosine is neuroprotective during ischemia (see above) any reduction in adenosine release leaves the brain more susceptible to excitotoxic damage during secondary strokes.

Furhtermore considering the brain's reliance on the purine salvage pathway, any loss of salvageable ATP degradation metabolites to the systemic circulation, as well as production of unsalvageable xanthine and uric acid by xanthine oxidase, might limit the potential recovery of post-ischemic TAN and ATP levels (Pearson et al., 2003).

Since the purine *de novo* synthesis in the brain is not up-regulated after ischemia (Gerlach et al., 1971) a complete restoration of normal nucleotide levels may be achieved by *de novo* synthesis at a slow rate, which may last several hours or days (Gerlach et al., 1971; Kleihues et al., 1974; Ljunggren et al., 1974). This could explain the slow and incomplete recovery of ATP during short reperfusion periods, and – considering intracellular ATP as a primary source of adenosine - the reduced adenosine release, after subsequent ischemic/hypoxic periods.

Balancing these two competing consequences of ATP degradation – the beneficial release of neuroprotective modulators and the concomitant depletion of the TAN pool respectively – can therefore only be achieved by enhancing the restoration of ATP in the post-ischemic brain, hence the purine salvage pathway.

1.5 Manipulations of purine salvage pathway

The main aim of this study was to improve post-ischemic ATP recovery by (i) increasing the availability of PRPP and/or by (ii) increasing the availability of the free purine bases hypoxanthine and adenine. This was achieved with simple manipulations, which are known to be tolerated in humans. Therefore, results of this study may provide important information for development of new treatments for stroke patients.

1.5.1 D-Ribose to increase the available PRPP pool

As in brain, brief periods of ischemia produces a rapid depletion in myocardial ATP levels (Zimmer, 1992). Likewise, the restoration of post-ischemic ATP levels is slow, due to the heart's dependence on the purine salvage pathway and the loss of salvageable purine metabolites to the systemic circulation (Zimmer, 1992, 1998; Pauly et al., 2003). It has been shown that due to the weak capacity of the oxidative PPP, the available pool of PRPP is small and limits post-ischemic cardiac adenine nucleotide synthesis via *de novo* and salvage pathways (Zimmer, 1998). Therefore, elevating the PRPP pool by bypassing the rate limiting step of the oxidative PPP is a

possibility to enhance adenine nucleotide synthesis. This can be achieved by administration of D-ribose, a simple pentose sugar, which is directly phosphorylated to ribose-5-phosphate by ribokinase (Park et al., 2007), and subsequently phosphoribosylated to PRPP by PRPP synthetase.

In fact, addition of D-ribose increases myocardial PRPP levels and efficiently improves postischemic recovery of the myocardial ATP in rat hearts by enhanced purine salvage as well as *de novo* synthesis (Zimmer and Gerlach, 1978; Zimmer, 1992, 1996, 1998). Accordingly this metabolic approach has been utilized in different experimental *in vivo* models: for example during myocardial infarction in rats (Zimmer, 1982; Zimmer et al., 1989) or after global myocardial ischemia in dogs (St Cyr et al., 1989), where it has been shown to enhance the functional recovery of the heart.

Ribose is known to be tolerated in humans (Gross and Zollner, 1991; Pauly et al., 2003) and administration of 10 mmol/kg per day has has no adverse effects in humans (Salerno et al., 1999). In patients with coronary artery disease D-Ribose improved cardiac function, exercise tolerance and general quality of life (Pliml et al., 1992). Ribose has also been given to a patient with fibromyalgia, a disease which is correlated with reduced ATP levels in muscles, where it decreased certain symptoms such as muscle pain, weakness or sleeping disturbances (Gebhart and Jorgenson, 2004).

In rat brain extracts ribose is phosphorylated to ribose-5-phosphate and subsequently PRPP, thereby implying the presence of ribokinase (Mascia et al., 2000; Barsotti and Ipata, 2002). Therefore – similar to the heart - increasing the available PRPP pool for APRT and HGPRT might help brain cells to recover their ATP pools faster after periods of ischemia and may improve functional recovery as well as cell viability. Therefore the D-Ribose administration will be tested as a potential neuroprotective intervention for the post-ischemic *in vitro* brain tissue.

1.5.2 Xanthine oxidase inhibition to increase available hypoxanthine levels

As explained above, the conversion of hypoxanthine to xanthine and uric acid, catalysed by xanthine oxidase, also contributes to a reduction of the TAN pool, since neither of these metabolites can be used in the purine salvage pathway. In rat forebrain following focal cerebral ischemia (Kanemitsu et al., 1988), as well as in cerebrospinal fluids of human stroke patients (Stover et al., 1997) xanthine and uric acid levels are increased, suggesting a role of xanthine oxidase in the degradation of hypoxanthine. Therefore, another possibility to enhance the purine salvage pathway could be to inhibit xanthine oxidase, and thereby increase the available hypoxanthine pool for HGPRT. The xanthine oxidase inhibitor allopurinol is known to be well tolerated in humans, since it is a commonly used drug to treat gout (Pacher et al., 2006).

This approach of inhibiting xanthine oxidase has already been studied in *in vivo* models of cerebral ischemia and pre-treatment of rodents with oxypurinol, the active inhibitor, has been shown to enhance the postischemic recovery of adenine nucleotide levels in the brain (Phillis et al., 1995). In other experiments pretreatment with allopurinol increased adenosine and inosine levels in cerebral cortex of newborn piglets, which was believed to be responsible for the protective effects of allopurinol during ischemia (Marro et al., 2006). Therefore, allopurinol will be used for comparative studies to D-ribose and its effect on postischemic recovery of cellular ATP levels and synaptic transmission will be studied.

1.5.3 Administration of the purine base adenine to enhance APRT activity

I further tested whether addition of the free purine base adenine can help to improve post-ischemic ATP recovery by enhancing the activity of APRT. In rat heart it has been shown that adenine is effectively converted to ATP and can further enhance the D-ribose mediated purine salvage (Brown et al., 1985; Zimmer, 1996; Kalsi et al., 1998). Likewise high concentrations of adenine can improve the post-ischemic recovery of ATP levels in brain slices (Newman et al., 1998).

Adenine has been given to humans suffering from Lesh-Nyhan syndrome (Schulman et al., 1971). However, adenine has to be administered in combination with allopurinol, to avoid its degradation by xanthine oxidase to an insoluble metabolite, 2,8-dihydroxy-adenine, that can cause the formation of kidney stones (Greenwood et al., 1982). Therefore it will be tested, whether adenine and adenine/allopurinol administration is an effective strategy to improve post-ischemic recovery of ATP and synaptic transmission, as well as cell viability.

Other work in this field attempted to maintain nucleotide levels by pre-incubation with creatine, to increase phospho-creatine levels, and thereby delay the degradation of ATP during ischemia (Balestrino et al., 1999; Balestrino et al., 2002). Therefore, experiments with creatine will be used for comparative purposes, but the main focus of this study will be on D-Ribose, allopurinol and adenine supplementation.

1.6 *In vitro* models for cerebral ischemia

As *in vitro* models of cerebral ischemia, I used hippocampal brain slices and cerebellar granule cells. *In vitro* models serve as a good cost-effective screening system for neuroprotective interventions. Furthermore the extracellular environment can be completely controlled, bypassing the blood brain barrier, and brain slices and cell cultures can be used for combined, functional, metabolic, morphological and cell viability analysis. However, the major limitations of *in vitro* models are the lack of inputs and outputs from the brain, the lack of blood-borne components (e.g. inflammatory mediators) as well as behavioural output. Nevertheless, cell cultures and brain slices show similar changes in response to the lack of oxygen and glucose with respect to biochemical and physiological properties of brain tissue, and are therefore widely used for electrophysiological, metabolic and cell viability studies into neuroprotection (Schurr and Rigor, 1989; Woodruff et al., 2011).

1.6.1 Hippocampal brain slices

The hippocampus is a bilateral structure embedded in the medial temporal lobe. The hippocampus is composed of two regions, the dentate gyrus (DG) and the cornu ammonis (CA), both of which are structured into layers (strata). The main cell types are granule cells in the DG and pyramidal cells in the CA regions. The DG has a stratum moleculare, a stratum granulosum with the cell bodies of granule cells, and a polymorphic layer. The CA regions can be separated into stratum moleculare (apical dendrites), stratum lacunosum, stratum radiatum, stratum lucidum, stratum pyramidale (cell body layer), stratum oriens (basal dendrites) and the alveus. The polymorphic layer and stratum radiatum and oriens contain various interneurons, basket cells, bipolar cells and mossy cells.

The CA region can be separated into 3[3] various subfields (CA1 - 3) with distinct connectivity, electrophysiological properties and vulnerability to insults. The hippocampus receives its afferents from various neighbouring brain regions, with the entorhinal cortex being the most important. The entorhinal cortex projects onto granule cells of the DG in the perforant path. DG granule cells send axons onto CA3 pyramidal cells in the mossy fibre pathway, and CA3 pyramidal cells send the so called Schaffer collateral-commisural fibres through the stratum radiatum to the CA1 pyramidal cells thereby forming the third pathway in the tri-synaptic circuit (see Figure 1.10) as well as to the contralateral hippocampus (Andersen et al., 2006).

[3] Sometimes the polymorphic layer of the DG is referred to as CA4, since the densely packed pyramidal cell layer begins to spread out into a more polymorphic layer.

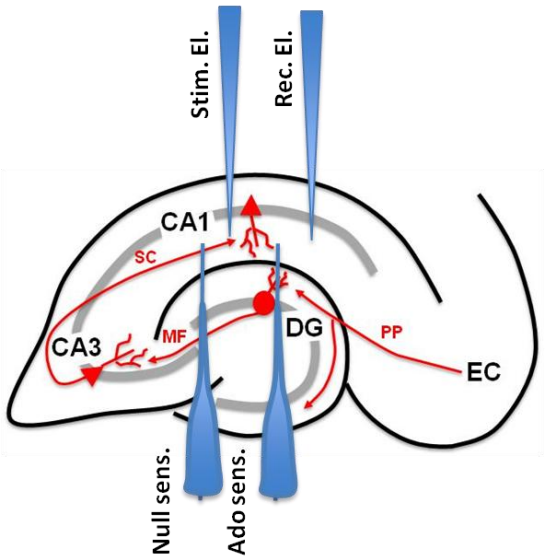

Figure 1.10: Sagittal hippocampal brain slice: *The entorhinal cortex (EC) projects to granule cells in the dentate gyrus (DG) in the perforant path (PP). Granule cells send axons to pyramidal cells in Cornu Ammonis 3 (CA3) in the mossy fiber pathway (MF). CA3 neurons project to CA1 pyramidal neurons in the Schaffer collateral pathway (SC), completing the trisynaptic circuit.The grey areas are the cell body layers of the DG (stratum granulosum) and CA subregions (stratum pyramidale). The position of the stimulating (Stim.) and recording (Rec.) electrodes (El.), as well as the null and Adenosine (Ado) biosensors (Sens.) during experiments are shown in blue.*

Hippocampal brain slices were introduced in the early 1950s (McIlwain, 1951) and have since been a widely used *in vitro* model system of CNS function. The hippocampus is best known for its role in learning and memory and hence hippocampal brain slices are frequently used in studies of synaptic transmission and plasticity.

Additionally, hippocampal neurons in the area CA1 are amongst the most vulnerable neurons to cerebral ischemia, and are therefore frequently as *in vitro* model for cerebral ischemia and neuroprotective interventions (Schurr and Rigor, 1989; Nitatori et al., 1995).

However, since their introduction it was heavily debated how similar the energetic state of the tissue is to the *in vivo* brain, since their preparation involves an ischemic period caused by cervical dislocation and decapitation. Accordingly many different

preparation and maintenance procedures have been suggested to make the *"best brain slices"* (Aitken et al., 1995; Lipton et al., 1995). Therefore a great part of the thesis will deal with the energetic state of the slices and the appropriate incubation conditions to achieve a metabolic state which is as close to the *in vivo* brain as possible as a prelude to investigating the influence of purine salvage manipulations. I further tested the consequences of improved energetic recovery on synaptic transmission and plasticity. After having established the optimal incubation conditions hippocampal brain slices were used for metabolic and combined adenosine release and electrophysiological studies, to investigate the effect of D-ribose, allopurinol and/or adenine as well as creatine on the recovery of postischemic ATP levels and synaptic transmission.

1.6.2 Cerebellar granule cells

To establish the effect of the various interventions of the purine salvage pathway on post-ischemic cell viability after prolonged reperfusion periods, I used cerebellar granule cells (CGC), a primary neuronal cell culture. CGCs were introduced about 30 years ago (Gallo et al., 1982) and are today a widely used primary neuronal cell culture for studies into developmental, functional, and pathological aspects of neurobiology. Unlike other cell cultures, such as hippocampal neurons, they represent a relatively pure (~ 90 %) neuronal culture. Accordingly CGC are frequently used for studies into neuronal cell death and neuroprotection (Contestabile, 2002).

Therefore, the combined use of these two *in vitro* models allowed me to establish the effect of enhanced purine salvage activity before or after OGD on the energetic state of the tissue (intracellular adenine nucleotide levels), adenosine release (adenosine biosensors) and the decline and recovery of synaptic transmission during brief ischemic (minutes) and reperfusion periods (hours) in hippocampal brain slices as well as on cell viability after longer ischemic (hours) and reperfusion periods (overnight) in CGC.

2 Material and Methods

2.1 Preparation and maintenance of Cerebellar granule cell cultures

Cerebellar granule cells (CGCs) were prepared from P 6 – 8 Sprague Dawley rats, as described previously (Tomaselli et al., 2008; Wall et al., 2010). For each preparation one or two pups were killed by cervical dislocation in accordance with Schedule 1 of the UK Government Animals (Scientific Procedures) Act 1986 and with local Ethical Review procedures. After decapitation the skin was removed, the skull was opened and the cerebellum was carefully isolated with tweezers and placed into a petri dish containing Krebs solution (NaCl 124 mM; KCl 5.4 mM; $NaH_2PO_4H_2O$ 1 mM; Glucose 14.4 mM; Phenolred 28 μM; HEPES 20 mM; $MgSO_4$ 150 μM; BSA 0.3 g; pH 7.4; 37°C) with 0.01 % Penicillin/Streptomycin (Pen/Strep). Meninges and blood vessels were removed and cerebella were triturated in 10 ml Krebs solution. After centrifugation (1500 rpm, 3 min), the tissue was resuspended in fresh Krebs solution containing 0.025 % trypsin and incubated for 15 min at 37°C in the water bath. Thereafter the trypsin containing cell suspension was diluted with 3.6 ml solution 3 (Krebs solution containing 0.52 mg/ml Trypsin inhibitor and 0.1 mg/ml DNAse) and 6.4 ml Krebs solution. After centrifugation (1500 rpm, 3 min), cells were thoroughly dissociated with a glass pasteur pipette (with a flamed opening, to reduce cell damage and improve dissociation of cells) in one volume solution 3 and two volumes solution 5, and passed through a 40 μm cell strainer (BD biosciences) to remove remaining cell clumps. The suspension was spun at 1900 rpm for 5 min and cerebellar granule neurons were purified from glial cells by a pre-plating step (1 h, 37°C) in 3 ml Neurobasal medium (supplemented with 2 % B27, 1.5 mM glutamine and 0.01 % Pen/Strep). During this incubation step glial cells will attach to the uncoated surface of the petri dish, whereas neurons will remain in suspension. The petri dish was washed with Neurobasal medium and the cells were spun at 1900 rpm for 5 min. The cell pellet was resuspended in 3 ml Neurobasal medium and cells were counted using a haemocytometer. CGCs were plated at a density of 1.3×10^5 on poly-l-ornithine coated borosilicate glass coverslips (placed in 12 well plates), at a density of 6×10^6 - 1×10^7 in 60 mm dishes, and at a density of 1×10^5/well in 96 well plates. Neurons were cultured for 7 - 8 days in Neurobasal medium, containing

KCl 25 mM, B27 2 %, glutamine 1.5 mM, and Pen/Strep 0.01% in a humidified atmosphere with 5 % CO_2, before being used for experiments. For coating of dishes/coverslips Poly-L-ornithine was added for 2 – 3 h, thereafter wells/coverslips/dishes were washed twice with sterile water and allowed to dry before being used. For compositions of the different solutions refer to Appendix 1, section 10.1.

CGC have to be maintained in high K^+ (Gallo et al., 1987), to depolarise the neurons, and promote a survival-supporting effect via Ca^{2+} influx and Ca^{2+}/calmodulin-dependent protein kinase (Hack et al., 1993). If maintained under these conditions CGCs form a neuronal network after 6 – 7 days *in vitro*, as seen by the neuronal marker MAP-2 (Microtubulus-associated protein 2) and the synaptic marker synapsin I (Figure 2.1).

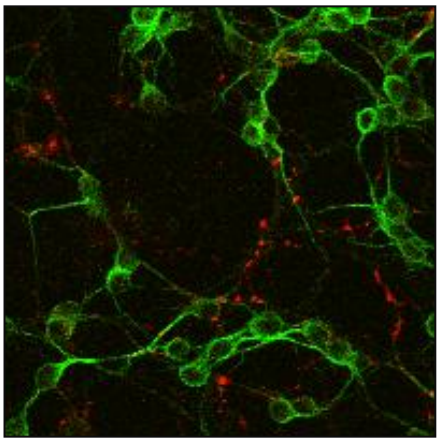

Figure 2.1: Staining of cerebellar granule cells after 7 days in vitro for MAP-2 (green stain) and synapsin I (red stain). *Cells were prepared from P 6 – 8 Sprague Dawley rats and maintained in a humidified atmosphere with 5 % CO_2 at 37°C in supplemented Neurobasal medium with 25 mM KCl. Cells were fixed in 4 % PFA for 15 min, washed twice with PBS and permeabilised with 0.3 % Triton X-100 in PBS for 15 min. After washing in PBS cells were blocked with 1 % BSA in PBS for 20 min, washed again and the primary antibodies were added in PBS containing 0.1 % BSA and Triton X-100 overnight at 4°C (1:500 dilution). On the next day cells were washed with PBS and the secondary Alexa labelled antibody was added in PBS containing 0.1 % BSA and Triton X-100, protected from light for 1 h at room temperature (1:1000 dilution). Coverslipes were washed and mounted onto microscopic slides in Vectashield, sealed with nail vanish and stored at 4°C, protected from light until being imaged (within 3 weeks).*

2.2 Preparation and maintenance of hippocampal brain slices

Male Sprague-Dawley rats (P 17 - 28) were killed by cervical dislocation in accordance with Schedule 1 of the UK Government Animals (Scientific Procedures) Act 1986 and with local Ethical Review procedures. To keep experiments consistent most animals were P 20 – P 25 and only occasionally younger/older animals had to be used. The animal was decapitated, the skull was opened, meninges were removed and the brain was quickly placed into ice cold 11 mM Mg^{2+}- containing artificial cerebrospinal fluid (aCSF). The temporal parts of the brain were trimmed, the hemispheres were separated along the midline and mounted onto a metal block using cyanoacrylate (RS components). Sagittal brain slices (400 μm), composed of hippocampus and overlying neocortex, were then prepared in ice-cold, 11 mM Mg^{2+}-containing aCSF using a Microm HM 650 V microtome. If not otherwise stated slices were transferred to a chamber (50 - 100 ml) (Edwards et al., 1989) and submerged in continuously circulating, oxygenated standard aCSF kept at 34°C. The composition of the standard aCSF solution was: NaCl 124 mM; KCl 3 mM; $CaCl_2$ 2 mM; $NaHCO_3$ 26 mM; NaH_2PO_4 1.25 mM; D-glucose 10 mM; $MgCl_2$ 1 mM; pH 7.4 with 95 % O_2/5 % CO_2 (Appendix 1, section 10.2).

In chapter 4 the preparation and maintenance of brain slices differed from the standard procedure described above, therefore the exact incubation conditions will be described individually for this chapter.

2.3 *In vitro* ischemia models

Oxygen/glucose deprivation (OGD) is a widely used model for *in vitro* ischemia in slices and cell cultures. It is comparable to transient global ischemia and reperfusion is easily achieved by exchanging the oxygen/glucose deprived medium/aCSF for standard medium/aCSF.

2.3.1 Induction of OGD in cerebellar granule cells

In cerebellar granule cells OGD was induced by replacing the Neurobasal medium with PBS or glucose free Neurobasal medium (supplemented with 0.01 % Pen/Strep, 1.5 mM Glutamine, 25 mM KCl and 2 % B27 supplement), which has been equilibrated with 95 % N_2/5 % CO_2 for 3 hrs in a sealed tupperware chamber. Cells were transferred into a tupperware chamber, which was then equilibrated with 95 % N_2/5 % CO_2 for another 30 min. Thereafter the chamber was thoroughly sealed with parafilm and tape and placed back into the incubator for 6 h, if not otherwise stated. After this ischemic insult cells were fixed immediately for Hoechst/Propidium iodide staining or the OGD medium was replaced with the previous culture medium for a 12 – 14 h reperfusion period.

2.3.2 Induction of OGD in brain slices

In hippocampal brain slice experiments OGD was induced by replacing glucose in the aCSF with 10 mM sucrose and bubbling the solution with 95 % N_2/5 % CO_2 for at least 1 h before slices were transferred (for HPLC analysis) or the perfusion system was switched (for electrophysiological recordings and sensor measurements). Slices were exposed to OGD for various time points and reperfusion was achieved by transferring the slices or switching the perfusion system back to standard aCSF for various time points.

2.4 Protein extraction

For each time point 2 - 3 brain slices were placed in ice cold aCSF to stop enzymatic activities. Slices were homogenised in 100 µl protein lysis buffer with a Kontes® pellet pestle motor (Sigma-Aldrich, UK). The suspension was centrifuged (30 min, 4°C, 16060 g) and the supernatant was stored at -80°C for kinase assays and western blot analysis. The composition of the protein lysis buffer was: Tris-HCl, pH 7.5 50

mM; EGTA 0.1 mM; EDTA 1 mM; Triton X-100 1%; sodium orthovanadate 1 mM; sodium fluoride 50 mM; sodium pyrophosphate 5mM; sucrose 270 mM; β-mercaptoethanol 0.1%; sodium azide 0.02%; 1 protease inhibitor tablet for 16.6 ml lysis buffer.

2.5 Nucleotide extraction

2.5.1 Nucleotide extraction of brain slices

Two brain slices were placed in ice cold standard aCSF to stop enzymatic degradation. Slices were transferred into 1 ml ice cold 5 % perchloric acid (PCA) with a small spatula, to minimise fluid transfer, and immediately homogenized with a Kontes® pellet pestle motor. After centrifugation (2 min, 4°C, 13000 rpm) the PCA was precipitated with 1 ml of tri-*n*-octylamine in 1,1,2-trichlorotrifluoroethane (1:1; v/v) (Khym, 1975). The suspension was vortexed for 20 s and kept on ice for 10 minutes. After centrifugation (2 min, 12100 g), the organic extraction was repeated twice with the upper aqueous phase. Thereafter the aqueous phase had a pH of 6 and contained water-soluble cell components, such as purine nucleotides/nucleosides and bases. HPLC analysis of extracts was performed on the same day (Zur Nedden et al., 2009). The protein pellet was resuspended in 1 ml 0.5 M NaOH, and protein concentration was determined by Bradford assay, with BSA as standard.

In chapter 4 the nucleotide extraction of brain slices differed from the standard procedure described above, therefore the exact extraction conditions will be described individually for this chapter.

2.5.2 Nucleotide extraction of cerebellar granule cells

The Neurobasal medium was removed and cells were washed with PBS twice before 500 µl ice cold 5 % PCA were added into the dish. Cells were kept on ice and

detached from the dish using a cell scraper. The cell suspension was transferred into a 1.5 ml eppendorf tube and cells were homogenised with a pellet pestle motor. After centrifugation (2 min, 4°C, 13000 rpm) the PCA extract was neutralized as described above. If not otherwise stated the extract was kept at - 20°C over night and analysed with HPLC on the next day.

2.6 Etheno-derivatisation

250 µl of the standard or sample mixture were incubated with 5 % chloroacetaldhyde at 80°C in a heating block for indicated time points. After addition of chloroacetaldehyde the pH of the solution was 3 - 5, as measured with a pH paper.

2.7 Bradford assay

BSA standards were prepared from 0.5 – 10 mg BSA/ml 1 M NaOH. 20 µl of standards and of sample extracts were diluted in 480 µl destilled water and 10 µl of these suspensions were added to 200 µl Bradford reagent in 96 well plates. Care was taken that all samples were well mixed at all times. The absorbance was read at a wavelength of 620 nm with a spectrophotometer, and the amount of protein in samples was calculated on the calibration curve of standard BSA.

2.8 High performance liquid chromatography

2.8.1 HPLC apparatus

The HPLC system (Thermo Scientific) consisted of a vacuum degasser (SCM 1000), Spectra System binary gradient pumps (P2000), an injector with a 20 µl injection valve and a Spectra System photodiode array UV detector (UV 6000), equipped with

a 10 µl flow cell. Unless otherwise stated a Supelcosil LC-18-T reverse phase column (150 mm x 4.6 mm i.d., 3µm) protected with a HPLC Security Guard Cartridge (C8, 4 x 3.0 mm, Phenomenex) was used for the UV detection of purine and pyrimidine metabolites. For fluorescence detection of etheno-metabolites a Luna C8 (2) (150 mm x 4.5 mm i.d., 5 µm) and a FL 3000 fluorescence detector (Spectra system) was used. Peak analysis and quantification was performed with the Chromquest 4.2.34 software. For UV detection HPLC chromatograms were obtained at a wavelength of 254 nm. However, the UV spectrum from 220-360 nm was scanned for all runs and used for spectral and purity analysis of sample and standard peaks. For fluorescence detection of etheno-adenine derivatives the FL 3000 detector was set to an excitation wavelength of 230 nm and an emission wavelength of 420 nm (Zur Nedden et al., 2009).

2.8.2 HPLC method for UV detection of purine and pyrimidine metabolites

If not otherwise stated the mobile phase consisted of buffer A (65 mM potassium phosphate buffer, composed of 39 mM dipotassium hydrogen phosphate and 26 mM potassium dihydrogen phosphate, adjusted to pH 6 with orthophosphoric acid, 4 mM TBAHS) and buffer B (65 mM potassium phosphate buffer composed of 39 mM dipotassium hydrogen phosphate and 26 mM potassium dihydrogen phosphate, adjusted to pH 6 with orthophosphoric acid and 25% methanol). The methanol in Buffer B was added after the pH of the solution was adjusted, and after addition of methanol the solution was mixed for 10 – 15 min. Both buffers were prepared in deionised water, and filtered through a 0.4 µm filter before use. For each day of analysis the Supelcosil LC-18-T column was equilibrated with 10 - 20 column volumes of buffer B, and 30 – 50 column volumes of buffer A (flow rate 1 ml/min). The retention times of standard compounds stabilised after two blank injections (gradient profile described below) and analytical separation could then be performed. The flow rate was 1 ml/min and the gradient profile used was: 1 min 100 % buffer A, 3 min to 30 % buffer B, 7.5 min to 80 % buffer B and 10 min to 100 % buffer B. The run was kept at 100 % buffer B for 3 more minutes before it was completed and the gradient was returned to 100 % buffer A. Run time for the elution of relevant

compounds was 13 min. A 10 minute re-equilibration between runs was sufficient to restore initial conditions. Concentrations were calculated by comparing the peak area of sample peaks with calibration curves for peak areas of each standard compound. All concentrations are expressed as nmol/mg protein (Zur Nedden et al., 2009). Standard solutions were prepared in deionised water/or 0.1 M NaOH as stock solutions at 1, 10 or 100 mM (if NaOH had to be used) concentration, and stored at -20°C. For preparation of HPLC buffers please refer to Appendix 1, section 10.3.

2.8.3 HPLC method for fluorescence detection of etheno-adenine-metabolites

For detection of etheno (ε)-metabolites a Luna C_8 (2) column (Phenomenex) and a Luna C_8 (2) guard column (Phenomenex) was used. Buffer A was composed of 20 mM potassium phosphate buffer, pH 6 and buffer B consisted of 20 mM phosphate buffer, pH 6 and 25 % methanol (see Appendix 1, section 10.3). For elution of ε - ATP, ε - ADP, ε - AMP and ε -adenosine a 10 min linear gradient from 100 % buffer A to 100 % buffer B at a flow rate of 1 ml/min was used. For preparation of reverse phase HPLC buffers please refer to Appendix 1, section 10.3.

2.8.4 Column protection

To keep the column performance optimal, special care was taken in column protection. The column (Supelcosil) was washed after each day with 25 column volumes of 25 % methanol in order to remove any residual phosphate buffer. The guard cartridge was changed after 200-300 injections. When the peak shapes started to show broadening and the backpressure increased (250 - 350 injections), the column was regenerated by flushing it with 30 column volumes of water (40-60°C), 100 % methanol, 100 % acetonitrile, 20 column volumes of 100 % tetrahydrofuran and 100 % methanol in reverse flow direction, at a flow rate of 0.4 ml/min, as per manufacturer's instructions (Zur Nedden et al., 2009).

For Luna C_8 (2) column a 95 % organic modifier/ 5 % water mixture was used, as per manufacturer's instructions. The flow rate, the order of organic modifiers and the volumes was the same as described above.

2.9 Electrophysiology

For electrophysiological recordings slices were transferred to a submerged type recording chamber, with a fluid volume of 2 - 3 ml kept at 33.5 ± 0.5°C and a flow rate of 6 - 8 ml/min. A small harp was placed onto the slice to prevent it from moving. A twisted bipolar teflon coated tungsten wire was placed to stimulate the Schaffer collateral/commissural pathway every 15 s and field excitatory postsynaptic potentials (fEPSPs) were recorded from stratum radiatum in area CA1 of the hippocampus with a glass microelectrode filled with aCSF (1 MΩ) as described previously (Frenguelli et al., 2007; Zur Nedden et al., 2011). The stimulus intensity was adjusted to 50 – 60 % of that required to evoke a population spike. Stimulus parameters and acquisition and analysis of fEPSPs were under the control of LTP software.

2.10 Adenosine biosensor measurements

Adenosine and null microelectrode biosensors (50 μm diameter /500 μm length) were purchased from Sarissa Biomedical Ltd (Coventry, UK). The adenosine sensor relies upon an enzyme cascade immobilized within a matrix on the surface of a Pt/Ir electrode to metabolize adenosine thereby liberating H_2O_2, which is oxidized on the Pt/Ir electrode. This gives rise to an oxidation current proportional to the concentration of adenosine. The null sensor lacks enzymes and is used to establish the presence of any electroactive interferents. Both sensors were inserted in the stratum radiatum of the CA1 region of hippocampal slices in between recording and stimulating electrodes, or with the stimulating electrode placed between both sensors

at an equal distance. Recording of fEPSP was started 30 – 45 min after insertion of sensors. fEPSPs, adenosine and null sensor traces were recorded simultaneously. After each experiment sensors were taken out of the tissue and calibrated with 10 µM adenosine in the recording chamber. To monitor the unspecific response to electroactive substances, 10 µM serotonin was applied and if the response was smaller than 50 pA, the adenosine signal during the experiment was assumed to be specific. Since no non-specific electroactive release could be detected on the null sensor, adenosine release was calculated without subtraction of the null trace and the values are given as µM´ to reflect that the adenosine sensor measures adenosine and its metabolites (Frenguelli et al., 2007). In order to integrate the area under the curve of adenosine sensor traces, the baseline had to be set to 0, which was achieved by subtracting from the sensor trace a linear regression based on 5 minutes of baseline (Zur Nedden et al., 2009).

2.11 Cell death staining with Hoechst and propidium iodide

Cells were incubated in the dark at 37°C for 10 minutes with Hoechst (cell permeable blue stain; 8 µM), followed by a further 5 minutes with propidium iodide (cell impermeable red stain; 5 µg/ml, see Appendix 1, section 10.4 for preparation). During this incubation all cells will be stained with Hoechst, and cells with broken membranes (dead cells) will be stained with propidium iodide (see Figure 2.2). Cells were washed twice with PBS and fixed with 4 % paraformaldehyde (PFA) for 15 min. After washing cells thoroughly with PBS, coverslips were mounted onto microscope slides using Vectashield (Vector Laboratories), sealed with nail vanish and stored at 4°C, protected from light until being imaged (within 3 weeks).

Imaging was conducted with a 20 x objective on an epifluoerescent microscope using the appropriate filter for Hoechst (UV) and propidium iodide (510 nm). Four to five images were captured of each coverslip, at distributed locations that were representative of the cells present.

Hoechst and propidium iodide pictures were merged in Photoshop (Adobe) and cells were assessed as being either viable (blue; Hoechst staining alone), or inviable (pink; co-merged Hoechst and propidium iodide staining). Only cells greater than 3 µm in diameter were included in the analysis. The percentage of cell death was calculated for each image (% cell death = dead cells x 100/total cell number), and the five values for each condition averaged to give total percentage of cell death per condition.

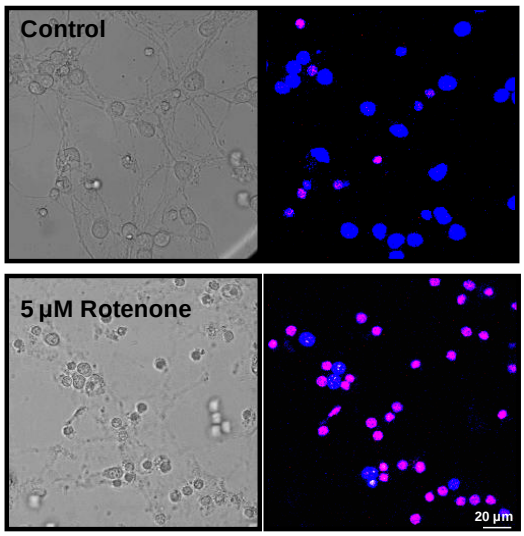

Figure 2.2: Cell death can be assessed with Hoechst (blue stain, all cells) and propidium iodide (red stain, dead cells): *Cerebellar granule cells were treated with 5 µM rotenone for 5 h to induce cell death. Cells were stained immediately with 10 µM Hoechst for 15 min and 2 µM propidium iodide for 5 min. Hoechst and propidium iodide images were merged and all pink cells were considered as being dead.*

2.12 XTT cell viability assay

In the XTT assay cell viability is assessed by measuring the activity of mitochondrial succinate dehydrogenases, which convert the yellow tetrazolium salt XTT (2,3-bis[2-methoxy-4-nitro-5-sulfopheny]-2H-tetrazolium-5-carboxyanilide) to orange formazan when incubated with the electron coupling agent phenazine methosulphate (PMS). The resulting colour change can then be quantified using a spectrophotometer.

For this assay cells were grown in 96 well plates. Cells were washed thoroughly with PBS and incubated for 4 hours at 37°C with 100 µl XTT solution in PBS per well (1mg/ml XTT; 25 µM PMS). Wells containing XTT solution in the absence of cells were used as blanks. The preparation of the XTT solution is described in Appendix 1, section 10.4. The intensity of the colour change was detected using a spectrophotometer (Labsystems; Multiscan Ascent). Plates were shaken to ensure even solutions and the absorbance at 450 nm was recorded, with a reference wavelength at 690 nm. After subtraction of the blank values average absorbance values (from 4 – 5 wells) for each condition were determined.

2.13 Chemicals and stocksolutions

All chemicals and stock solutions are summarised in Appendix 1, section 10.5.

2.14 Statistical analysis

All values are expressed as mean ± S.E.M. For the electrophysiological and adenosine sensor measurements N values refer to the number of slices per experimental condition, which for most cases is also equal to the number of animals used. Slices were used in duplicate for nucleotide extraction and in triplicate for protein extraction. In these cases N values represent the number of animals used. In experiments with CGC N values refer to the average of 5 images per coverslip per animal used. For statistical analysis of more than two groups one way ANOVA with Bonferroni's multiple comparison test was applied, whereas for comparisons between two independent groups unpaired t-tests were used. For comparison of adenosine release before and after application of different drugs a paired t-test was applied. Calculations were carried out with Prism 4; p-values < 0.05 were considered as statistically significant.

3 Development of a high performance liquid chromatography method for accurate detection of purine metabolites in brain slices

3.1 Introduction

An important part of this project was the assessment of adenine nucleotide levels in hippocampal brain slices, before, during and after ischemic insults, under control conditions and after various interventions of the purine salvage pathway. In addition to absolute adenine nucleotide values, equations that describe the relation of the individual nucleotides in the total adenine nucleotide pool ([TAN] = Σ ([ATP] + [ADP] + [AMP]), such as the adenylate energy charge (EC = ([ATP] + 0.5[ADP]/[TAN])) (Atkinson, 1968), are frequently used to assess the energetic state of tissues or cells, since it reflects the energy supply (ATP) to demand (ADP, AMP) relationship better than the absolute adenine nucleotide values (Kammermeier, 1993). The EC describes the relative proportion of charged adenine nucleotides (in terms of their phospho-anhydride bonds) in the TAN pool, and has a maximum value of 1, when all the adenine nucleotides are in the form of ATP. As such, accurate determinations of *in situ* adenine nucleotide concentrations are required for many investigations into the energetic state of tissue.

There are several possible ways of measuring tissue adenylate levels, with bioluminescence assays and high performance chromatography methods (HPLC) most frequently used (Manfredi et al., 2002). HPLC has the advantage of high sensitivity and it allows the separation and quantification of a wide range of purine and pyrimidine nucleotides/nucleosides and free bases in one run. Therefore the main aim of this chapter was to develop a HPLC method for the simultaneous and accurate detection of tissue adenylate levels and most metabolites involved in the purine salvage pathway. For measurement of purine nucleotides, nucleosides and bases, ion-pair reversed-phase HPLC is commonly used (Stocchi et al., 1987; Kochanowski et al., 2006), since the separation of purine nucleotides is difficult with reverse phase columns and purine nucleosides are only poorly retained in anion exchange HPLC (Zakaria and Brown, 1981).

In reverse phase HPLC the stationary phase is packed into a column and consists of spherical silica particles (usually 3 – 5 μm in diameter) masked with alkyl chains

(such as C_4, C_8 or C_{18}), and therefore provides a nonpolar, hydrophobic environment. The mobile phase is polar and consists of an aqueous solution, buffered to a certain pH. After injection of the sample or standard mixture, separation is achieved because individual sample/standard compounds (analytes) will interact with the mobile and stationary phase to different extents, based on their hydrophobic characteristics (or their relative polarity)[4]. Elution of analytes from the column is generally achieved by gradually reducing the polarity of the mobile phase by increasing the percentage of an organic modifier (such as methanol or acetonitrile).

Purine nucleosides or bases, which are uncharged and relatively nonpolar, can be easily separated with this type of HPLC. However, in order to achieve a separation of charged molecules (such as nucleotides), which will not sufficiently interact with the stationary phase, an ion pairing agent can be added to the mobile phase. The most commonly used ion pairing agents for negatively charged analytes are quaternary amines such as tetrabutylammonium hydrogen sulphate (TBAHS). TBAHS consists of 4 alkyl chains, which interact with the stationary phase, and a positively charged ammonium head group, which will form ion pairs with the negatively charged compounds in the sample mixture and thereby prolong their retention time. The addition of TBAHS to the mobile phase still allows uncharged/non polar compounds to interact with the stationary phase.

In this section I will describe the disadvantages of fluorescence-based detection of adenine nucleotides for the accurate detection of the *in situ* energetic state and the development of a fast, sensitive, ion-pair reversed-phase UV-based HPLC method, which allows the analysis of at least 11 purine metabolites, including adenine nucleotides and their most important degradation metabolites. This method is suitable for low analyte concentrations and its rapidity (13 min runtime) means that many fresh samples can be run in one day avoiding degradation of adenine nucleotides in frozen tissue or upon thawing (Cappeln et al., 1999). Furthermore, keeping the separation runtime short also helps to save the cost of each analysis,

[4] The actual nature of the interaction of analytes with the stationary/mobile phases is debated in the literature: Vailaya A., Horváth C. (1998) Retention in reversed-phase chromatography: partition or adsorption? *J. Chrom. A* 829:1-27.

since ion-pairing agents are expensive.

I will describe how the analytical separation is obtained using a 3-µm Supelcosil LC-18-T column, with a gradient elution at room temperature. I have used this method to determine the energetic state of hippocampal brain slices and furthermore to evaluate changes in adenine nucleotide levels caused by snap-freezing in liquid nitrogen.

3.2 Results

3.2.1 Reversed phase HPLC

3.2.1.1 Fluorescence-based detection of adenine nucleotides and adenosine

There are two possible ways to detect adenine nucleotides/nucleosides in biological samples: with UV detectors at a wavelength of 240 - 270 nm, or with fluorescence detection of etheno-adenine (ε-adenine) metabolites. The latter method is achieved by derivatising adenine metabolites in samples with chloroacetaldhyde ($ClCH_2CHO$) to fluorescent $1,N^6$-ε-adenine derivatives. During this process (at an ideal pH of 3 – 5) a new imidazol ring structure is formed by an "ethylene bridge" that links the nitrogen (N-1) of the ring structure with the aminogroup at the C-6 atom (Kost and Ivanov, 1980) as shown in Figure 3.1. The presence of an aminogroup ($-NH_2$) is necessary and therefore this process is limited to adenine and cytosine metabolites, and to a lesser extent (at a pH of 6.5) to guanosine metabolites. In order to achieve an efficient derivatisation samples/standards have to be incubated with chloroacetaldehyde at 60°C - 100°C (Sonoki et al., 1989; Howard et al., 1998), with increasing incubation times at lower temperatures, such as 24 hrs at 37°C (Ramos-Salazar and Baines, 1985). A commonly-used temperature for the derivatisation of adenine metabolites is 80°C (Fenton and Dobson, 1992).

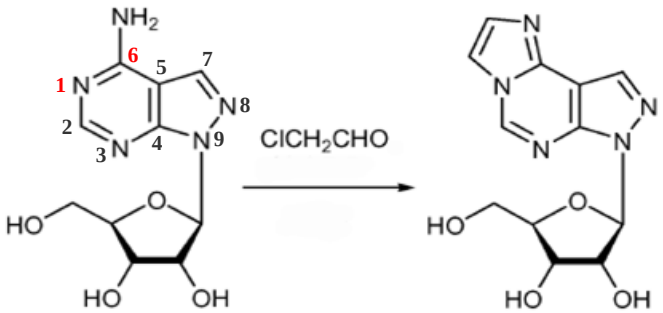

adenosine **1,N^6-ε-adenosine**

Figure 3.1: Principle of etheno-derivatisation *adapted from (Lin et al., 2004): 1,N^6-ε-adenosine is formed when adenosine is incubated with chloroacetaldehyde ($ClCH_2CHO$) at high temperatures.*

The advantage of using 1,N^6-ε-derivates and fluorescence detection is the very low detection limit (picomolar to femtomolar range) (Katayama et al., 2001). Furthermore, the problem of co-eluting purine/pyrimidine metabolites can be disregarded since, as mentioned above, only adenine and cytosine metabolites will be effectively derivatised and detected.

In a first set of experiments I determined the derivatisation efficiency of 100 µM standard ATP upon incubation with 5 % chloroacetaldehyde in aqueous solution (pH 3 - 4) at 80°C. The integrated peak areas obtained from derivatised ε-ATP after various incubation time points (10 min – 2 h) were compared to the peak area obtained from 100 µM standard ε-ATP (indicated by the black dotted line in Figure 3.2 A). As seen in Figure 3.2 A, a complete derivatisation of 100 µM ATP to 100 µM ε-ATP was never reached and, although the derivatisation efficiency improved with increasing incubation duration (to a maximum of 60 % after 40 min incubation), a simultaneous degradation of ATP could be observed, as seen in the increase of ε-ADP, ε-AMP and ε-Adenosine peak areas (Figure 3.2 AB). Due to degradation of ATP during this process this precludes an accurate determination of the energetic state, and thereby underestimates key parameters such as the energy charge (Figure 3.2 C). The derivatisation efficiency could not be improved by incubating standard ATP at lower temperatures (37°C - 4°C) or with higher chloroacetaldehyde concentrations (10 %; data not shown).

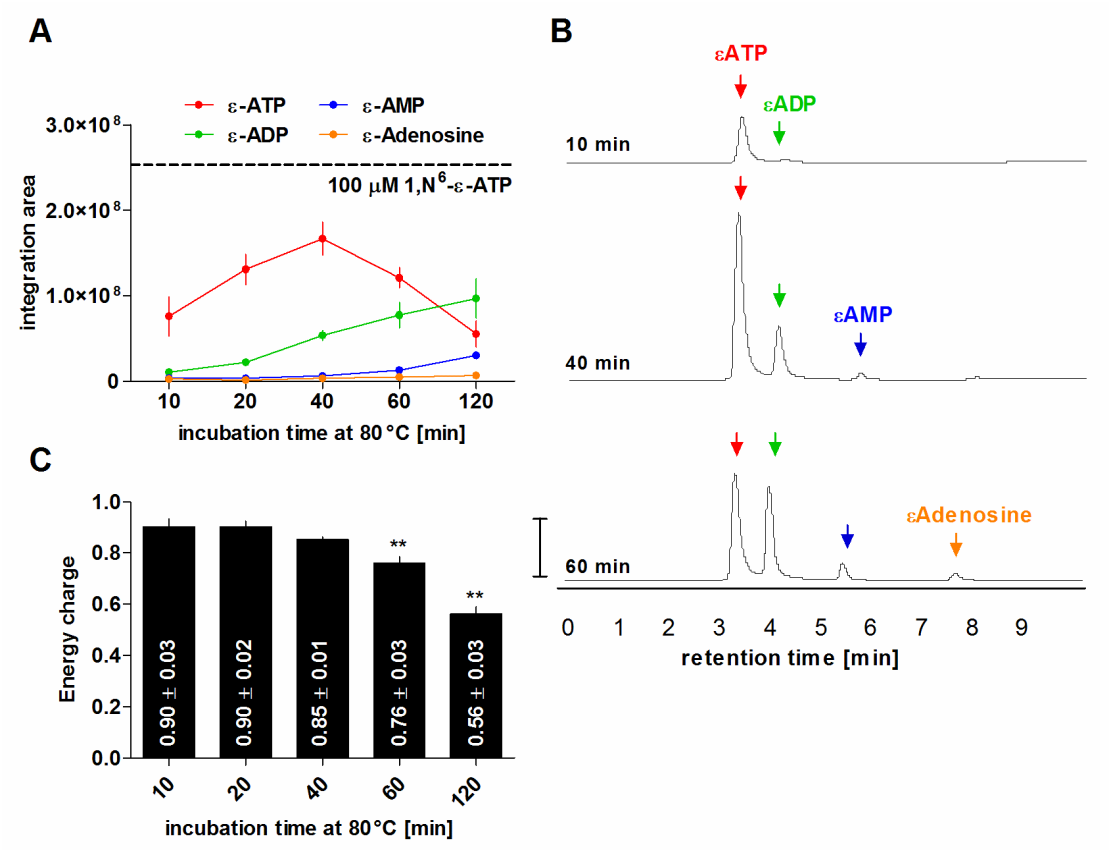

Figure 3.2: Etheno-derivatisation results in degradation of adenine nucleotides. A *100 µM ATP was incubated with 5 % chloroacetaldehyde for various time points at 80°C and analysed by fluorescence-based HPLC. The peak area of standard 100 µM 1,N^6-etheno-ATP is indicated by the horizontal black dotted line. Longer incubation periods resulted in better derivatisation efficiency, peaking after 40 minutes. However, due to degradation of ATP, peak areas of ADP, AMP and adenosine progressively increased with longer incubation time points; All values are presented as mean ± S.E.M.; N = 3 - 8.* ***B*** *Representative HPLC traces of 100 µM ATP after 10, 40 or 60 min incubation with 5 % chloroacetaldehyde at 80°C. Arrowheads refer to ε-ATP (red), ε-ADP (green), ε-AMP (blue) or ε-adenosine (orange). Scalebar indicates 10 V.* ***C*** *Calculation of the energy charge (EC = [ATP]+0.5[ADP])/[TAN] of derivatised 100 µM ATP from (A) after various incubation time points at 80°C. An energy charge value of 1 (all ATP) was never reached, indicating that an accurate determination of the energy charge is not possible due to degradation of ATP. All values are presented as mean ± S.E.M.; N = 3 - 8.*

For the derivatisation of tissue samples, brain slice extracts were incubated with 5 % chloroacetaldehyde at 80°C for 20 min, to avoid major degradation of ATP seen after 40 min incubation (Figure 3.2 AB). As seen in Figure 3.3 not only was the yield of ε-derivatised adenine metabolites very variable (Figure 3.3 B) but also the relative increases in adenosine levels (Figure 3.3 C). These observations most likely reflect differences in the derivatisation efficiency and degradation of ATP, rather then differences of *in situ* adenine nucleotide levels in brain slices. Furthermore the retention times of sample peaks were not stable: peaks showed tailing, and sometimes closely co-eluted (Figure 3.3 D), suggesting that the HPLC method lacked sufficient reproducibility.

Despite the inaccurate detection of *in situ* tissue adenylate levels, another disadvantage of this detection method was the fact that other purine salvage metabolites such as hypoxanthine or IMP could not be detected. Therefore the system had to be optimised for UV-based detection.

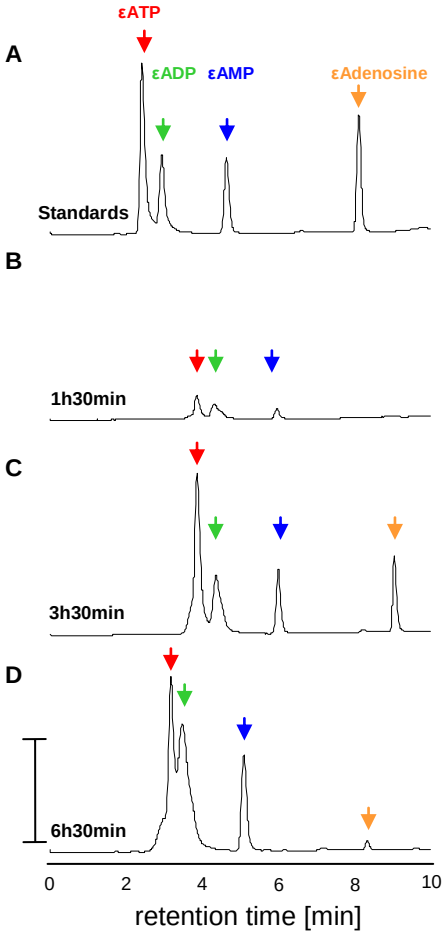

Figure 3.3: Etheno-derivatisation of brain slice extracts results in variable derivatisation efficiency and degradation of ATP. ***A*** *Separation of standard ε-adenine metabolites.* ***B-C*** *Brain slices were incubated in standard aCSF at room temperature for indicated time points, snap frozen in liquid nitrogen and stored at -80°C for < 1 month. After extraction and neutralisation, brain slice extracts were etheno-derivatised by incubating extracts with 5 % chloroacetaldehyde for 20 min at 80°C (pH 4 – 5). 20 min incubation was chosen in order to avoid massive degradation of ATP, which was observed after 40 min (Figure 3.2 AB). HPLC analysis was performed on the day of etheno-derivatisation. Note the very unstable retention times of ε-metabolites and the unreliable derivatisation efficiency. Arrowheads refer to ε-ATP (red), ε-ADP (green), ε-AMP (blue) or ε-adenosine (orange). Scalebar indicates 2 V.*

3.2.1.2 UV-based detection of purine and pyrimidine metabolites

All pyrimidine- and purine-based metabolites absorb at UV ranges around 240 - 270 nm, due to the ring structures of their bases. Therefore, by using a UV detector, a very good separation method is necessary in order to obtain pure peaks, which are not contaminated by other co-eluting compounds. By applying the same HPLC method as used for fluorescence-based detection (see Chapter 2, section 2.8.3), purine/pyrimidine metabolites could not be sufficiently separated in a standard mixture (Figure 3.4 A) or brain slice extracts (Figure 3.4 B).

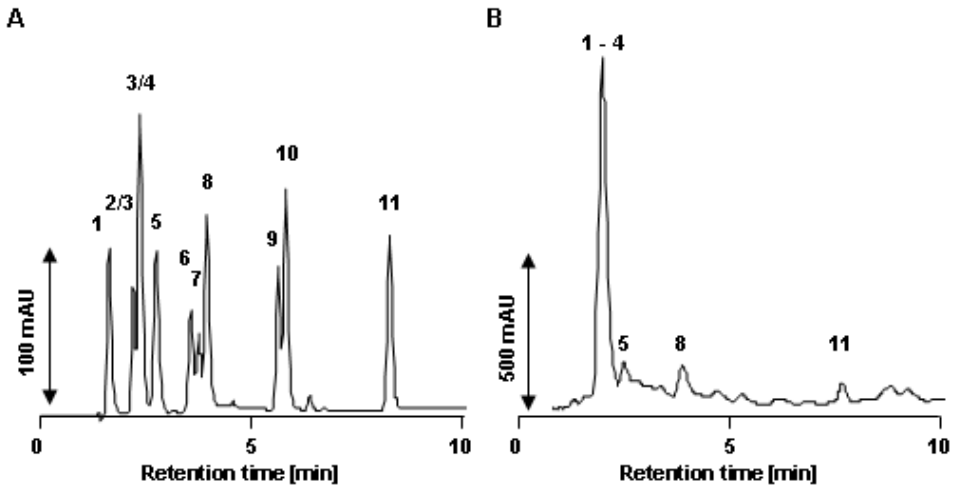

Figure 3.4: Sufficient separation of purine/pyrimidine metabolites is not possible with the HPLC method used for detection of 1,N^6ε-adenine metabolites: *Standard/sample compounds were separated on a Luna-C8(2) column using a 10 min linear gradient from 20 mM phosphate buffer, pH 6 to 20 mM phosphate buffer with 25% methanol.* ***A*** *Separation of standard metabolites and* ***B*** *Separation of nucleotide extracts from a brain slice; 1 GTP, 2 GMP, 3 IMP, 4 ATP, 5 ADP, 6 hypoxanthine, 7 xanthine, 8 AMP, 9 inosine, 10 guanosine, 11 adenosine. Note the co-elution of GTP, GMP, IMP and ATP. Arrowheads indicate milli absorbance units (mAU)*

There are numerous parameters that influence the separation of sample compounds in reverse phase HPLC, some of which are shown in Appendix 2, Table 11.1. In general, changes to the mobile phase will affect its elutive capacity whereas changes to the stationary phase will affect its retentive capacity.

Before adding an ion pairing agent, which permanently changes a reverse phase HPLC column, I tried to change several parameters of the mobile phase and the stationary phase as summarised in Appendix 2, Table 11.2. However, none of these parameters resulted in a sufficient resolution of ATP/GMP and/or IMP as well as AMP/hypoxanthine/xanthine. This is due to the fact that the primary phosphate group of nucleotides is a strong acid ($pK_A < 2$) (Jordan, 1952). Therefore, in order to suppress phosphate ionisation the pH would have to be adjusted to < 1, which cannot be done with silica based columns, since they have a pH operating range of 2 - 8 (with decreases in column efficiency upon long exposure to low (<3) or high (>7) pH).

3.2.2 Ion pairing reversed phase HPLC

The addition of an ion pairing agent to the HPLC buffers (Tetrabutylammonium hydrogen sulphate, TBAHS see Figure 3.5) greatly improved separation. TBAHS consists of an alkyl chain, which allows it to interact with the stationary phase, and a positively charged ammonium group, which forms ion pairs with negatively charged analytes, such as ATP. Upon addition of TBAHS the retention times of nucleotides will be greater compared to nucleosides, therefore the elution of compounds is reversed compared to conventional reverse phase HPLC methods, and the retention time will increase with increasing number of phosphate groups.

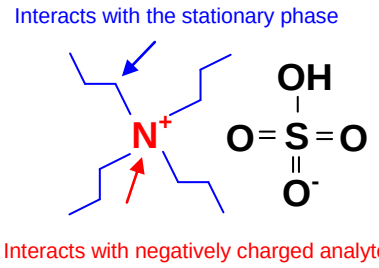

Figure 3.5: Tetrabutylammonium hydrogen sulphate (TBAHS).

I tried to avoid using high TBAHS (8 mM) and buffer concentrations (100 mM) (Stocchi et al., 1987) because of salt precipitations in the HPLC system. A good and reproducible separation of standard compounds was achieved by using a Luna-C_8 (2) column, 50 mM potassium phosphate buffer (pH 6), 15 min linear gradient to 25%

methanol and 4 mM TBAHS in both buffers. With this method most compounds (apart from GMP/IMP) could be well separated in standard mixtures (Figure 3.6). However, further peaks appeared at the end of the run (Figure 3.6 peaks 11 and 13), which were classified as ghost peaks (Williams, 2004), since they were not caused by any of the standard compounds injected.

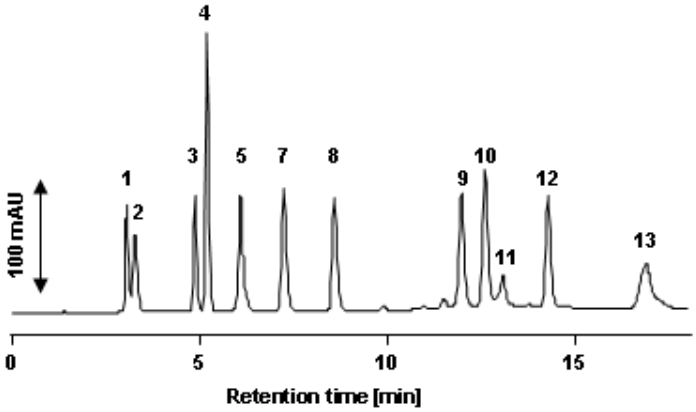

Figure 3.6: Separation of a standard mixture of purine and pyrimidine metabolites on Luna C8 (2) column with 4 mM TBAHS: *1 hypoxanthine, 2 xanthine, 3 inosine, 4 IMP/GMP, 5 guanosine, , 7 adenosine, 8 AMP, 9 ADP, 10 GTP, 11 ghost peak, 12 ATP, 13 ghost peak. mAU milliabsorbance units*

The same method was used to analyse brain slice extracts obtained from brain slices, which had been incubated in standard aCSF at room temperature for various timepoints (0.5 – 6 h), snap frozen in liquid nitrogen and kept at -80°C for 3 - 5 weeks. However, after HPLC analysis (Figure 3.7 A) and calculation of the energy charge of these brain slice extracts (Figure 3.7 B) two things became obvious: Firstly the separation of un-retained material and hypoxanthine/xanthine as well as IMP and GMP was very poor and/or not possible, and secondly the energy charge obtained for brain slices from 1 to 6 h incubation was very low (0.6 – 0.78), potentially reflecting partial adenine nucleotide degradation in the samples and/or compromised energetic state of the tissue. I therefore tried to improve the qualitiy of the separation by using a column with longer alkyl chains (C_{18}) and a smaller silica particle size (3 µm), a higher buffer concentration and by adjusting the gradient profile of the run to achieve optimal separation of these compounds. Furthermore, I aimed to improve the extraction of brain slices to ensure an accurate detection of *in situ* adenine nucleotide levels and energetic parameters.

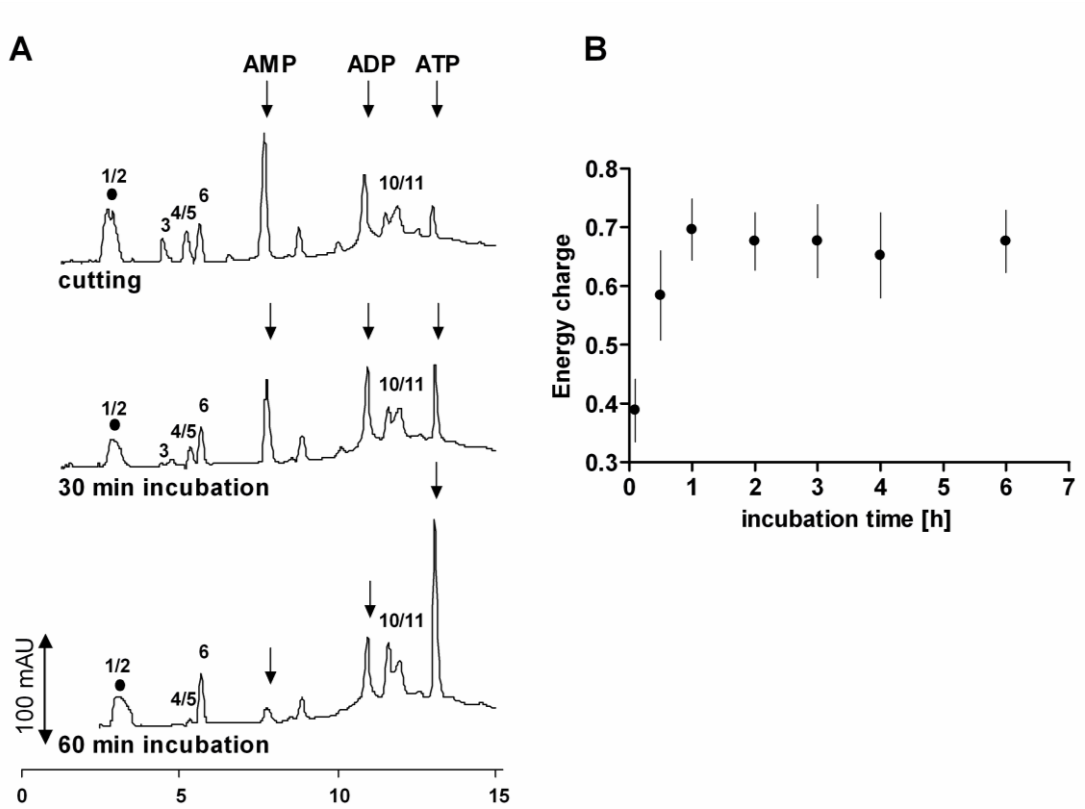

Figure 3.7: Separation of brain slice extracts on a Luna C_8 (2) column with 4 mM TBAHS: *Brain slices were snap frozen in liquid nitrogen at various timepoints after cutting and incubation in aCSF at room temperature. Slices were stored at -80°C for 3 - 5 weeks before being used for perchloric acid extraction and HPLC analysis.* ***A*** *Representative HPLC traces of brain slices at time of cutting and after 30 or 60 min incubation in aCSF at RT. Numbers on traces refer to the following compounds: ● unretained material, 1 hypoxanthine, 2 xanthine, 3 inosine, 4 IMP/GMP, 5 Guanosine, 6 NAD, 7 Adenosine, 8 AMP, 9 ADP, 10 GTP, 11 ghost peak, 12 ATP – note the poor separation of HX/X and IMP/GMP.* ***B*** *Calculation of the Energy charge (EC = ATP + 0.5 x ADP / (ATP + ADP + AMP)) of brain slices after various incubation times in aCSF at RT. Values are presented as mean ± S.E.M, N = 3 - 6, mAU milliabsorbance units.*

The best separation of all purine metabolites (including IMP/GMP) was achieved by using 65 mM potassium phosphate buffer and 4 mM TBAHS, pH 6 for buffer A and 65 mM potassium phosphate buffer, pH 6 with 25 % methanol for buffer B (Figure 3.8). The gradient profile used was 1 min 100% buffer A, 3 min at up to 30% buffer B, 7.5 min at up to 80% buffer B and 10 min at up to 100% buffer B. The run was kept at 100% buffer B for 3 more minutes before it was completed and the gradient was returned to 100% buffer A.

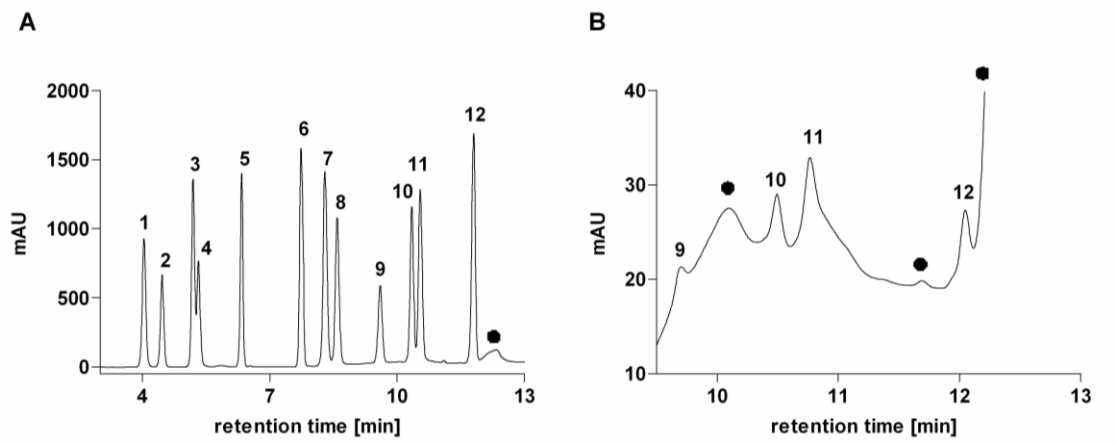

Figure 3.8: HPLC chromatograms of purine standards. A *100 µM standard mixture of 12 compounds.* ***B*** *500 nM mixture of CTP, GTP, ADP and ATP injected after 5 minutes re-equilibration time. Numbers on traces refer to the following compounds: 1 hypoxanthine, 2 xanthine, 3 GMP, 4 IMP, 5 inosine, 6 adenosine, 7 AMP, 8 GDP, 9 CTP, 10 GTP, 11 ADP, 12 ATP.* ● *ghost peaks; mAU milli absorbance units.*

3.2.2.1 Method validation

3.2.2.1.1 *Chromatographic separation*

Using the chromatographic procedure, described above, at least 12 different purine metabolite standards could be separated within 13 minutes, as shown in Figure 3.8 A (100 µM standard mixture; 2000 pmol).

To keep the relative standard deviation of the retention times for each compound (Table 3.1) below ± 2.5 %, the re-equilibration time after each run was kept at 10 minutes. Shorter re-equilibration times (~ 5 min) led to unstable retention times of hypoxanthine and xanthine, whereas longer re-equilibration times (~ 15 min) resulted in co-elution of GMP and IMP at 5.5 minutes (Figure 3.9). Although the retention times of CTP, GTP, ADP and ATP were very stable, even after a 5 minutes re-equilibration time (Figure 3.8 B, 500 nM, 10 pmol), I chose to adopt a constant re-equilibration time of 10 minutes as this allowed optimal and consistent separation of all compounds of interest. Furthermore, the retention times of all standard

compounds did not change when the flow direction of the column was reversed, which allowed me to use the column for longer.

At high gain, the baseline showed several small peaks, eluting after 10 minutes and a larger ghost peak eluting after ATP (black dots in Figure 3.8 B) whose size increased, and whose retention time decreased with the column life time. The nature of these peaks could not be clearly determined. They were not due to an impurity in any of the buffer components, to contamination of the injection valve, to the re-equilibration time, or to the fact that the ion-pairing agent was only used in buffer A. A possible reason could be a precipitation of TBAHS during the gradient elution, which can occur when using potassium phosphate buffers. However, since the ghost peak could be clearly distinguished from the ATP peak, even at low concentrations of ATP, and in order to keep the runtime to a reasonable length, neither the gradient profile nor buffer composition were changed.

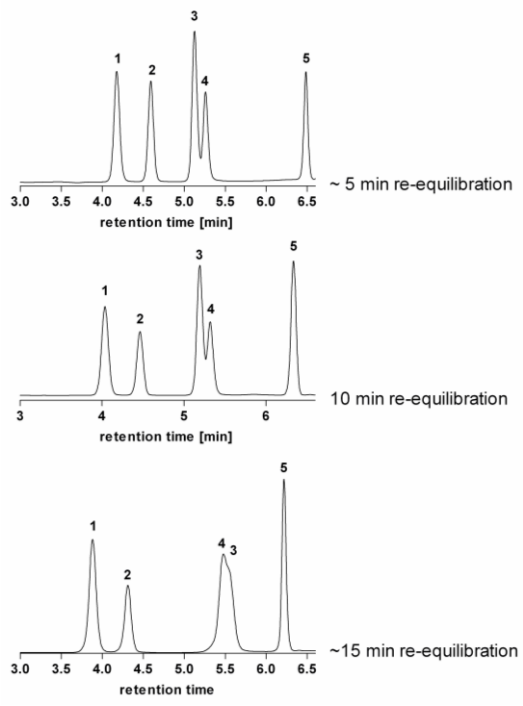

Figure 3.9: Re-equilibration time influences the retention times of early eluting compounds: *After 5 min equilibration the retention times of hypoxanthine (1) and xanthine (2) were variable. After 10 min re-equilibration time the retention times stabilised. However, after 15 min re-equilibration times GMP (3) and IMP (4) co-eluted around 5.5 min. Therefore a 10 min re-equilibration time was chosen between all runs; Numbers on traces refer to following compounds: 1 hypoxanthine, 2 xanthine, 3 GMP, 4 IMP, 5 inosine.*

3.2.2.1.2 *UV absorbance spectra*

The UV absorbance spectra (220-360 nm) for all standard and sample compounds were measured for all runs. Figure 3.10 A shows a contour graph and Figure 3.10 B shows the respective three dimensional graphs of all standard compounds (100 µM, 2000 pmol). The two dimensional UV absorbance spectrum for trinucleotides, nucleosides and free purine bases are shown in Figure 3.10 C and D and the respective UV absorbance maxima are summarised in Table 3.1. Hypoxanthine, inosine and IMP had the lowest UV absorbance maximum (247 nm), whereas xanthine (267 nm) and CTP (270 nm) had the highest absorbance maxima. The quantitative analysis was performed at a wavelength of 254 nm (black line in Figure 3.10 A). This was chosen to encompass the absorbance spectra of all separated compounds.

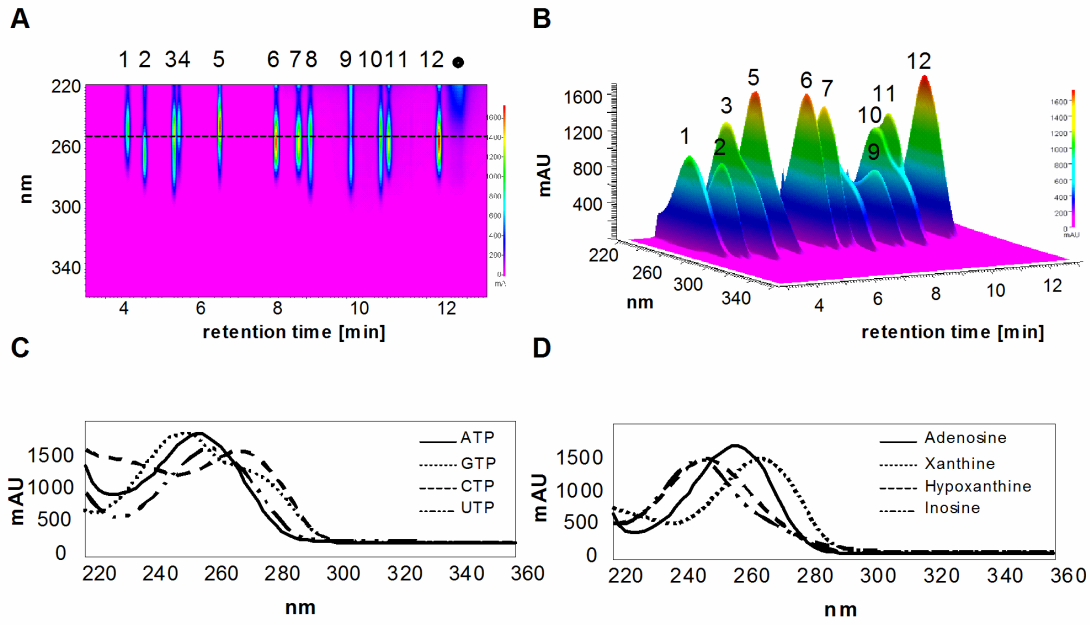

Figure 3.10: Spectral view of HPLC chromatograms obtained from a 100 µM standard mixture. ***A*** *contour graph,* ***B*** *three dimensional graph of all separated standard compounds; Y axis indicates the wavelength (220-360 nm); X axis shows the retention time, Z axis shows the absorbance intensity in milli absorbance units (mAU). The black dotted line in A indicates 254 nm, the wavelength that was used for quantitative analysis of standard and sample compounds. Compounds are numbered as in Figure 1.* ***C****,* ***D*** *UV absorbance spectra (220-360 nm) for* ***C*** *purine nucleotides and* ***D*** *purine nucleosides and free bases; UV absorbance maxima are summarised in Table 3.1.*

3.2.2.1.3 *Limit of detection/quantification*

The limits of detection (LOD, evaluated with a signal to noise ratio > 3) and quantification (LOQ, evaluated with a signal to noise ratio > 10) are summarised in Table 3.1 and shown for AMP in Figure 3.11. The LOD for standard compounds dissolved in deionised water ranged between 0.1-10 pmol, whereas the LOQ ranged between 0.5-10 pmol at 254 nm. The higher LOD and LOQ for GTP, ADP and ATP were due to the baseline peaks shown in Figure 3.8 B, which merged with the standard peaks at concentrations below 500 nM (10 pmol) and thereby made an accurate determination of the analyte peaks unreliable.

The LOQ estimated for sample peaks was between 1 pmol (hypoxanthine, xanthine, IMP, GMP, inosine), 2 pmol (adenosine, AMP, GDP) and 10 pmol (CTP, GTP, ADP, ATP). The smallest amount of standards added to samples, which could be reliably detected by an increase in peak height ranged between 1 – 2 pmol for hypoxanthine, xanthine, IMP, GMP, inosine, adenosine, AMP and GDP. Due to the baseline peaks eluting after 10 minutes (see Figure 3.8 B) and due to the larger size of GTP and ATP peaks in samples (see Figure 3.12), the smallest amount of reliably detectable standards, determined by an increase in the peak area, for CTP, GTP, ADP and ATP was 10 pmol.

3.2.2.1.4 *Linearity*

A linear response, as indicated by correlation coefficients (R^2) in excess of 0.99, was observed for each compound ranging from the LOQ for standard compounds in water to at least 2000 pmol (100 µM). The calibration curves for ATP, ADP, and AMP are shown in Figure 3.11 B and the respective R^2 values for all resolvable standard metabolites are summarised in Table 3.1.

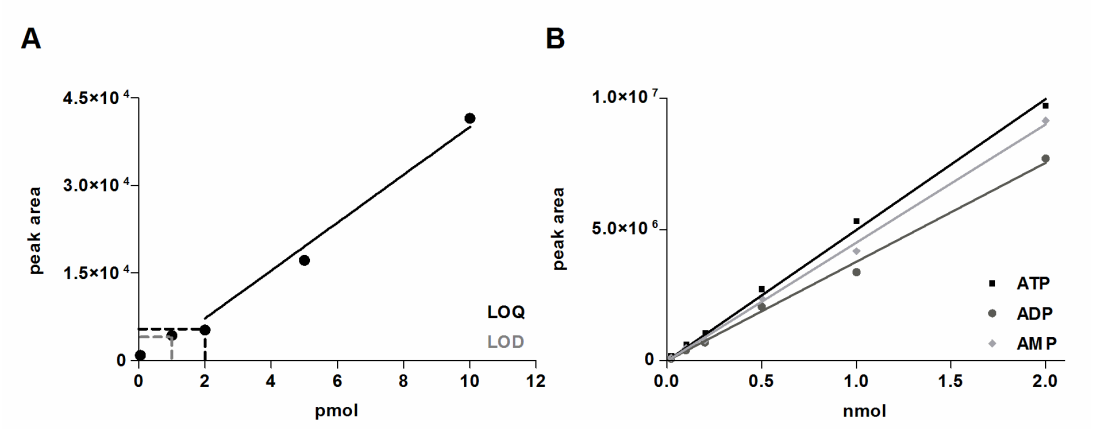

Figure 3.11: Calibration curves for adenine nucleotides. A *limit of detection (LOD; signal to noise ratio > 3) and quantification (LOQ; signal to noise ratio > 10) for AMP* ***B*** *calibration curves for ATP, ADP and AMP (LOQ-2000 pmol).*

3.2.2.1.5 *Recovery of standard compounds after perchloric acid extraction*

Perchloric acid (PCA) is commonly used to precipitate proteins of tissue samples and thereby to extract acid-soluble cell compounds, such as nucleotides, for subsequent analysis. However during the neutralisation process of PCA extracts, ATP can be adsorbed to the perchlorate precipitate (Wiener et al., 1974; Williams and Forrester, 1976). To evaluate to what extent PCA extraction influenced the yield of nucleotides and metabolites, standard compounds were added to half of a brain slice sample, whilst the other half had an equivalent volume of distilled water added. Both samples were subjected to PCA extraction and subsequently neutralised to pH 6 by a threefold organic extraction with tri-*n*-octylamine/trichlorotrifluoroethane.

Since this protocol required the injection of two aliquots from the same brain sample (spiked and unspiked), I needed first to determine the intra-sample variability of these two injections. For two unspiked aliquots of the same brain samples, as treated above, the difference between the two peak areas, expressed as a percentage of the mean peak area, was between 2.1 ± 0.9 % (ATP), 6.8 ± 1.6 (ADP) and 14.4 ± 8.2 (AMP) (N = 4). These values likely overestimate any variability as the percentages do not take into account the size of the peak areas. Thus for smaller peaks (eg AMP), subtle differences between aliquots would have a proportionately larger effect. This

may also explain the reduction in apparent variability as the peaks become larger from ADP to ATP.

Nonetheless, to test whether these values reflected variability in the detection system, I injected sequential aliquots from solutions of standard compounds. This yielded much lower variability: the difference of the peak areas of subsequent injections of 20 μM (400 pmol) ATP, ADP and AMP standards from the mean peak area was 1.3 ± 0.5 %, 1.1 ± 0.4 % and 0.2 ± 0.1 %, respectively (N = 7). Hence, the variability between the peak areas of two aliquots from the same brain slices is not due to poor precision of the system, but more likely reflects subtle differences between the initial aliquots, which involved separating the homogenised tissue in two, a possible source of intra-sample variability. This was only performed during these spiked sample experiments.

I observed that the recovery of all standard compounds in spiked brain samples was between 90 and 109 % of the standard when dissolved in water (Table 3.1). Given the intra-sample variability described above, we assumed a 100 % recovery for all standard metabolites.

Compound	LOD	LOQ	T_R [min]	λ_{max} [nm]	(R^2)	% Recovery after PCA extraction
ATP	500 nM (10 pmol)	500 nM (10 pmol)	11.99	258	0.996	102.8 ± 4.0
ADP	500 nM (10 pmol)	500 nM (10 pmol)	10.6	259	0.996	109.3 ± 7.4
GTP	500 nM (10 pmol)	500 nM (10 pmol)	10.47	252	0.999	95.3 ± 5.7
CTP	100 nM (2 pmol)	500 nM (10 pmol)	9.68	270	0.999	90.9 ± 4.9
GDP	50 nM (1 pmol)	100 nM (2 pmol)	8.65	252	0.998	100.5 ± 2.4
AMP	50 nM (1 pmol)	100 nM (2 pmol)	8.3	259	0.997	99.4 ± 2.5
Adenosine	5 nM (0.1 pmol)	25 nM (0.5 pmol)	7.76	259	0.999	103.8 ± 2.5
Inosine	5 nM (0.1 pmol)	25 nM (0.5 pmol)	6.32	247	0.991	95.8 ± 2.6
IMP	10 nM (0.2 pmol)	100 nM (2 pmol)	5.47	247	0.999	98.1 ± 2.3
GMP	10 nM (0.2 pmol)	50 nM (1 pmol)	5.35	252	0.999	99.4 ± 1.7
Xanthine	10 nM (0.2 pmol)	50 nM (1 pmol)	4.48	267	0.994	103.7 ± 10.1
Hypoxanthine	10 nM (0.2 pmol)	50 nM (1 pmol)	3.9	250	0.999	102.2 ± 5.5

Table 3.1: HPLC Method validation: *Limit of detection (LOD) of standard compounds dissolved in deionised water was classified as the concentration of the analyte 3 times the noise level, limit of quantification (LOQ) was classified as the analyte concentration 10 times the noise level. At 10 min re-equilibration between runs the retention times (R_T) varied by ≤ ± 2.5%. The correlation coefficient values (R^2) for each calibration curve (LOQ-2000 pmol), measured at 254 nm are also indicated. Furthermore the UV absorption maximum (λ_{max}) is given for every compound. Recovery of standard compounds after perchloric acid (PCA) extraction was determined by spiking sample homogenates with various concentrations of standard compounds; all values are presented as means from 3 – 9 determinations.*

3.2.2.1.6 *Analysis of brain slice extracts*

To evaluate whether this HPLC method is suitable for studying the adenine nucleotide levels of biological tissue, I applied it to neutralised PCA extracts of hippocampal brain slices. A representative HPLC chromatogram is shown in Figure 3.12 A, and the contour and three dimensional graphs of the absorbance spectra are shown in Figure 3.12 B and C. The identity of each sample peak was determined by comparison of the retention times with the respective standard compound, by spiking samples with standards, by comparison of the UV spectra with the particular standard compound, and by peak purity analysis, as shown for ATP in Figure 3.12 D. Peak purity analysis showed that sample adenine nucleotides were as pure as standard adenine nucleotides. However, the GTP peak was contaminated due to co-elution with UTP. It is possible that these compounds could be individually resolved by appropriate changes to the buffer gradient profile, but since all adenine nucleotides were clearly separated, this was not pursued.

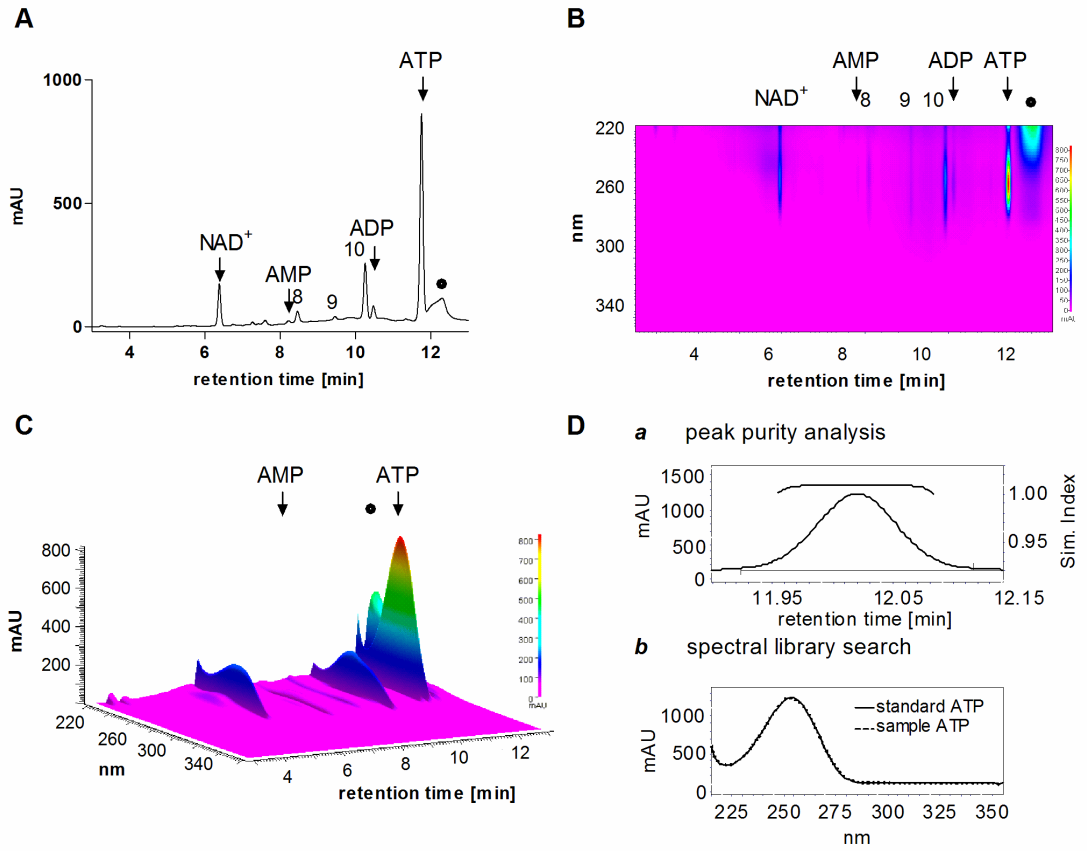

Figure 3.12: Representative HPLC chromatogram from neutralised hippocampal brain slice extracts. *Brain slices were incubated for 3 hours in aCSF at 34°C and nucleotide extraction was performed on fresh tissue without prior freezing in liquid nitrogen.* ***A*** *representative HPLC chromatogram obtained from brain slice extracts at 254 nm.* ***B*** *Respective contour and* ***C*** *three dimensional graph for separated compounds. Numbers on traces refer to the following compounds: 8 GDP 9 CTP 10 GTP/UTP ● ghost peak; mAU milli absorbance units;* ***D*** *Sample ATP peak verification by* ***a*** *peak purity analysis, Sim. Index similarity index = 0.99* ***b*** *spectral library search; sample ATP UV absorbance spectrum was 100% similar to standard ATP absorbance spectrum.*

3.2.2.1.7 *Effect of liquid nitrogen freezing on tissue adenylate levels*

It is often convenient to snap-freeze tissue after the experiment for analysis at a later date. This may be the case when the analysis procedure or HPLC runtime is lengthy, thereby obviating the possibility of running several fresh samples on the day of the experiment. Given the known labile nature of adenine nucleotides and the low energy charge values observed for snap-frozen brain slices after various incubation time points (see Figure 3.7 B), I sought to determine whether snap freezing in liquid nitrogen and/or subsequent extraction results in a change of adenine nucleotide levels. For this purpose brain slices were transferred into ice-cold aCSF. One set of slices was immediately homogenised in PCA, and another set of slices was frozen in liquid nitrogen for 30 - 60 minutes. Frozen slices were powdered under liquid nitrogen and subsequently homogenised in PCA. All neutralised extracts were analysed on the same day of slice preparation.

Representative HPLC chromatograms, adenine nucleotide and EC levels of fresh and liquid nitrogen frozen brain slices are shown in Figure 3.13. EC values from fresh tissue slices, are very high (0.95 ± 0.003; N = 4), indicating that the slices are in good metabolic condition. In contrast, snap-freezing in liquid nitrogen led to significantly higher ADP (1.1 ± 0.2 nmol/mg protein for fresh slices and 2.5 ± 0.3 nmol/mg protein for snap-frozen slices; N = 4; $p < 0.01$; unpaired t-test) and AMP levels (0.2 ± 0.02 nmol/mg protein for fresh slices and 0.5 ± 0.04 nmol/mg protein for snap-frozen slices; N = 4; $p < 0.001$; unpaired t-test), indicating degradation of ATP during the freezing/extraction process. This results in significantly lower EC values (0.95 ± 0.003 for fresh slices and 0.88 ± 0.009 for snap-frozen slices, N = 4; $p < 0.001$, unpaired t-test). However, there was no further degradation of adenine nucleotides in snap frozen slices, since the TAN pool was not significantly different between both groups (15.9 ± 1.4 nmol/mg protein for fresh slices; 14.2 ± 1.4 nmol/mg protein for snap frozen slices, N = 4, $p > 0.05$, unpaired t-test). This degradation of ATP is dependent on the presence of tissue since freezing of standard ATP in liquid nitrogen did not lead to ATP breakdown (data not shown).

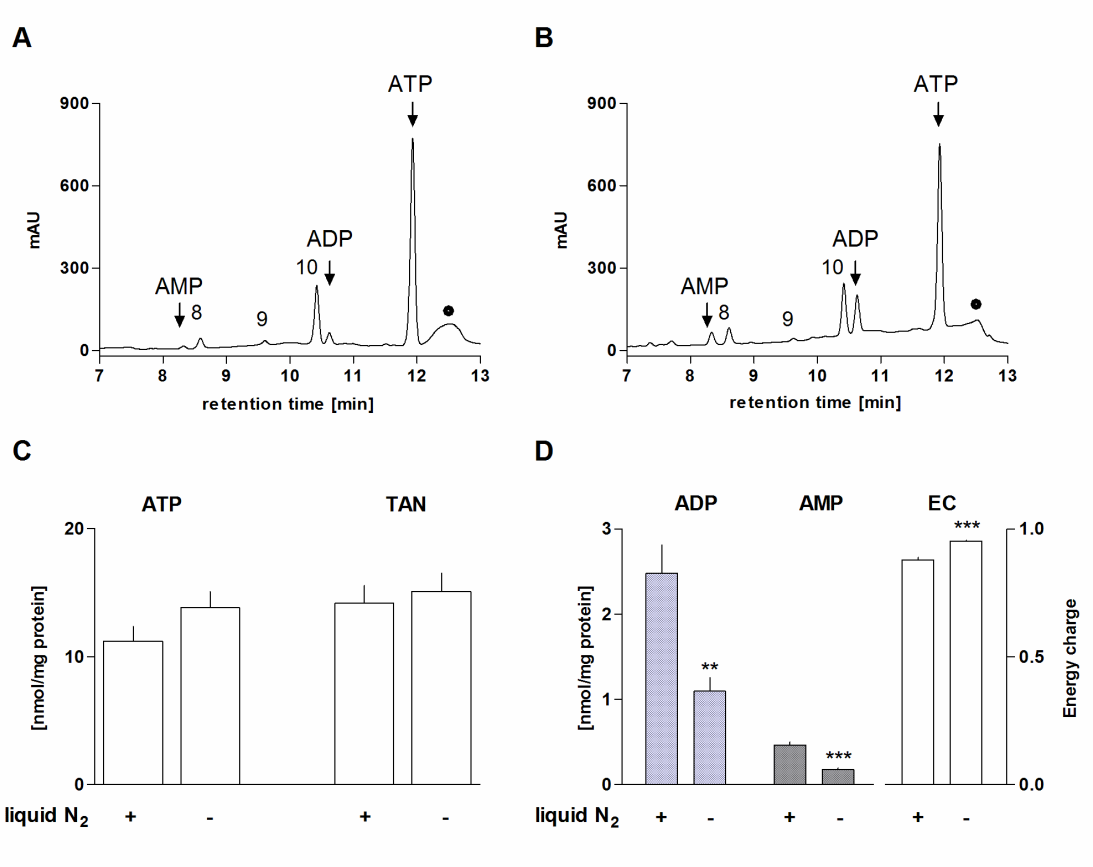

Figure 3.13: Effect of liquid nitrogen freezing on adenine nucleotide levels. *HPLC chromatograms from **A** unfrozen brain slices, **B** frozen slices. Numbers on traces refer to the following compounds: 8 GDP 9 CTP 10 GTP/UTP ● ghost peak. The rising baseline in Figure 5B is due to a short re-equilibration time between runs. **C** ATP and TAN levels, D ADP, AMP and EC values of fresh and liquid nitrogen frozen slices. Values are expressed as mean ± S.E.M., N = 4, (**) p < 0.01, (***) p < 0.001 for AMP and EC, unpaired t-test.*

3.3 Discussion

Since the accurate determination of adenine nucleotides is most significant in the study of energy metabolism, I aimed to develop a fast, high-resolution ion-pair reversed-phase HPLC method that allows the analysis of multiple fresh samples in one day, thereby avoiding freeze-thaw degradation of nucleotides. Reverse phase HPLC methods without ion pairing agents or ion-exchange methods, usually take long runtimes in order to achieve sufficient separation of analytes (Zakaria and Brown, 1981). With the method described here at least 11 different purine compounds can be separated within 13 minutes, with a subsequent 10 minutes re-equilibration time. This method is particularly useful for studying changes in the adenine nucleotide levels associated with experimental manipulations, extraction efficiency or tissue storage. The short time of analysis and the accurate evaluation of the compounds, make this method useful for routine and relatively high throughput use.

The sensitivity, as determined by the LOQ, lies in the range of previously published UV-based HPLC methods (Tomiya et al., 2001; Kochanowski et al., 2006), and calibration curves for standard compounds showed that they were linear over a wide concentration range (LOQ-2000 pmol). Since the signal of each standard compound increases linearly with increasing injection volume (Kochanowski et al., 2006), injecting more than 20 µl on the column may result in even lower LOD and LOQ. Nonetheless, the absolute sensitivity is still lower than fluorescence-based HPLC analysis of adenine nucleotides (Katayama et al., 2001). However, for this method purine compounds of sample extracts have to be etheno-derivatised with chloroacetaldehyde, a process that requires incubation at high temperatures (most commonly 80°C), and limits the analysis to compounds containing an amino group in the purine or pyrimidine ring (such as adenine and cytosine). Furthermore, the derivatisation efficiency of standard ATP is variable and never reached 100 % (Figure 3.2 A). This precludes an accurate determination of the energetic state, due to degradation of ATP during this process and thereby underestimates key parameters such as the energy charge (Figure 3.2 C). Therefore, UV-based HPLC

analysis of adenine nucleotides, although less sensitive, results in a more reliable detection of the *in situ* energetic state.

This method is also suitable for analysis of hippocampal brain slices, which are the main *in vitro* stroke model for this thesis. Tissue nucleotides were extracted with PCA and for neutralisation a threefold organic extraction with tri-*n*-octylamine/trichlorotrifluoroethane was used. It is known that acid extraction and subsequent neutralization can lead to adsorption of ATP to the acid-salt precipitate (Wiener et al., 1974; Williams and Forrester, 1976) and the recovery of ATP has been reported to be between 45 - 96 % (Levitt et al., 1984; Shryock et al., 1986; Au et al., 1989; Kochanowski et al., 2006), depending on the type of extraction and neutralization. In this study there was a complete recovery of standard compounds added to sample extracts. This may be due to the use of tri-n-octylamine/trichlorotrifluoroethane since it has been reported that the neutralisation of PCA with tri-n-octylamine/trichlorotrifluoroethane can result in a better recovery of nucleotides than, for example, precipitation as $KClO_4$ (Brown et al., 1982). The additional advantages of using tri-*n*-octylamine/trichlorotrifluoroethane for neutralisation of acid extracts have been pointed out previously (Pogolotti and Santi, 1982). Most importantly this method does not introduce additional salts into the extracts, which could interfere with HPLC separations. Furthermore, there is no possibility of making the solution too alkaline. In fact the threefold organic extraction used in this study always resulted in a pH of 6, which allowed the best separation of all sample/standard compounds in the method described here, since the buffers used had the same pH.

HPLC chromatograms obtained from hippocampal brain slice extracts showed that all purine nucleotide compounds were clearly separated. Peak purity analysis and UV absorbance spectra comparisons further established the nature of the specific sample compounds. Including the time for slice preparation (30 minutes), slice incubation (3 hours), extraction for tissue nucleotides (30 minutes) and washing of the column after use (50 minutes), at least 10 sample extracts could be analysed in one day.

An interesting observation of this study is that freezing the brain tissue in liquid nitrogen and/or subsequent extraction can result in a significant change of adenine nucleotide levels. This has implications for the storage of tissue, especially if it is to be used for metabolic studies and might explain the low EC values of brain slices obtained after 3 - 4 weeks storage at -80°C (Figure 3.7).

Due to the high activities of ATPases in fresh samples, changes in the adenine nucleotide levels take place very quickly when ATPase enzymes are not inactivated immediately. Snap-freezing of tissues in liquid nitrogen is a simple and widely used way to instantly stop any enzymatic activities and to store the sample for subsequent extraction. However the maintenance of freezing conditions during the nucleotide extraction procedure is critical, since thawing of the tissue will result in a recovery of enzymatic activities and potential degradation of ATP. Although samples in this report were kept and powdered in liquid nitrogen, there was a significant change in adenine nucleotide levels. This resulted in significantly lower EC values compared to fresh sample extracts (Figure 3.13), and is potentially responsible for the even lower observed EC values after longer storage conditions (Figure 3.7 B). Freezing of standard ATP in liquid nitrogen did not lead to a degradation of ATP. Furthermore it is unlikely that snap freezing is not quick enough to stop enzymatic degradation of ATP or that enzymatic activities recover at such low temperatures. Since brain slices were powdered under liquid nitrogen the degradation of ATP most likely occurs during the homogenisation procedure. The tissue powder might thaw and therefore ATPase activities might recover before proteins are effectively precipitated with PCA.

Since tissue is frequently frozen in liquid nitrogen and stored at -80 to -20°C for subsequent extraction and HPLC analysis, assumptions about the EC have to be made very carefully, as they might not reflect the *in situ* values. Hence, transferring tissue slices into ice-cold aCSF and performing the PCA extraction immediately leads to a more reliable evaluation of adenine nucleotide levels.

In summary I report a method which is suitable for the detailed analysis of tissue adenine nucleotide levels and, due to its rapidity, allows within-day sample analysis.

This helps to bypass the problem of freeze/thaw degradation of adenine nucleotides, and results in an accurate determination of the tissue energy charge.

The development of this method (Zur Nedden et al., 2009) further allowed me to study the basal energetic state of brain slices under control conditions in Chapter 4 and the effects of various interventions of the purine salvage pathway before during and after OGD in subsequent chapters.

4 Metabolic recovery of hippocampal brain slices after preparation

4.1 Introduction

The use of brain slices has revolutionised the study of the mammalian central nervous system and has now become a standard preparation in many laboratories and in many areas of neuroscience. Their versatility lends them to many types of investigation into the genomic, proteomic, molecular and cellular properties of the brain. A major advantage of brain slices is that they can be used for combined functional, metabolic, morphological and pharmacological experiments with maximal control over the extracellular environment and greater experimental access. Hippocampal brain slices are particularly widely used for studies into the fundamental properties of synaptic transmission and plasticity. Furthermore, given the vulnerability of the mammalian hippocampus to a wide variety of insults, including stroke, they are a common *in vitro* model system for the study of cerebral ischemia (Whittingham et al., 1984a; Schurr et al., 1989; Schurr et al., 1999; Kreisman et al., 2000) and for the assessment and screening of the efficacy of putative neuroprotectants (Galeffi et al., 2000).

Notwithstanding the value of brain slices it is an unavoidable fact that the preparation of brain slices is associated with ischemia (decapitation) and tissue trauma (dissection/slice cutting) and thereby results in a substantially compromised energetic state of the tissue at time of cutting (Fredholm et al., 1984; Whittingham et al., 1984b). However, as described as far back as the 1950s (McIlwain et al., 1951; McIlwain, 1952), brain slices show remarkable metabolic recovery after preparation and it is now common practise to allow a period of incubation (usually 1 hour) before they can be used for experiments. Although every *in vitro* model system is a naturally simplified representation of the *in vivo* situation, it should strive to approach the *in vivo* condition as closely as possible, in particular with respect to the specific problem of interest. For "*in vitro* ischemia" studies the energetic state of the tissue is of special importance. The fact that control conditions in hippocampal slices might represent a post-ischemic recovery state (Hossmann, 2008), and the fact that high energy phosphate levels (ATP, phosphocreatine) of brain slices have traditionally been registered as lower than their *in situ* values (Thomas, 1957;

Whittingham et al., 1984a; Schurr and Rigor, 1989), are strong arguments against their usefulness as *in vitro* models for ischemia studies. However, as brain slice preparations have an irreplaceable role for the investigation and separation of the many variables that interact in the *in vivo* situation a balance has to be struck that at least includes some key parameters approaching the *in vivo* condition.

Since hippocampal brain slices will be the main *in vitro* model for ischemia studies in this thesis the aims of this chapter were to study the metabolic recovery after slice preparation and to determine the best incubation conditions in order to approach the *in vivo* situation as closely as possible. This was achieved by (1) establishing the influence of the incubation temperature on the recovery of adenine nucleotides and energetic parameters, including the activity of AMP activated protein kinase (AMPK), an enzyme exquisitely sensitive to the cellular ATP/AMP ratio; and (2) separating and investigating the potential causes for the reduced ATP content of brain slices compared to the values reported *in vivo.* Through this we have added more information to existing work in this field about the recovery and stability of adenine nucleotides after slice cutting (Zur Nedden et al., 2011).

4.2 Materials and methods

4.2.1 Preparation of brain slices

Rat brain slices were prepared as described in the Methods section (Chapter 2, Section 2.2) and were either analysed immediately upon cutting for their purine nucleotide content or transferred to an incubation chamber with continuously circulating, oxygenated standard aCSF, at room temperature (RT; 22 ± 0.5°C) or 34 ± 1°C.

In a separate set of experiments nucleotide concentrations of 1) the intact hippocampus and cortex, and 2) slices of varying thickness were analysed. For this purpose one hemisphere was used to dissect and separate hippocampus and cortex,

and the other hemisphere was used to cut slices of varying thickness (200 µm – 3600 µm). Since with the microtome used no slices over 1500 µm could be cut automatically, 3600 µm had to be measured with a guide. For these experiments all nucleotide extractions of were performed immediately after preparation.

4.1.1 Nucleotide extraction

Nucleotide extraction was performed as described in Chapter 2, section 2.5.1. For analysis of the TAN content of whole hippocampus and neocortex, and 1200, 1500 and 3600 µm slices, the tissue was first homogenized in 500 µl 5% PCA. The amount of this suspension containing 20 mg wet weight (equivalent to four 200 µm, two 400 µm, or one 800 µm slice) of the tissue was mixed with 5 % PCA to a final volume of 1 ml and neutralized as described above.

4.2.2 Kinase assays

Kinase assays of brain slice protein extracts were performed by Simon Hawley and Grahame Hardie at the University of Dundee. AMPK from extracts was immunoprecipitated with a mixture of α1 and α2 antibodies and AMPK activity in the immunoprecipitates was determined using the AMARA peptide assay as described in (Hardie et al., 2000; Gadalla et al., 2004). The enzyme activity is expressed as units (U)/ mg protein. 1 U is the amount of enzyme that catalyses the conversion of 1 µmol substrate/min.

4.2.3 Western blot analysis

Western blot analysis of brain slice protein extracts was performed by Simon Hawley and Grahame Hardie at the University of Dundee. The detection of dual-labelled western blots by infrared imaging was carried out as previously described (Hawley et al., 2003), except that in the present study the phosphorylation state of the native full length protein was determined.

4.3 Results

4.3.1 Metabolic recovery of hippocampal brain slices after preparation

4.3.1.1 Recovery of adenine nucleotides

To study the recovery of adenine nucleotides after slice preparation, HPLC analysis of slice extracts was performed on fresh slices immediately after cutting and after various incubation time points in aCSF (10 min - 5 h) at room temperature (22°C) and 34°C (Figure 4.1 A).

Immediately after cutting ATP, ADP and AMP were present in nearly equal amounts (6.0 ± 0.3, 4.0 ± 0.4 and 5.2 ± 0.8 nmol/mg protein, respectively; N = 7; Figure 4.1 B-D). ATP levels significantly increased after only 10 min incubation (10.7 ± 1.0 and 11.0 ± 0.9 nmol/mg protein at 22°C and 34°C, respectively; N = 7; $p < 0.001$, one way ANOVA) with a concomitant decrease of ADP (1.9 ± 0.3 and 1.5 ± 0.1 nmol/mg protein at 22°C and 34ºC, respectively; N = 7; $p < 0.001$, one way ANOVA) and AMP levels (1.1 ± 0.3 and 0.5 ± 0.1 nmol/mg protein at 22°C and 34ºC respectively; N = 7; $p < 0.001$, one way ANOVA).

After the initial recovery, ATP, ADP and AMP levels did not significantly change during the incubation time points tested (up to 5 h incubation) and there were no significant differences between adenine nucleotides of slices kept at 22°C and 34°C (Figure 4.1 B-D). As a consequence of these complementary changes in individual nucleotides, the total adenine nucleotide pool (TAN = [ATP] + [ADP] + [AMP]; Figure 4.1 E) did not significantly change when slices were transferred from the ice-cold cutting solution (15.2 ± 1.1 nmol/mg protein; N = 7) into aCSF at 22°C (13.7 ± 1.4 nmol/mg protein; N = 7) or 34°C (13.0 ± 1.1 nmol/mg protein; N = 7), suggesting that most of the accumulated AMP is rephosphorylated to ATP rather then dephosphorylated to adenosine (via cytosolic 5'-nucleotidase) or deaminated to IMP (via AMP deaminase).

The TAN pool remained stable over an incubation period of 5 h. Average TAN concentrations from all time points tested (10 min – 5 h) were 14.1 ± 0.3 nmol/mg protein in slices at 22°C and 15.4 ± 0.9 in slices at 34°C, with ATP accounting for about 85 % and 89 %, respectively.

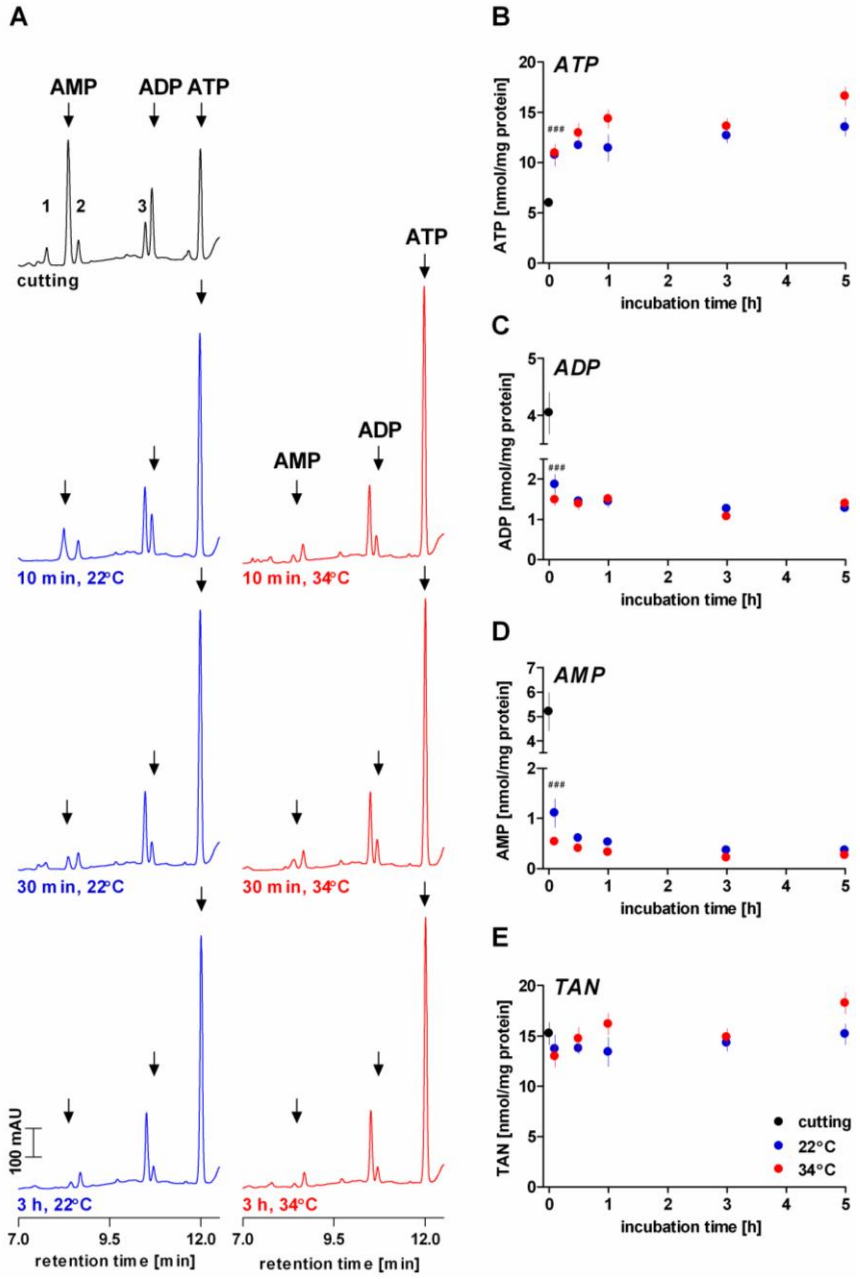

Figure 4.1: Rapid recovery of adenine nucleotides after slice preparation. A *Representative HPLC traces obtained from brain slices after slice cutting (black trace) and various incubation times in aCSF at room temperature (22ºC, blue traces) and 34ºC (red traces). Note the consistently higher AMP levels in slices incubated at 22ºC. Numbers on traces refer to the following compounds: 1 adenosine 2 GDP 3 GTP/UTP; arrowheads indicate, from left to right, AMP, ADP and ATP; mAU milli absorbance units.* ***B-E*** *Recovery of* ***B*** *ATP,* ***C*** *ADP,* ***D****, AMP and* ***E*** *total adenine nucleotides (TAN = [ATP]+[ADP]+[AMP]) from time of cutting (black circles, time zero) and various incubation times (0.1 – 5 h) in aCSF at 22ºC (blue circles) or 34ºC (red circles). Values are expressed as mean ± S.E.M, N = 5 – 7; (###) p < 0.001 for slices at 22°C and 34°C compared to time of cutting, one way ANOVA with Bonferroni's multiple comparison test. Where no error bars can be seen they are smaller than the symbol.*

4.3.1.2 Recovery of energetic parameters

The energetic state of a tissue is commonly reported as the ratio of adenine nucleotides, since this reflects the energy supply (ATP) to demand (ADP, AMP) relationship better than their individual concentrations. Additionally to the EC, another sensitive parameter of the energetic state is the ATP/AMP ratio. This ratio is predominantly controlled by adenylate kinase (see Chapter 1, section 1.4.1.1), which catalyses the reversible reaction $2ADP \leftrightarrow ATP + AMP$. As it works at equilibrium it is mainly regulated by the availability of ADP and AMP, thereby generating ATP and AMP, as soon as ADP levels rise via increased metabolic activity or inadequate energy supply (Hardie and Hawley, 2001).

Due to the nearly equal amounts of ATP, ADP and AMP at the time of cutting, the EC was very low (0.54 ± 0.03; N = 7; Figure 4.2 A), but it recovered significantly after only 10 min incubation at 22°C (0.86 ± 0.019, N = 7, $p < 0.001$, one way ANOVA) and 34°C (0.90 ± 0.007, N = 7; $p < 0.001$, one way ANOVA). After 3 h the EC stabilized at 0.93 ± 0.003 for slices kept at 22°C and at 0.95 ± 0.002 for slices kept at 34°C and, as for adenine nucleotides, there were no significant differences between slices incubated at 22°C and 34°C.

The ATP/AMP ratio significantly recovered from time of cutting (1.4 ± 0.4; N = 7; Figure 4.2 B) after only 10 min in slices at 34°C (22.9 ± 2.7; N = 7; $p < 0.001$; one way ANOVA) whereas it took approximately 30 min to recover in slices incubated at 22°C (20.1 ± 1.8; N = 6; $p < 0.001$; one way ANOVA). Similar to the EC, the ATP/AMP ratio stabilized after 3 h, but with considerable differences between slices incubated at 22°C and at 34°C. At 22°C the ATP/AMP ratio ranged between 35.2 - 38.0, whilst at 34°C the ATP/AMP ratio was much higher at between 63.5 - 64.2. The differences in the ATP/AMP ratio values between the two incubation temperatures became statistically significant after 30 min (N = 6 - 8; $p < 0.01$; one way ANOVA) and remained statistically significant for the rest of the incubation period (N = 5 - 8; $p < 0.001$; one way ANOVA).

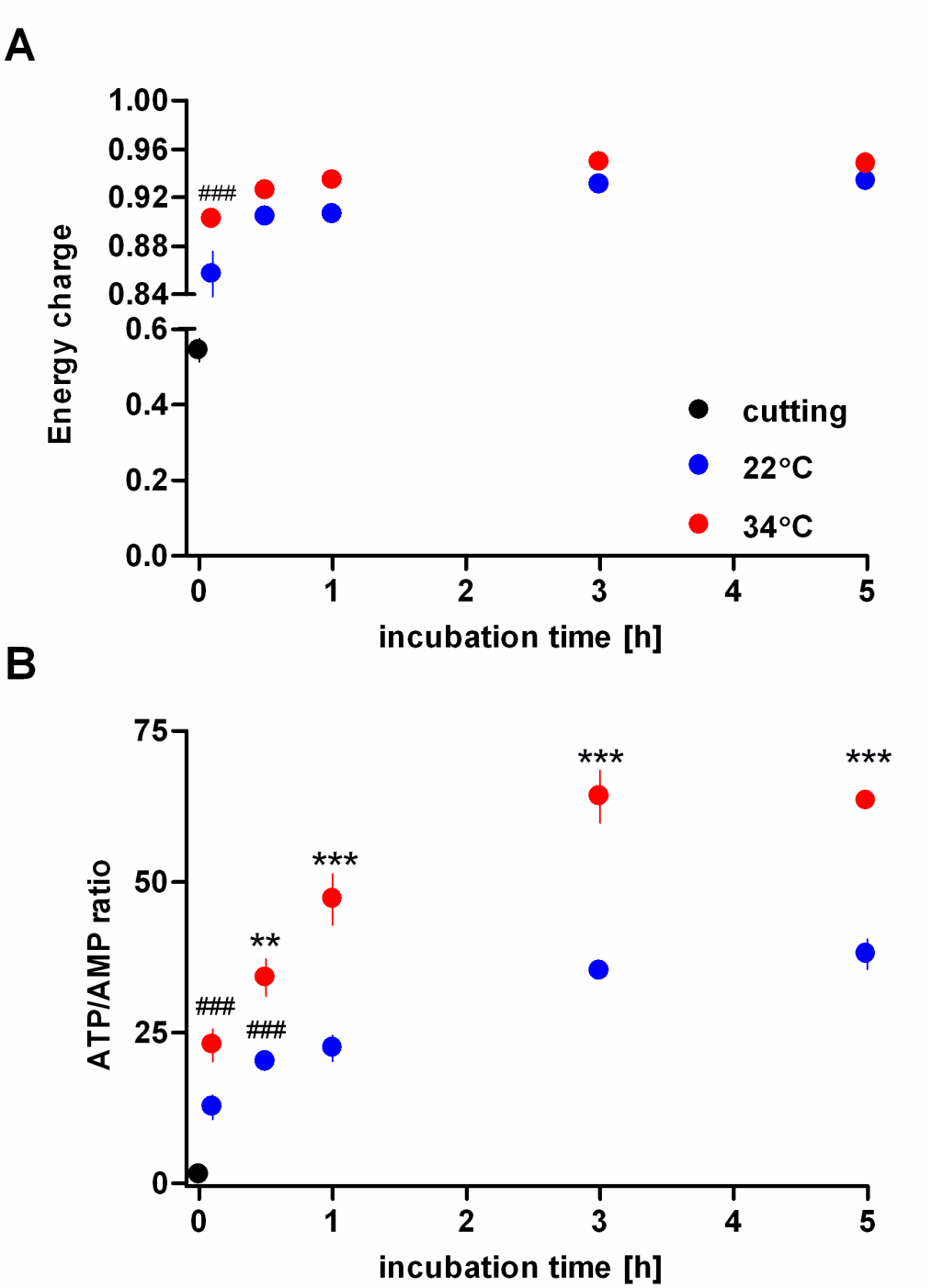

Figure 4.2: Differential influence of temperature on the recovery of energetic parameters after slice cutting. ***A*** *Recovery of the tissue energy charge ((ATP + 0.5ADP)/TAN) is not influenced by temperature, whereas* ***B*** *the ATP/AMP ratio is significantly higher at elevated temperature (N = 5 – 7). All values are expressed as mean ± S.E.M. (###) p < 0.001 for slices at 22°C and 34°C compared to time of cutting; (**) p < 0.01, (***) p < 0.001 compared between slices at 22°C and 34°C, one way ANOVA with Bonferroni's multiple comparison test. Where no error bars can be seen they are smaller than the symbol.*

4.3.1.3 Recovery of AMPK activity

Since the cellular ATP/AMP ratio is monitored by AMP-activated protein kinase (AMPK), a main sensor and regulator of cellular energy metabolism (Hardie and Hawley, 2001; Hardie, 2007) I further investigated whether the lower ATP/AMP ratio in slices at 22°C is reflected by a higher AMPK activity.

Kinase assays and western blot analysis of AMPK activity and phosphorylation status supported this assumption. The AMPK activity (Figure 4.3 A) decreased from 0.066 ± 0.003 U/mg protein at time of cutting to 0.04 ± 0.001 U/mg protein after 30 min at 22°C (1.6 fold decrease; N = 3; $p < 0.001$, one way ANOVA), by which time at 34°C AMPK activity had fallen 3.4-fold (N = 2). After 3 h AMPK was 3 times more active in slices at 22°C (0.03 ± 0.003 U/mg protein, N = 3) than in slices at 34°C (0.01 ± 0.001 U/mg protein; N = 3; $p < 0.001$, one way ANOVA).

Western blot analysis of the phosphorylation status of AMPK and one of its downstream targets, acetyl-CoA carboxylase (ACC), was performed to further support these findings and to evaluate whether a higher AMPK activity is reflected in a higher phosphorylation of its substrates (Figure 4.3 BC). ACC-1 catalyses the first step of fatty acid synthesis, whereas ACC-2 inhibits fatty acid oxidation. Both isoforms are phosphorylated, and thereby inactivated by AMPK, resulting in inhibition of fatty acid synthesis and activation of fatty acid oxidation, respectively (Hardie and Pan, 2002). The phospho-AMPK/total-AMPK ratio decreased from 2.8 at time of cutting to 1.9 in slices at 22°C and to 1.1 in slices at 34°C after 3 h incubation (N = 2, Figure 4.3 C). Likewise the phospho-ACC/total-ACC ratio decreased from 1.6 at time of cutting to 1.0 in slices at 22°C and to 0.5 in slices at 34°C after 3 h incubation.

These observations suggest that despite similarities between TAN pools and EC values between slices incubated at room temperature and more physiological temperatures, the ATP/AMP ratio can influence the activity of key intracellular enzymes with potentially important consequences for neuronal and glial properties.

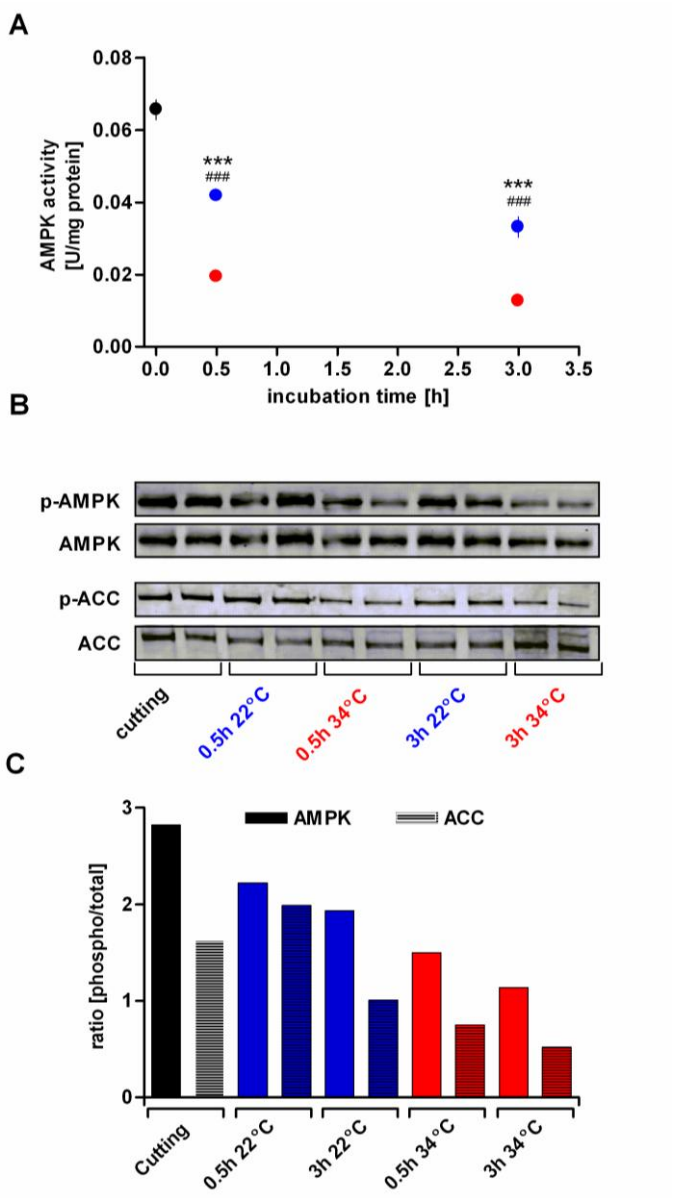

Figure 4.3: Differential influence of temperature on the recovery of AMPK activity after slice cutting. ***A*** *AMPK activity in brain slices, as measured by pseudo-substrate phosphorylation, is lower at higher incubation temperature reflecting the higher ATP/AMP ratio (N = 3 except for 0.5 hr, 34°C, N = 2). Black circles: slices at time of cutting (time zero); blue circles: slices incubated in aCSF at room temperature (22°C); red circles: slices incubated in aCSF at 34°C; All values are expressed as mean ± S.E.M. (###) p < 0.001 for slices at 22°C and 34°C compared to time of cutting; (**) p < 0.01, (***) p < 0.001 compared between slices at 22°C and 34°C, one way ANOVA with Bonferroni's multiple comparison test. Where no error bars can be seen they are smaller than the symbol.* ***B*** *Confirmation of increased AMPK activity through western blot analysis of increased phosphorylation of AMPK (p-AMPK) and a downstream target, Acetyl CoA carboxylase (p-ACC) in two separate sets of slices. Also shown is total AMPK and ACC at different durations and temperature of incubation.* ***C*** *Mean ratio of phospho-AMPK/ACC to total AMPK/ACC signal of two separate sets of slices.*

4.3.2 Basis of reduced TAN concentration in slices

Although EC values of brain slices reported here (Figure 4.2 A) show that slices are in a very good metabolic condition, and comparable to those reported *in vivo* (see Appendix 3, Table 12.1), absolute TAN levels (Figure 4.1 E) are about 60 - 40 % lower than published *in vivo* values, which are typically around 33.6 ± 4.7 nmol/mg protein (arithmetic mean ± SD of all published data in Appendix 3 Table 12.1). However, there is considerable variability in published TAN levels for the rat brain *in vivo* ranging from 27 – 44.5 nmol/mg protein with most values below the arithmetic mean (Figure 4.4). This variability most likely reflects different extraction and/or detection methods rather than differences in the *in situ* TAN levels.

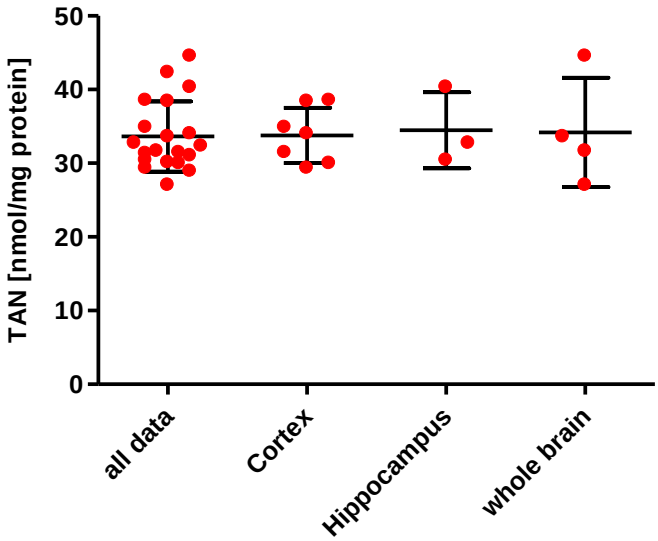

Figure 4.4: *Scatter plot for reported TAN values from Appendix 3 Table 12.1. Data is presented as individual values (red circles) and in black the mean ± SD for either all values (all data), values reported for cortex, hippocampus or the whole brain.*

Despite this, published ATP and TAN values for rat brain *in vitro* (Appendix 3 Table 12.2), including my own results, clearly show that brain slices have lower ATP and TAN levels. This raises questions as to the basis of this discrepancy and the nature of the adenine nucleotide loss in brain slices.

In this study the loss of adenine nucleotides occurred either before or during slice preparation, since TAN levels were already ~ 55 % (~ 18.4 nmol/mg protein) lower at the time of cutting than published *in vivo* studies. There are several possible explanations underlying this observation. (1) The ischemic period leads to accumulation and subsequent loss of diffusible ATP degradation products, thereby resulting in a reduced TAN pool. (2) The tissue might suffer from physical damage, during decapitation, dissection and slicing, thereby resulting in further metabolic stress. (3) The slicing procedure leaves a layer of damaged and dead tissue on each side of the slice (35 - 50 µm) (Feig and Lipton, 1990; Siklos et al., 1997; Frenguelli et al., 2003), which might not contain adenine nucleotides, but which will contribute to the protein content of the tissue. Therefore, by relating the observed nucleotide levels to the total protein content of the tissue one would underestimate the amount of cellular nucleotides in the viable core of the slice. I investigated each of these parameters in turn.

4.3.2.1 The ischemic period leads to loss of diffusible ATP degradation products

As regards the loss of diffusible ATP metabolites, the sum of ATP degradation metabolites (adenosine, inosine, hypoxanthine, xanthine, IMP) at time of cutting is approximately ~ 5 nmol/mg protein (Table 4.1). Like ADP and AMP levels, these metabolites declined during the first 10 - 30 min of incubation, but since no similar rise in the TAN pool was observed, they are likely to be mostly lost from the tissue, rather than being incorporated into the adenine nucleotide pool, and thereby contribute to the reduced adenine nucleotide content of brain slices.

time [min]	Adenosine [nmol/mg protein]		Inosine [nmol/mg protein]		Hypoxanthine [nmol/mg protein]	
	22°C	**34°C**	**22°C**	**34°C**	**22°C**	**34°C**
cutting	0.6±0.2		0.7±0.4		0.63±0.17	
10	0.28±0.15	0.17±0.08	0.32±0.1	0.05±0.01	0.34±0.19	0.16±0.08$^{\#\#}$
30	0.21±0.18	0.16±0.12	0.19±0.02	0.09±0.04	0.12±0.02$^{\#\#\#}$	0.05±0.01
60	0.13±0.09$^{\#}$	0.05±0.01$^{\#}$	0.08±0.02$^{\#}$	0.04±0.02$^{\#}$	0.07±0.02	0.05±0.01
180	0.04±0.01	0.05±0.01	0.08±0.02	0.10±0.01	0.09±0.01	0.14±0.09
300	0.10±0.06	0.10±0.05	0.04±0.03	0.20±0.09	0.04±0.01	0.07±0.02

time [min]	IMP [nmol/mg protein]		Xanthine [nmol/mg protein]	
	22°C	**34°C**	**22°C**	**34°C**
cutting	2.5±0.3		0.7±0.2	
10	2.13±0.43	0.74±0.17$^{\#\#\#,***}$	0.14±0.05$^{\#\#}$	0.14±0.01$^{\#\#}$
30	0.89±0.08$^{\#\#\#}$	0.40±0.06	0.12±0.02	0.09±0.04
60	0.55±0.09	0.23±0.01	0.07±0.02	0.06±0.03
180	0.30±0.04	0.16±0.03	0.15±0.05	0.11±0.03
300	0.28±0.03	0.33±0.07	0.09±0.03	0.23±0.11

Table 4.1: Recovery of purine nucleosides, bases and inosine monophosphate (IMP) after slice cutting in slices incubated at 22°C or 34°C. *All values are presented as mean ± S.E.M.; N = 4 - 7; ($^{\#\#\#}$) p < 0.001; ($^{\#\#}$) p < 0.01; ($^{\#}$) p < 0.05 compared to slices after cutting; (***) p < 0.001 between slices at different temperatures, one way ANOVA with Bonferroni's multiple comparisons test.*

4.3.2.2 The tissue suffers from physical damage causing additional loss of adenine nucleotides

To establish if the additional dissection of tissue associated with slicing caused further loss of adenine nucleotides, I determined the TAN content immediately after decapitation/dissection in entire hippocampus and cortex (since slices in this study were composed of hippocampus and overlaying neocortex). The TAN content of intact hippocampal and cortical tissue was higher than that in combined hippocampal/neocortical slices at 23.0 ± 2.1 and 28.9 ± 2.9 nmol/mg protein, respectively (Figure 4.5 A, N = 5; p > 0.05 between hippocampal and cortical tissue,

unpaired t-test). The value for cortex is close to that reported *in vivo* (33.6 ± 4.7 nmol/mg protein; Figure 4.5 A), but TAN levels in the hippocampus are somewhat lower than those reported *in vivo*. This suggests that the ischemic period during decapitation results in a loss of adenine nucleotides, especially in hippocampal tissue (~ 10 nmol/mg protein, ~ 29 %), which additionally requires more physical and potentially traumatic dissection for removal. The differences between TAN levels in hippocampal and cortical tissue may also be due to the fact that the cortex undergoes more rapid cooling when the whole brain is dropped into ice cold aCSF.

To analyse whether the difference in TAN levels between cortex and hippocampus can also be seen in slices, I separated neocortical/hippocampal slices after cutting into hippocampus and cortex and analysed them immediately for their TAN content (Figure 4.5 A). I observed the same pattern as for the whole tissue: the TAN levels of hippocampal slices were significantly lower than the TAN levels of cortical slices (16.4 ± 1.1 nmol/mg protein and 20.7 ± 0.7 nmol/mg protein, respectively, N = 3, $p < 0.05$, unpaired t-test). However, these values were about 28 % lower than the respective whole tissue values reported above (~ 8.2 nmol/mg protein for cortical tissue and ~ 6.6 nmol/mg protein for hippocampal tissue), and about 38 (cortex, ~ 12.9 nmol/mg protein) – 50 % (hippocampus, ~ 17.5 nmol/mg protein) lower than reported *in vivo* values (33.6 ± 4.7 nmol/mg protein as shown by the grey area for the mean ± SD in Figure 4.5 A). This additional difference might be either caused by ongoing ischemia and/or physical damage during slice preparation, or by the protein content of dead slice edges, which might distort the calculation of metabolite levels in the viable core of the tissue.

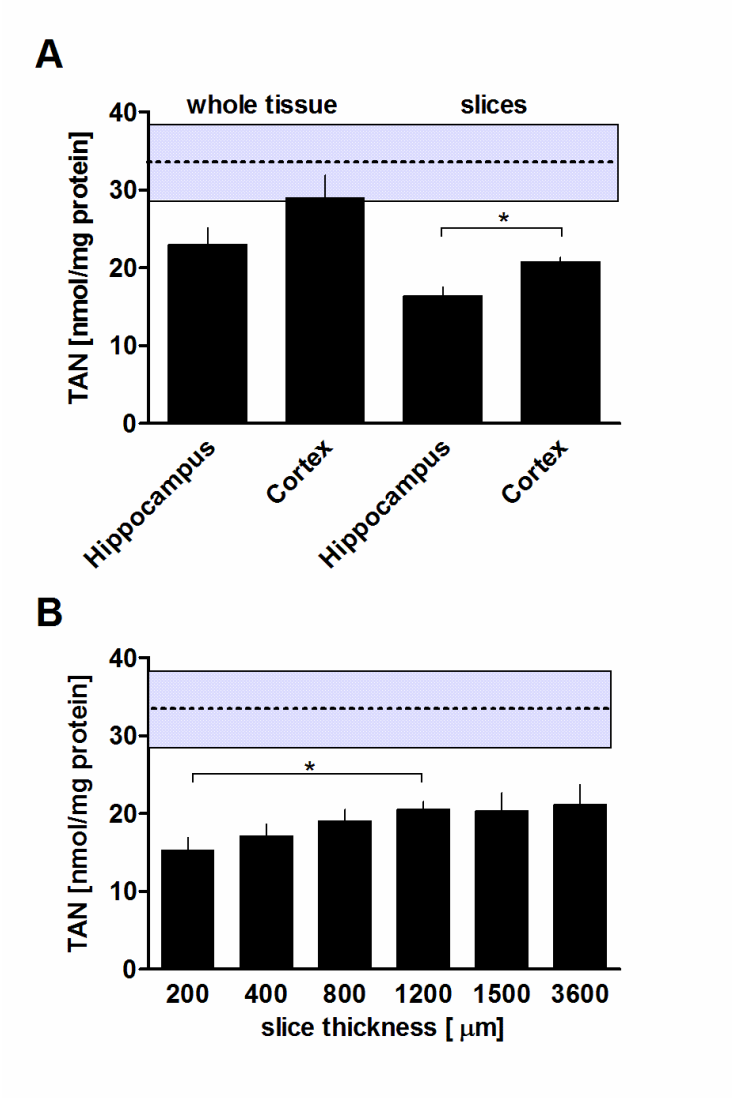

Figure 4.5: Tissue thickness and handling influences calculation of adenine nucleotide content of brain tissue. ***A*** *Total adenine nucleotide (TAN) content of whole hippocampus (N = 5) and cortex (N = 5), immediately after dissection, and hippocampal (N = 3) and neocortical slices (N = 3) immediately after cutting. Note that whole tissue TAN levels of hippocampus are lower than reported in vivo values (grey area represents the arithmetic mean ± SD for all reported values from Appendix 3 Table 12.1), possibly reflecting increased handling/trauma, with only whole cortex approaching in vivo values. Slices of these regions show the same pattern, but have substantially lower TAN levels than the in vivo brain.* ***B*** *TAN levels of neocortical/hippocampal slices of varying thickness (200, 400, 800, 1200, 1500, 3600 μm) immediately after cutting. All values are presented as mean ± S.E.M.; N = 3 – 8. (*) p < 0.05, unpaired t-test.*

4.3.2.3 The dead layer on slice surfaces distorts adenine nucleotide measurements

To test the latter hypothesis, I prepared neocortical/hippocampal slices of different thickness, thereby changing the ratio of dead to viable tissue. As there were no significant changes in the TAN levels between slice cutting and 5 h incubation (Figure 4.1 E) and in order to bypass the problem of a possible emerging ischemic core in very thick slices, the analysis was performed immediately after cutting.

Interestingly, the TAN content of slices, relative to the amount of protein, increased approximately 26 % with increasing thickness from 15.2 ± 1.7 nmol/mg protein in a 200 µm slice to 20.6 ± 1.0 nmol/mg protein in a 1200 µm slice (Figure 4.5 B, N = 5 - 8, $p < 0.05$, unpaired t-test). There was no further increase in the TAN levels in 1500 µm slices (20.3 ± 2.3 nmol/mg protein, N = 4) and I obtained a value of 21.1 ± 2.6 nmol/mg protein (N = 3) for 3600 µm slices.

To better understand the dependence of TAN content on slice thickness, Professor Nicholas Dale assisted in the formulation of a mathematical model for the relation between slice thickness and TAN levels. In this method the assumption is made that the TAN is proportional to the volume of the tissue (l^3) as defined by a unit of length l (Figure 4.6). If in a slice there is a layer of dead tissue devoid of adenine nucleotides at either face of the slice of thickness d then the volume of tissue contributing to the TAN is $l^2(l-d)$. I further assumed that d is constant and does not depend on slice thickness and expressed d as a proportion of l ($d = \alpha l$). The volume of tissue contributing to the TAN is thus $l^3(1 - \alpha)$. If a unit of volume is considered (i.e. $l=1$), then a plot of $1-\alpha$ against the normalized TAN for different slice thicknesses, assuming constant d, should fit the observed data and provide a theoretical estimate of the dead layer of tissue at either face of the slice.

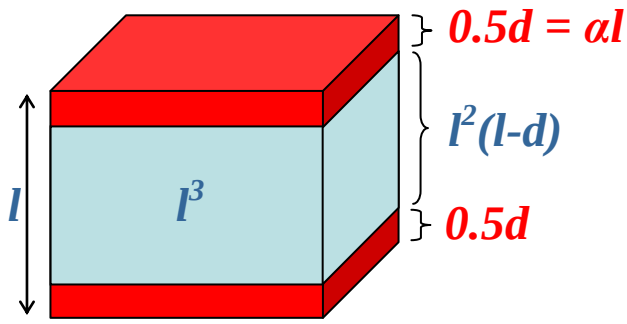

Figure 4.6: Illustration of the development of mathematical model describing the volume of the tissue contributing to the TAN levels*: **l** length; **l^3** total volume of the tissue, **d** thickness of the dead tissue layer, **$l^2(l-d)$** volume of the tissue contributing to the TAN level; **α** constant describing the thickness of d as a proportion of l.*

In Figure 4.7 AB I have plotted theoretical curves for the relative contribution of a dead tissue layer (*d*) of 20 µm (40 µm in total), 35 µm (70 µm in total) and 50 µm (100 µm in total) on both slice edges to the total tissue thickness (*l*, from 100 to 3600 µm slices in 20 µm steps). By normalizing the measured TAN values in Figure 4.5 B to the TAN value obtained for 3600 µm slices (21.1 nmol/mg protein) and plotting it on the same graph, I observed a very good fit of these measured values to the theoretical curve obtained for an estimated total dead cut edge layers of 70 µm, or 35 µm for each edge (Figure 4.7, black dotted line). Based on histological assessment of 400 µm slices an estimate of 35 µm of the dead slice layer has been reported previously (Frenguelli et al., 2003), revealing a remarkable degree of consistency between this experimental observation and the theoretical model, described here.

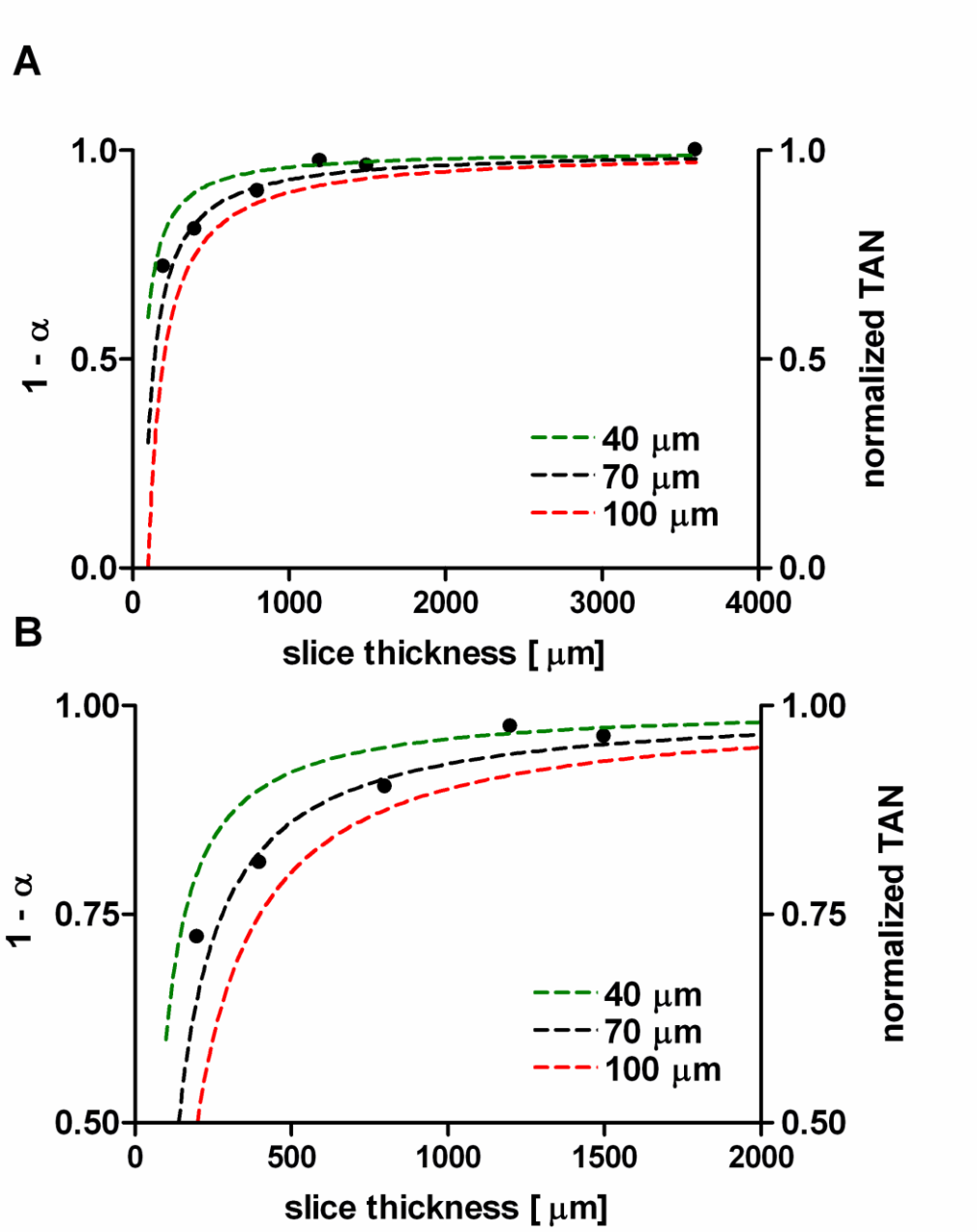

Figure 4.7: *Theoretical curves (Y = 1-α; α = d/l; dotted lines) to estimate the relative contribution of dead cut edges (d) to the total tissue thickness of slices (l, ranging from 100 µm to 3600 µm in 20 µm steps in* ***A*** *and to 2000 µm in* ***B****), assuming a total thickness for the two dead cut edges of 40 µm (green dotted line, 20 µm on each side of the slice), 70 µm (black dotted line, 35 µm on each side of the slice) or 100 µm (red dotted line, 50 µm on each side of the slice). By normalising the TAN levels obtained from slices at different thicknesses from Figure 4.5 B to the TAN values obtained for 3600 µm slices (plotted as black dots), I found that these normalized values fit the curve for a total dead cut edge layer of 70 µm (black dotted line), which is in agreement with histological estimates obtained previously for dead slice edges in 400 µm hippocampal slices (Frenguelli et al., 2003).*

With this curve (for a total dead tissue layer of 70 µm) an asymptotic value is approached at a tissue thickness of 3600 µm (1-α = 0.980), suggesting that the dead cut edges account for only 2 % of the whole tissue thickness. Therefore, assuming a maximal TAN value of 21.1 nmol/mg protein (3600 µm slices) in slices, the TAN content of the viable core tissue in a 400 µm slice (17.1 ± 1.5 nmol/mg protein) is underestimated by ~ 4 nmol/mg protein, approximately 19 %.

Nonetheless, when corrected for this amount, slice TAN levels in 400 µm neocortical/hippocampal slices remain ~ 37 % (~ 12.5 nmol/mg protein) lower than reported *in vivo* values (33.6 ± 4.7 nmol/mg protein). Hence, this difference is likely due to the loss of adenine nucleotides and precursors during the physical trauma and ischemia during slice preparation.

4.4 Discussion

Although brain slice preparations have become widely used *in vitro* model systems for studying the central nervous system, the extent to which they accurately reflect the energetic status of the *in vivo* brain has been a subject of debate since their introduction. Many investigations have been carried out to study and/or improve the metabolic integrity of brain slices (Thomas, 1957; Orrego and Lipmann, 1967; Fredholm et al., 1984; Whittingham et al., 1984b; Hesse and Shashoua, 1990). The aim of this chapter was to re-address this issue and to study (i) the energetic recovery of brain slices and (ii) the reasons for reduced levels of ATP.

4.4.1 Metabolic recovery after slice preparation

My results show that adenine nucleotide levels in brain slices recover quickly and remain stable for at least 5 h, independently of the incubation temperature. This is supported by earlier findings, which reported that slice ATP levels recover during the first hour of incubation, and remain stable and/or improve over a period of 8 h (Fredholm et al., 1984; Whittingham et al., 1984b; Whittingham et al., 1984a).

Likewise the EC and ATP/AMP ratio show a very rapid recovery after slice preparation, but it takes 3 h until they approach a steady state. EC values presented here for slices at 34°C (0.95 ± 0.002), are higher than values reported by others *in vitro* (EC = 0.73-0.9) (Kass and Lipton, 1982; Fredholm et al., 1984; Whittingham et al., 1989; Paschen and Djuricic, 1995; Milusheva et al., 1996; Galeffi et al., 2000). However, in this study the nucleotide extraction was performed on fresh tissue, since snap freezing in liquid nitrogen and subsequent extraction can lead to changes of *in situ* adenine nucleotide levels (see Chapter 3 Figure 3.13) (Zur Nedden et al., 2009). This makes a comparison with data in the literature somewhat difficult, since it cannot be said whether the higher EC is due to a better metabolic integrity of slices or to different extraction procedures. Likewise published EC values from *in vivo* brain vary between 0.80-0.97 (Appendix 3 Table 12.1), which might also be due to different extraction methods rather than differences in the energetic state of the

tissue. Therefore, the only conclusion that can be drawn is that the EC of hippocampal brain slices recovers to an asymptotic value after 3 h, which is similar to those reported at the higher end of the *in vivo* range and values predicted to reflect metabolic integrity.

It is worth noting that not only adenine nucleotide levels, but also other metabolites, such as the second messengers cGMP and cAMP, lactate or phospho-creatine require 1 - 3 h to achieve a steady state (Whittingham et al., 1984b). Similarly the phosphorylation state of proteins involved in synaptic plasticity, such as GluA1, ERK2 and MEK1/2, undergoes changes especially during the first 3 h of incubation (Ho et al., 2004). A recovery period of 4 h has also been suggested on the basis of achieving stable and reliable long term recordings for synaptic plasticity studies in brain slices (Sajikumar and Frey, 2004; Sajikumar et al., 2005; Redondo et al., 2010). Therefore the recovery period of slices after cutting is critical and should be carefully selected for the specific purpose for which the brain slices are to be used.

Hence, slices for future studies were allowed to rest for 3 h, to avoid running the risk of exposing pre-stressed slices to experimental manipulations.

4.4.2 Higher AMPK activity at lower temperatures

My results further showed that slices at 34°C have a significantly higher ATP/AMP ratio compared to slices at room temperature. The potential basis for this might lie in the activity of adenylate kinase (2 ADP ↔ ATP + AMP). In a computational model of this enzyme, it has been predicted that the rate of conformational switching, which is the rate limiting step of the catalysis (Sheng et al., 1999), is faster at temperatures beyond 32°C (Lu and Wang, 2008). According to this, adenylate kinase would work more efficiently at 34°C, resulting in a better turnover of AMP and ATP to ADP.

Since AMPK is exquisitely sensitive to the cellular ATP/AMP ratio, this translated into slices incubated at 22°C showing a 3 fold higher activity of AMPK than slices at 34°C. AMPK is activated upon phosphorylation by upstream kinases, and binding of AMP inhibits its dephosphorylation and causes allosteric activation of the enzyme,

whereas both effects are antagonized by high intracelluar ATP levels (Hardie et al., 2006; Sanders et al., 2007). Downstream targets of AMPK are involved in metabolism of lipids, carbohydrates, proteins as well as cell signalling (Hardie, 2007). Furthermore it has been shown that the function of $GABA_B$ receptors, which participate in the suppression of neuronal excitation, is increased by phosphorylation through AMPK (Hardie and Frenguelli, 2007; Kuramoto et al., 2007) and it was reported that AMPK activation inhibits calcium-activated potassium channels (αβ-BK_{Ca}) by direct phosphorylation (Wyatt et al., 2007).

A proteomic *in vitro* screen for identification of new brain specific substrates revealed 12 further potential downstream targets (Tuerk et al., 2007). The authors proposed that AMPK might have a general role in shutting down neuronal excitation during energy shortage by phosphorylation of synapsin I, thereby affecting synaptic vesicle transport and release of neurotransmitters, and by phosphorylation of PACSIN1 (protein kinase C and casein kinase substrate in neurons 1), thereby causing endocytosis of NMDA receptors. Therefore, AMPK activity should be preferentially low in brain slices in order to better mimic the state of energy metabolism of normal *in vivo* tissue, with respect to the activity of metabolic enzymes and synaptic transmission. Since ACC, one of the downstream targets of AMPK, shows a higher phosphorylation in slices incubated at room temperature than at 34°C (Figure 4.3 BC), other downstream targets are likely to show the same pattern. Hence, incubating slices at elevated temperatures will help to approach the state of energy metabolism of the *in vivo* situation more closely.

4.4.3 Reduced ATP and TAN concentrations of brain slices

As seen in this and many other reports (Appendix 3, Table 12.2), brain slices have lower ATP and TAN concentrations compared to the respective values of *in vivo* brain (~ 40 - 50 %).

The ischemic period during slice preparation is inevitable, and, as seen in the accumulation of ATP degradation metabolites in the tissue at time of cutting (Table 4.1), clearly contributes to a reduction in the TAN pool.

The extent to which the dead slice edges affect the calculation of slice metabolites has been raised previously (Fredholm et al., 1984; Whittingham et al., 1984a). My data shows that decreasing the ratio of dead tissue to viable tissue by increasing the slice thickness results in an increase of TAN levels, suggesting that the protein content of the dead slice edges contributes to an underestimation of the TAN levels in the viable core tissue by ~ 4 nmol/mg protein (~ 20 %).

However, given that the brain tissue remains more or less inactive, as soon as it is placed into ice cold aCSF and unable to further metabolise ATP, the EC values obtained from slices immediately after cutting (0.54 ± 0.03) would reflect the severity of the ischemic insult, caused by decapitation and removal of the brain. Similar EC values were observed within 3 min of decapitation-induced ischemia (Whittingham et al., 1984a).

There are many reports showing that cerebral TAN/ATP levels after brief periods of ischemia (1 - 5 min) recover close to preischemic control values, upon short reperfusion time points (60 - 90 min) (Ljunggren et al., 1974; Kobayashi et al., 1977; Nowak et al., 1985). However, there was no significant increase in TAN levels in slices over a 5 h incubation period (Figure 4.1 E). This might be due to a lack of purine precursor metabolites in the aCSF which could be used to restore tissue ATP levels via purine salvage or *de novo* synthesis. In fact it has been shown that addition of adenine or adenosine to the aCSF can increase the adenine nucleotide content of cortical slices from 0.85 ± 0.03 μmol/g wet weight to 1.01 ± 0.02 μmol/g wet weight (0.85 mM adenine) (Thomas, 1957). In aCSF supplemented with 1 mM adenosine, tissue TAN levels in 400 μm hippocampal slices can be increased up to 26.54 ± 1.33 nmol/mg protein within 2 h, and are maintained even if adenosine is removed from the incubation medium (Whittingham et al., 1989), showing that brain slices have the capacity to improve the recovery of ATP levels in the viable core tissue. However, the use of adenosine should be carefully considered since it has strong receptor based actions (see Chapter 1, section 1.4.3.4) (Cunha, 2001; Dunwiddie and Masino, 2001; Fredholm et al., 2001).

In conclusion I report that the full recovery of energetic parameters (EC, ATP/AMP ratio) in neocortical/hippocampal brain slices is reached 3 h after slice preparation. The incubation of slices closer to physiological temperatures helps to approach the energy state of the *in vivo* situation more closely and reduce the activation of AMPK, which is known to influence ion channel and $GABA_B$ receptor function. I further showed that the ischemic period during slice preparation results in a substantial loss of adenine nucleotides, but that the protein content of the dead slice edges likewise distorts the calculation of TAN levels. Although the TAN levels in slices are clearly not identical to the *in vivo* situation, the metabolic integrity (EC, ATP/AMP ratio) of brain slices is robust.

5 Effect of purine salvage metabolites on the post-ischemic recovery of ATP levels in brain slices after preparation

5.1 Introduction

As seen in the previous Chapter hippocampal brain slices have lower ATP levels compared to the *in vivo* brain. This is due to i) the ischemic period during slice preparation leading to an accumulation and loss of ATP degradation/precursor metabolites, and ii) the protein content of the dead slice edges resulting in an underestimation of the ATP content of the viable core tissue. However, as shown in the literature hippocampal brain slices have the capacity to increase basal ATP levels if incubated with ATP precursor/degradation metabolites, such as adenosine or adenine (Thomas, 1957; Whittingham et al., 1989). Thus, brain slices are a good model system to screen the efficiency of purine salvage pathway metabolites on improving the recovery of basal ATP levels after slice preparation.

In the purine salvage pathway (see Figure 5.1) the ATP degradation metabolite hypoxanthine (HX) or adenine[5] (Ade) are combined with the activated sugar donor PRPP (5-phospho-ribosyl-1-pyrophosphate) in order to form the respective purine nucleotides inosine monophosphate (IMP, derived from hypoxanthine) or AMP (derived from adenine). The enzymes catalyzing these reactions are hypoxanthine guanine phosphoribosyltransferase (HGPRT) and adenine phosphoribosyltransferase, respectively (APRT, see Figure 5.1). IMP can then be reconverted to AMP, via the intermediate adenylosuccinate, a process which involves the two enzymes adenylosuccinate synthetase and adenylosuccinate lyase.

The purine salvage pathway is a quick and energy efficient way of maintaining adenine nucleotide levels. In a slower and energy dependent process ATP can be generated from low molecular weight precursors in the purine *de novo* synthesis. As for the purine salvage pathway the sugar donor is PRPP and the end product is IMP, but its synthesis is not dependent on pre-existing purine metabolites. It has been shown that in heart tissue the availability of PRPP is a limiting factor for both the purine salvage pathway and the purine *de novo* synthesis (Zimmer, 1983). The basis for the low PRPP pool lies in the weak capacity of the pentose phosphate pathway to

[5] Adenine derives from polyamine synthesis, see introduction 1.4.6

synthesise ribose-5-phosphate and subsequently PRPP (Zimmer, 1992, 1996). Since the brain, like the heart, mainly relies on the purine salvage pathway to maintain constant ATP levels (Gerlach et al., 1971; Mascia et al., 2000), the availability of PRPP and/or the free purine bases Ade or HX might be a limiting factor for the complete recovery of ATP levels in brain slices after slice preparation.

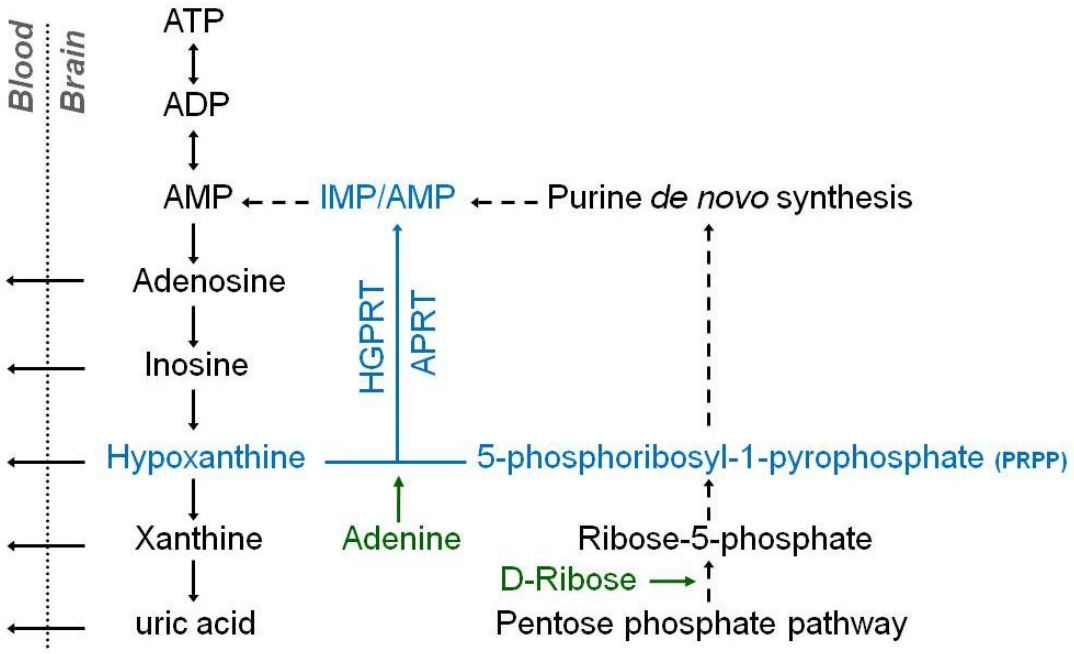

Figure 5.1: Degradation/restoration of ATP levels pathway for adenine and D-ribose utilization: *Adenine nucleotides (ATP, ADP and AMP) are degraded to adenine nucleosides (adenosine and inosine), purine bases (hypoxanthine and xanthine) and uric acid. Substances indicated with an arrowhead can be released from the cell and lost to the systemic circulation. In the purine salvage pathways (shown in blue) the free purine bases hypoxanthine or adenine are combined with the activated sugar donor 5-phosphoribosyl-1-pyrophosphate (PRPP) to build up the respective purine nucleotide IMP via hypoxanthine-guanine phosphoribosyl transferase (HGPRT) or AMP via adenine phosphoribosyl transferase (APRT). Solid lines indicate direct routes, dashed lines indicate indirect routes.*

Therefore, the main aim of this chapter was to test the hypothesis that tissue adenine nucleotide levels of hippocampal brain slices can be increased upon incubation with the pentose D-Ribose (Rib) and/or the free purine bases Ade and HX (see Figure 5.1 and Chapter 1, section 1.5). Rib bypasses the rate limiting step of the pentose phosphate pathway as it can be directly phosphorylated to ribose-5-phosphate by

ribokinase and subsequently to PRPP by and PRPP synthetase (Zimmer, 1996). The beneficial effects of Rib on postischemic myocardial ATP recovery and function have been demonstrated in many *in vitro* (Smolenski et al., 1998; Wallen et al., 2003) and *in vivo* animal models (Zimmer and Gerlach, 1978; Zimmer, 1982; St Cyr et al., 1989; Zimmer et al., 1989; Zimmer, 1992). However, the effect of Rib or combined Rib/Ade, Rib/HX application on adenine nucleotide levels and their functional consequences in *in vitro* or *in vivo* brain tissue has not been studied yet.

I will show that Rib/Ade are used by brain slices to produce ATP, and that slice TAN levels, when corrected for the influence of the dead cut edges values (~ 4 nmol/mg protein), closely approach reported *in vivo* values. Furthermore I tested the effect of acute Rib/Ade application on basal electrophysiological properties as well as the recovery of synaptic transmission after slice preparation.

5.2 Results

5.2.1 Screening of the effects of purine salvage metabolites on basal ATP levels

To screen the effect of purine salvage metabolites on basal ATP levels, brain slices were incubated with Rib alone or in combination with Ade or HX for 3 h at 34°C immediately after slice preparation, and nucleotide extraction was performed thereafter. The incubation time was chosen on the basis of previous results, which showed that the full recovery of energetic parameters after slice preparation takes 3 h (see Chapter 4, Figure 4.2).

The values for adenine nucleotides as well as IMP (since this is the end product of Rib/HX) are shown in Table 5.1. The concentrations of Rib and/or Ade/HX are based on previous studies in heart tissue (Brown et al., 1985; Smolenski et al., 1998; Zimmer, 1998). Rib on its own was not effective at increasing ATP or TAN levels, even at high concentrations (10 mM). In contrast, the combination of Rib and Ade significantly increased slice ATP and TAN levels, whereas Rib/HX (N = 2) was less

effective. However, basal IMP levels in slices treated with 10 mM Rib were significantly higher compared to control slices, suggesting that Rib might stimulate purine slavage and/or *de novo* synthesis. Likewise, the combination of Rib/HX resulted in elevated IMP levels, likely due to enhanced salvage of intracellular HX.

Since Rib/Ade treatment was more effective at increasing TAN levels than Rib/HX, I focused on Rib/Ade supplementation.

Substrate	ATP [nmol/mg protein]	ADP [nmol/mg protein]	AMP [nmol/mg protein]	TAN [nmol/mg protein]	IMP [nmol/mg protein]
Control (N = 4)	16.21 ± 1.10	1.33 ± 0.20	0.25 ± 0.06	17.8 ± 1.1	0.14 ± 0.01
2.5 mM Rib (N = 3)	15.47 ± 2.41	1.42 ± 0.07	0.23 ± 0.03	17.1 ± 2.5	0.15 ± 0.03
10 mM Rib (N = 5)	16.55 ± 1.18	1.1 ± 0.12	0.29 ± 0.04	17.9 ± 1.2	0.25 ± 0.03*
2.5 mM Rib/ 50 uM Ade (N = 3)	22.89 ± 1.01*	1.64 ± 0.23	0.21 ± 0.01	24.7 ± 0.8*	0.21 ± 0.02
2.5 mM Rib/ 50 uM HX (N = 2)	18.77	1.56	0.225	20.6	0.31

Table 5.1: Effect of various purine salvage metabolites on basal ATP levels. *Brain slices were incubated with D-Ribose (Rib), adenine (Ade) or hypoxanthine (HX) immediately after slice preparation for 3 h at 34°C. Control slices were incubated with 2.5 mM Sucrose. Supplementation of aCSF with 2.5 mM Rib and 50 µM Ade resulted in significant elevation of basal ATP and TAN levels. (*) p < 0.05 compared to Control slices, one way ANOVA, Bonferroni's multiple comparison test.*

5.2.2 Effect of Ribose and adenine on basal ATP levels

Since 2.5 mM Rib/50 µM Ade treatment resulted in significant elevation of basal ATP/TAN levels (Table 5.1), I further aimed to study the effect of various Ade (50 or 100 µM) and Rib(0.5 – 10 mM) concentrations on basal adenine nucleotide and adenine levels after a 3 h treatment period at 34 °C.

I observed a significant elevation of ATP and TAN levels after 3 h incubation in 1 mM Rib/50 µM Ade (Figure 5.2, 25.8 ± 0.7 nmol/mg protein compared to 19.1 ± 1.2 nmol/mg protein, N = 3 - 5; $p < 0.01$ one way ANOVA). The tissue Ade content reached a maximum after 1 h incubation with no further increase after 3 h ((Figure 5.2 B, $p < 0.001$ compared to control slices, one way ANOVA). In order to establish whether these elevated levels of TAN and ATP persisted when Rib/Ade was removed, I incubated slices in standard aCSF for 2 h after 3 hrs in Rib/Ade (slice age was 5 h). During this time tissue adenine content decreased back to baseline (Figure 5.2 B). However, the higher TAN levels were maintained even when Rib and Ade were washed out of the slices (Figure 5.2 A 24.8 ± 0.4 nmol/mg protein, N = 3; $p < 0.01$ compared to standard slices, one way ANOVA).

When corrected for the influence of the protein content of the dead slice edges (~ 4 nmol/mg protein; Figure 4.4), these values (~ 30 nmol/mg protein, light green bar in Figure 5.2 A) are close to the values reported for *in vivo* tissue (33.6 ± 4.7 nmol/mg protein as shown by the grey area for the mean ± SD in Figure 5.2 A). The elevated TAN and ATP levels in Rib/Ade treated slices did not significantly impact on the EC, which stabilised at 0.96 ± 0.001, and the ATP/AMP ratio (141.7 ± 17.5 in Rib/Ade treated slices, compared to 94.9 ± 23.5 for slices incubated in standard aCSF; Figure 5.2 C, N = 3 to 5, $p > 0.05$, one way ANOVA).

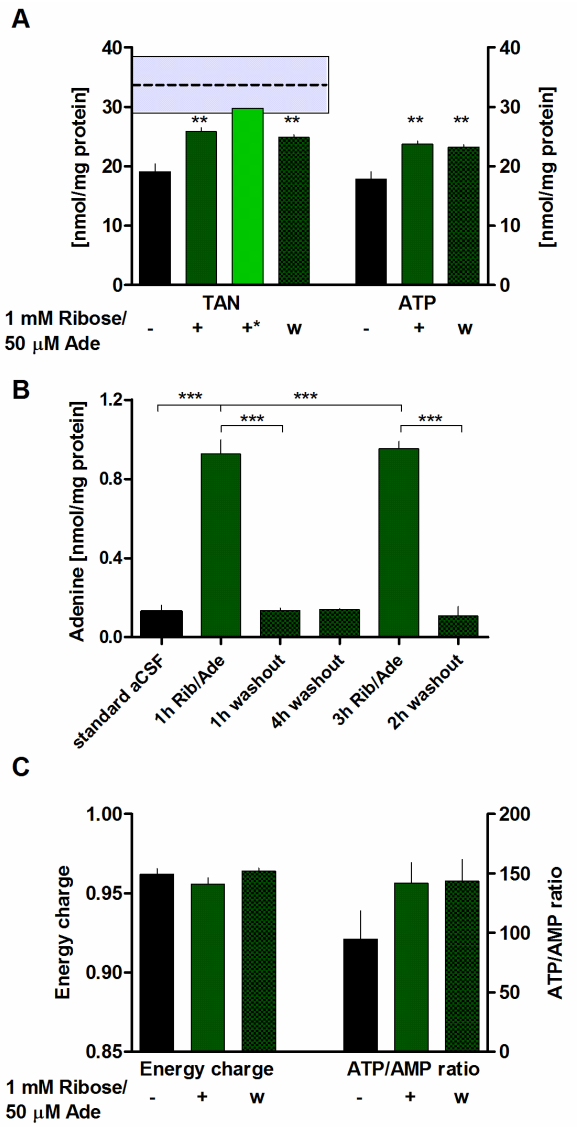

Figure 5.2: A *TAN (left y axis) and ATP (right y axis) levels in slices after 3 h incubation in standard aCSF (-, black bars) or aCSF supplemented with 1 mM D-Ribose (Rib)/50 μM Adenine (Ade) (+, green bars). Under these conditions, and with the correction for dead tissue on the edge of slices (~ 4 nmol/mg protein), slice TAN levels (+*, light green bar) are close to those reported in vivo (grey area represents the arithmetic mean ± SD for all reported values from Figure 4.4). Elevated TAN levels are maintained when Rib/Ade are washed out (w) of the tissue (dashed green bars) by transferring the slices to standard aCSF for 2 h.* ***B*** *Tissue Adenine levels are significantly elevated after 1 h incubation in Rib/Ade (green bar), but decline back to baseline within 1 h washout (dashed green bars).* ***C*** *Energy charge (left y axis) and ATP/AMP levels (right y axis) are not significantly different in slices after 3 h incubation in standard aCSF (-, black bars), in aCSF supplemented with Rib/Ade (+, green bars) or after washout (w) of Rib/Ade (dashed green bars) by transferring the slices to standard aCSF for 2 h. All values are expressed as mean ± S.E.M, N = 3 – 5; (**) p < 0.01, (***) p < 0.001 compared to slices incubated in standard aCSF, one way ANOVA with Bonferroni's multiple comparison test. Where no error bars can be seen they are smaller than the symbol.*

The full time course of recovery of adenine nucleotide levels, EC and ATP/AMP ratio in 1 mM Rib/50 µM Ade supplemented aCSF slices from 0.5 - 5 h is shown in Figure 5.3. From these data it became clear that the maximal TAN levels were reached after a 2 h incubation (25.4 ± 2.3 nmol/mg protein) with no further increase after 3 h (25.8 ± 0.7 nmol/mg protein) or 5 h (25.4 ± 0.91 nmol/mg protein, Figure 5.3 AB). Likewise the Energy charge (EC) stabilised after 1 - 2 h incubation (0.96 ± 0.004, Figure 5.3 C). However, the ATP/AMP ratio showed a significant recovery after 2 h (127 ± 1.3, $p < 0.01$ compared to 30 min at 67 ± 7.6, one way ANOVA), stabilising after a 3 h incubation period (141.7 ± 17.5, $p < 0.001$ compared to 30 min, one way ANOVA).

Higher Rib or Ade concentrations did not result in a further increase of ATP or TAN levels (Table 5.2). In contrast, tissue Ade levels were significantly elevated by increasing the Ade concentration from 50 µM to 100 µM (Table 5.2). However, there was no significant increase in the adenine nucleotide content, suggesting that the accumulated Ade was not salvaged to produce more ATP. Interestingely, the tissue Ade content was higher if slices were incubated with 1mM Rib/50 µM Ade than with 50 µM Ade on its own, suggesting that Rib facilitated Ade uptake.

These data suggest that the full recovery of slice ATP levels is limited by the lack of ATP precursors in the aCSF, and that incubation in Rib/Ade-supplemented aCSF for a recovery period of 2 - 3 h helps the viable core of brain slices to restore ATP levels close to reported *in vivo* values.

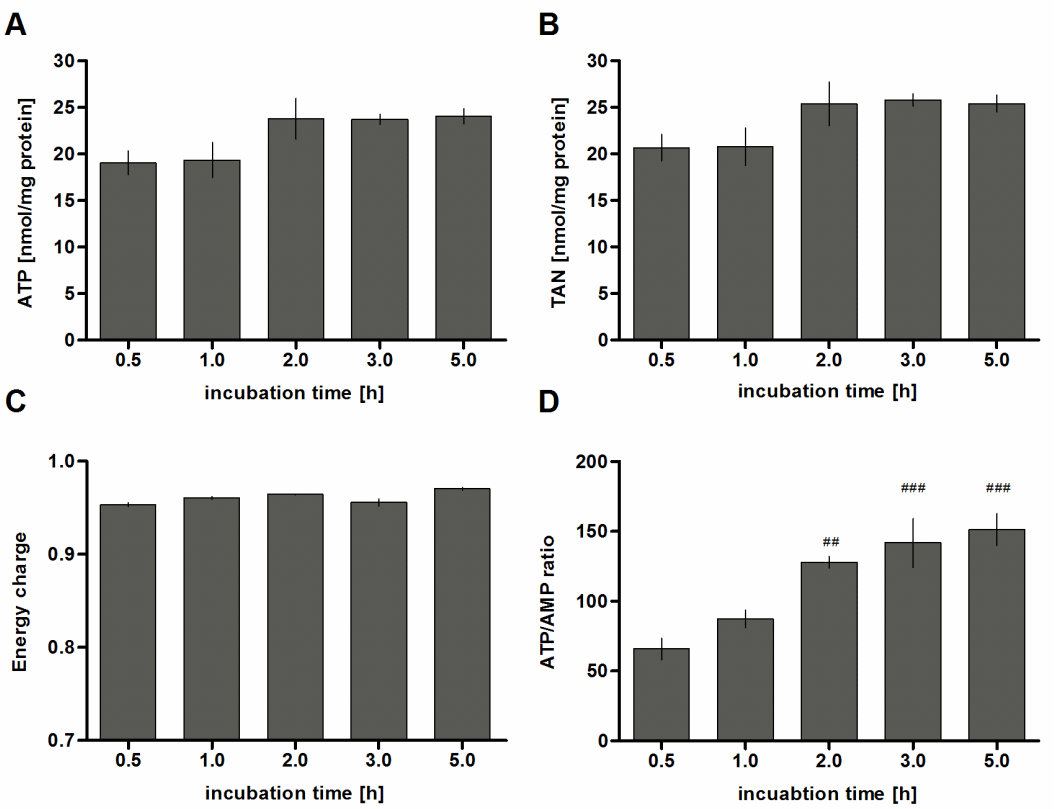

Figure 5.3: Full time-course of recovery of adenine nucleotide levels and energetic parameters from 30 min to 5 h incubation in aCSF supplemented with 1 mM Ribose and 50 µM adenine. *Maximum TAN levels were reached after 2 h (25.4 ± 2.3 nmol/mg protein) and did not further increase after 3 h incubation (25.8 ± 0.6 nmol/mg protein). The ATP/AMP ratio significantly recovered after 2 h and stabilised after 3 h at 141.7 ± 17.5. Values are expressed as mean ± S.E.M, N = 3 – 5.Where no error bars can be seen they are smaller than the symbol.*

Substrate	ATP [nmol/mg protein]	ADP [nmol/mg protein]	AMP [nmol/mg protein]	TAN [nmol/mg protein]	Adenine [nmol/mg protein]
50 uM Ade (N = 3)	20.7 ± 0.3	1.00 ± 0.14	0.15 ± 0.02	21.8 ± 0.4	0.55 ± 0.09
1 mM Rib/ 50 uM Ade[#] (N = 5)	23.7 ± 0.5	1.93 ± 0.25	0.18 ± 0.03	25.8 ± 0.7*	0.95 ± 0.03*
5 mM Rib/ 50 uM Ade (N = 5)	22.5 ± 0.2	1.70 ± 0.20	0.16 ± 0.02	23.1 ±1.1	0.8 ± 0.06
10 mM Rib/ 50 uM Ade (N = 5)	21.7 ± 1.4	1.79 ± 0.32	0.19 ± 0.02	24.4 ± 1.3	0.82 ± 0.06
100 uM Ade (N = 3)	20.9 ± 1.7	2.11 ± 0.42	0.25 ± 0.06	23.3 ± 1.3	1.55 ± 0.18***
10 mM Rib/ 100 uM Ade (N = 3)	22.8 ± 1.0	1.84 ± 0.39	0.12 ± 0.02	25.9 ± 0.7	1.36 ± 0.14**

Table 5.2: Effect of various D-Ribose (Rib) and/or adenine (Ade) concentrations on basal adenine nucleotide and adenine levels*: Slices were incubated with Rib and/or Ade immediately after cutting for 3 h at 34°C. (*) p < 0.05, (**) p < 0.01, (***) p<0.001 compared to 50 µM Ade, one way ANOVA with Bonferri's multiple comparison test.(#) data taken from Figure 5.2 A.*

5.2.3 Effect of Ribose and adenine on synaptic transmission

To my knowledge no other metabolic effects have been reported for Rib at the concentration used, however a G_0-protein coupled adenine receptor has been described and cloned recently (Bender et al., 2002; von Kugelgen et al., 2008). Therefore, to test whether Ade or Rib/Ade had any effects on the presynaptic release probability, via activation of adenine P0 receptors, I compared paired pulse ratios of slices incubated in standard aCSF before and after 10 min application of Ade or Rib/Ade. As shown in Figure 5.4 acute application of 50 µM Ade (Figure 5.4 A, N = 4) on its own or in combination with 1 mM Rib (Figure 5.4 B, N = 5) did not change paired-pulse ratios when applied acutely to slices. Furthermore I did not observe any effects on the fEPSP baseline (105.7 ± 2 % after 10 min application of Rib/Ade).

These results show that the adenine receptor, if present in the hippocampus, does not have any presynaptic effects on neurotransmitter release.

To study the effect of Rib/Ade application after slice cutting on the recovery of synaptic transmission, freshly cut slices were immediately transferred to a recording chamber submerged in aCSF at 33.4 ± 0.3°C. The stimulation strength was adjusted to obtain a fiber volley amplitude of -0.12 – -0.16 mV and the recovery of fEPSPs were monitored for 1 h in slices perfused with standard aCSF or Rib/Ade supplemented aCSF.

The recovery of synaptic transmission after slice cutting was not different between control and Rib/Ade-treated slices (Figure 5.5). Within one hour after slice cutting fEPSP slopes recovered to -0.7 ± 0.1 mV/ms in slices incubated in standard aCSF and to -0.8 ± 0.1 mV/ms in slices incubated in Rib/Ade-supplemented aCSF ($N = 5$; $p > 0.05$, unpaired t-test). In two experiments the fEPSPs were monitored for ≥ 2 hrs, with no further substantial increase in slope or fEPSP amplitude.

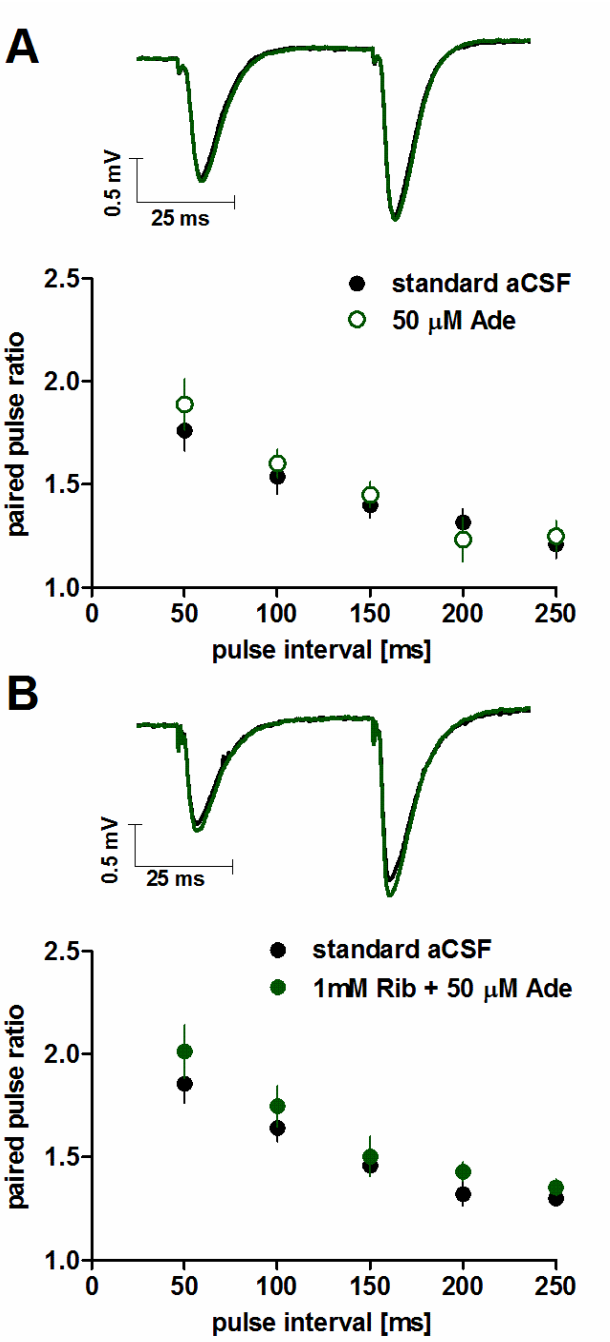

Figure 5.4: Acute application of Ade and Rib/Ade does not change presynaptic release probability. *Paired pulse ratios for slices incubated in standard aCSF before (black circles) and after 10 min acute application of* ***A*** *50 µM Ade (open green circles, N = 4) or* ***B*** *50 µM Ade and 1 mM Rib (green circles, N = 5). Insets are representative fEPSPs at 50 ms interpulse interval before (black trace) and after (green trace) application of Ade or Rib/Ade. All recordings were performed at 33.4 ± 0.2 °C at a flow rate of 7 – 8 ml/min after a ≥ 3 h recovery period from slice cutting.*

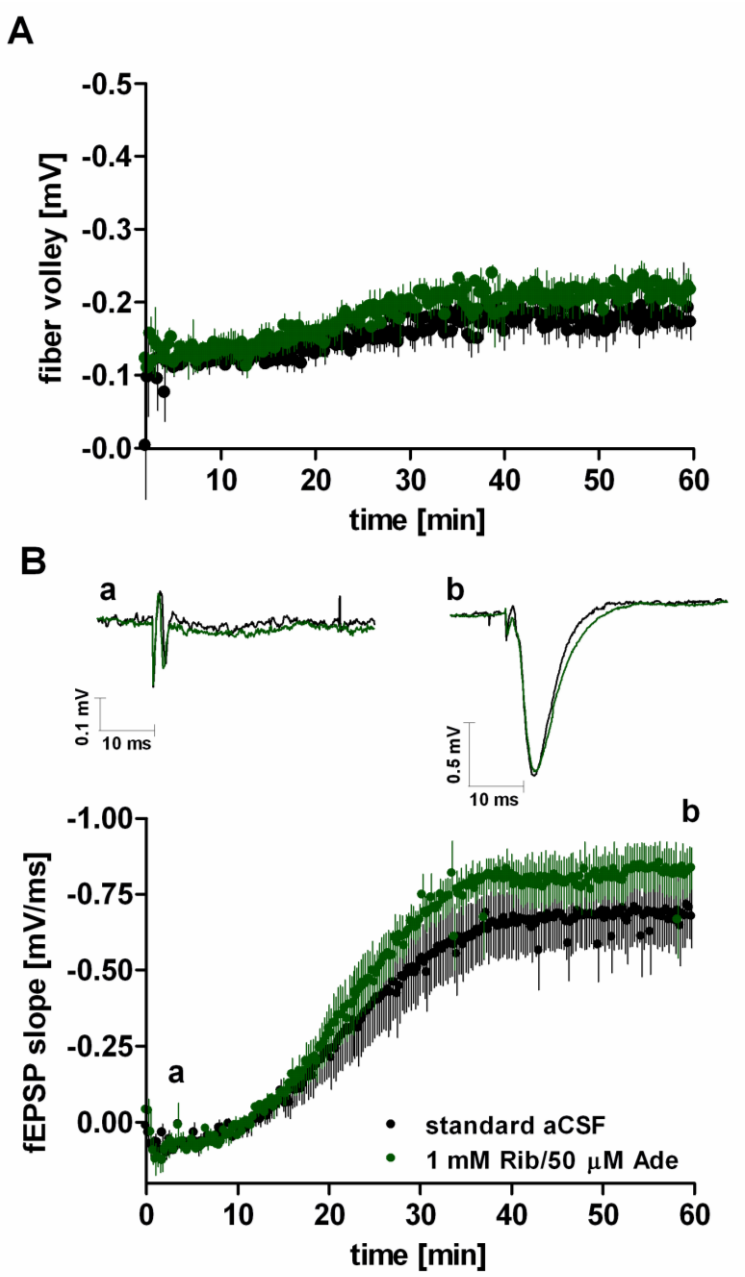

Figure 5.5: 1 mM Ribose (Rib) and 50 µM adenine (Ade) do not affect the time-course of recovery of the fEPSP after slice cutting. *Slices were removed from the vibratome upon cutting and immediately placed into the recording chamber. Stimulating and recording electrodes were inserted into stratum radiatum of area CA1 and the afferent Schaffer pathway stimulated to evoke a fiber volley of -0.12 to -0.16 mV as seen in* ***A****. The delay between slice cutting and evoking a fiber volley was typically ~ 2 min.* ***B*** *The growth of the fEPSP at a fixed stimulation strength was monitored for 60 min until it stabilised. Insets are fEPSPs taken at the time points indicated. There was no appreciable difference between control slices in standard aCSF (black dots, black traces) and slices perfused with Rib/Ade (green dots, green traces).*

5.3 Discussion

The results of this Chapter show that brain slices have the capacity through the purine salvage pathway to restore their intracellular ATP pool in the viable core tissue to levels close to the *in vivo* brain if incubated with Rib and the purine base Ade.

Rib on its own was not sufficient to cause a significant increase in basal ATP levels during a 3 h treatment period. The reason for this could be that after slice cutting the capacity of the purine salvage pathway is mostly limited by the loss of purine metabolites (see Chapter 4, Table 4.1). However, brain slices treated with 10 mM Rib had significantly elevated IMP levels. Therefore the accumulated PRPP might be mainly used for purine *de novo* synthesis, which is not sufficiently fast to increase tissue ATP levels during that short reperfusion period (Gerlach et al., 1971; Kleihues et al., 1974). Likewise a 3 h incubation with Ade on its own did not result in a significant elevation of basal ATP levels. This is in agreement with previous *in vivo* studies in rat heart, where for a significant increase of postischemic ATP levels during a 5 h reperfusion period only the combination of Rib and Ade was found to be effective (Zimmer, 1996). In myocytes the incorporation of HX and Ade into the adenine nucleotide pool is enhanced in the presence of Rib (Brown et al., 1985) and the authors found a maximal salvage of HX or Ade in the presence of 1 mM Rib (at a range of 10 µM – 10 mM Rib). In the same report, Rib/HX seemed to be less efficiently incorporated into the adenine nucleotide pool compared to Rib/Ade, which is in agreement with my own results (Table 5.1). However, tissue IMP levels of brain slices were elevated after 3 h Rib/HX incubation, suggesting that HX is efficiently salvaged by HGPRT. Compared to Ade the incorporation of HX into the adenine nucleotide pool is more complex since IMP can be converted to AMP or guanosine monophosphate (GMP), via different intermediates. Therefore the conversion of IMP to AMP also depends on the activity of the two enzymes adenylosuccinate synthetase and adenylosuccinate lyase and in myocytes the incorporation of HX into the ATP pool has been shown to be limited by the slow rate of catalysis by adenylosuccinate synthetase (Brown et al., 1985). That might explain

why Rib/HX treatment results in elevated IMP in brain slices but is still less effective in increasing ATP or TAN levels compared to Rib/Ade treatment. Thus I mainly focused on Rib/Ade supplementation since these metabolites are directly converted to AMP and since a 2 - 3 h incubation period resulted in a significant increase of basal ATP levels. Furthermore both substances are (i) known to be tolerated in humans, as discussed below and (ii) can cross the blood brain barrier, as discussed later.

The metabolism of orally and intravenously administered Rib has been extensively studied in humans (Segal and Foley, 1958; Gross and Zollner, 1991; Seifert et al., 2008) and the only side effect observed was mild hypoglycemia, the reason for which has not been found yet. At very high concentrations (1M) Rib has been shown to result in glycolation of tau and α-synuclein *in vitro* (Chen et al., 2009; Wei et al., 2009; Chen et al., 2010a). However, these concentrations are not physiological, with the normal Rib blood concentration being around 0.1-0.5 mM and blood levels reaching a maximum of about 5 - 6 mM (Gross and Zollner, 1991) after intravenous Rib infusion. Rib has been given successfully given to patients suffering from a variety of conditions such as congestive heart failure (Omran et al., 2003), coronary artery disease (Pliml et al., 1992), AMP deaminase deficiency (Gross et al., 1989) or fibromyalgia (Gebhart and Jorgenson, 2004).

Likewise Ade has been given to humans. However, it has been shown that Ade can be metabolised by xanthine oxidase to 2,8-dihydroxy-adenine (Bendich et al., 1950). This metabolite per se is not toxic but due to its insolubility in water 2,8-dihydroxy-adenine precipitates in the kidneys and can result in formation of kidney stones, as seen in patients suffering from APRT deficiency (Van Acker et al., 1977). To avoid this side effect Ade has to be applied with the xanthine oxidase inhibitor allopurinol (Greenwood et al., 1982; Simmonds, 1986). Ade/Allopurinol has been given to patients suffering from Lesch-Nyhan syndrome (Schulman et al., 1971; Benke et al., 1973; Watts et al., 1974) and adenylosuccinate lyase deficiency (Jaeken et al., 1988). Despite the fact that adenine therapy was not successful in preventing the neurological damage or improving the neurological outcome in these patients, no adverse effects of adenine administration have been reported in these studies. In *in*

vitro studies Ade has been shown to have neurotrophic effects in cerebellar purkinje cells (Yoshimi et al., 2003). Furthermore a G_i-protein coupled adenine P0 receptor has been described (Bender et al., 2002) and cloned recently (von Kugelgen et al., 2008) and Ade has been suggested to have a pronociceptive role in nociceptive sensory transmission (Matthews and Dickenson, 2004). Quantitative reverse transcriptase–PCR analyses of rat adenine receptor transcripts showed the highest expression levels in dorsal root ganglia, moderate expression in hypothalamus and very low expression levels in the other brain regions, including the hippocampus (Bender et al., 2002). I did not observe any effects of acute Ade or Rib/Ade application on paired pulse ratios or fEPSP baseline in brain slices, suggesting that the P0 receptor, if present in the hippocampus, does not have any presynaptic effects on neurotransmitter release.

Ade is taken up by the brain by a transport mechanism shared with HX (Betz, 1985; Spector, 1989; Redzic et al., 2001) and the K_m value of adenine transport across the blood brain barrier was estimated to be 27 µM (Cornford and Oldendorf, 1975). Cell membranes are highly permeable to Rib (Sacerdote and Szostak, 2005) and it has been shown that Rib can cross the *in vitro* choroid plexus from the frog to the blood (Prather and Wright, 1970) and that its uptake competes with that of glucose (Betz et al., 1975). This may explain why in one study the presence of glucose may have affected Rib uptake (Agnew and Crone, 1967). Furthermore Rib is converted to PRPP in heart (Zimmer, 1998) and in brain extracts (Barsotti and Ipata, 2002), which might underestimate its uptake and may explain the low levels of Rib detected in both brain and heart in another study (Park et al., 1957). Administration of Rib to a patient suffering from adenylosuccinate lyase deficiency has been shown to reduce seizure frequency (Salerno et al., 1999), suggesting that Rib is taken up by human brain. However, this was not replicated in another study (Jurecka et al., 2008), which may reflect differences in dosing and dietary regime. These studies indicate that both Rib and Ade can enter the brain from the periphery, which may be exaggerated after injury, such as stroke, when the BBB may is compromised for several weeks (Strbian et al., 2008).

In summary this chapter shows that enhancing the purine salvage pathway with Rib/Ade is an effective strategy to improve the recovery of ATP levels in brain tissue after an ischemic insult. Furthermore my results demonstrate that brain slices have the capacity to increase their ATP levels close to *in vivo* values, which shows that the traditionally reported lower ATP levels (see Chapter 4 and Appendix 3) are due to a loss and lack of ATP precursors and not a generally compromised energetic state of the tissue. Therefore in the next chapter I investigated whether the increased ATP content of brain slices had any consequences on the electrophysiological properties of the tissue, before studying the effect of Rib/Ade application in *in vitro* ischemia models.

6 Influence of elevated tissue ATP levels on synaptic transmission

6.1 Introduction

The findings of the previous chapters provide new insights into the energetic status of brain slices. They show that the loss of ATP precursors is responsible for the decreased ATP content of brain slices, and by supplementing the aCSF with adenine and D-Ribose, the recovery of tissue ATP levels can be improved. Since I have shown that neither Ade nor the combination of Rib/Ade had any appreciable effects on basic electrophysiological properties I further wanted to test whether the elevated tissue ATP levels had measurable consequences on synaptic transmission. Both ATP and its degradation metabolite adenosine can participate in regulation of synaptic transmission via activation of P1 receptors by adenosine and P2 receptors by ATP and other nucleotides (Cunha, 2001; Burnstock, 2006).

In the CNS ATP acts as a sole neurotransmitter or as a cotransmitter, such as with GABA or glutamate (Pankratov et al., 2009). There are seven characterised ionotropic P2X receptors forming homo or heteromers and eight metabotropic P2Y receptors (Burnstock, 2006) and many of these receptor subtypes have been shown to be widely expressed in neurons and glial cells. Purinergic signalling is involved in neurotransmission and modulation as well as neuron-glial and glial-glial signalling (Fields and Burnstock, 2006). Activation of P2X receptors allows the passage of sodium, potassium and calcium ions and is responsible for fast excitatory purinergic neurotransmission (Pankratov et al., 2009). Activation of P2Y receptors can release calcium from intracellular stores or inhibit adenylyl cyclase activity and modulate ion channels (Abbracchio et al., 2009). Functional studies in hippocampal synaptosomes showed that ATP can modulate glutamate release via facilitation by $P2X_{(1,2/3,3)}$ receptor activation as well as inhibition by $P2Y_{(1,2,4)}$ receptor activation (Rodrigues et al., 2005). Furthermore ATP release has been implicated in hippocampal long term potentiation (LTP) (Wieraszko and Ehrlich, 1994), the electrophysiological correlate of learning and memory. However, the exact mechanism by which ATP influences synaptic plasticity is controversial since P2X receptor activation has been reported to facilitate (Almeida et al., 2003) and inhibit (Pankratov et al., 2002) LTP, which might reflect the complex nature of LTP

induction and maintenance, which is sensitive to cytosolic calcium levels (Abraham and Williams, 2003; Abbracchio et al., 2009).

Additionally ATP can modulate synaptic transmission via its extracellular degradation to adenosine (see Chapter 14.3.3). A_{2A} and A_{2B} receptors generally mediate excitatory actions in the central nervous system. Activation of A_2 receptors has been shown to result in increased acetylcholine and glutamate release as well as A_1 receptor desensitisation (Lopes et al., 2002; Pedata et al., 2007). Likewise A_3 receptors can inhibit the action of A_1 receptors resulting in enhanced neurotransmission (Dunwiddie et al., 1997; Pedata et al., 2007). A_{2A} and A_3 receptor activation can exert excitatory effects on hippocampal LTP (Costenla et al., 2001; Almeida et al., 2003). Despite this, the main role of adenosine in the CNS is inhibitory via activation of A_1 receptors, which results in combined postsynaptic hyperpolarisation due to activation of potassium conductance and presynaptic inhibition of neurotransmitter release (Dunwiddie and Masino, 2001). In hippocampal brain slices there is a low inhibitory adenosine tone in the extracellular space (Dunwiddie and Diao, 1994). Furthermore adenosine release has been shown to modulate synaptic plasticity, such as paired pulse facilitation, long term depression (LTD) and LTP via A_1 receptor activation (de Mendonca and Ribeiro, 1997).

Considering the above actions of ATP and adenosine, the main aim of this chapter was to test whether the elevated tissue ATP levels in Rib/Ade-treated hippocampal brain slices had any measurable consequences on basal synaptic transmission as well as LTP via increased ATP and/or adenosine release.

I will show that the elevation of tissue ATP levels, by Rib/Ade treatment, results in greater activity-dependent release of adenosine and, via activation of adenosine A_1 receptors, leads to the raising of the threshold for the induction of LTP. I further confirmed the greater adenosine release during LTP induction in Rib/Ade-treated slices by measurements with adenosine biosensors and tried to determine the mechanism of release by using inhibitors of extracellular nucleotidases and equilibrative adenosine transporters.

6.2 Results

6.2.1 Electrophysiological properties of slices incubated in Rib/Ade

To establish whether the higher ATP and TAN levels in slices incubated in Rib/Ade would alter the electrophysiological properties of brain slices I performed extracellular recordings from the CA1 region of hippocampal slices. For this purpose input-output curves, paired-pulse facilitation and long-term potentiation (LTP) were compared between slices incubated for 3 - 8 h in standard aCSF, and slices incubated for 2 h in 1 mM Rib and 50 μM Ade then for 1 - 6 h in standard aCSF, to wash these agents out of the tissue. A 2 h incubation period in Rib/Ade was chosen, since slice TAN levels reached an asymptotic value at that time (Chapter 5, Figure 5.3).

6.2.1.1 Basal synaptic transmission is normal in Rib/Ade-treated slices

There was no significant difference in input-output curves (Figure 6.1 A; N = 15 - 16) and paired-pulse ratios (Figure 6.1 B; N = 18 - 22) between the two set of slices ($p > 0.05$, one way ANOVA). This suggests that under conditions of low-frequency stimulation of afferent fibers, the enhanced tissue ATP levels in Rib/Ade-treated slices is not being released to form adenosine in the extracellular space which would, via inhibitory adenosine A_1 receptors (A_1R), inhibit glutamate release and raise the paired-pulse facilitation ratio.

To further exclude possible differences in A_1R sensitivity or adenosine uptake caused by treatment with Rib/Ade, I applied the selective A_1R agonist N^6-cyclopentyladenosine (N^6-CPA, 10 nM) (Gadalla et al., 2004) and the adenosine uptake inhibitors nitrobenzylthioinosine (NBTI, 5 μM)/dipyridamole (DIPY, 10 μM) (Frenguelli et al., 2007; Etherington et al., 2009) to both sets of slices (Figure 6.1 CD). The concentrations chosen were submaximal for complete depression of the fEPSP to avoid a “floor effect” obscuring potential differences between the two sets of slices. Furthermore, it has been previously shown that NBTI/DIPY caused a depression of the fEPSP which is caused by an increased accumulation of

extracellular adenosine (Frenguelli et al., 2007; Etherington et al., 2009) and which can be reversed with A_1R antagonists (Pearson et al., 2001).

The rate and extent of fEPSP depression after a 15 min application of N^6-CPA was the same in control (50.0 ± 1.6 %; N = 5) and Rib/Ade-treated slices (50.4 ± 1.6 %; N = 5; $p > 0.05$, unpaired t-test, Figure 6.1 C). Likewise, application NBTI/DIPY for 40 min resulted in the same rate and amount of depression in both sets of slices (40 ± 5.9 % for standard slices; 43 ± 3.3 % for Rib/Ade treated slices; N = 4; $p > 0.05$, unpaired t-test, Figure 6.1 D). These data suggest that Rib/Ade pre-treatment and/or increased tissue ATP levels do not influence the sensitivity of the A_1R to agonists nor the activity of equilibrative adenosine transporters.

To further exclude the possibility of differences in adenylyl cyclase activation and cAMP formation, due to adenine exposure and potential activation of the adenine P_0 receptor (Bender et al., 2002) between Rib/Ade-treated slices and slices incubated in standard aCSF, I applied 50 μM forskolin, an adenylyl cylcase activator, to both sets of slices and compared the increase in fEPSP slopes. There was no significant difference in forskolin-induced potentiation between Rib/Ade-treated slices and slices incubated in standard aCSF (Figure 6.1 E; 147.4 ± 9.8 % in standard slices and 159.1 ± 12.9 % in Rib/Ade-treated slices; N = 3 - 4; $p < 0.05$ compared to baseline prior to application of forskolin, $p > 0.05$ between standard slices and Rib/Ade-treated slices at 20 min after application of forskolin, one way ANOVA). Paired-pulse facilitation was similarly affected by forskolin in standard slices and Rib/Ade-treated slices (Figure 6.1 F; N = 3 - 4, $p > 0.05$ between standard slices and Rib/Ade-treated slices, unpaired t-test). This suggests that adenylyl cyclase activation and cAMP production is not impaired in Rib/Ade-treated slices.

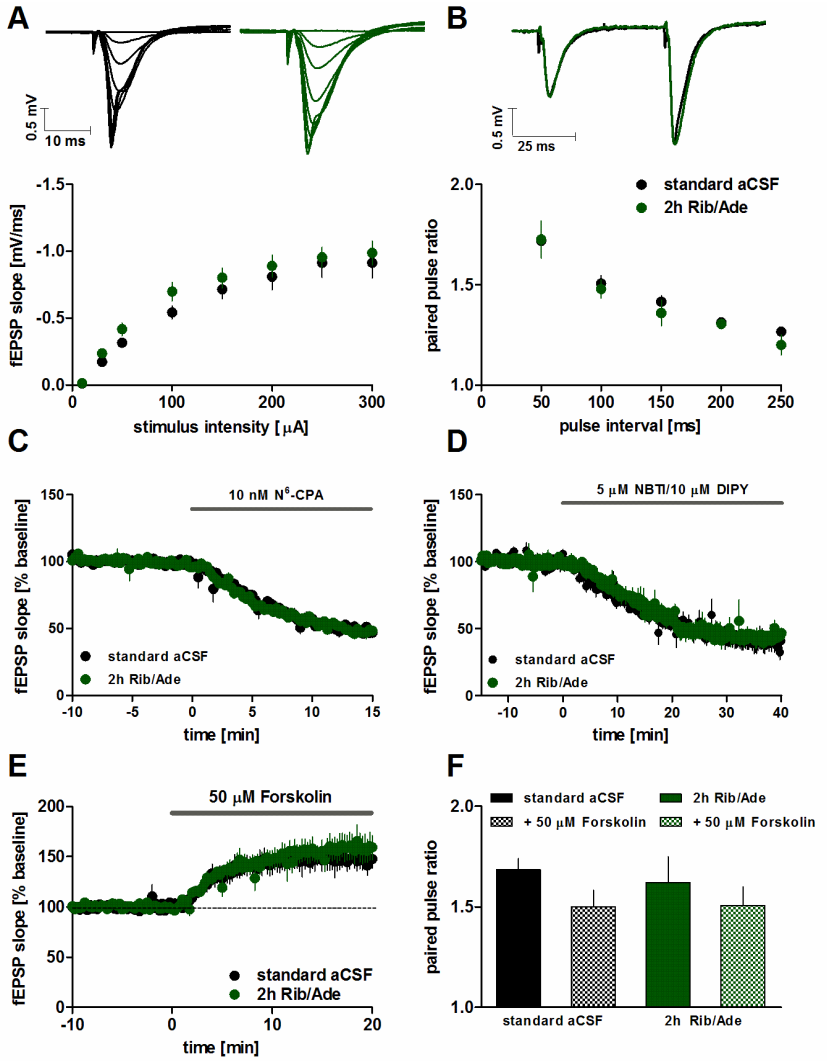

Figure 6.1: Basal synaptic transmission is not different between slices incubated in standard aCSF and slices treated for 2 h in 1mM D-Ribose (Rib) and 50 µM Adenine (Ade). A *Input-output curves (N = 15 - 16) and* ***B*** *paired-pulse ratios (N = 18 - 22) for slices incubated in standard aCSF (black dots) and slices treated for 2 h with Rib/Ade supplemented aCSF (green dots). Insets are representative fEPSPs from 10 – 300 µA (A) and at 50 ms interpulse intervals (B) for control (black traces) and Rib/Ade treated slices (green traces).* ***C*** *There was no difference in the rate or magnitude of fEPSP depression in response to the selective A_1R agonist N^6-cyclopentyladenosine (N^6-CPA, 10 nM; N = 5) or* ***D*** *the combination of the adenosine uptake inhibitors nitrobenzylthioinosine (NBTI, 5 µM)/dipyridamole (DIPY, 10 µM; N = 4) in standard slices (black dots) or Rib/Ade-treated slices (green dots).* ***E*** *Likewise forskolin-induced potentiation (50 µM) in standard slices (black dots) and Rib/Ade treated slices (green dots) was not different (N = 3 - 4) and* ***F*** *the decrease in paired-pulse facilitation (N = 3 - 4) was similar in both sets of slices. Recordings were performed at 33.4 ± 0.2 °C at a flow rate of 7 - 8 ml/min after a ≥ 3 h recovery period from slice cutting. All values are presented as mean ± S.E.M. No significant differences observed between standard and Rib/Ade-treated slices with unpaired t-tests or one way ANOVA with Bonferroni's multiple comparison test. Where no error bars can be seen they are smaller than the symbol.*

6.2.1.2 Long-term potentiation is impaired in Rib/Ade-treated slices

Slices incubated in standard aCSF showed robust LTP 55 - 60 min after tetanic stimulation (1 train of 100 shocks at 100 Hz; Figure 6.2 A; 135 ± 5.8 % of baseline; N = 9; $p < 0.001$ compared to 5 min baseline prior to tetanic stimulation, one way ANOVA). However, LTP in slices incubated for 2 h in 1 mM Rib and 50 µM Ade decayed back to baseline 60 min after tetanic stimulation, (108 ± 4.9 % of baseline; N = 11; $p > 0.05$ compared to 5 min baseline prior to tetanic stimulation, one way ANOVA), and was significantly lower in amplitude than LTP in control slices incubated in standard aCSF (Figure 6.2 B, $p < 0.001$ from 55 – 60 min after LTP induction, one way ANOVA).

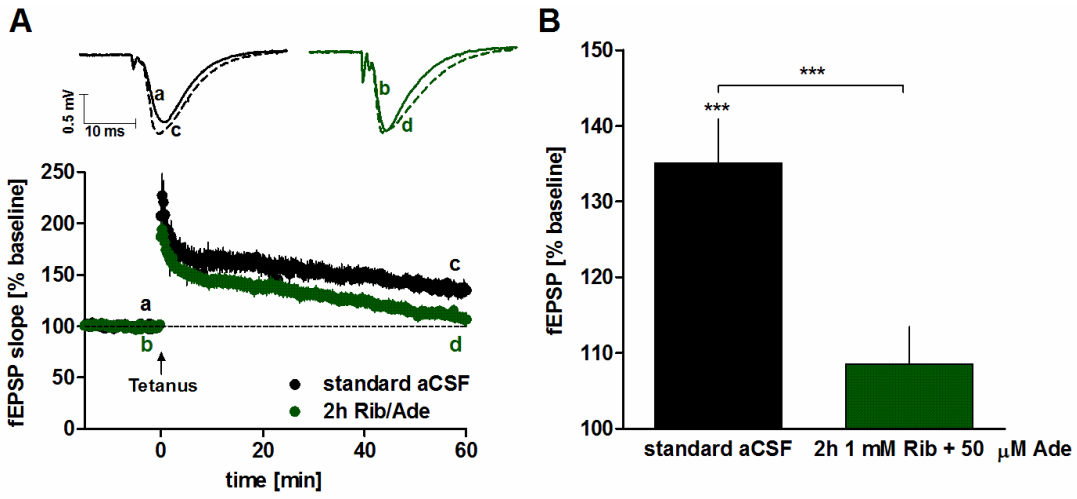

Figure 6.2: LTP induction with tetanic stimulation is impaired in slices treated for 2 h in 1 mM D-Ribose (Rib) and 50 µM Adenine (Ade) A *LTP after tetanic stimulation (1 x 100 stimuli at 100 Hz) in slices incubated in standard aCSF (black dots, N = 9) and slices incubated for 2 h in Rib/Ade-supplemented aCSF (green dots , N = 11).* ***B*** *Comparison of the last five minutes of LTP in each set of slices. Insets are representative of fEPSPs before (solid lines) and 60 min after the induction of LTP (dashed lines). Recordings were performed at 33.4 ± 0.2 °C at a flow rate of 7 - 8 ml/min after a ≥ 3 h recovery period from slice cutting. All values are presented as mean ± S.E.M. (***) p < 0.001, one way ANOVA.*

The fact that stable recordings could be achieved in Rib/Ade-treated slices over the same time period (Figure 6.3 A) argues against baseline drift as being the cause for the observed decay in LTP. Furthermore acute application of Ade (Figure 6.3 B) or Rib (Figure 6.3 C) alone, or both in combination (Figure 6.3 C) did not impair tetanus-induced LTP implying a requirement for uptake and intracellular conversion to adenine nucleotides.

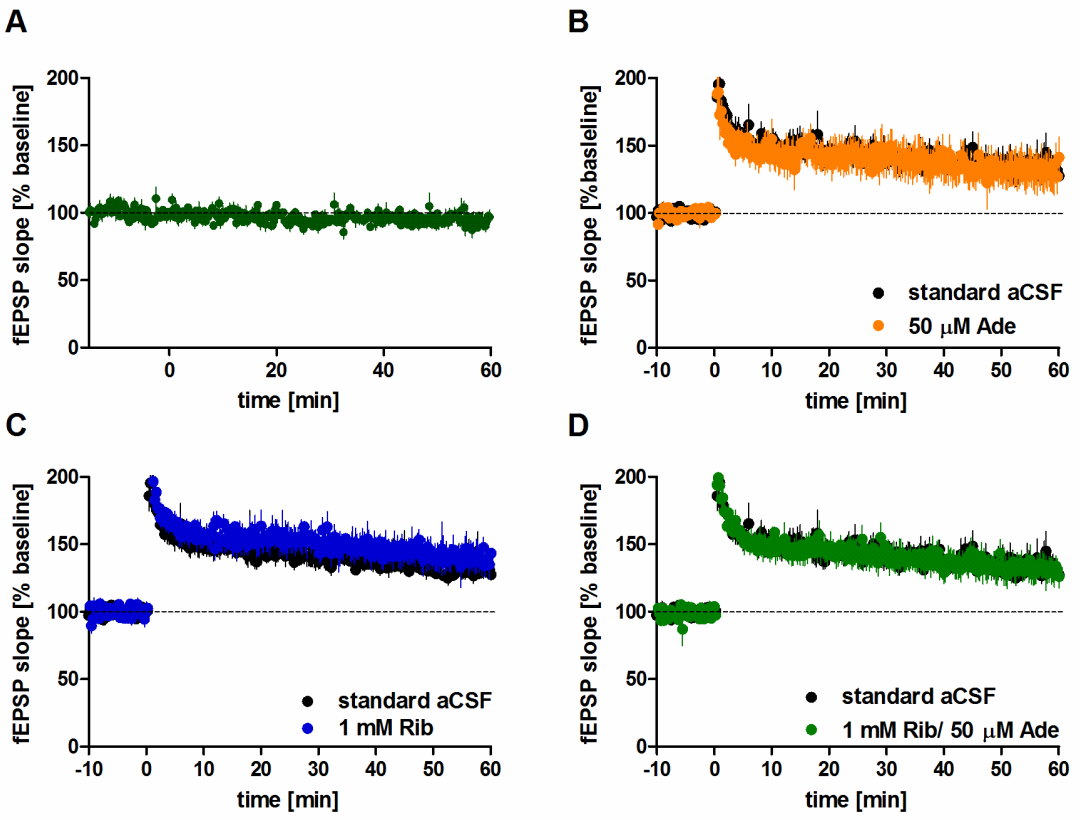

Figure 6.3: ***A*** *Baseline stability in electrophysiological recordings of slices treated with 1 mM D-Ribose and 50 µM Adenine for 2 h over the time course of LTP experiments, N = 4. Acute application for 10 min of* ***B*** *50 µM Adenine (Ade),* ***C*** *1 mM Ribose (Rib) or* ***D*** *both in combination, does not prevent a stable induction of tetanus-induced LTP (1 train of 100 pulses at 100 Hz). Recordings were performed at 33.4 ± 0.2 °C at a flow rate of 7 - 8 ml/min after a ≥ 3 h recovery period from slice cutting. All experiments were performed interleaved over the same time period, however for the presentation of the data the different treatments were split up in Figure 6.3 BCD with the control values being the same in all three figures. For statistical tests all values were compared simultaneously. Values are expressed as mean ± S.E.M, N = 4 - 5. No statistical differences between groups were observed with one way ANOVA and Bonferroni's multiple comparison test.*

A potential reason for the impaired LTP stabilisation in Rib/Ade-treated slices might be that, due to the higher TAN pool, enhanced synaptic activity during tetanic stimulation causes the activity-dependent release of ATP and/or its metabolite adenosine. To test this I incubated slices in the ATP P2 receptor antagonist PPADS (10 µM) and A_1R antagonist 8-CPT (1 µM) prior to the induction of LTP.

Pre-incubation with PPADS did not prevent the decay of LTP in Rib/Ade-treated slices (Figure 6.4; N = 4). These observations suggest that if ATP is being released during tetanic stimulation it is not directly responsible via P2 receptors for the impairment of LTP.

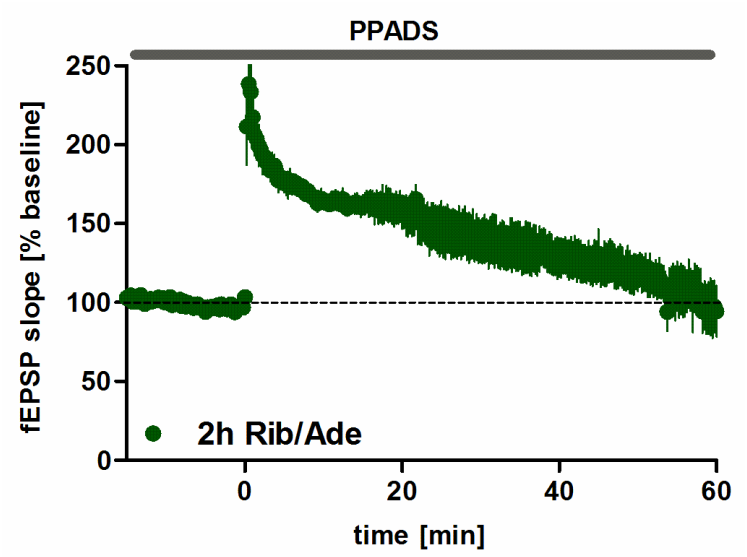

Figure 6.4: *10 µM PPADS applied for 10 min prior to tetanic stimulation (1 train of 100 pulses at 100 Hz) in slices treated with 1 mM D-Ribose and 50 µM Adenine for 2 h does not prevent the impairment of LTP. Recordings were performed at 33.4 ± 0.2 °C at a flow rate of 7 - 8 ml/min after a ≥ 3 h recovery period from slice cutting. Values are expressed as mean ± S.E.M, N = 4.*

To test for a role for adenosine A_1 receptors, I applied 8-CPT (1 µM), a selective A_1R antagonist, to slices which had either been pre-treated with Rib/Ade or incubated in standard aCSF. Ten minutes after acute application of 8-CPT fEPSPs increased to 121.4 ± 0.7 % in standard slices (N = 6; data not shown) and to 124.1 ± 0.5 % in Rib/Ade-treated slices (N = 8) and was associated with a similar decrease in PPF in both (7.5 %). Both these changes in synaptic transmission are indicative of

the removal of a basal adenosine A_1R-dependent inhibitory tone. The fact that the changes were similar between the two conditions argues against the possibility of an increased basal adenosine tone in Rib/Ade-treated slices. This is consistent with observations of similar tissue adenosine levels in both sets of slices after a 3 h incubation (see next chapter Figure 7.6 E, standard slices: 0.05 ± 0.004 nmol/mg protein; N = 3; Rib/Ade-treated slices: 0.04 ± 0.002 nmol/mg protein; N = 3; $p > 0.05$, unpaired t-test), and of normal basal transmission and paired-pulse facilitation in Rib/Ade-treated slices (Figure 6.1).

Having established that the basal handling and effects of adenosine were similar in control and Rib/Ade-treated slices I next examined the effect of the A_1R antagonist on tetanus-induced LTP with or without prior Rib/Ade-treatment. LTP was induced when a stable fEPSP baseline of 15 min was collected, approximately 30 - 40 min after application of 8-CPT. Both sets of slices showed robust LTP in the presence of 8-CPT 55 - 60 min after tetanic stimulation (Figure 6.5 AB, 143 ± 6.0 % in standard slices and 154 ± 6.7 % in Rib/Ade-treated slices; N = 5 - 6; $p < 0.001$ compared to 5 min baseline prior to tetanic stimulation, $p > 0.05$ between standard slices and Rib/Ade-treated slices 55 - 60 min after tetanic stimulation, one way ANOVA). This suggests that the activity-dependent accumulation of extracellular adenosine contributes to the impairment of LTP induction in Rib/Ade-treated slices.

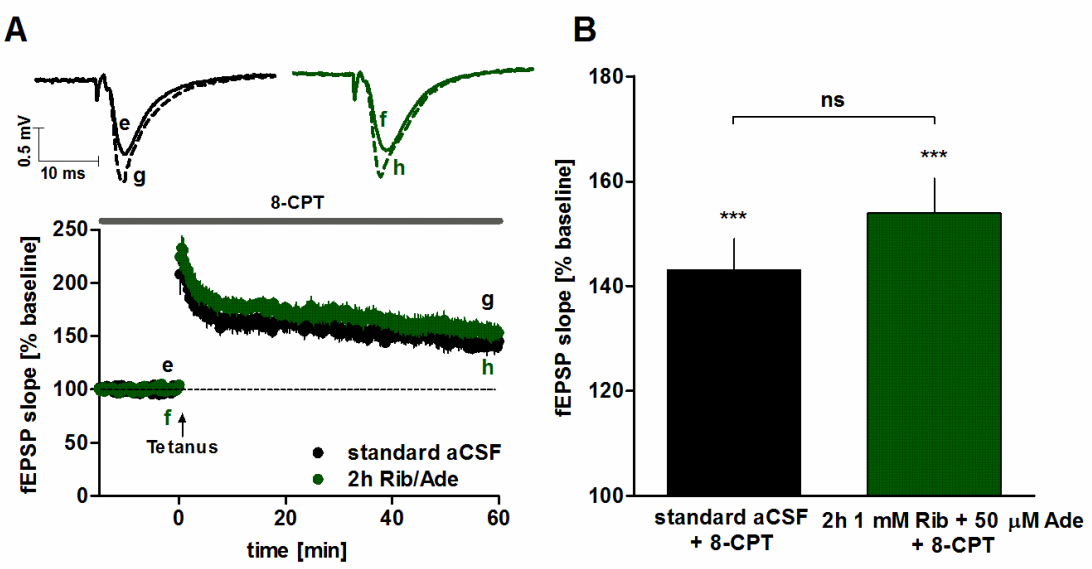

Figure 6.5: ***A*** *LTP after tetanic stimulation and in the presence of 8-CPT in slices incubated for 2 h in Rib/Ade-supplemented aCSF (grey circles, N = 6) and slices incubated in standard aCSF (black circles, N = 5).* ***B*** *Comparison of the last five minutes of LTP in each set of slices. Insets are representative of fEPSPs before (solid lines) and 60 min after the induction of LTP (dashed lines). Recordings were performed at 33.4 ± 0.2 °C at a flow rate of 7 - 8 ml/min after a ≥ 3 h recovery period from slice cutting. All values are presented as mean ± S.E.M. (***) p < 0.001 compared to 5 min baseline prior to LTP induction, one way ANOVA.*

The deficit in LTP induction upon tetanic stimulation in Rib/Ade treated slices might represent a raising of the threshold for LTP by the activity-dependent accumulation of extracellular adenosine and activation of inhibitory A_1Rs. This hypothesis predicts that stronger activation of postsynaptic neurons should overcome this threshold. Accordingly, I utilised a theta-burst stimulation (TBS) LTP induction protocol (Larson et al., 1986), which is known to deliver sustained glutamatergic excitation whilst causing fatigue of GABA-mediated inhibition and hence greater activation of NMDA receptors (Chen et al., 2010b).

Control and Rib/Ade-treated slices were stimulated with two TBS at 5 min intervals (2 x 10 trains of 4 pulses at 100 Hz with 200 ms intervals, ie 80 pulses in total). This protocol resulted in robust LTP in both standard and Rib/Ade-treated slices 55 - 60 min after TBS (Figure 6.6 A; 150.2 ± 7.6 % in standard slices and 140.0 ± 7.1 % in Rib/Ade-treated slices; N = 6 - 7; p < 0.001 compared to 5 min baseline prior to

TBS, $p > 0.05$ between standard slices and Rib/Ade-treated slices at 55 - 60 min after TBS, one way ANOVA). One TBS (40 pulses) resulted in smaller LTP 55 - 60 min after TBS and showed little difference between standard and Rib/Ade-treated slices (Figure 6.6 B; 137.7 ± 9.5 % in standard slices and 126.2 ± 5.0 % in Rib/Ade-treated slices; $N = 6$; $p < 0.01$ for standard slices and $p < 0.05$ for Rib/Ade treated slices compared to 5 min baseline prior to TBS, $p > 0.05$ between standard slices and Rib/Ade-treated slices at 55 - 60 min after TBS, one way ANOVA). However, 20 pulses (5 x 4 pulses at 100 Hz, 200 ms apart) resulted in significant LTP in standard slices, but not in Rib/Ade-treated slices 55 - 60 min after TBS (Figure 6.6 C; 131.6 ± 2 % in standard slices and 117.8 ± 6.6 % in Rib/Ade-treated slices; $N = 3 - 4$; $p < 0.01$ for standard slices and $p > 0.05$ for Rib/Ade treated slices compared to 5 min baseline prior to TBS, one way ANOVA). A comparison of the magnitude of LTP vs the number of TBS pulses (Figure 6.6 D) reveals a consistent inhibitory influence of Rib/Ade treatment on the magnitude of LTP.

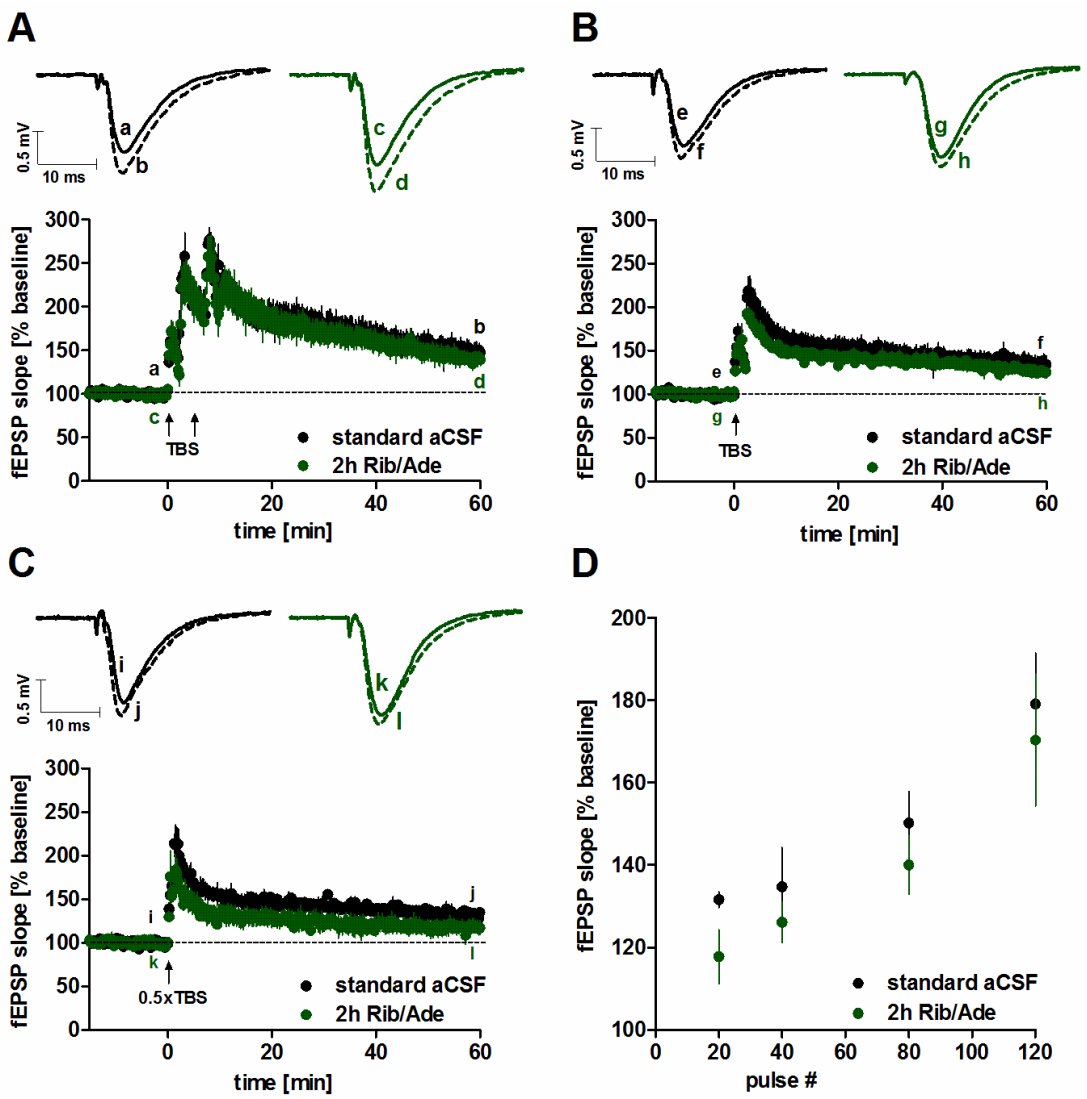

Figure 6.6: *LTP is not different in slices incubated for 2 h in Rib/Ade-supplemented aCSF (green circles) and standard aCSF (black circles) when either two (**A**; 10 trains of 4 pulses delivered at 100 Hz and at 200 ms interval, 5 min apart; 80 pulses in total; N = 6 - 7) or one (**B**; 40 pulses in total; N = 6 for both) theta-burst stimulation (TBS) are delivered. **C** In contrast, a briefer TBS (5 trains of 4 pulses, 20 pulses in total) resulted in significant LTP in standard slices 55 - 60 min after TBS (black circles, N = 3 from 2 animals), but not Rib/Ade-treated slices (green circles, N = 4 from 3 animals). **D** Plot of pulse number versus magnitude of LTP 55 - 60 min (20, 40, 80 pulses) or 30 min (120 pulses) after induction in standard and Rib/Ade-treated slices. Note that throughout the pulse number range Rib/Ade-treated slices give rise to lower LTP, which falls below significant LTP induction threshold at 20 pulses. Data for 120 pulses is obtained from Figure 6.9 A with 120 pulses delivered via 3 x 40 pulse theta trains at 10 s intervals with LTP measured after 30 min. All insets are representative of fEPSPs before (solid lines) and 60 min after the induction of LTP (dashed lines). Recordings were performed at 33.4 ± 0.2 °C at a flow rate of 7 - 8 ml/min after a ≥ 3 h recovery period from slice cutting. All values are presented as mean ± S.E.M.*

To confirm that TBS resulted in greater depolarisation compared to tetanic stimulation, I measured the area associated with each pulse induced by tetanic stimulation (100 pulses) and TBS (40 pulses) in a manner similar to that recently described (Chen et al., 2010b). In accordance with the authors findings, a comparison of the normalized cumulative area evoked by each pulse in a tetanus and TBS (Figure 6.7) revealed a dramatic difference between the two: during a tetanus, most of the depolarisation had occurred within the first 20 pulses, whereas during TBS the depolarisation increased almost linearly during the 40 pulse train.

Furthermore, during a tetanus, there was evidence of a fatigue of transmission in Rib/Ade-treated slices occurring at the later stages of the train (> 20 pulses; Figure 6.7 A). This was prevented in slices treated with 8-CPT (Figure 6.7 B) and is consistent with a gradual synaptic accumulation of adenosine. Indeed, the apparent enhancement in CPT/Rib/Ade-treated slices may reflect an action of adenosine on facilitatory adenosine A_2 (Kessey and Mogul, 1998; Fujii et al., 1999; Almeida et al., 2003) or A_3 receptors (Costenla et al., 2001). In contrast, this Rib/Ade-induced fatigue was hardly present during 1 TBS (Figure 6.7 A), 2 TBS given 5 min apart (Figure 6.7 C), or 3 TBS given 10 seconds apart (Figure 6.7 D/E) suggesting rapid clearance of adenosine in the 200 ms between each 4 x 100 Hz stimuli. An examination of the cumulative depolarisation evoked by tetanic stimulation (Figure 6.7 A) predicted that around 20 pulses was the threshold for Rib/Ade-treated slices to inhibit the induction of TBS LTP since this was the exactly the point at which cumulative tetanic depolarisations diverged between standard and Rib/Ade treated slices and also equivalent to the number of TBS pulses required to evoke the maximal tetanic depolarisation in Rib/Ade. Interestingly, as shown before this theta-burst induction protocol (20 pulses) resulted in significant LTP in standard slices but not in Rib/Ade treated slices (Figure 6.6 E).

These data point to the release of either ATP or adenosine upon electrical stimulation, which, via adenosine A_1Rs, inhibits the induction of LTP in response to tetanic stimulation in Rib/Ade treated slices. Importantly, this impairment can be overcome by additional stimulation suggesting that the elevated levels of tissue ATP translate into raising the threshold for LTP induction.

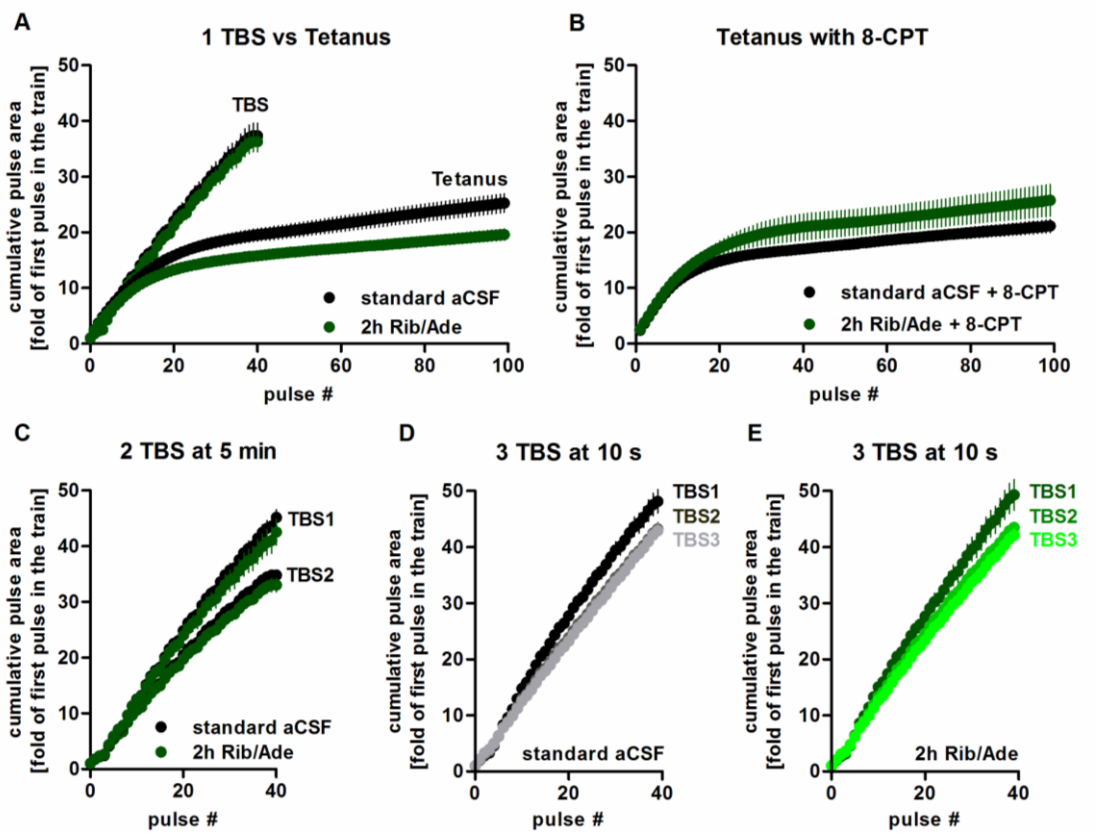

Figure 6.7: ***Theta-burst stimulation (TBS) results in stronger depolarisation than tetanic stimulation.*** ***A*** *The cumulative pulse area (mV*ms) from the data from Figure 6.2 A and Figure 6.6 B is expressed as the fold increase of the first pulse area for tetanic stimulation (100 pulses, 100 Hz) and TBS (10 trains of 4 pulses, 200 ms apart, 100 Hz) in both standard slices (black dots) and slices pre-treated with 1 mM D-Ribose (Rib)/ 50 µM adenine (Ade) for 2 h (green dots). TBS stimulation resulted in significantly greater depolarisation than tetanic stimulation in both sets of slices. Furthermore, during a tetanus, there was evidence of an influence of Rib/Ade in causing fatigue of transmission during the later stages of the train (> 20 pulses), which is consistent with a gradual synaptic accumulation of adenosine.* ***B*** *A similar analysis of the tetanus train files of standard and Rib/Ade slices in the presence of 8-CPT (Figure 6.5 A) shows that the fatigue observed in Rib/Ade slices is prevented and may reflect an action of adenosine on facilitatory adenosine A_{2A} or A_3 receptors. N = 6. The Rib/Ade-induced fatigue was not obvious during* ***A*** *1 TBS* ***C*** *2 TBS given 5 min apart (Figure 6.6 A) or* ***D/E*** *3 TBS given 10 seconds apart (Figure 6.8 A). Cumulative pulse areas were expressed as fold increase from the first pulse area in each train. N = 4 – 7; All values are presented as mean ± S.E.M.*

6.2.2 Real time measurement of adenosine release during LTP induction

To further test whether the higher TAN levels in Rib/Ade-treated slices results in a greater accumulation of extracellular adenosine during periods of electrical stimulation of afferent fibers I used adenosine biosensors (Frenguelli et al., 2003) to measure the real-time release of adenosine during TBS stimulation and LTP induction. The sensors (adenosine and null sensors) were placed in stratum radiatum of the CA1 region of hippocampal slices between the recording and stimulating electrodes.

I could not detect any measurable release of adenosine during tetanic stimulation (100 Hz, 1 s, Figure 6.8) or consistently with one TBS, presumably because the released adenosine is below the limit of detection for adenosine biosensors (50 nM) or because the released adenosine remained close to the side of release unavailable to the enzymes in the sensor.

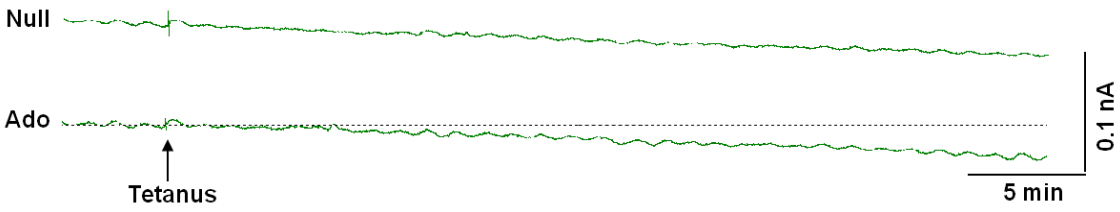

Figure 6.8: *LTP induction using tetanic stimulation does not result in adenosine release. Shown is an example trace for a Rib/Ade treated slice with the null sensor (Null, upper trace) and adenosine biosensor trace (Ado, lower trace). The traces were not subtracted and the baseline is shown by the dashed black line in the adenosine sensor trace.*

For this reason I used a more intense protocol that would be more likely to result in greater adenosine release and sufficient spill-over of adenosine to be detected by the sensors. Accordingly, with a multiple TBS stimulation protocol (10 trains of 4 pulses at 100 Hz, 200 ms apart, repeated 3 times at 10 s intervals; Figure 6.9 A) I was able to detect a rise in extracellular adenosine in slices incubated in standard aCSF and slices treated with Rib/Ade (Figure 6.9 B).

Rib/Ade-treated slices released significantly more adenosine during TBS stimulation as measured by integrating the area under the adenosine signal at the start of TBS stimulation to 5 min after stimulation (Figure 6.9 B; 0.64 ± 0.1 μM'*min in slices incubated in standard aCSF and 1.98 ± 0.1 μM'*min in Rib/Ade-treated slices; N = 3; $p < 0.01$, unpaired t-test). Despite this greater release of adenosine I did not observe any differences in LTP (Figure 6.9 A) between the 2 sets of slices. This is likely due to the fact that the strong stimulation protocol (Figure 6.7 DE) overcame the inhibitory effects of A_1R.

These results suggest that higher intracellular TAN/ATP levels result in increased activity-dependent adenosine release during periods of strong electrical stimulation, which can modulate the induction threshold for LTP.

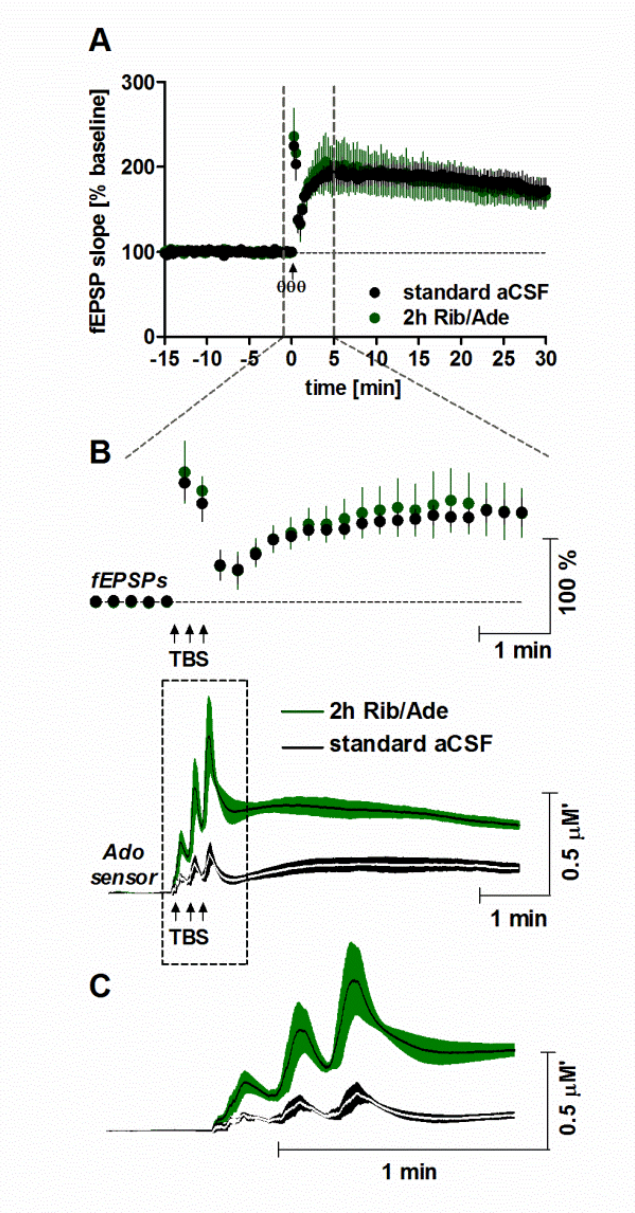

Figure 6.9: *Real time measurement of adenosine release during LTP induction reveals significantly higher adenosine release in slices treated for 2 h in 1mM D-Ribose (Rib) and 50 µM Adenine (Ade).* ***A*** *fEPSP slopes after LTP induction with TBS (10 trains of 4 pulses, at 100 Hz 200 ms apart, applied 3 times with 10 s intervals) are not different in slices incubated for 2 h in Rib/Ade-supplemented aCSF (green dots, N = 4) and slices incubated in standard aCSF (black dots, N = 5).* ***B*** *fEPSP slopes and adenosine sensor traces from 1 min before and 5 min after TBS, as shown by the grey dotted lines in A. Adenosine sensor traces show pooled traces of all experiments for standard slices (black line with green area for mean ± S.E.M., respectively, N = 3) and Rib/Ade treated slices (white line with black area for mean ± S.E.M., respectively, N = 3). Adenosine sensors placed between the recording and stimulating electrodes show significantly higher adenosine release in Rib/Ade-treated slices during LTP induction.* ***C*** *Expanded time scale of the adenosine sensor trace during TBS, as shown in the dashed rectangle in D. All values are presented as mean ± S.E.M.*

6.2.2.1 Mechanism of theta-burst induced adenosine release

To establish whether the released adenosine arose from direct release of adenosine or from extracellular degradation of ATP, I used adenosine uptake inhibitors (NBTI/DIPY) and sodium polyoxotungstate (POM-1), a non-competitive inhibitor of ectonucleotidases (Müller et al., 2006; Wall et al., 2008). To assess the effect of these drugs on adenosine release, TBS-induced adenosine release was evoked twice (45 - 60 min apart). The first TBS stimulation was in control aCSF (in either standard slices or Rib/Ade-treated slices) and the second was in the presence of NBTI (5 μM)/DIPY (10 μM) or POM-1 (100 μM), which were applied 30 min after the initial TBS stimulation. Repeating TBS twice within 45 - 60 min did not affect adenosine release (see Figure 6.10 A). If adenosine was released directly one would expect the transport inhibitors to reduce TBS-induced adenosine accumulation as they represent a major efflux pathway for adenosine into the extracellular space (Baldwin et al., 2004). If extracellular adenosine arose from the metabolism of ATP, POM-1 should reduce TBS-induced adenosine release.

The effectiveness of POM-1 to inhibit ATP breakdown in hippocampal brain slices was assessed by inserting adenosine biosensors into slices and measuring adenosine production following exogenous ATP application in the presence and absence of POM-1 (Wall et al., 2008). In the absence of POM-1 50 μM ATP yielded 3.5 ± 0.2 μM' adenosine. After POM-1 application for 5 min ATP breakdown was inhibited by 30 ± 3 % (2.5 ± 0.1 μM'; N = 3; $p > 0.05$ compared to initial response, one-way ANOVA) and after 15 min application by 42 ± 2 % (2 ± 0.2 μM'; N = 3; $p < 0.05$ compared to initial response, one-way ANOVA; Figure 6.10 BC), which was reversible after 10 min washout. I therefore decided to wait 15 min after POM-1 application to study the effect of POM-1 on TBS-induced adenosine release.

In the presence of POM-1 TBS-induced adenosine release was variable but showed no evidence of inhibition of adenosine release. In fact the reverse was observed: POM-1 seemed to increase TBS-induced adenosine release in both standard and Rib/Ade slices (Figure 6.10 A). This could represent an off-target effect, as has been suggested exist in the use of POM-1 (Wall et al., 2008), or could reflect a previously

described ATP-mediated facilitation of adenosine release via the activation of ATP P2 receptors (Almeida et al., 2003). To address this I incubated Rib/Ade-treated slices with the P2 Receptor antagonist PPADS (10 μM) for 10 min before TBS stimulation. PPADS had no significant effect on adenosine release in Rib/Ade-treated slices (2.0 ± 0.41 μM'*min for Rib/Ade treated slices; N = 10; and 2.0 ± 0.61 μM'*min for Rib/Ade-treated slices in the presence of PPADS; N = 3; $p > 0.05$, one way ANOVA) and indeed did not affect the increased TBS-induced adenosine release in the presence of POM-1 (2.8 ± 0.45 μM'*min for Rib/Ade-treated slices after POM-1 application; N = 4, and 2.3 and 3.3 μM'*min in two Rib/Ade-treated slices in the presence of POM-1 and PPADS; Figure 6.10 A). These negative results with the ectonucleotidase inhibitor POM-1 argue against an appreciable release of ATP and extracellular conversion to adenosine.

In contrast, application of NBTI/DIPY for 30 min resulted in a 50 % reduction in TBS-induced adenosine release in both sets of slices (Figure 6.10 A, 50.3 ± 17.0 % for control slices; N = 4; $p = 0.06$; 49.2 ± 11.0 % for Rib/Ade-treated slices; N = 3; $p = 0.04$, paired t-test), suggesting a role of equilibrative adenosine transporters in the release of adenosine in response to high-frequency stimulation of afferent fibers.

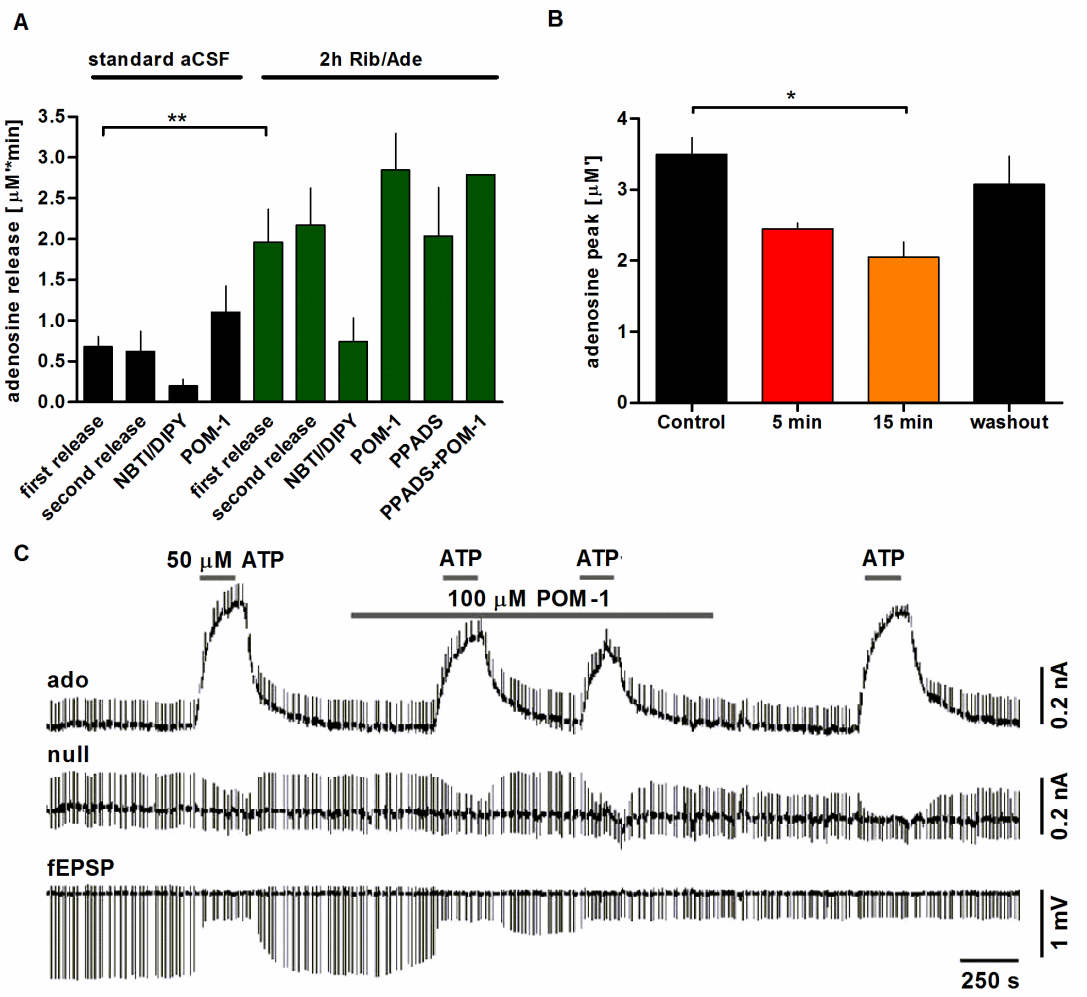

Figure 6.10: *Effect of adenosine uptake and ectonucleotidase inhibitors on adenosine release upon TBS (10 trains, 4 pulses, 100 Hz, 200 ms apart, repeated 3 times with 10 s intervals) in standard slices (black bars) and slices pre-treated with 1 mM D-Ribose (Rib)/50 µM adenine (Ade) (green bars).* ***A*** *Adenosine release was measured by integrating the area under the adenosine signal from the start of TBS to 5 min after stimulation. Rib/Ade-treated slices release significantly more adenosine in response to the first TBS than standard slices (N = 8 - 13; p < 0.01, one-way ANOVA with Bonferroni's multiple comparison test). To assess the effect of the above mentioned drugs on adenosine release, TBS-induced adenosine release was evoked twice. The first TBS was in standard aCSF (first release), whereas the second one was either in standard aCSF (second release, 45 - 60 min later) or in the presence of adenosine uptake inhibitors nitrobenzylthioinosine (NBTI, 5 µM) and dipyridamole (DIPY, 10 µM), or the ectonucleotidase inhibitor sodium polyoxotungstate (POM-1, 100 µM). Both drugs were applied 30 min after LTP induction, and NBTI/DIPY was washed on for 30 min, whereas POM-1 was washed on for 15 min before the second TBS. The effect of PPADS was only tested in Rib/Ade-treated slices and the first release was induced after 10 min application of 10 µM PPADS, whereas the second release was induced 45 min later after 15 min application of POM-1 in the continuous presence of PPADS (N = 2). NBTI/DIPY resulted in a consistent 50 % reduction in adenosine release in both sets of slices (N*

= 3 - 4), whereas POM-1 resulted in a variable increase of adenosine release (N = 4 - 5). All values are presented as mean ± S.E.M. ***B*** *POM-1-mediated inhibition of ATP breakdown in hippocampal brain slices was assessed by inserting adenosine biosensors in slices and measuring the adenosine production following ATP application (50 μM), under control conditions (black bar, control) and after application of POM-1 for 5 min (red bar) or 15 min (orange bar), as well as after washout of POM-1 for 10 min (black bar, washout). The adenosine production induced by ATP breakdown was reduced by 41 % after 15 min application of POM-1, which reversed on POM-1 removal (N = 3; p < 0.05, one-way ANOVA with Bonferroni's multiple comparison test.). All values are presented as mean ± S.E.M.* ***C*** *An example of unprocessed traces obtained from null and adenosine (ado) biosensors in parallel with continuous extracellular field recordings (fEPSP) showing the effects of POM-1. Periodic deflections reflect fEPSPs evoked at 15 s intervals.*

6.3 Discussion

As shown in the previous chapter Rib/Ade-treatment is an effective intervention to restore tissue nucleotide levels close to those observed *in vivo*. Results from this chapter show that this does not have a bearing on basal synaptic transmission, paired-pulse facilitation, or the tonic handling and effects of extracellular adenosine in terms of sensitivity to an agonist (N^6-CPA), antagonist (8-CPT) or uptake inhibition (DIPY/NBTI). Instead, I observed a slow decline of LTP after tetanic and weak TBS in Rib/Ade-treated slices. A likely explanation for this is that the higher TAN levels resulted in greater activity-dependent adenosine release, thereby preventing a stable expression of LTP in an A_1R-dependent manner. This is further emphasised by the analysis of the individual responses during the tetanus, which were consistently lower in Rib/Ade-treated slices than in control slices. Additionally, the application of the A_1R antagonist rescued the decline of tetanus-induced LTP in Rib/Ade-treated slices and reversed the fatigue of the fEPSP during the tetanus. This latter observation may reflect a facilitatory action on the fEPSP by adenosine acting on A_2 or A_3 receptors (Kessey and Mogul, 1998; Fujii et al., 1999; Costenla et al., 2001; Almeida et al., 2003).

It is known that activity-dependent adenosine release regulates synaptic transmission (Mitchell et al., 1993; Manzoni et al., 1994; Wall and Dale, 2008). Indeed, the use of A_1R antagonists facilitate LTP, suggesting that endogenous adenosine exerts an inhibitory influence on LTP induction (de Mendonca and Ribeiro, 1994; Forghani and Krnjevic, 1995; Fujii et al., 2000; Rex et al., 2005), especially when used with weak stimulation protocols (Arai and Lynch, 1992; de Mendonca and Ribeiro, 2000). Interestingly, the threshold for adenosine-dependent regulation of TBS, based on the facilitatory actions of an A_1R antagonist, was 20 pulses (Arai and Lynch, 1992; de Mendonca and Ribeiro, 2000), consistent with my predictions based on tetanic and TBS cumulative depolarisations, and experiments with Rib/Ade-treated slices. These observations and my own results point towards an adenosine A_1R-dependent regulation of LTP, which is influenced by the levels of intracellular adenine nucleotides.

The inhibitory effect of A_1R activation on LTP induction in Rib/Ade-treated slices could be overcome by using stronger TBS protocols (40, 80 or 120 pulses). This likely arises through greater postsynaptic depolarisation across the duration of the train compared to tetanic stimulation, allowing more effective engagement of NMDA receptors (Chen et al., 2010b). My analysis of the stimulus trains provides a potential additional mechanism: the adenosine A_1R-dependent fatigue of the fEPSP during a tetanus was not observed during TBS. This may reflect the fact that the 200 ms burst spacing may allow time for the removal of extracellular adenosine between stimulus trains either through reuptake, metabolism or diffusion. Thus, to the two known actions of TBS that make it an effective and naturalistic stimulus for LTP induction, postsynaptic depolarisation and GABA-ergic fatigue, my results may now potentially add a third: minimising the intraburst synaptic accumulation of extracellular adenosine.

Earlier studies using HPLC have shown increased adenosine release during prolonged electrical stimulation (Lloyd et al., 1993; Sciotti et al., 1993; Cunha et al., 1996). In the present study I was able to detect in real time the release of adenosine during TBS, effectively ~ 6 s of stimulation. Rib/Ade-treated slices released significantly more adenosine, consistent with the availability of a greater precursor

pool of ATP. My attempts to establish whether ATP or adenosine was released in response to high-frequency stimulation were made using an ectonucleotidase inhibitor, POM-1 (Müller et al., 2006; Wall et al., 2008) and the equilibrative nucleoside transporter (ENT) inhibitors DIPY/NBTI (Dunwiddie and Diao, 1994; Frenguelli et al., 2007; Etherington et al., 2009). As described previously (Wall et al., 2008), POM-1 is an effective inhibitor of ATP breakdown in slices, but failed to reduce, and indeed facilitated, TBS-induced adenosine release. This is unlikely to be due to ATP P2 receptor-mediated facilitation of adenosine release reported by others (Almeida et al., 2003) since the facilitation was not affected by the P2 antagonist PPADS. Instead, this facilitation may involve non-specific actions of POM-1 (Wall et al., 2008) or could potentially involve ATP heteroexchange with adenosine (Sperlagh et al., 2003), which is insensitive to P2 receptor antagonists, but sensitive to ENT inhibition. Accordingly, my observations of a 50 % reduction in TBS-induced adenosine release by DIPY/NBTI are consistent with the direct release of adenosine during high-frequency stimulation.

In summary the data presented here and in a recent publication (Zur Nedden et at., 2011) shows that the physiological consequences of elevated tissue ATP levels are in the greater activity-dependent release of adenosine and the subsequent inhibition of LTP upon tetanic or weak theta-burst stimulation of afferent fibers.

In a wider context, the reduced tissue ATP levels observed *in vivo* after cerebral ischemia may, via reduced extracellular adenosine and reduced activation of the inhibitory A_1R may contribute to a further loss of neurons due to imbalances of their energy metabolism. Accordingly, elevation of tissue ATP levels with Rib/Ade may be of value in the post-ischemic brain, *in vitro*, *in vivo*, and potentially in humans. As described in the previous chapter both, Rib and Ade/Allopurinol have been given to humans. Allopurinol may itself be beneficial (Phillis et al., 1995) as it would prevent the metabolism of salvageable hypoxanthine to non-salvageable xanthine thereby providing greater substrates for the purine salvage pathway in the post-ischemic brain. Therefore in the next chapter I investigated the effect of Rib, Ade and Allopurinol on the recovery of postischemic ATP levels, the electrophysiological consequences, as well the effect on cell viability.

7 Modulation of intracellular high energy phosphate levels in *in vitro* models of cerebral ischemia – effect on synaptic transmission and adenosine release

7.1 Introduction

The brain's energy stores are limited and therefore it relies on a constant supply of oxygen and glucose to maintain high intracellular levels of ATP. The depletion of ATP levels during periods of ischemia, as occurs during stroke, results in a loss of neuronal function and viability (Lipton, 1999). Furthermore, the complete recovery of post-ischemic ATP levels may take up to 24 hours (Kleihues et al., 1974; Phillis et al., 1996) thereby prolonging the period of energy depletion and leaving the brain less able to deploy reparative mechanisms as well as more vulnerable to secondary insults. The brain mainly relies on the purine salvage pathway to restore its ATP levels (Gerlach et al., 1971; Mascia et al., 2000) and the reduction and incomplete recovery of post-ischemic ATP levels is due to a loss of salvageable ATP degradation metabolites, such as adenosine, inosine or hypoxanthine (Hillered et al., 1989; Kobayashi et al., 1998; Valtysson et al., 1998; Weigand et al., 1999) as well as the production of the unsalvageable metabolites xanthine and uric acid by xanthine oxidase (Kanemitsu et al., 1988; Stover et al., 1997) (see Figure 7.1).

However, as explained in the Introduction (Chapter 1 section 1.4.3) the release of purine metabolites is important since for example the purine nucleoside adenosine is known to be neuroprotective during ischemia. Adenosine, via activation of A_1 receptors reduces synaptic transmission and thereby helps cells to preserve their energy homeostasis during short ischemic periods (Rudolphi et al., 1992; Dunwiddie and Masino, 2001; Ribeiro et al., 2003). Additionally adenosine can activate A_2 receptors in cerebral blood vessels and thereby increase cerebral blood flow (Phillis, 1989; Soricelli et al., 1995).

Considering the importance of ATP in maintaining cerebral function and the neuroprotective role of adenosine, there are two scenarios which might improve cell viability and function after ischemia: pre-treatment of brain tissue with substances, that can either (i) increase the release of adenosine during ischemia or (ii) delay the degradation of ATP, or treatment of brain tissue after the ischemic insult with substances that help to improve the post-ischemic recovery of ATP, thereby helping

the brain to restore the balance of its energy metabolism. The first scenario might be useful for high risk stroke patients, whereas the second scenario is more useful for acute stroke patients.

The aim of this chapter was to manipulate the decline and recovery of intracellular ATP levels during *in vitro* ischemia by (i) enhancing the purine salvage pathway and/or (ii) delaying the degradation of ATP during ischemia and to study the effect on intracellular adenine nucleotides, synaptic transmission and adenosine release.

This was achieved by (i) increasing basal ATP levels with D-Ribose and Adenine (Rib/Ade, see Chapter 5) and/or inhibiting xanthine oxidase with allopurinol (see Figure 7.1). Due to the greater ATP pool in Rib/Ade-treated slices there might be a greater adenosine release during ischemia and additionally Rib/Ade might be useful in restoring post-ischemic ATP levels. Likewise pre-treatment with allopurinol has been shown to increase hypoxic adenosine levels in the *in vivo* brain (Marro et al., 2006) and enhance the recovery of post-ischemic ATP levels (Phillis et al., 1995).
(ii) On the other hand I aimed to delay the degradation of ATP during ischemia upon incubation with creatine, which is converted to the high energy phosphate phosphocreatine in a reversible reaction catalyzed by creatine kinase (see Chapter 1 section 1.4.2.1). Creatine kinase can then delay the degradation of ATP even in the absence of oxygen and glucose, by transferring the phosphate group from phosphocreatine back to ADP (see Figure 7.1). This is shown in the fact that the decline of neuronal phosphocreatine levels during ischemia precedes the decline in ATP (Lipton and Whittingham, 1982).

Pre-treatment of brain tissue with allopurinol (Lin and Phillis, 1991, 1992; Phillis et al., 1995; Marro et al., 2006) or creatine (Whittingham and Lipton, 1981; Balestrino et al., 2002; Berger et al., 2004; Zhu et al., 2004) has been shown to have a neuroprotective effect in various *in vitro* and *in vivo* models of cerebral ischemia. As discussed before Rib/Ade or Rib on its own has been successfully used in various *in vitro* and *in vivo* models of myocardial ischemia (Zimmer, 1992, 1996).

Allopurinol is widely used in the treatment of gout (Smalley et al., 2000; Terkeltaub, 2003; Pea, 2005) and leukaemia (Sahasranaman et al., 2008). Likewise creatine is known to be tolerated in humans (Kim et al., 2011) and is used as a performance enhancing supplement for athletes (Williams and Branch, 1998). Additionally therapeutic effects on myopathies and neurodegenerative diseases have been reported (Gualano et al., 2011).

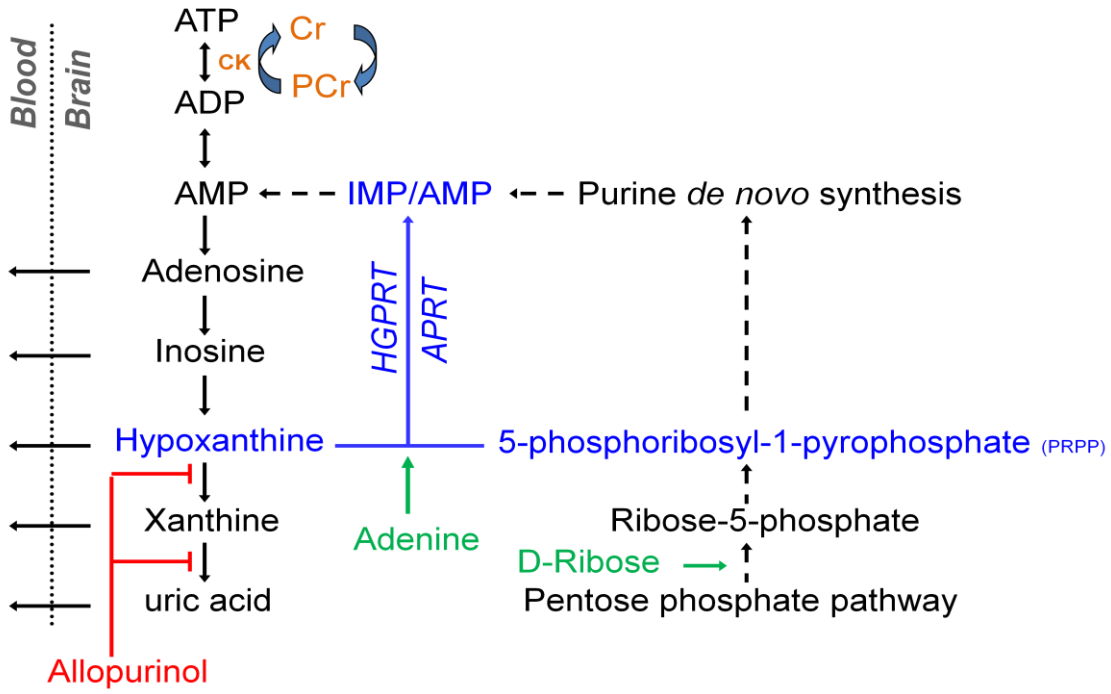

Figure 7.1: Degradation and restoration of ATP levels. *Adenine nucleotides (ATP, ADP and AMP) are degraded to adenine nucleosides (adenosine and inosine), purine bases (hypoxanthine and xanthine) and uric acid. Substances indicated with an arrowhead can be released from the cell and lost to the systemic circulation. In the purine salvage pathways (shown in blue) the free purine bases hypoxanthine or adenine are combined with the activated sugar donor 5-phosphoribosyl-1-pyrophosphate (PRPP) to build up the respective purine nucleotide IMP via hypoxanthine-guanine phosphoribosyl transferase (HGPRT) or AMP via adenine phosphoribosyl transferase (APRT). D-Ribose and Adenine can be used to increase basal ATP levels via the activity of APRT. Allopurinol is a xanthine oxidase inhibitor, that can be used to prevent the degradation of hypoxanthine to xanthine and uric acid. ATP levels can be maintained through the action of creatine kinase (CK) by transferring a phosphate group from phosphocreatine (PCr) to ADP generating ATP and Creatine (Cr).*

In this chapter I will show that it is possible to influence the decline and recovery of synaptic transmission as well the amount and pattern of adenosine release during ischemia by modulation of intracellular high energy phosphate levels with substances that are known to be tolerated in humans.

7.2 Results

7.2.1 Oxygen/glucose deprivation as an *in vitro* model for cerebral ischemia

In order to test the effect of these various intereventions on the post-ischemic energetic and functional recovery, I first wanted to establish an *in vitro* ischemia protocol in hippocampal brain slices that would result in partial reduction of the tissue ATP and TAN levels as well as partial recovery of synaptic transmission. Oxygen/glucose deprivation (OGD), which is a commonl-used *in vitro* model of cerebral ischemia, was induced by exposing slices to aCSF devoid of glucose and bubbled with 95% N_2/5% CO_2. The glucose in the aCSF was substituted with an equimolar amount of sucrose. For reperfusion (rep) studies slices were transferred back to standard aCSF bubbled with 95% O_2/5%CO_2.

7.2.1.1 Effect of OGD on adenine nucleotide levels and energetic parameters

7.2.1.1.1 *Adenine nucleotide levels*

Representative HPLC traces of brain slices exposed to 5 or 10 min OGD and subsequent reperfusion are shown in Figure 7.2. As seen in the individual peaks, the extent of the decrease of ATP levels upon OGD and the recovery during reperfusion depends on the duration of the ischemic insult. The decline in ATP levels is accompanied by a significant rise in AMP levels and other ATP degradation metabolites, such as adenosine and IMP.

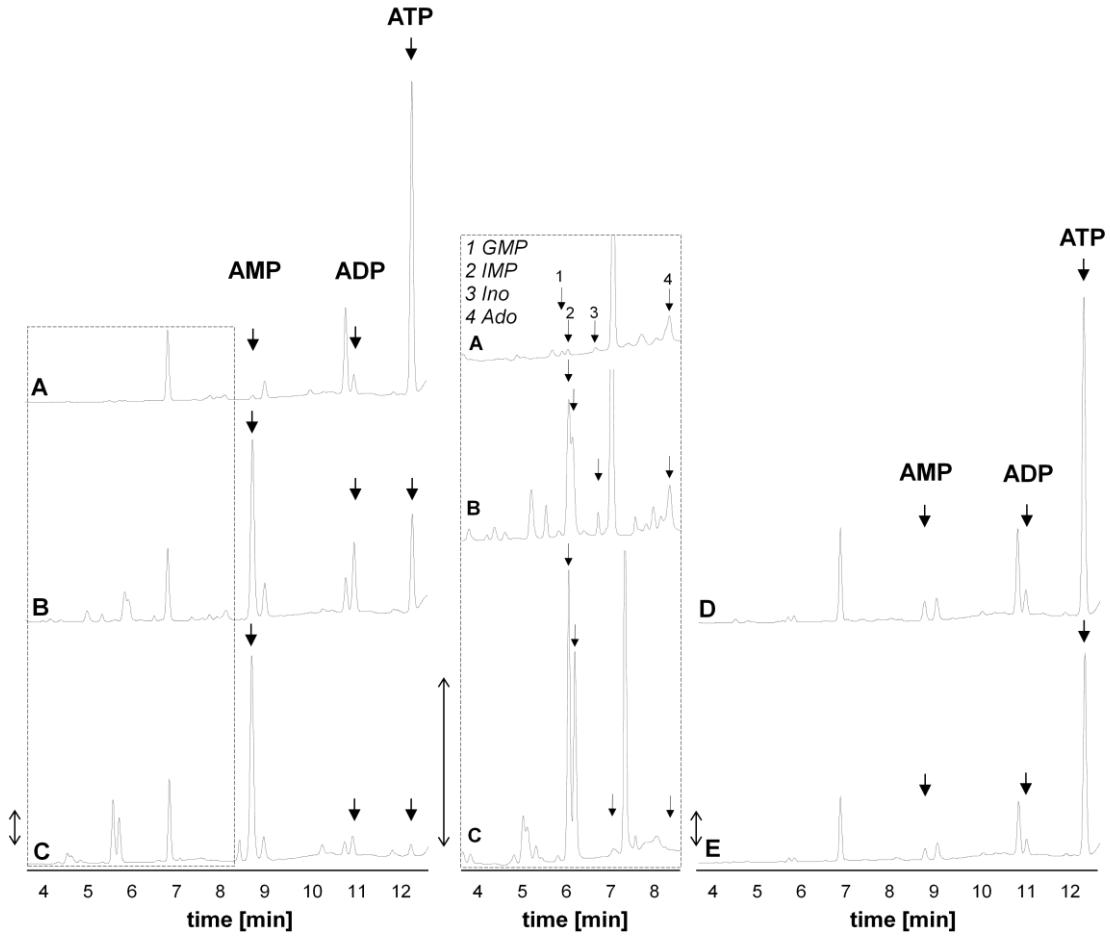

Figure 7.2: Representative HPLC traces of slices exposed to oxygen/glucose deprivation (OGD) and subsequent reperfusion. *After a 3 h recovery period from slice cutting* ***(A)*** *slices were exposed to* ***B*** *5 min OGD or* ***C*** *10 min OGD. Dashed rectangle is shown enlarged next to the traces.* ***D*** *5 min OGD and subsequent 10 min reperfusion and* ***E*** *10 min OGD and subsequent 60 min reperfusion. Note the incomplete recovery of ATP after 10 min OGD. Numbers on traces refer to the following compounds: 1 GMP, 2 IMP, 3 Inosine (Ino) and 4 Adenosine (Ado). All these metabolites are elevated during OGD and decline during reperfusion. Bidirectional arrowheads indicate 100 milli absorbance units.*

The changes in individual adenine nucleotide and adenosine levels are summarised in Figure 7.3. ATP levels decreased approximately 71 % after 5 min OGD and 93 % after 10 min OGD (Figure 7.3 A; from 14.0 ± 1.1 to 4.0 ± 0.9 and 0.9 ± 0.1 nmol/mg protein respectively, N = 6 - 8, $p < 0.001$, one way ANOVA). ADP showed an initial 2.7 fold increase after 5 min of OGD (Figure 7.3 B, from 1.3 ± 0.2 nmol/mg protein to 3.6 ± 0.5 nmol/mg protein, N = 6 - 8, $p < 0.001$, one way ANOVA) but decreased back to pre-ischemic levels after 10 min OGD (1.2 ± 0.2 nmol/mg protein, N = 6, $p > 0.05$ compared to pre-ischemic values, one way ANOVA). This observation has been made before *in vitro* (Mitani et al., 1994) as well as *in vivo* brain during global ischemia (Hertz, 2008). AMP levels increased 38-fold after 5 min OGD and 46-fold after 10 min OGD (Figure 7.3 C; from 0.2 ± 0.02 to 7.5 ± 0.7 and 9.1 ± 0.5 nmol/mg protein respectively, N = 6 - 8, $p < 0.001$, one way ANOVA). Likewise adenosine levels, showed a significant increase after 5 and 10 min OGD (Figure 7.2 D; from 0.02 ± 0.005 to 0.25 ± 0.05 and 0.5 ± 0.03 nmol/mg protein respectively, N = 5 - 8, $p < 0.001$, one way ANOVA). Due to degradation of AMP the total adenine nucleotide (TAN) pool, composed of ATP, ADP and AMP, declined up to 23 % after 10 min OGD (Figure 7.3 E, from 15.1 ± 1.2 to 11.5 ± 0.7 nmol/mg protein, N = 6 - 8, $p > 0.05$ compared to pre-ischemic levels, one way ANOVA)

Upon the reperfusion time points tested, there was a trend towards recovery to pre-ischemic values for all metabolites. However, the extent of the recovery was delayed after 10 min OGD compared to 5 min OGD, as seen in the still significant elevation of AMP levels after 10 min OGD and 10 min reperfusion (Figure 7.3 C, 2.3 ± 0.24 nmol/mg protein, N = 5, $p < 0.05$ compared to pre-ischemic values, one way ANOVA). Likewise TAN levels remained significantly reduced by about 33 % after 10 min OGD and 10 min reperfusion (Figure 7.2 D, 10.3 ± 1 nmol/mg protein, N = 4, $p < 0.05$ compared to pre-ischemic values, one way ANOVA), with no improved recovery after 60 min reperfusion (10 ± 0.4 nmol/mg protein, N = 4). The reduced TAN pool limits the potential recovery of ATP and accordingly ATP levels only recovered to 61 % of pre-ischemic levels after 10 min OGD and 60 min reperfusion (8.6 ± 0.4 nmol/mg protein, N = 4, $p < 0.01$, one way ANOVA).

Longer reperfusion periods (6 h) did not result in complete recovery of TAN levels (data not shown), however after 9 h incubation a ~ 20 % drop in TAN could be observed in time control slices (see Appendix 4, Figure 13.1), suggesting a slow deterioration of brain slices after prolonged incubation periods.

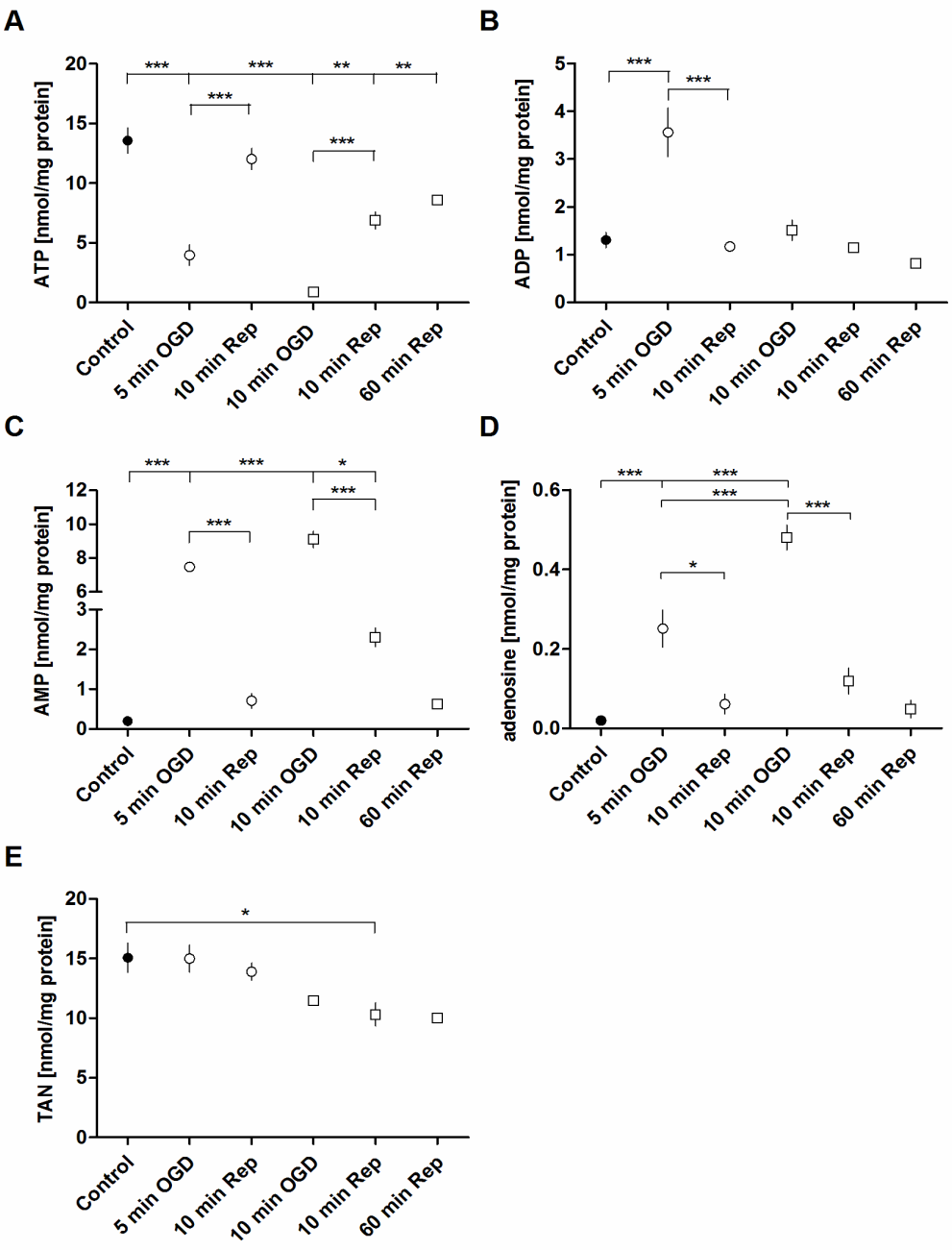

Figure 7.3: Effect of oxygen/glucose deprivation (OGD) and reperfusion (Rep) on tissue adenine nucleotide and adenosine levels: ***A*** *ATP,* ***B*** *ADP,* ***C*** *AMP,* ***D*** *adenosine and* ***E*** *total adenine nucleotide (TAN) levels. Symbols refer to pre-ischemic values (Control, 3 h recovery after slice cutting, black dots), 5 min OGD and subsequent 10 min reperfusion (open circles) and 10 min OGD and subsequent 10 and 60 min reperfusion (open squares). 10 min OGD and 10 min reperfusion resulted in a significant reduction of the TAN pool, indicating a loss of ATP degradation metabolites and limiting the potential recovery of ATP upon reperfusion. All values are expressed as mean ± S.E.M. N = 4 - 8, (*) p < 0.05, (**) p < 0.01, (***) p < 0.001 between indicated groups, one way ANOVA with Bonferroni's multiple comparison test. Where no error bars can be seen they are smaller than the symbol. All incubations were done at 34°C.*

7.2.1.1.2 *Energetic parameters*

The energy charge (EC) decreased to 0.14 ± 0.02 after 10 min OGD (Figure 7.4 A). Upon reperfusion, aerobic energy metabolism is resumed and cellular EC recovers, despite a decreased TAN and ATP pool (Ljunggren et al., 1974). However, pre-ischemic EC values are not completely restored, due to the decreased ATP and still elevated AMP levels. Accordingly, values returned close (0.91 ± 0.01 after 5 min OGD 10 min reperfusion and 0.90 ± 0.005 after 10 min OGD and 60 min reperfusion, N = 6 - 8, $p > 0.05$ compared to pre-ischemic values, one way ANOVA) but not completely to pre-ischemic values (0.95 ± 0.001) during reperfusion. Furthermore the energy metabolism in slices exposed to 10 min OGD showed a more severe disturbance, as indicated by the slower recovery of the EC.

As explained in Chapter 4, a more sensitive parameter of the energetic state of the tissue is the ATP/AMP ratio. Like the EC this ratio severely declined during OGD (Figure 7.4 B, from 70 ± 6 to 0.63 ± 0.2 after 5 min OGD and to 0.1 ± 0.01 after 10 min OGD, N = 6 - 8, $p < 0.001$, one way ANOVA). Furthermore the ATP/AMP ratio remained significantly reduced and never reached pre-ischemic values upon the reperfusion time points tested (22 ± 5 after 5 min OGD and 10 min reperfusion and 14 ± 1.1 after 10 min OGD and 60 min reperfusion, N = 4 - 5, $p < 0.001$ compared to preischemic values), suggesting a severe disturbance of the energy metabolism.

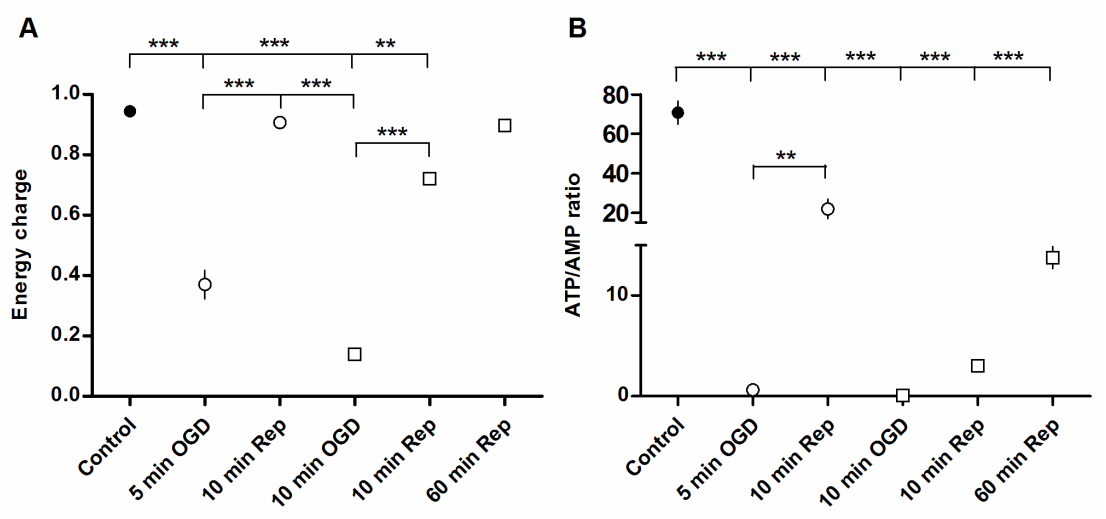

Figure 7.4: Effect of oxygen/glucose deprivation (OGD) and reperfusion (Rep) on energetic parameters: ***A*** *Energy charge and* ***B*** *ATP/AMP ratio. Symbols refer to pre-ischemic values (Control, 3 h recovery after slice cutting, black dots), 5 min OGD and subsequent 10 min reperfusion (open circles) and 10 min OGD and subsequent 10 and 60 min reperfusion (open squares). Note the incomplete recovery of the ATP/AMP ratio after OGD. All values are expressed as mean ± S.E.M. N = 4 - 8 , (**) p < 0.01, (***) p < 0.001 between indicated groups, one way ANOVA with Bonferroni's multiple comparison test. Where no error bars can be seen they are smaller than the symbol. All incubations were done at 34°C.*

These results show that ATP and TAN concentrations decrease progressively with the duration of ischemia and that the severity of the ischemic insult negatively affects the recovery of ATP upon reperfusion. This is due to a reduction of the TAN pool, caused by a loss of ATP degradation metabolites such as adenosine. Furthermore the severe disruption of the energy metabolism is reflected in an incomplete recovery of energetic parameters upon reperfusion.

7.2.1.2 Effect of OGD on synaptic transmission

To study the effect of OGD on synaptic transmission I performed extracellular field recordings in hippocampal brain slices and exposed them to 5 or 10 min OGD and subsequent reperfusion, similar to previous HPLC studies.

As shown in Figure 7.5 synaptic transmission declined very rapidly upon exposure to OGD, which is mainly mediated by release of adenosine and subsequent A_1 receptor activation (Pearson et al., 2006; Dale and Frenguelli, 2009). After 5 min OGD and 30 min reperfusion there was a nearly complete, but still significantly reduced recovery of synaptic transmission (92 ± 2 % of pre-ischemic baseline, $N = 4$, $p < 0.01$, paired t-test). However after 10 min OGD there was no recovery of synaptic transmission in the two slices tested (Figure 7.5 B). This is due to the fact that the anoxic depolarisation (AD) occurred in those slices. AD is caused by a complete loss of ion homeostasis, due to functional inactivation of the Na^+/K^+ ATPase (Somjen, 2002), and if the AD is prolonged beyond a critical time point there is no recovery of electrophysiological activity in brain tissue. The occurrence of AD is marked by a disappearance of the presynaptic fibre volley (Frenguelli et al., 2007) (as shown by the arrowhead in Figure 7.5 B). The mean time to AD in control slices was 7.2 ± 0.2 min (see Figure 7.10 C).

In order to achieve a partial recovery of synaptic transmission in combination with a partial reduction of the total adenine nucleotide pool for studies on interventions of the purine salvage pathway, I choose to adjust the OGD exposure period for HPLC analyses to the value for the 75 % percentile of the mean time to AD in control slices, which was 8 min.

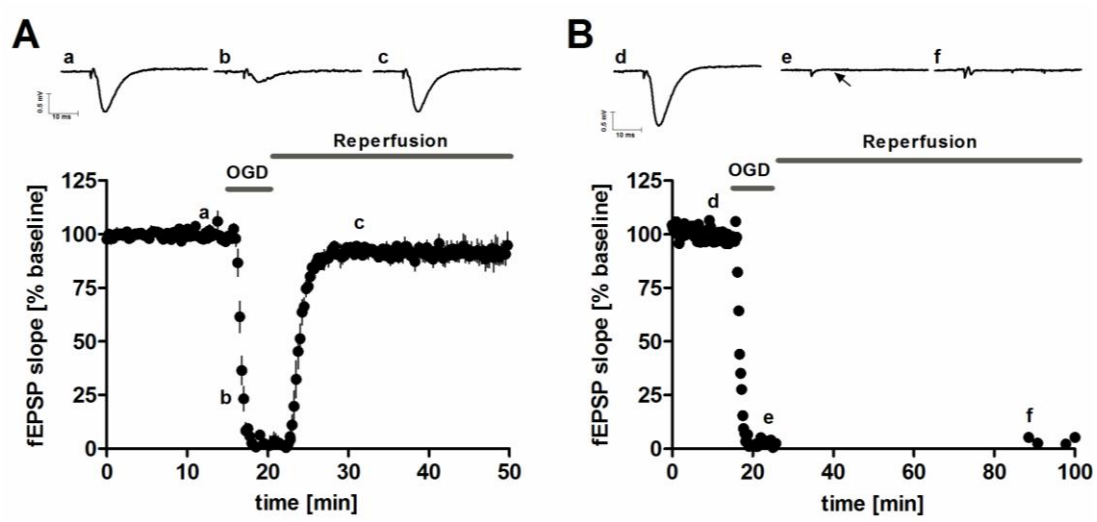

Figure 7.5: Effect of oxygen/glucose deprivation (OGD) and reperfusion on synaptic transmission: *Brain slices were exposed to either* ***A*** *5 min (N = 4) or* ***B*** *10 min OGD (N = 2) and subsequent reperfusion. Whereas 5 min OGD resulted in a nearly complete recovery of synaptic transmission there was no recovery of synaptic transmission after 10 min OGD. Arrowhead in B indicates the disappearance of the presynaptic fiber volley, which marks the time of anoxic depolarisation observed during 10 min OGD. Values in A are expressed as mean ± S.E.M. and values in B are expressed as mean only. Insets are fEPSP traces taken from the indicated timepoints. Recordings were performed at a flow rate of 6 – 7 ml/min, at 33.4 ± 1°C and after a ≥ 3 h recovery period from slice cutting.*

7.2.2 Modulation of intracellular high energy phosphate levels with Rib/Ade Creatine and Allopurinol – Effect on adenine nucleotide levels and ratios

I next wanted to test the effect of manipulations of intracellular ATP and phosphocreatine levels on the decline and recovery of adenine nucleotides and energetic parameters in brain slices during OGD. The interventions were (1) pre-treatment with 1 mM D-Ribose/50 µM Adenine (Rib/Ade) to increase basal ATP and TAN levels, (2) pre-treatment with 10 µM allopurinol to inhibit xanthine oxidase and the production of unsalvageable ATP degradation metabolites, and (3) pre-treatment with 1 mM creatine to increase phosphocreatine levels and buffer the initial decline of ATP upon energy shortage. Brain slices were treated with these

metabolites immediately after slice cutting at 34 °C. After 3 h slices were exposed to 8 min OGD and transferred back to the supplemented aCSF for 1 h reperfusion.

The concentration of Rib/Ade (1 mM/50 µM) is based on results of Chapter 5, creatine was used at an equimolar concentration to Rib (1 mM) and allopurinol has been shown to inhibit xanthine oxidase at 10 µM in cerebellar granule cells (Atlante et al., 1997). The effectiveness of 10 µM allopurinol was further tested on adenosine biosensors, since xanthine oxidase is part of the enzyme complex (see Appendix 4, Figure 13.2). Allopurinol is converted to oxypurinol, the active inhibitor (Lin and Phillis, 1991), by xanthine oxidase itself. Therefore allopurinol gives a signal on the adenosine sensor trace, which gradually decreases over time due to inhibition of xanthine oxidase. There was a time-dependent inhibition of the initial adenosine response in sensors treated with allopurinol, and the response was reduced by about 96 % after 3 h.

7.2.2.1 Effect of Rib/Ade, creatine and allopurinol on pre- and post-ischemic adenine nucleotide levels

The changes observed in individual adenine nucleotide, adenosine and IMP levels in slices pre-treated with Rib/Ade, creatine and allopurinol are shown in Figure 7.6. It was difficult to measure phosphocreatine and creatine levels with this HPLC method since the retention time was very close to the void volume of the column (~ 1. 5 min) and was contaminated by other unretained materials. However, it has been shown that treatment of brain slices with 1 mM creatine increases basal phoshocreatine levels upon a 2 h treatment period (Balestrino et al., 1999).

As shown before (Chapter 5) Rib/Ade treatment results in significant elevation of basal ATP levels (Figure 7.6 A, 24.0 ± 1.3 nmol/mg protein compared to 18.8 ± 0.4 nmol/mg protein in control slices, $N = 5$, $p < 0.01$, one way ANOVA), while having no effect on basal adenosine levels (Figure 7.6 E, 0.04 ± 0.002 nmol/mg protein compared to 0.05 ± 0.002 nmol/mg protein in control slices, $N = 4$, $p > 0.05$, one way ANOVA). Creatine and allopurinol did not change any of the metabolites tested under control conditions, although I observed a slight but insignificant elevation of

basal adenosine levels in allopurinol-treated slices (Figure 7.6 E, 0.07 ± 0.02 nmol/mg protein, N = 4, p > 0.05 compared to control slices, one way ANOVA).

As shown in Figure 7.3, upon exposure to OGD (8 min, 75 % percentile of the time to AD in control slices) I observed significant a decline in ATP levels (Figure 7.6 A), a significant rise in ADP (Figure 7.6 B), AMP (Figure 7.6 C), adenosine (Figure 7.6 E) and IMP levels (Figure 7.6 F) upon all conditions tested.
Interestingly, there were differences in adenosine and IMP levels (Figure 7.6 EF) in Rib/Ade and creatine pre-treated slices. Rib/Ade treatment resulted in significantly higher adenosine levels during OGD (Figure 7.6 E, 1.1 ± 0.08 nmol/mg protein in Rib/Ade treated slices compared to 0.8 ± 0.08 nmol/mg protein in control slices, N = 4, p < 0.01, one way ANOVA), suggesting that the greater ATP pool results in greater production of adenosine upon energy shortage. Although allopurinol-treated slices also had elevated adenosine levels during OGD, this did not reach statistical significance (Figure 7.6 D, 1.0 ± 0.1, N = 3, p > 0.05 compared to control slices, one way ANOVA). Creatine-treated slices had significantly reduced adenosine levels during OGD (0.5 ± 0.03 nmol/mg protein, p < 0.05 compared to control slices, p < 0.001 compared to Rib/Ade treated slices, N = 4, one way ANOVA), due to increased buffering capacity of the phosphocreatine pool and the delayed degradation of ATP. This is also supported by the slightly elevated ADP levels during OGD (Figure 7.6 B, 4.0 ± 0.6 for creatine treated slices compared to 2.6 ± 0.1 for control slices, N = 4, p > 0.05, one way ANOVA).

IMP levels were significantly higher in Rib/Ade-treated slices compared to control slices (Figure 7.6 F, 6.3 ± 0.2 for Rib/Ade treated slices compared to 3.6 ± 0.3 nmol/mg protein for control slices, N = 4, p < 0.001, one way ANOVA). This suggests either increased degradation of AMP due to the higher ATP levels and/or increased salvage of accumulated hypoxanthine and/or Ade via the purine salvage pathway. The latter hypothesis is supported by the fact that incubation of brain slices with high Rib concentrations alone, which does not affect pre-ischemic ATP levels, also resulted in increased production of IMP during OGD (see Appendix 4, Figure 13.3 C). In contrast, creatine-treated slices had significantly lower IMP levels (0.5 ±

0.03 for creatine-treated slices, N = 4, $p < 0.05$ compared to control slices, $p < 0.001$ compared to Rib/Ade-treated slices, one way ANOVA).

Upon reperfusion Rib/Ade treatment resulted in significantly better recovery of ATP (Figure 7.6 A, 21.8 ± 0.4 nmol/mg protein for Rib/Ade treated slices compared to 15.3 ± 0.9 nmol/mg protein for control slices, N = 4, $p < 0.001$, one way ANOVA) and TAN levels (Figure 7.6 D, 22.0 ± 1.2 nmol/mg protein for Rib/Ade treated slices compared to 17.0 ± 0.9 nmol/mg protein, N = 4, $p < 0.05$, one way ANOVA). Despite the improved recovery of ATP in Rib/Ade treated slices there was still a 14 % reduction of the TAN pool upon reperfusion, which is similar to that observed for control slices. In contrast, creatine treatment prevented the reduction of TAN levels upon reperfusion (18.9 ± 1.4 nmol/mg protein for pre-ischemic TAN levels and 19.2 ± 1.0 upon 1 h reperfusion).

These results show that it is possible, by Rib/Ade or creatine pre-treatment to modulate the decline and recovery of intracellular adenine nucleotide levels as well as the production of ATP degradation and precursor metabolites, such as adenosine and IMP during OGD. Interestingly, allopurinol did not have a significant effect on any of the metabolites tested, potentially suggesting that the concentration used was too low.

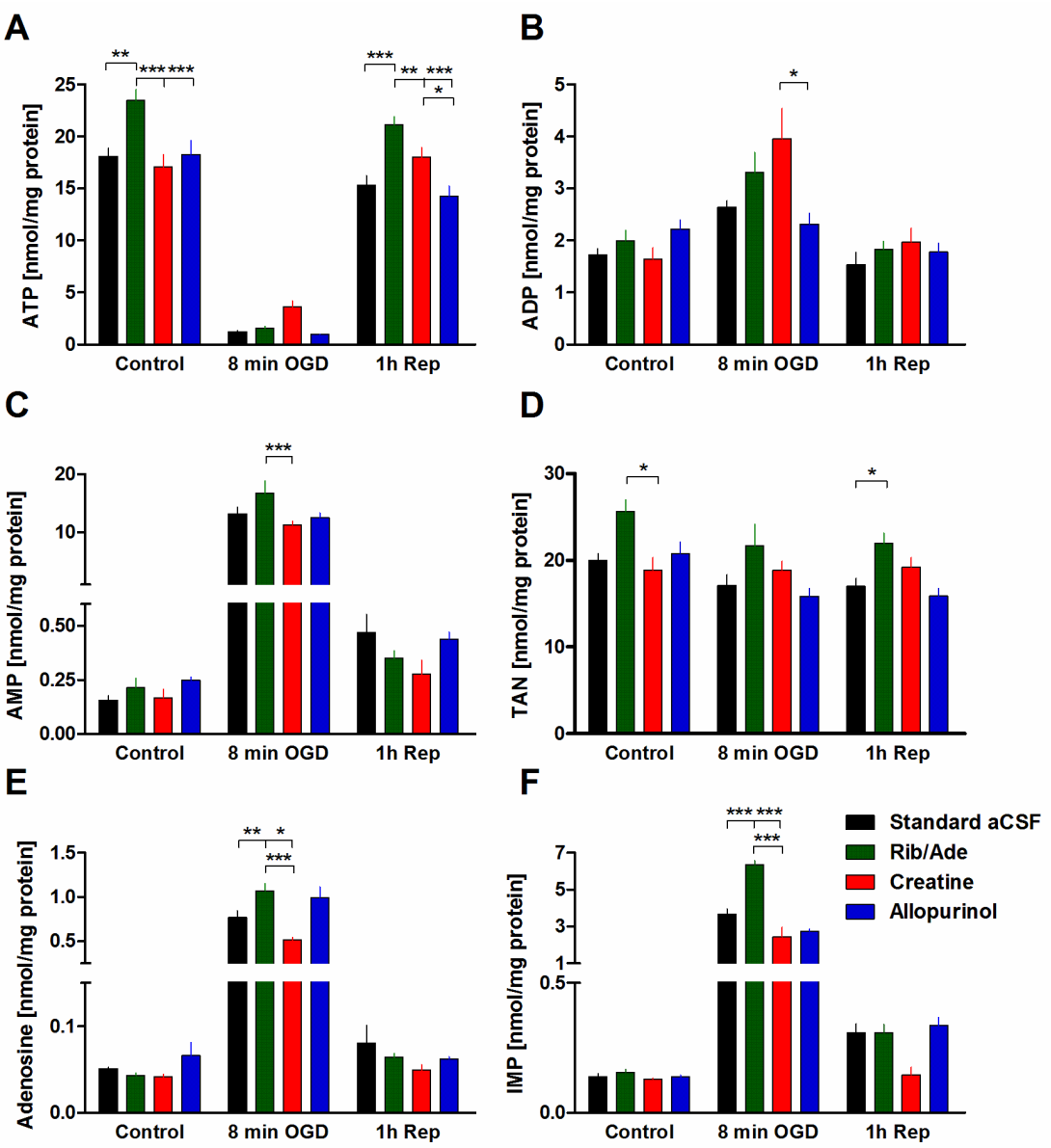

Figure 7.6: Effect of Ribose/Adenine (Rib/Ade), creatine and allopurinol on the decline and recovery of adenine nucleotide, adenosine and IMP levels upon oxygen/glucose deprivation (OGD) and reperfusion (Rep). *Brain slices were incubated in standard aCSF (black bars) or pre-treated with Rib/Ade (green bars, 1 mM/50 µM), creatine (red bars, 1 mM) or allopurinol (blue bars, 10 µM) for 3 h at 34°C before being exposed to 8 min OGD. For reperfusion, slices were transferred back to control aCSF or aCSF supplemented with these substances. HPLC analysis was performed immediately and* ***A*** *ATP,* ***B*** *ADP,* ***C*** *AMP,* ***D*** *total adenine nucleotides (TAN) as well as* ***E*** *adenosine and* ***F*** *IMP levels were measured. All values are expressed as mean ± S.E.M. N = 3 - 5 , (*) p < 0.05, (**) p < 0.01, (***) p < 0.001 between indicated groups, one way ANOVA with Bonferroni's multiple comparison test.*

7.2.2.2 Effect of Rib/Ade, creatine and allopurinol on pre- and post-ischemic energetic parameters

As seen in Figure 7.7 none of the treatments tested had any significant effects on the basal EC values or the ATP/AMP ratio, although a consistently lower ATP/AMP ratio, due to slightly elevated AMP levels (Figure 7.6 C) was observed in allopurinol-treated slices (74.5 ± 8 for allopurinol treated slices compared to 125 ± 16 for control slices, N = 4 - 5, $p > 0.05$, one way ANOVA).

During OGD creatine-treated slices had significantly higher EC values compared to all other conditions (Figure 7.7 A, 0.3 ± 0.03 for creatine-treated slices compared to 0.01 ± 0.001 for control and Rib/Ade-treated slices and 0.01 ± 0.004 for allopurinol-treated slices, N = 3 - 4, $p < 0.001$, one way ANOVA), due to a better preservation of ATP and ADP levels as seen in Figure 7.6 AB. During reperfusion EC recovered nearly completely and there was no difference in any of the conditions.

The ATP/AMP ratio (Figure 7.7 B) was significantly reduced upon reperfusion in control (38 ± 11 after 1 h reperfusion compared to a pre-ischemic value of 125 ± 16, N = 4 – 5, $p < 0.001$, one way ANOVA) and Rib/Ade-treated slices (58 ± 8 after 1 h reperfusion compared to a pre-ischemic value of 125 ± 20, N = 4 - 5, $p < 0.01$, one way ANOVA), but was not different in creatine- and allopurinol-treated slices. The reason for the first observation might be that due to the better preservation of post-ischemic ATP and TAN levels, there was a better recovery of the energetic metabolism. However, the reason for the latter observation might be that the basal ATP/AMP ratio of allopurinol-treated slices was lower under control conditions.

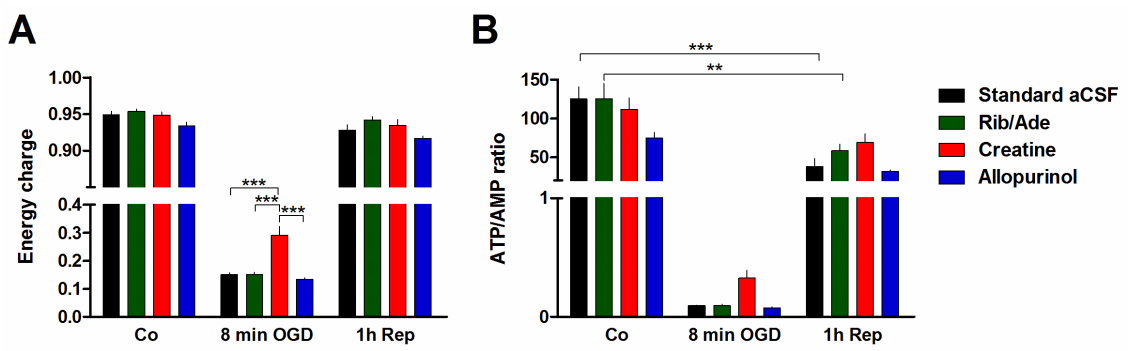

Figure 7.7: Effect of Ribose/Adenine (Rib/Ade), creatine and allopurinol on the decline and recovery of energetic parameters upon oxygen/glucose deprivation (OGD) and reperfusion (Rep): *Brain slices were incubated in standard aCSF (black bars) or pre-treated with Rib/Ade (green bars, 1 mM/50 µM), creatine (red bars, 1 mM) or Allopurinol (blue bars, 10 µM) for 3 h at 34°C before being exposed to 8 min OGD. For reperfusion, slices were transferred back to control aCSF or aCSF supplemented with these substances. HPLC analysis was performed immediately and* ***A*** *the energy charge (EC = (ATP + 0.5ADP)/TAN) as well as* ***B*** *the ATP/AMP ratio were determined. All values are expressed as mean ± S.E.M. N = 3 - 5 , (**) p < 0.01, (***) p < 0.001 between indicated groups, one way ANOVA with Bonferroni's multiple comparison test. Where no error bars can be seen they are smaller than the symbol.*

In summary these data show that creatine pre-treatment effectively preserves pre-ischemic adenine nucleotide levels and energetic parameters upon reperfusion. Despite the fact that Rib/Ade increased both, pre- and post-ischemic ATP levels, there was still a reduction of the TAN pool by 14 % and a decreased ATP/AMP ratio upon 1 h reperfusion. Furthermore I observed differences in tissue adenosine levels during OGD upon the conditions tested. Therefore I next wanted to test the electrophysiological consequences of the modulation of tissue ATP and adenosine levels during OGD in Rib/Ade, creatine and allopurinol treated slices.

7.2.3 Modulation of intracellular high energy phosphate levels by Rib/Ade Creatine and Allopurinol – Effect on synaptic transmission

7.2.3.1 Effect of creatine and allopurinol on basic synaptic transmission

In the previous chapters I have shown that Rib/Ade had no effect on input-output curves or paired pulse ratios. I further wanted to test whether creatine or allopurinol had any effect on basic synaptic transmission. I therefore compared input-output curves (Figure 7.8 A) and paired pulse ratios (Figure 7.8 B) of brain slices incubated for 3 - 6 hrs in creatine, allopurinol or Rib/Ade + creatine and Rib/Ade + allopurinol with control slices. I did not observe any significant differences between any of the treatments tested, although a slightly elevated output was observed for Rib/Ade + creatine treated slices. Likewise a consistently higher paired pulse ratio was observed in allopurinol and Rib/Ade + allopurinol treated slices, which might reflect the slightly elevated basal tissue adenosine levels observed upon allopurinol treatment (see Figure 7.6 E).

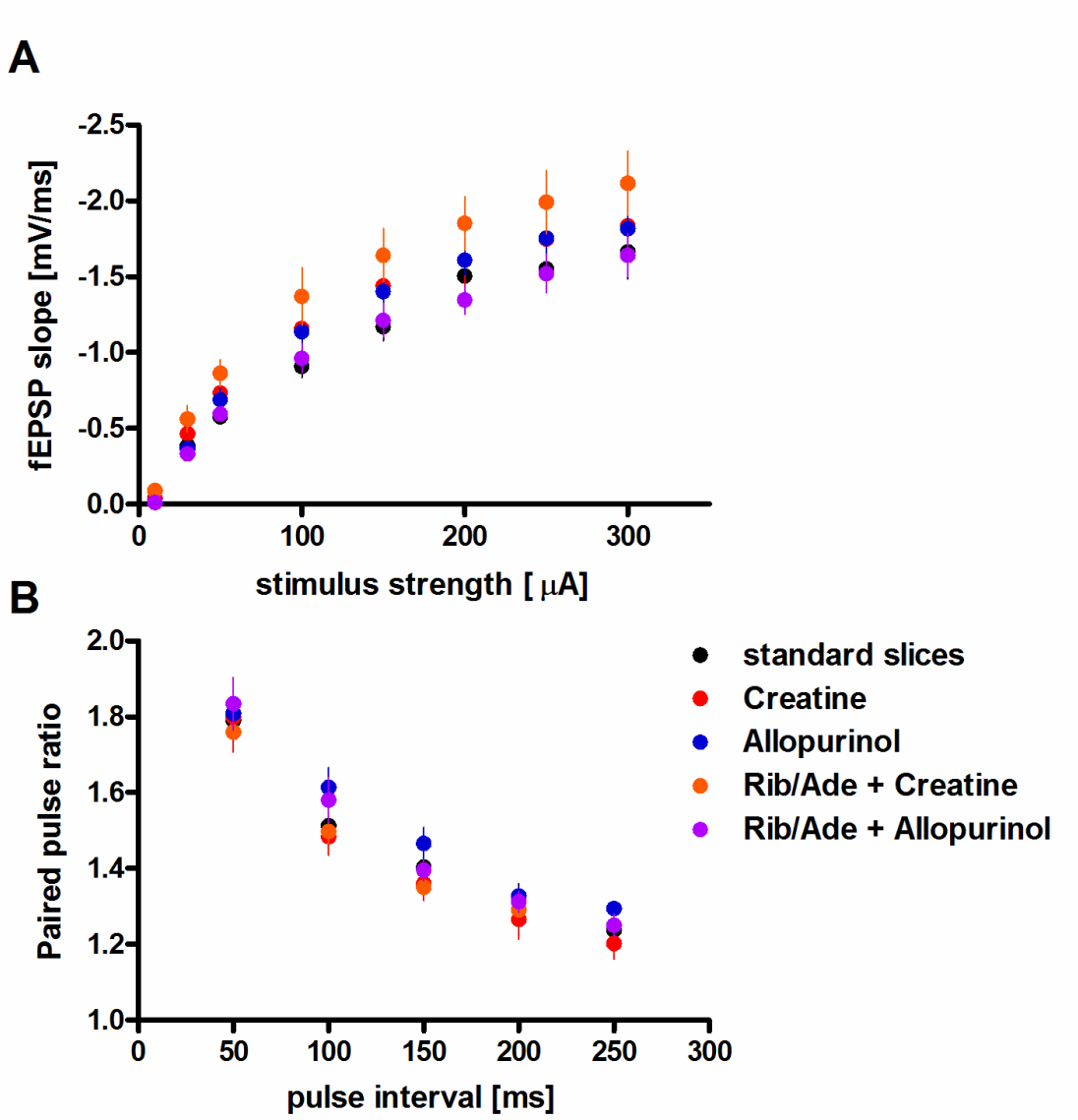

Figure 7.8: ***A*** *input/output curves and* ***B*** *paired pulse ratios for slices incubated in standard aCSF (black dots, N = 6), or in the continuous presence of creatine (red dots, 1 mM, N = 6), allopurinol (blue dots, 10 µM, N = 3), creatine + Ribose/Adenine (1 mM Rib/ 50 µM Ade, pink dots, N = 3) and allopurinol + Rib/Ade (green dots, N = 3). All values are presented as mean ± S.E.M. No significant differences observed between standard and Rib/Ade-treated slices with one way ANOVA with Bonferroni's multiple comparison test. Where no error bars can be seen they are smaller than the symbol. Recordings were performed at 33.4 ± 0.2 °C at a flow rate of 7 - 8 ml/min after a ≥ 3 h recovery period from slice cutting.*

7.2.3.2 Effect of Rib/Ade, creatine and allopurinol on the decline of synaptic transmission during OGD

Brain slices were incubated for ≥ 3 h in Rib/Ade, creatine, allopurinol or indicated combinations. After a stable baseline of 20 min was collected in the continuous presence of these substances, slices were perfused with oxygen and glucose-free aCSF. The decline of synaptic transmission, which is primarily mediated by the release of adenosine and the activation of A_1 receptors (Pearson et al., 2006; Dale and Frenguelli, 2009), and the time to 50 % inhibition of the initial fEPSP response is shown in Figure 7.9.

Rib/Ade significantly accelerated the time to 50 % inhibition of fEPSP upon onset of OGD (Figure 7.9 B, 106 ± 2.5 seconds for Rib/Ade treated slices compared to 128 ± 2.7 seconds for control slices, N = 10 - 12, $p < 0.001$, one way ANOVA) whereas creatine had the opposite effect (168 ± 7 seconds, N = 8, $p < 0.001$ compared to control slices, one way ANOVA), reflecting potential differences in adenosine release. Allopurinol on its own did not affect the time to 50 % inhibition (129 ± 9.5 seconds, N = 5, $p > 0.05$ compared to control slices, one way ANOVA). I further studied the effect of combined treatment with allopurinol + Rib/Ade, since Ade has to be applied with allopurinol to prevent its degradation to the nephrotoxic metabolite 2,8-dihydroxy-adenine (see Chapter 5). Interestingly, this combination further accelerated the time to 50 % inhibition of fEPSPs during OGD (96 ± 5.2 seconds, N = 6, $p < 0.001$ compared to control slices, one way ANOVA). This suggests that xanthine oxidase inhibition can influence the adenosine release during OGD, which becomes more obvious if the adenosine production is enhanced by Rib/Ade supplementation and is consistent with slightly elevated tissue adenosine levels during OGD in allopurinol treated slices (Figure 7.6 E). The combination of Rib/Ade and creatine, which would result in both increased ATP and phosphocreatine levels, thereby potentially counteracting each other, resulted in similar decline of fEPSPs as in control slices (133 ± 5 seconds, $p > 0.05$ compared to control slices, one way ANOVA).

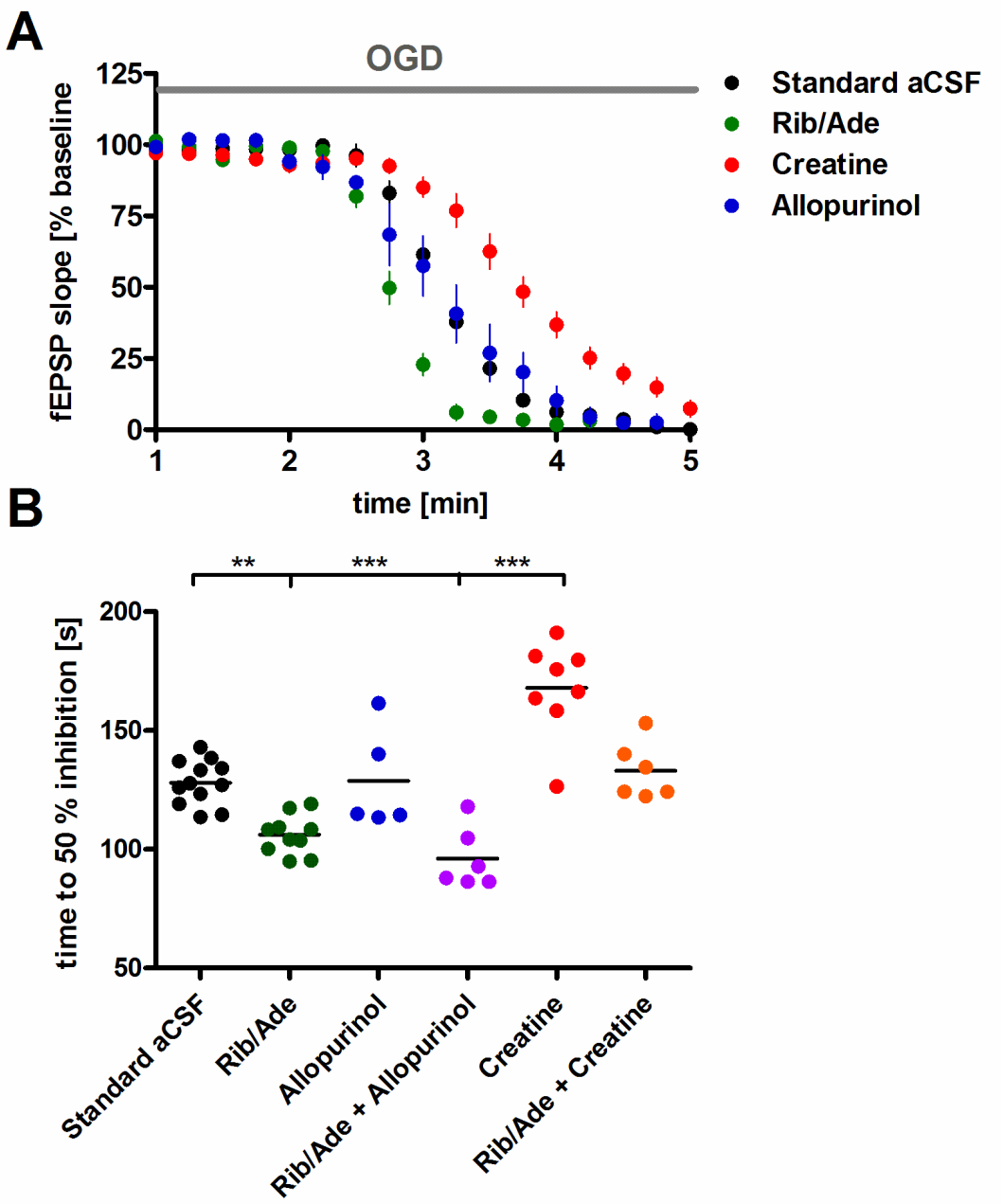

Figure 7.9: Decline of synaptic transmission during OGD in Ribose/Adenine (Rib/Ade), creatine and allopurinol treated slices: *The decline of fEPSP traces during the first 5 min of OGD is shown in* ***A*** *and the time to 50 % inhibition of the initial response, as calculated by fitting a Boltzmann sigmoidal curve to each individual experiment is shown in a scatter plot in* ***B****. Symbols refer to: Control slices (black dots, N =12) and slices treated with Rib/Ade (green dots, 1 mM/50 µM, N = 10), creatine (red dots, 1 mM, N = 8), allopurinol (blue dots, 10 µM, N = 5), Rib/Ade + Creatine (orange dots, N = 6) and Rib/Ade + Allopurinol (pink dots, N = 6). Recordings were performed at 33.4 ± 0.2 °C at a flow rate of 7 - 8 ml/min after a ≥ 3 h recovery period from slice cutting. Values in A are presented as mean ± S.E.M and values in B as individual experiments with the mean shown as black horizontal line. (**) p < 0.01, (***) p < 0.001, one way ANOVA with Bonferroni's multiple comparison test.*

7.2.3.3 Effect of Rib/Ade, creatine and allopurinol on the time to anoxic depolarisation

As explained above, the anoxic depolarisation (AD) marks the time of a complete loss of ion homeostasis. If the duration of AD is prolonged beyond a critical point there is an irreversible loss of synaptic transmission (Frenguelli, 1997; Balestrino et al., 2002; Somjen, 2002; Frenguelli et al., 2007). In order to test whether any of the treatments prolonged the time to AD, brain slices were exposed to OGD until the AD occurred, as measured by the disappearance of the presynaptic fibre volley.

In order to make sure that the age of the animal, as well as the age of the slice did not affect the time to AD, I have plotted the data obtained for control slices from different aged animals and slices against the time to AD (Figure 7.10). Neither the age of the animal (Figure 7.10 A) nor the age of the slice (Figure 7.10 B) had an effect on the time to AD. However, I have tried to avoid using animals younger than P 20 and older than P 26 and most slices were between 3 and 7 h old.

The time to AD was not different between control (N = 18), Rib/Ade (N = 7), allopurinol (N = 5) or Rib/Ade + allopurinol (N = 5) treated slices (Figure 7.10 C, values are given in the bar graphs, $p > 0.05$, one way ANOVA). However creatine (N = 4) as well as Rib/Ade + creatine (N = 4[6]) significantly delayed the occurrence of AD ($p < 0.001$ compared to other groups, one way ANOVA). Interestingly, in 3 out of 4 slices treated with creatine and in 4 out of 4 slices treated with Rib/Ade + Creatine, I observed epileptiform activity during OGD, which occurred about 1 min before AD. Furthermore in one experiment of Rib/Ade + Creatine treated slices the time to AD was delayed by 18.25 min, and this experiment was not included in the main data set since the time to AD was longer than twice the standard deviation of the mean time to AD. This slice had strong epileptiform activity for about 5 min.

[6] One experiment was excluded since the time to AD was longer than double the standard deviation.

These results show that increasing pre-ischemic ATP levels, or increasing adenosine levels during OGD does not affect the time to AD, whereas, in agreement with previous reports (Balestrino et al., 1999), delaying the degradation of ATP by creatine supplementation delays the time to AD by 60 %. These results further show that even if the pre-ischemic ATP levels are increased by Rib/Ade supplementation the combined treatment with creatine is still effective in delaying the time to AD.

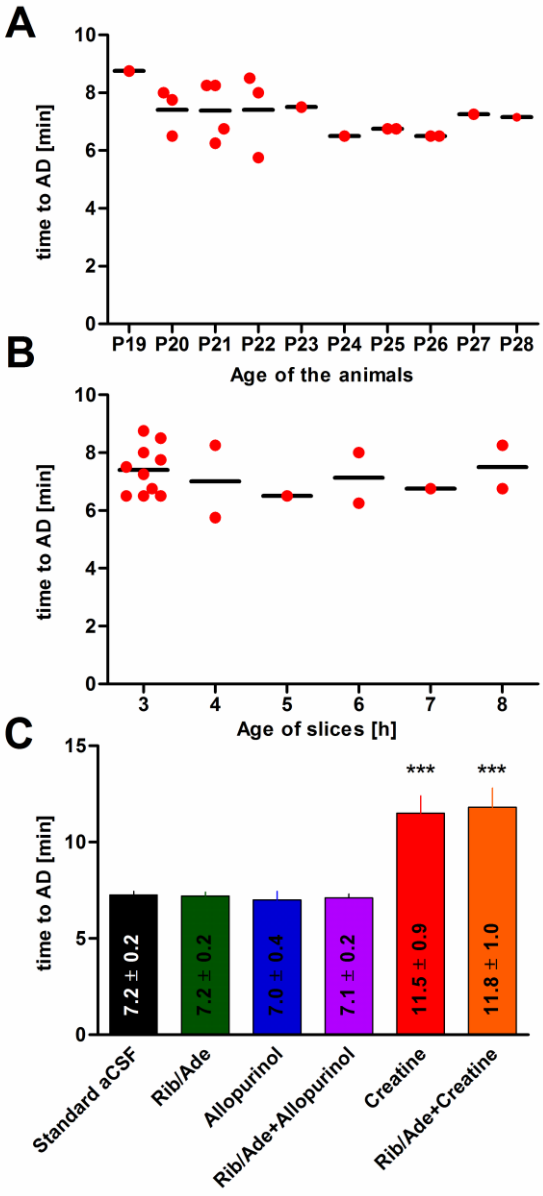

Figure 7.10: The time to Anoxic depolarisation (AD) in Ribose/Adenine (Rib/Ade), creatine and allopurinol treated slices: *Brain slices were exposed to OGD until the presynaptic fibre volley disappeard, which marks the time of AD. Neither the age (P postnatal) of the animals as shown in the scatter plot in* ***A*** *nor the age of the slices as shown in* ***B*** *seemed to influence the time to AD in control slices. For most experiments the animals were P 20 – P 26, and the slices were between 3 and 7 h old.* ***C*** *Time to AD in control slices (black bars, N = 18), slices pre-treated with Ribose and Adenine (Rib/Ade, 1 mM/ 50 µM, green bar, N = 7), allopurinol (blue bar, 10 µM, N = 5), Rib/Ade + allopurinol (pink bar, N = 7), creatine (red bar, 1 mM, N = 4) or Rib/Ade + creatine (orange bar, N = 4). Creatine as well as Rib/Ade + creatine significantly delayed the time to AD. Recordings were performed at 33.4 ± 0.2 °C at a flow rate of 7 - 8 ml/min after a ≥ 3 h recovery period from slice cutting. Values in A and B are presented as individual experiments with the mean shown as horizontal line and values in C are shown as mean ± S.E.M. (***) p < 0.001, one way ANOVA with Bonferroni's multiple comparison test.*

7.2.3.4 Effect of Rib/Ade, creatine and allopurinol on the recovery of synaptic transmission after OGD

I further aimed to study the effect of Rib/Ade, creatine and allopurinol on the recovery of synaptic transmission after OGD. Therefore pre-treated slices were exposed to OGD until the AD occurred (mean times are shown in Figure 7.10 C) and then super-fused again for 1 h with aCSF supplemented with the previous treatment (Figure 7.11).

The recovery of synaptic transmission 1 h after the ischemic insult was not different between control (Figure 7.11 A, 21 ± 7.6 % of the intial fEPSP baseline), Rib/Ade (27 ± 5.6 %) or allopurinol treated slices (42 ± 10 %, $p > 0.05$ compared to control slices, one way ANOVA). Surprisingly creatine and Rib/Ade + creatine treated slices showed a nearly complete recovery of synaptic transmission (92 ± 3.2 % for creatine treated slices and 94 ± 2 % in Rib/Ade + creatine treated slices, $p < 0.001$ compared to all other groups, one way ANOVA).

In three experiments I applied 8-CPT after 1 h reperfusion to Rib/Ade treated slices, to test whether the incomplete recovery was due to increased adenosine levels (Appendix 4, Figure 13.4). In one slice the baseline increased by 250 %, however in the other two the baseline increased by 28 %, which is slightly higher but still close to the effect of 8-CPT on pre-ischemic baseline in control slices (see Chapter 6, 21 % increase). This suggests that extracellular adenosine levels might be slightly elevated after 1 h reperfusion in Rib/Ade slices, but do not alone account for the incomplete recovery of synaptic transmission.

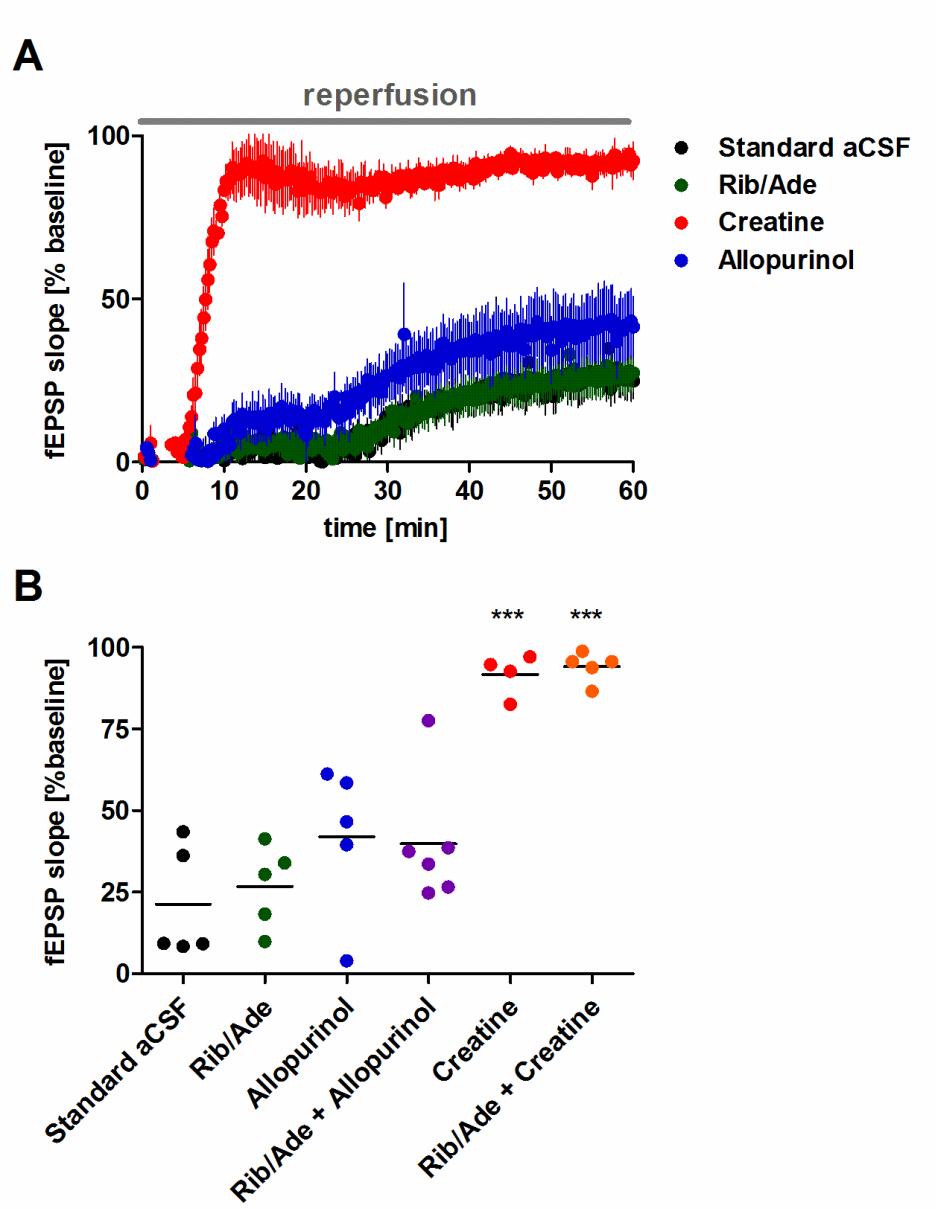

Figure 7.11: Recovery of synaptic transmissionin Ribose/Adenine (Rib/Ade), creatine and allopurinol treated slices: *Slices were exposed to OGD until AD occurred and reperfusion was induced as soon as the presynaptic fiber volley disappeared. It took ~ 1 min until the fibre volley appeared again. Slices were reperfused with the treatment they obtained before, which was either standard aCSF (black dots, N = 5), or aCSF supplemented with Ribose and Adenine (Rib/Ade, 1 mM/ 50 µM, N = 5), creatine (1 mM, N = 4), allopurinol (10 µM, N = 5), Rib/Ade + creatine (N = 5) or Rib/Ade + allopurinol (N = 6). The recovery of fEPSP traces during 1 h of reperfusion is shown in **A** and a scatter plot of the degree of recovery for individual treatments 60 min after OGD, expressed as a percentage of the pre-ischemic fEPSP baseline is shown in **B**. Recordings were performed at 33.4 ± 0.2 °C at a flow rate of 7 - 8 ml/min after a ≥ 3 h recovery period from slice cutting. Values in A are presented as mean ± S.E.M and values in B as individual experiments with the mean shown as horizontal line. (***) p < 0.001, one way ANOVA with Bonferroni's multiple comparison test.*

The creatine concentrations used in other *in vitro* studies (Whittingham and Lipton, 1981; Lipton and Whittingham, 1982) were higher (5 – 25 mM) than 1 mM, and a dose dependent increase in the phosphocreatine content between 1 and 10 mM creatine upon a 2 h incubation period has been described (Balestrino et al., 1999). I did not observe any differences in the decline of synaptic transmission during OGD in two slices treated with 5 mM Creatine compared to 1 mM Creatine (see Appendix 4 Figure 13.5 A). The mean time to AD in 5 mM Creatine-treated slices was slightly longer at 13.25 (compared to 11.5 min in 1 mM Creatine treated slices). However in 1 slice treated with 10 mM creatine the AD occurred after 10.25 min (data not shown), which is similar to slices treated with 1 mM Creatine, suggesting that during this long incubation period (≥ 3 h) the phosphocreatine content of slices is saturated with 1 mM Creatine exposure.

In a few experiments (N = 2 – 4) I exposed control slices to OGD and then reperfused them with Rib/Ade or creatine (Appendix 4 Figure 13.6) and measured the functional recovery over a 3 h reperfusion period. However, I obtained very variable results, although a trend towards better recovery was seen in Rib/Ade and creatine treated slices.

7.2.4 Modulation of intracellular high energy phosphate levels by Rib/Ade creatine and allopurinol – Effect on adenosine release

Since I observed differences in the decline of synaptic transmission during OGD I next wanted to measure the real time release of adenosine with biosensors in Rib/Ade and creatine treated slices. Slice were treated for 3 - 6 hrs with Rib/Ade or creatine and these substances were washed out in standard aCSF for 30 min before slices were transferred into the recording chamber. I have shown before that adenine levels decline back to baseline within 1 h washout (see Chapter 5, Figure 5.5) therefore tissue adenine levels did not interfere with the adenosine signal. I did not test allopurinol treated slices since xanthine oxidase is part of the enzyme complex in the adenosine biosensor, and allopurinol interferes with the adenosine signal (see

Appendix 4, Figure 13.1). 45 min after insertion of the sensors, fEPSPs were recorded for 20 - 30 min and then slices were exposed to 5 min OGD, to avoid the occurrence of AD, and subsequent reperfusion in standard aCSF. fEPSPs and adenosine sensor traces were recorded simultaneously (Figure 7.12).

As reflected in the faster decline of synaptic transmission and the increased tissue adenosine levels during OGD, Rib/Ade treated slices released significantly more adenosine during OGD and upon reperfusion (Figure 7.12 AB, 16 ± 1.3 μM' compared to 11 ± 0.4 μM' in control slices, N = 4, $p < 0.05$, one way ANOVA), whereas creatine treated slices released significantly less adenosine (5 ± 0.5 μM', N = 3, $p < 0.01$ compared to control slices, one way ANOVA) as measured by the peak during the post-ischemic purine efflux (Frenguelli et al., 2003). This correlates with a delayed recovery of synaptic transmission in Rib/Ade treated slices, due to increased extracelluar adenosine levels (Figure 7.12 AD). Furthermore, Rib/Ade and standard slices showed the same pattern of adenosine release, whereas creatine treated slices seemed to differ (Figure 7.12 A), by showing a peak and then a plateau at an elevated level. The full time course of adenosine release and fEPSP traces, for Rib/Ade, creatine and Rib/Ade + creatine treated slices is shown in Appendix 4, Figure 13.7. Interestingly the adenosine release in Rib/Ade + Creatine treated slices was more similar to the trace observed for creatine treated slices than to Rib/Ade treated slices. This further shows that the intracellular phosphocreatine levels can still buffer the decline of the higher ATP levels and hence the production of adenosine in Rib/Ade treated slices and is in agreement with the similar time to AD in creatine and Rib/Ade + creatine treated slices (Figure 7.10 C).

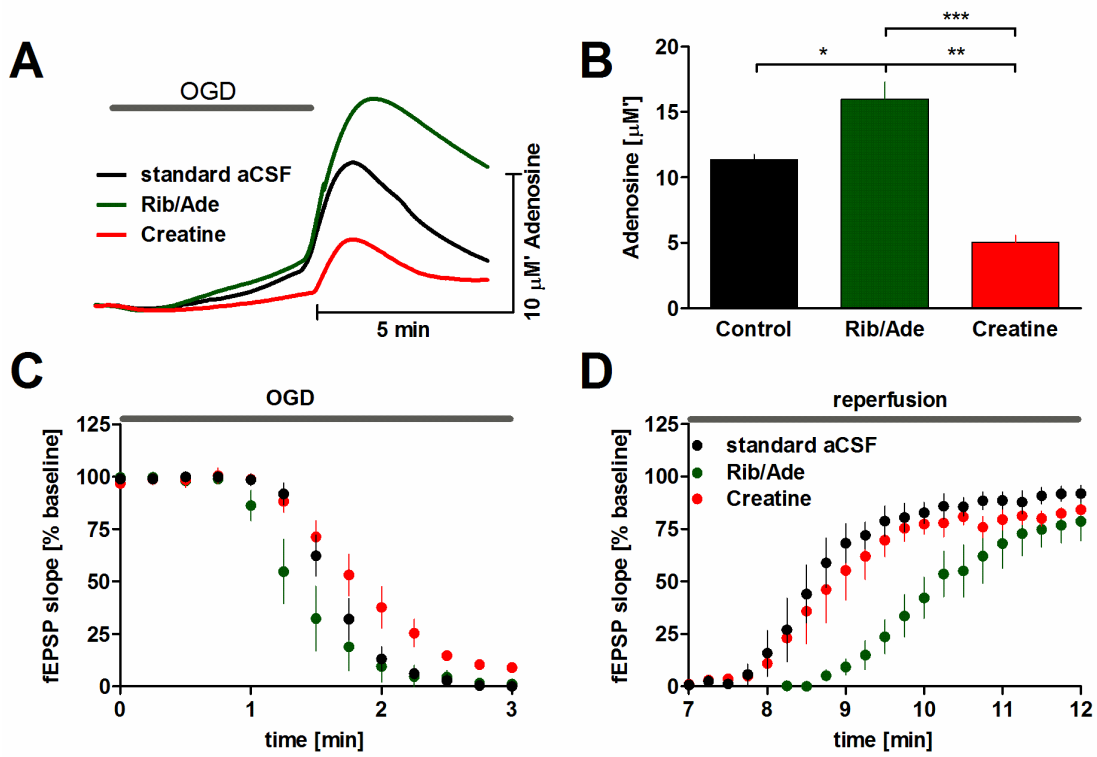

Figure 7.12: Modulation of intracellular adenine nucleotides with Ribose/Adenine (Rib/Ade) or creatine influences adenosine release during OGD: A *mean traces for adenosine sensor recordings of control slices (black trace, N = 4), slices pre-treated with Ribose and Adenine (Rib/Ade, green trace, N = 4) or Creatine (red trace, N = 3).* ***B*** *The peak height during the postischemic purine efflux was calculated and expressed as µM' Adenosine. Simultaneously to sensor traces fEPSPs were recorded as shown in C and D.* ***C*** *Decline of synaptic transmission during the first 3 min of OGD and* ***D*** *recovery of synaptic transmission after OGD. Note the accelerated decline and delayed recovery of fEPSPs in Rib/Ade treated slices, which reflects the increased extracellular adenosine levels. Values in A are expressed as mean and values in BCD are expressed as mean ± S.E.M. (*) p < 0.05, (**) p < 0.01, (***) p < 0.001, one way ANOVA with Bonferroni's multiple comparison test.*

I further wanted to study the effect of two brief ischemic periods on adenosine release, to test whether Rib/Ade could replenish the reduced adenosine release observed during subsequent ischemic periods *in vitro* (Pearson et al., 2001) and *in vivo* (Valtysson et al., 1998). Therefore I wanted to find a protocol, which would result in partial recovery of synaptic transmission during the first ischemic period and accelerated recovery of synaptic transmission during the second ischemic period of the same duration, as shown before (Pearson et al., 2001). However, I was not able to establish an appropriate protocol due to very inconsistent results (see Appendix 4, Figure 13.8). In slices exposed to 6.25 or 6 min OGD (Pearson et al., 2001), I sometimes observed a complete recovery of synaptic transmission during the first and second ischemic period, and sometimes the AD occurred during the second ischemic insult resulting in delayed and incomplete recovery of synaptic transmission. Shorter ischemic periods (5 min) always resulted in complete recovery of synaptic transmission and longer ischemic period (6.5 min or 7 min, data not shown) always resulted in the occurrence of AD during the second ischemic insult. This might be due to different age of the animals since it has been shown that the AD in older animals (P 20) occurs faster than in younger animals (P 12) (Madry et al., 2010) and the animals in (Pearson et al., 2001) were P 12 – P 24, as opposed to P 20 – P 26 in this study.

7.3 Discussion

In summary these data show that it is possible to modulate the decline and recovery of intracellular ATP levels, by increasing the pre-ischemic tissue ATP content with Rib/Ade or the tissue phosphocreatine content with creatine. This has measurable consequences on the decline and recovery of synaptic transmission and release of neuroprotective adenosine during OGD.

7.3.1 Effect of OGD on adenine nucleotide levels and synaptic transmission

Data in the literature (Whittingham et al., 1984a; Milusheva et al., 1996; Newman et al., 1998) and my own results show that brain slices behave in the same way as the *in vivo* brain with respect to the rapid deline and incomplete recovery of ATP levels and synaptic transmission (Schurr and Rigor, 1989). That is that ATP and TAN concentrations decrease progressively with the duration of ischemia which negatively affects the recovery of ATP, due to a reduction in the TAN pool. Likewise the decline and recovery of synaptic transmission in hippocampal brain slices reflects observations reported for *in vivo* brain, showing that if the ischemic period is prolonged beyond a critical point there is no recovery of synaptic transmission (Somjen, 2002; Krnjevic, 2008). Therefore, by establishing a protocol which results in incomplete recovery of TAN levels as well as synaptic transmission, brain slices can be easily used to screen for the effect of potential neuroprotective interventions on energetic and functional recovery from ischemic insults.

7.3.2 Manipulations of intracellular high energy phosphate levels

The approach of pre-treating brain tissue with neuroprotective substances might be useful for clinical interventions, where a known risk of global or cerebral ischemia exists, such as operations on the open heart, atherectomy of carotid arteries or high stroke risk patients. From the manipulations tested in this chapter (Rib/Ade, creatine, allopurinol) the most effective ones were Rib/Ade and creatine. Rib/Ade-treatment results in increased tissue ATP levels, increased adenosine release and improved

recovery of post-ischemic ATP levels. Creatine treatment on the other hand delays the degradation of ATP during ischemia, improves the EC during ischemic periods, helps to maintain post-ischemic ATP levels, and results in a nearly complete recovery of synaptic transmission after OGD.

7.3.2.1 Pre-treatment with Rib/Ade to increase adenosine release and improve post-ischemic ATP recovery

To my knowledge there is one report, where the recovery of post-ischemic ATP levels in brain slices was improved upon addition of 1 mM Ade (Newman et al., 1998). However, despite this study, pre- or post-ischemic Rib/Ade or Ade administration has not been studied in brain tissue. In contrast, the positive effect of Rib or Rib/Ade on the recovery of post-ischemic myocardial ATP and TAN levels in *in vitro* and *in vivo* preparations is well documented (Zimmer, 1982; Mauser et al., 1985; Zimmer et al., 1989; Zimmer, 1996; Muller et al., 1998; Smolenski et al., 1998; Perkowski et al., 2007). The improved post-ischemic ATP recovery has been linked to an enhanced functional recovery of the heart, as seen in improved cardiac contractility (Pasque and Wechsler, 1984; Lamberts et al., 2007; Schneider et al., 2007). Rib was also effective in improving renal ischemic injury (Nishiyama et al., 2009; Sato et al., 2009). Likewise administration of Rib to patients suffering from congestive heart failure (Pliml et al., 1992; Omran et al., 2003; Omran et al., 2004; Maccarter et al., 2008) has been shown to have beneficial effects on cardiac function. Hence, Rib has been suggested as a supplement to improve cardiac energy metabolism (Pauly and Pepine, 2000; Shecterle et al., 2010). However, despite the improved recovery of post-ischemic ATP levels in Rib/Ade-treated slices, I did not observe any positive effect on the functional recovery in brain slices. This might be due to the fact that, despite the higher post-ischemic ATP levels in Rib/Ade slices, the reduction compared to pre-ischemic values (14 %) was similar to that in control slices, and that the ATP/AMP ratio has not completely recovered during 1 h reperfusion. Most of these studies, cited above, were done over a reperfusion period of minimally 5 h and up to 24 h. Even for combined administration of Rib/Ade a 5 h reperfusion period was chosen (Zimmer, 1998). Therefore the lack of any effect on

Rib/Ade supplementation on the functional recovery of brain slices in this chapter might be due to a too short reperfusion period.

However, Rib/Ade treated slices released significantly more adenosine during ischemia, which might have protective effects in the *in vivo* ischemic brain. It has been shown that pre-ischemic administration of adenosine deaminase inhibitors increases adenosine release from rat brain during ischemia (Phillis et al., 1991). Adenosine can via activation of A_2 receptors enhance cerebral blood flow (Phillis et al., 1985; Phillis, 1989) which would improve the oxygen and glucose supply to hypoperfused areas. Accordingly pre-ischemic administration of the adenosine deaminase inhibitor deoxycoformycin has been shown to protect the *in vivo* brain from ischemic brain injury (Phillis and O'Regan, 1989; Lin and Phillis, 1992). Furthermore the reduced tissue ATP levels observed *in vivo* after cerebral ischemia may via reduced extracellular adenosine and reduced activation of the anticonvulsant A_1R (Boison and Stewart, 2009; Dale and Frenguelli, 2009) contribute to the development of post-ischemic epilepsy (Camilo and Goldstein, 2004; Kadam et al., 2010). The influence of intracellular ATP on extracellular adenosine and neuronal excitability has recently been described (Kawamura et al., 2010), and an increase in intracellular ATP with a concomitant increase in extracellular adenosine has been proposed of being the basis for reduced incidence of seizures during a ketogenic diet (Masino and Geiger, 2008). Therefore Rib/Ade treatment and increased adenosine release during periods of energy depletion might be useful to enhance cerebral blood flow through A_2 receptor activation and inhibit post-ischemic seizure activity through greater activation of the anticonvulsant adenosine A_1 receptor.

7.3.2.2 Pre-treatment with Creatine to delay the degradation of ATP

The alternative approach of delaying the degradation of ATP by pre-incubation with creatine proved more effective in terms of delaying the time to AD and improving the functional recovery during the short reperfusion period tested. The protective effect of creatine pre-treatment by delaying the time to AD in ischemic brain slices (Kass and Lipton, 1982; Lipton and Whittingham, 1982; Balestrino et al., 1999) and improving the anoxia-induced impairment of protein synthesis (Carter et al., 1995)

has been reported earlier. Furthermore it has been shown that pre-ischemic administration of creatine and Rib was effective in preserving cell viability of myocytes (Caretti et al., 2010). Since creatine is well tolerated in humans, the approach of treating high stroke risk patients with creatine supplementation has been suggested (Zhu et al., 2004; Gualano et al., 2011).

Creatine can enter the cells through creatine transporters and an increased phosphocreatine content in *in vivo* rat brain has been shown after intracerebroventricular creatine application (Rebaudo et al., 2000). However after a single bolus intraperitoneal administration with a high creatine dose (160 mg/kg at its solubility limit) brain creatine levels only increased by 70 µM, which is a minor amount compared to the total cellular creatine and phosphocreatine pool of about 10 mM (Balestrino et al., 2002; Perasso et al., 2003). This suggests a weak blood-brain permeability of creatine through the creatine transporter, and it has been shown that prolonged continuous oral administration of creatine (weeks) is required to raise brain creatine levels of healthy human subjects , and even then only by 10 % (Dechent et al., 1999; Lyoo et al., 2003). Accordingly prophylactic creatine administration for 1 month is effective in reducing the post-ischemic caspase-cell death cascades in mice and thereby preserving cell viability (Zhu et al., 2004). Creatine has also been shown to improve hypoxic/ischemic damage in neonatal rats at even shorter pre-treatment periods (days) (Berger et al., 2004). Shorter pre-treatment periods in adult animals (1 week) (Zhu et al., 2004) or addition of creatine after the ischemic insult (Berger et al., 2004) were not protective. However, a novel Phosphocreatine-Mg-acetate complex has been developed which can cross the blood-brain barrier independently of the creatine transporter. This complex increases cerebral phosphocreatine levels and has been shown to be neuroprotective even if given 30 or 60 min prior to ischemic insults in mice (Perasso et al., 2009). Interestingly, another study showed that the reduced infarct volume in mice which were pre-treated that creatine was not linked to increased cerebral phosphocreatine levels but to improved cerebrovascular protection (Prass et al., 2007).

Slices in this report were exposed to OGD until the AD occurred, so the severity of the ischemic insult was the same in all conditions. Nevertheless, creatine was still

effective in improving the post-ischemic recovery of synaptic transmission, which might not be solely linked to increased phosphocreatine levels. For example creatine itself has been shown to have mild antioxidant effects, primarily against free radical ions (Lawler et al., 2002; Sestili et al., 2006). During both ischemia and reperfusion, neuronal injury is worsened by the generation of oxygen radicals which damage essential cellular components and activate apoptotic signalling mechanism (Schmidley, 1990; Doyle et al., 2008). Radical scavengers improve cell viability (Ginsberg, 2008), and this effect does not depend upon pre-incubation and might therefore explain why the continuous presence of creatine upon reperfusion might further improve functional recovery.

However the fact that creatine pre-treated slices exposed to OGD undergo a short epileptiform activity before occurrence of the AD, has to be considered. This might be caused by the fact that adenosine levels are lower, and therefore the high extracellular potassium concentrations during ischemia (Dirnagl et al., 1999) might shift the brain slice towards epileptiform activity. Nevertheless, from all treatments tested creatine was the most effective intervention in terms of improving functional recovery.

7.3.2.3 Pre-treatment with allopurinol to inhibit production of unsalvageable metabolites

Unlike Rib/Ade or creatine pre-treatment of brain slices, allopurinol had no measurable effects on the recovery of adenine nucleotides or synaptic transmission. However, I did observe slightly elevated tissue adenosine levels under control and ischemic conditions. This effect has been reported *in vivo* as well, and was linked to the antinociceptive role of allopurinol administration (Schmidt et al., 2009). The fact that xanthine oxidase inhibition can influence adenosine levels is further emphasised by an increased decline of synaptic transmission during OGD in Rib/Ade + allopurinol treated slices. In agreement with these results pre-treatment of newborn piglets with allopurinol increased adenosine and inosine levels in cerebral cortex during hypoxia (Marro et al., 2006).

Pre-treatment with oxypurinol, the active xanthine oxidase inhibitor, enhanced postischemic recovery of adenine nucleotide levels (Phillis et al., 1995) and helped to reduce the cerebral infarct zone in the ischemic rat brain (Lin and Phillis, 1991, 1992). Interestingly the neuroprotective effect was still evident when allopurinol or oxypurinol was administered after the ischemic insult (Lin and Phillis, 1992; Palmer et al., 1993) and the authors proposed that this effect is not likely linked to increased adenosine levels, since at that time adenosine levels have fallen back to baseline values. In addition to enhancing the purine salvage pathway, allopurinol has been shown to act as a scavenger of free radicals (Das et al., 1987), which as explained above can improve cell viability and function. Therefore, it has been suggested that the protective effect of oxypurinol on post-stroke treatment might be linked to its radical scavenging action (Phillis and Sen, 1993) as well as inhibition of further degradation of hypoxanthine levels (Lin and Phillis, 1992), which are elevated for up to several hours after ischemia (Hillered et al., 1989).

In summary these results show that it is possible to modulate ATP levels using compounds safe for use by humans and they have the expected effects on the release of adenosine and the energetic recovery of the tissue.

The brain slice is a good model system to study neuroprotective interventions, and establish their short term effect on a variety of functional and metabolic conditions. However, in order to study long term reperfusion acute brain slices are not suited since they can only be maintained for $\leq$ 9 h incubation period (see Appendix 4, Figure 13.1). The limitations of brain slices required me to move to long term reperfusion *in vitro* model of cerebral ischemia. Hence, in order to establish the effect of Rib/Ade on cell viability if added after the ischemic insult andfor longer reperfusion studies (12 – 14 h) I used a primary neuronal cell culture. Therefore in the next chapter I will present data obtained from cerebellar granule cells, pre- or post-treated with various combinations of Rib and/or Ade.

8 Modulation of intracellular ATP levels in *in vitro* models of cerebral ischemia – Effect on cell viability

8.1 Introduction

As shown in Appendix 4, Figure 13.1 the metabolic integrity of slices is limited, and I observed a 20 % reduction of TAN levels after 9 h incubation. In an earlier report brain slice TAN levels have been shown to be stable for 8 h (Whittingham et al., 1984b), therefore the experimental window in brain slices (after a 3 h recovery period) is limited. Hence, in order to test the effect of Rib/Ade on cell viability during prolonged reperfusion periods I used cerebellar granule cells.

In addition to the incomplete recovery of post-ischemic ATP levels observed in *in vivo* models of stroke (Kleihues et al., 1975; Levy and Duffy, 1977) and as seen in the previous chapter in hippocampal brain slices, a secondary deterioration of ATP and phosphocreatine levels can be observed during prolonged reperfusion (Hata et al., 2000a), suggesting marked imbalances between energy use and production (Schaller and Graf, 2004). At the cellular level reperfusion injury involves a reduction in the mitochondrial respiratory chain, increased production of reactive oxygen species, transient but large imbalances in mitochondrial Ca^{2+} homeostasis, suppression of protein synthesis, as well as activation of deleterious signalling cascades. This eventually leads to cell death via necrosis and apoptosis (Schaller and Graf, 2004). It has therefore been suggested that the compromised ATP levels might contribute to the ongoing loss of tissue upon reperfusion (Hashimoto et al., 1992; Lust et al., 2002).

Prophylactic treatment of brain tissue with substances that can delay the degradation of ATP, such as creatine (Berger et al., 2004; Perasso et al., 2009), or improve the post-ischemic recovery of ATP, such as allopurinol (Lin and Phillis, 1991; Phillis et al., 1995), have been shown to be neuroprotective in the *in vivo* ischemic brain. In agreement with these reports, results from the previous chapter show that creatine pre-treatment significantly delays the time to anoxic depolarisation and helps to improve the functional recovery after ischemia. However, an intervention that could improve cell viability and function if given after the ischemic insult would be more helpful for acute stroke patients.

Therefore the aim of this chapter was to test whether Rib and/or Ade administration, which increase post-ischemic ATP levels in hippocampal brain slices, is an effective intervention to improve cell viability after OGD in a long term model of reperfusion. As an *in vitro* model for these studies I used cultures of cerebellar granule cells (CGC), since they are reported to contain 95% neurons (Thangnipon et al., 1983) and are therefore a good model system to study in a relatively pure neuronal population.

In this chapter I will show that the combined treatment of post-ischemic neurons with Rib/Ade helps to preserve cell viability during prolonged reperfusion periods.

8.2 Results

8.2.1 Effect of various D-Ribose concentrations on basal cell viability

In a first set of experiments I studied the effect of various Rib concentrations on cell viability in CGC. Neurons were cultured with 2.5 – 50 mM Rib for 2 days and cell viability was assessed with Hoechst (stains all cells, blue) and propidium iodide (stains dead cells, red). As seen in Figure 8.1, Rib at concentrations from 2.5 - 10 mM had no adverse effects on cell viability. These concentrations were also used in myocardial cell cultures (Kalsi et al., 1998; Smolenski et al., 1998) and blood Rib concentrations up to 6 mM has been shown to be well tolerated in humans (Salerno et al., 1999). However, incubating cells with 50 mM Rib led to a nearly complete loss of all neurons (Figure 8.1 A). This might be either caused by osmotic stress or impurities of the drug. In addition recent publications, have shown that Rib, at high concentrations (1 M), can result in non-enzymatic ribosylation of α-synuclein (Chen et al., 2010a) and tau (Chen et al., 2009). These ribosylated proteins aggregate and exert cytotoxic effects. However, this effect was only observed with 1 M Rib and after a ≥ 24 h incubation of the pure protein.

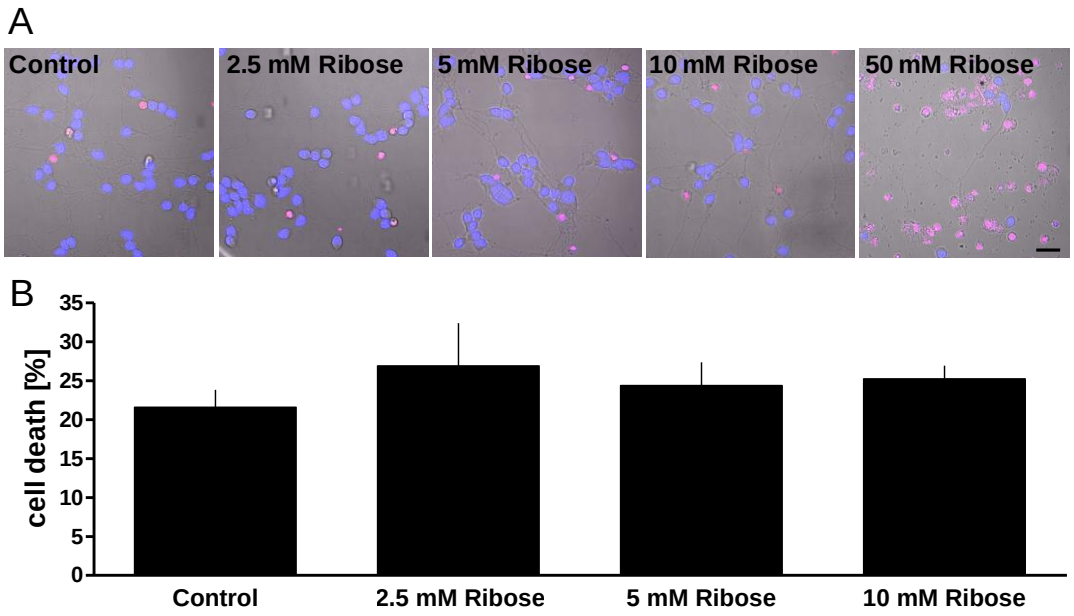

Figure 8.1: Effect of Ribose on cell viability: *After 6 - 7 days in vitro cells were incubated with various Ribose concentrations (2.5 - 50 mM) and were stained for cell death 48 h later with Hoechst (blue stain, all cells) and propidium iodide (red stain, dead cells).* ***A*** *Representative images showing the merged bright field/Hoecht/propidium iodide staining. All pink cells are dead cells. Scale bar represents 20µm.* ***B*** *The percentage of dead cells was calculated ((propidium positive cells x 100)/Hoechst positive cells). There was no difference between control cells or cells treated with 2.5, 5 or 10 mM Ribose (N = 4). However most cells maintained in 50 mM Ribose were dead (N = 2), potentially due to osmotic stress or due to the ribosylation and aggregation of cellular proteins. All values are presented as mean ± S.E.M. No statistical differences were observed with one way ANOVA and Bonferroni's multiple comparison test for control cells versus Rib-treated cells (2.5 – 10 mM).*

I further wanted to establish the effect of various Rib concentrations on the energy charge (EC) of CGC (Figure 8.2). The EC for cells cultured in Rib was not different from control cells. However, the measured EC values were very low (~0.79, Figure 8.2 A) as compared to the values obtained in brain slices (~0.96) (see previous chapters). This might be due to the fact that extracts were kept at -20°C for at least 1 month before analysis, possibly resulting in degradation of ATP (see Chapter 3) (Zur Nedden et al., 2009), as seen in the high AMP levels (Figure 8.2 B). Therefore for further analysis of intracellular nucleotides CGC cell extracts were maintained over night at -20°C.

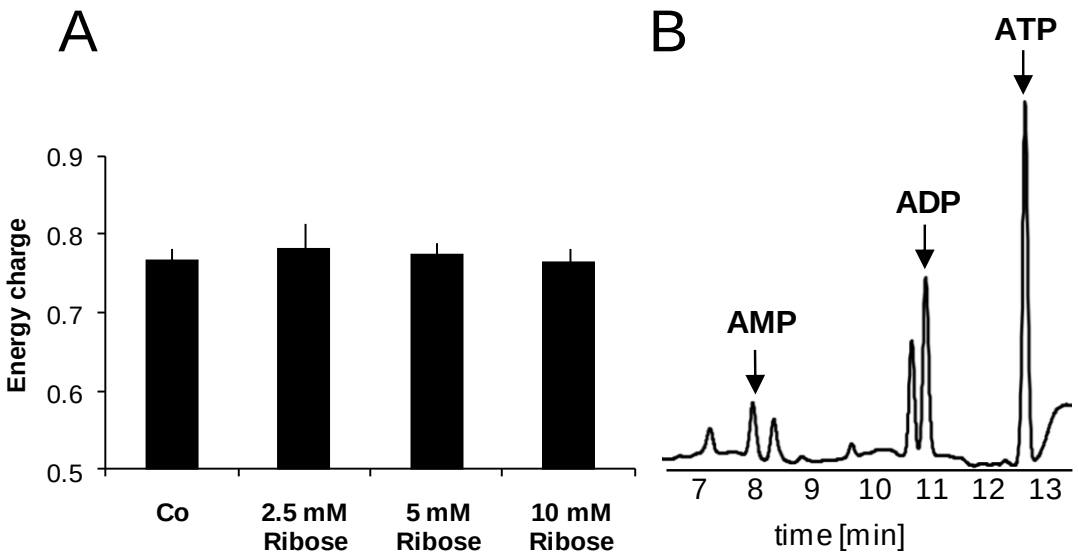

Figure 8.2: Effect of various Ribose concentrations on the cellular energy charge: *After 6 - 7 days in vitro cells were incubated with various Ribose concentrations (2.5 - 10 mM) for 2 days. Cell extracts were prepared and maintained at - 20°C for ≥ 1 month.* ***A*** *Energy charge values (EC = (ATP+0.5ADP)/TAN) from cell nucleotide extracts, N = 3.* ***B*** *Representative HPLC trace obtained from control cells. Note the very high AMP and ADP concentrations, potentially reflecting partial degradation of ATP upon prolonged storage at -20°C. All values are presented as mean ± S.E.M. No statistical differences were observed with one way ANOVA and Bonferroni's multiple comparison test.*

8.2.2 Development of an OGD model in cerebellar granule cells

For OGD in CGC the culture medium was exchanged for glucose-free PBS (Wise-Faberowski et al., 2001)(supplemented with glutamine, Pen/Strep, KCl and B27 and equilibrated with 95 % N_2/5 % CO_2), and cells were kept for 3 - 14 h in an air-tight chamber equilibrated with 95 % N_2/5 % CO_2 (Figure 8.3). 3 h OGD did not result in increased cell death (25 %, N = 2 compared to 25 ± 5 % in control slices, N = 5). However, 6h OGD resulted in significantly increased cell death (Figure 8.3 B, 59.5 ± 6.3 %, N = 5, $p < 0.001$, one way ANOVA). Therefore 6h OGD was chosen for all future experiments.

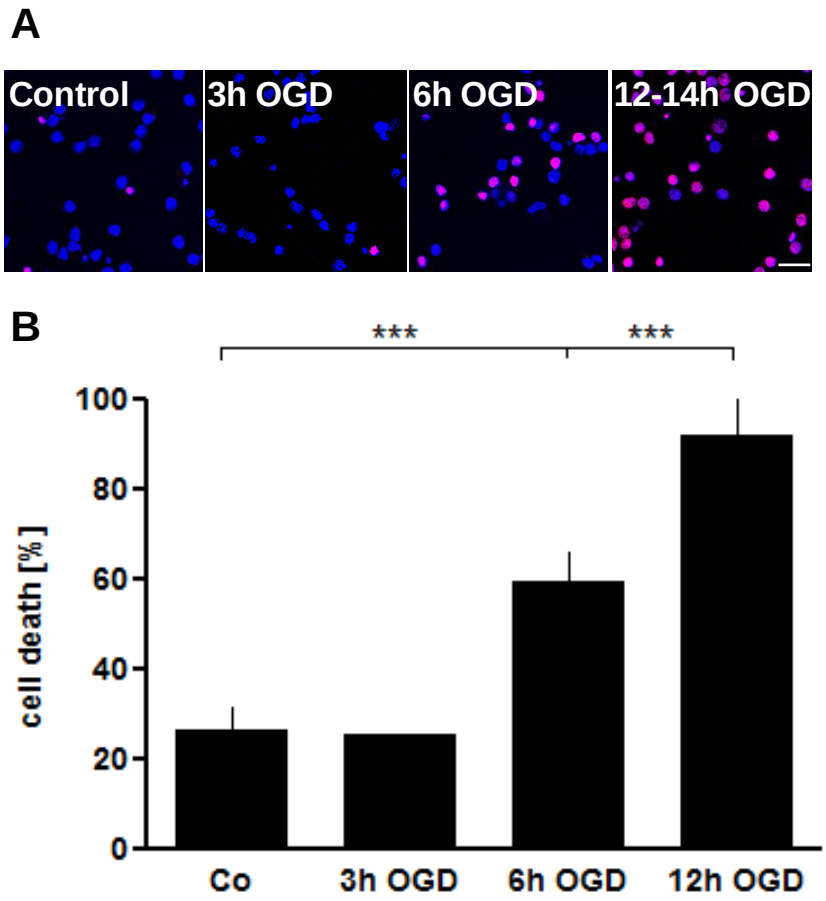

Figure 8.3: Effect of various durations of OGD on cell viability in cerebellar granule cells. *After 7 - 8 days in culture, cells were incubated in PBS (supplemented with glutamine, Pen/Strep, KCl and B27 and equilibrated for 3 h with 95 % N_2/5 % CO_2) in an airtight chamber, equilibrated with 95 % N_2/5 % CO_2. Control (Co) cells were incubated in supplemented Neurobasal medium.* ***A*** *Cell death was analysed by Hoechst (blue, all cells) and propidium iodide (red, dead cells) staining. All pink cells are dead cells. Scale bar refers to 20µm.* ***B*** *The percentage of dead cells was calculated: ((propidium iodide positive cells x 100)/ Hoechst positive cells); Values for Co, 6 h OGD and 12 h OGD are expressed as mean ± S.E.M.; N = 3 – 5. Values for 3 h OGD are presented as mean (N = 2); (***) p < 0.001 compared to Co, one way ANOVA, Bonferroni's multiple comparison test.*

8.2.3 Effect of D-Ribose and adenine on cell viability in CGC if added before the ischemic insult

In a first set of experiments I studied the effect of prophylactic administration of various Rib and/or Ade concentrations on post-ischemic cell viability in CGC. Cells were pre-treated for 3 h with various Rib and/or Ade concentrations and subsequently exposed to 6 h OGD. Cell death was assessed immediately afterwards. Control cells were incubated with Neurobasal medium (Co NB) or in PBS supplemented with glucose (equimolar to NB medium) for the same time period.

As seen in Figure 8.4 the amount of cell death in cells exposed to 6 h OGD (58 ± 5 %, N = 7) was significantly higher compared to cells incubated in Neurobasal medium (27 ± 4 %, N = 6, $p < 0.001$, one way ANOVA) as well as cells incubated for 6 h in glucose-supplemented PBS (22 ± 4 %, N = 3, $p < 0.001$, one way ANOVA). Furthermore there was a significant increase in cell death between cells incubated in glucose-free PBS but under normoxic conditions (36 ± 5 %, N = 5) and cells incubated in OGD ($p < 0.05$, one way ANOVA), showing that the lack of oxygen further contributes to a loss of neurons.

Rib seemed to preserve cell viability in a concentration-dependent manner, with 10 mM Rib being most effective (37 ± 2 %, N = 6, $p < 0.05$ compared to 6 h OGD, $p > 0.05$ compared to Co NB and PBS + Glucose, one way ANOVA). Ade on its own had a similar effect to 1 mM Rib on its own (48 ± 5 % for both conditions, N = 4 – 5) and the combination of Rib and Ade did not further improve the cell viability compared to Rib alone.

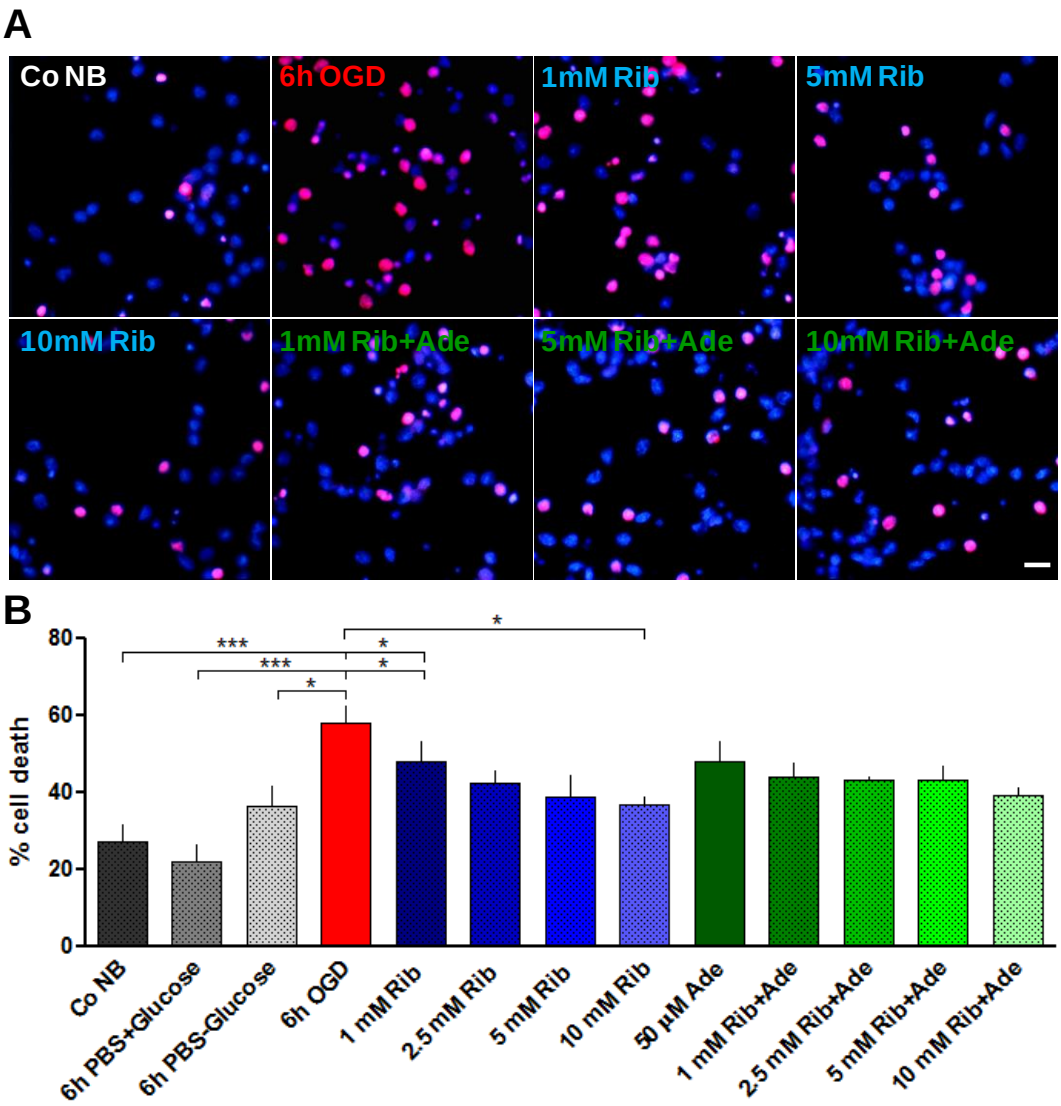

Figure 8.4: Cell death after 6 h OGD in cells pre-treated for 3 h with or without D-ribose (Rib) and/or adenine (Ade). *For control experiments cells were: (i) incubated in Neurobasal medium (Co NB), in (ii) glucose supplemented PBS (PBS + Glucose) or in (iii) glucose-free PBS but under normoxic conditions (PBS – Glucose).* ***A*** *Cell death was analysed by Hoechst (blue, all cells) and propidium iodide (red, dead cells) staining immediately after 6 h OGD. All pink cells are dead cells. Scale bar refers to 20µm.* ***B*** *The percentage of cell death calculated: ((propidium iodide positive cells x 100)/ Hoechst positive cells). All values are expressed as mean ± S.E.M; N = 3 - 6; (***) $p < 0.001$, (**) $p < 0.01$, (*) $p < 0.05$, one way ANOVA with Bonferroni's multiple comparison test.*

8.2.4 Effect of D-Ribose on TAN levels in CGC before and after ischemia

To investigate whether the improved cell viability after OGD in Rib pre-treated cells was due to a better preservation of ATP levels or energetic parameters, HPLC analysis was performed immediately after OGD. In order to prevent adenine nucleotide degradation seen in Figure 8.2, the cell extracts were stored over night at -20 °C and analysed on the next day.

However, as seen in Figure 8.5 no difference was observed in TAN, energy charge or ATP/AMP ratio levels between Rib-treated cells and control cells exposed to 6 h OGD. I further performed a nucleotide extraction after 3 h OGD, to investigate whether Rib helps cells to maintain higher ATP levels for a longer period. Preliminary results suggest that there is no change in TAN levels (Figure 8.5 E, N = 1). Further experiments, looking at pre-ischemic TAN levels and earlier time points during OGD in Rib-treated cells, will give a better idea as to how ribose and/or adenine may improve cell viability after OGD. However, there was not enough time to finish these experiments.

Interestingly the basal EC (0.98 ± 0.001) and ATP/AMP ratio values (311 ± 19) in cells were higher than in slices (EC ~ 0.96, ATP/AMP ratio ~ 100, see Chapter 4, 5 and 7). This might be due to a higher incubation temperature (37°C as compared to 34°C), since I have shown before that the ATP/AMP ratio is temperature-dependent.

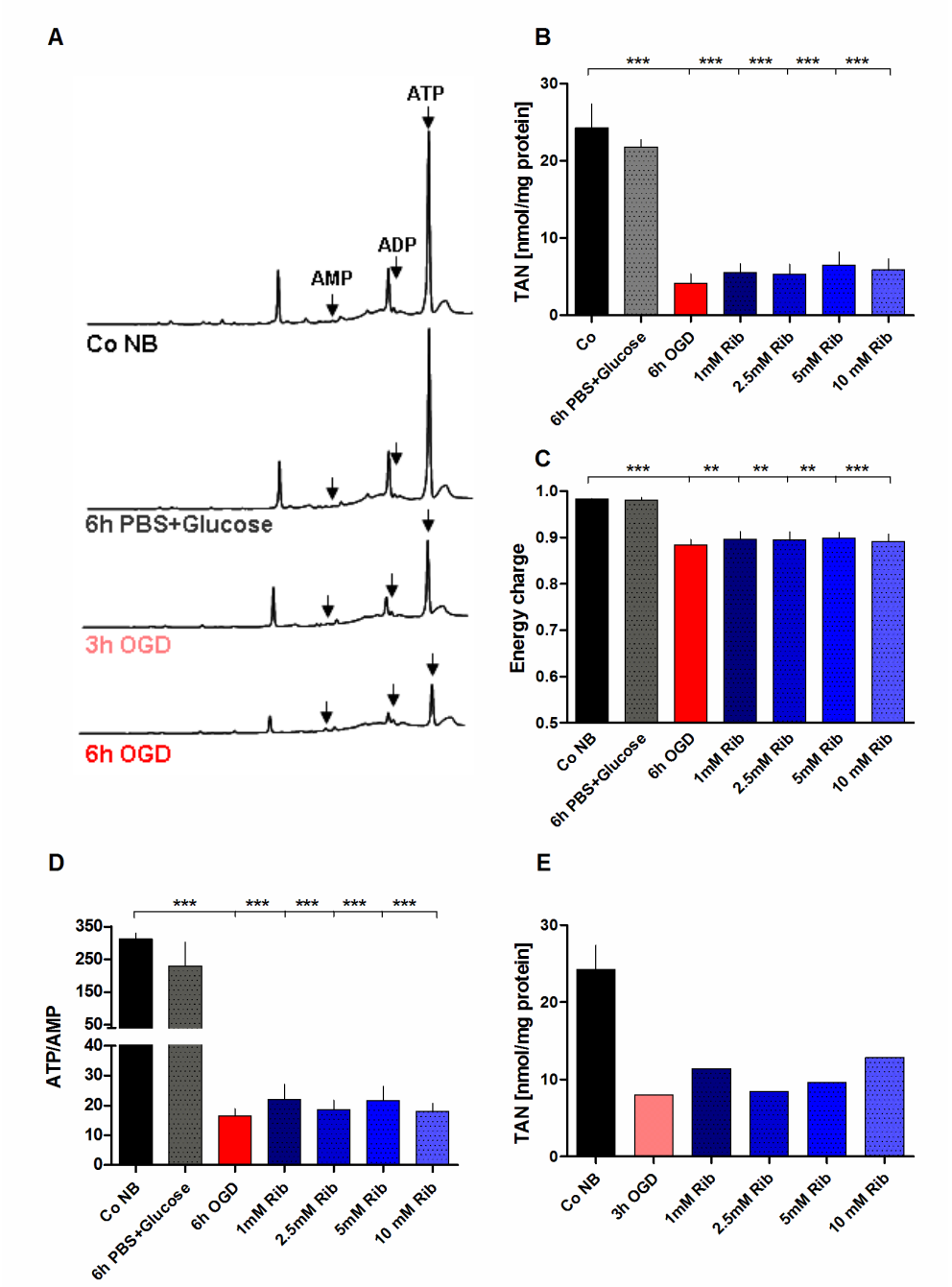

Figure 8.5: HPLC analysis of CGC extracts after 6 h OGD. A *Representative HPLC traces obtained from CGC extracts under control conditions in Neurobasal medium (Co NB), after 6 h incubation in PBS + Glucose, as well as after 3 or 6 h OGD.* ***B*** *TAN and* ***C*** *energy charge (EC) and* ***D*** *ATP/AMP ratio values obtained for CGC before and after 6h OGD and with or without prophylactic treatment (3 h) with 1 - 10 mM Ribose (Rib). B-D: All values are expressed as mean ± S.E.M; N = 4 - 5. (**) p < 0.01, (***) p < 0.001, one way ANOVA with Bonferroni's multiple comparison test.*

8.2.5 Effect of D-Ribose and adenine on cell viability in CGC after OGD for 12 – 14 h reperfusion

Having established, that Rib/Ade was beneficial if given before OGD, I further aimed to test the effect of Rib and/or Ade on cell viability, if added after the ischemic insult for prolonged reperfusion periods (12 – 14 h). Cells were therefore exposed to 6 OGD (or 6 h PBS + Glucose) and thereafter the OGD medium was replaced by the previous Neurobasal culture medium, which was supplemented with or without Rib and/or Ade. Rib and Ade had no adverse effects on cell viability, when added for 24 h (Figure 8.6) and there was no significant difference between control cells, cells treated with 10 mM Rib, 50 or 100 µM Ade or the combination of Rib/Ade ($p > 0.05$, one way ANOVA).

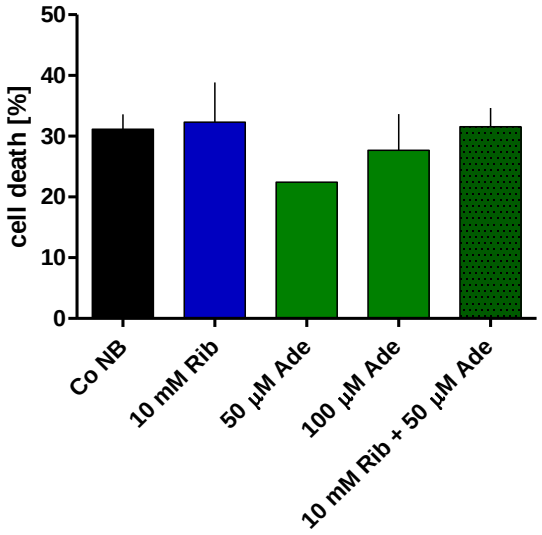

Figure 8.6: Effect of adenine (Ade) and/or Ribose (Rib) on cell viability: *After 6 - 7 days in vitro cells were incubated with Rib and/or various Ade concentrations for 24 h and stained for cell death with Hoechst and propidium. Values for control cells incubated in standard Neurobasal medium (Co NB) or cells incubated in 10 mM Rib, 100 µM Ade and 10 mM Rib + 50 µM Ade are expressed as mean ± S.E.M.; N = 3 - 5. Values for 50 µM Ade are presented as mean (N = 2). No statistical differences were observed with one way ANOVA and Bonferroni's multiple comparison test.*

After 12 - 14 h reperfusion there was no significant difference between cells that were continuously cultured in Neurobasal medium (Figure 8.7, Co NB, 30 ± 4 %, N = 4) and cells that were exposed to 6 h PBS + glucose and subsequent 12 -14 h reperfusion in Neurobasal medium (PBS + Glucose, 25 ± 9 %, N = 3, $p > 0.05$, one way ANOVA). However there was a significant amount of cell death in cells that were exposed to 6 h OGD and subsequent 12 - 14 h reperfusion (83 ± 7 %, $p < 0.001$ compared to Co NB and 6 h PBS + Glucose, one way ANOVA). Likewise cells that were treated with 1 - 5 mM Rib (N = 3) or 50 µM Ade (N = 2) after OGD showed the same amount of cell death ($p < 0.01$ compared to Co NB , $p < 0.001$ compared and Glucose + PBS, one way ANOVA). However, a trend could be seen towards better cell survival in cells pre-treated with 10 mM Rib (60 ± 10 %, N = 3, $p > 0.05$ compared to control cells, one way ANOVA). Interestingly, the combination of Rib and Ade was effective in preserving cell viability at even lower Rib concentrations (57 ± 9 % for cells which were treated with 1 mM Rib/50 µM Ade, N = 3, $p > 0.05$ compared to Co NB and PBS + Glucose, one way ANOVA) and there was no further improvement upon higher Rib concentrations.

This suggests that the approach of enhancing the recovery of post-ischemic ATP levels with Rib/Ade administration (as shown in hippocampal brain slices, see Chapter 7) can improve cell viability. Further experiments looking at the intracellular ATP levels after 12 – 14 h reperfusion could have clarified this point. However, this was beyond the scope of this study.

The major disadvantage of propidium iodide staining is that it only stains cells with broken membranes, which does not necessarily imply that all propidium negative cells are still viable. To complement findings of cell death assays in CGC, I wanted to use an XTT (2,3-Bis(2-methoxy-4-nitro-5-sulfophenyl)-2H-tetrazolium-5-carboxanilide inner salt)-based cell viability assay. In this assay cell viability is assessed by measuring the activity of mitochondrial dehydrogenases, which convert the yellow tetrazolium salt to orange formazan. Furthermore, the results of an XTT assay are analysed by a spectrophotometer reading, which is a more un-biased way of analysis than manually counting propidium iodide positive cells.

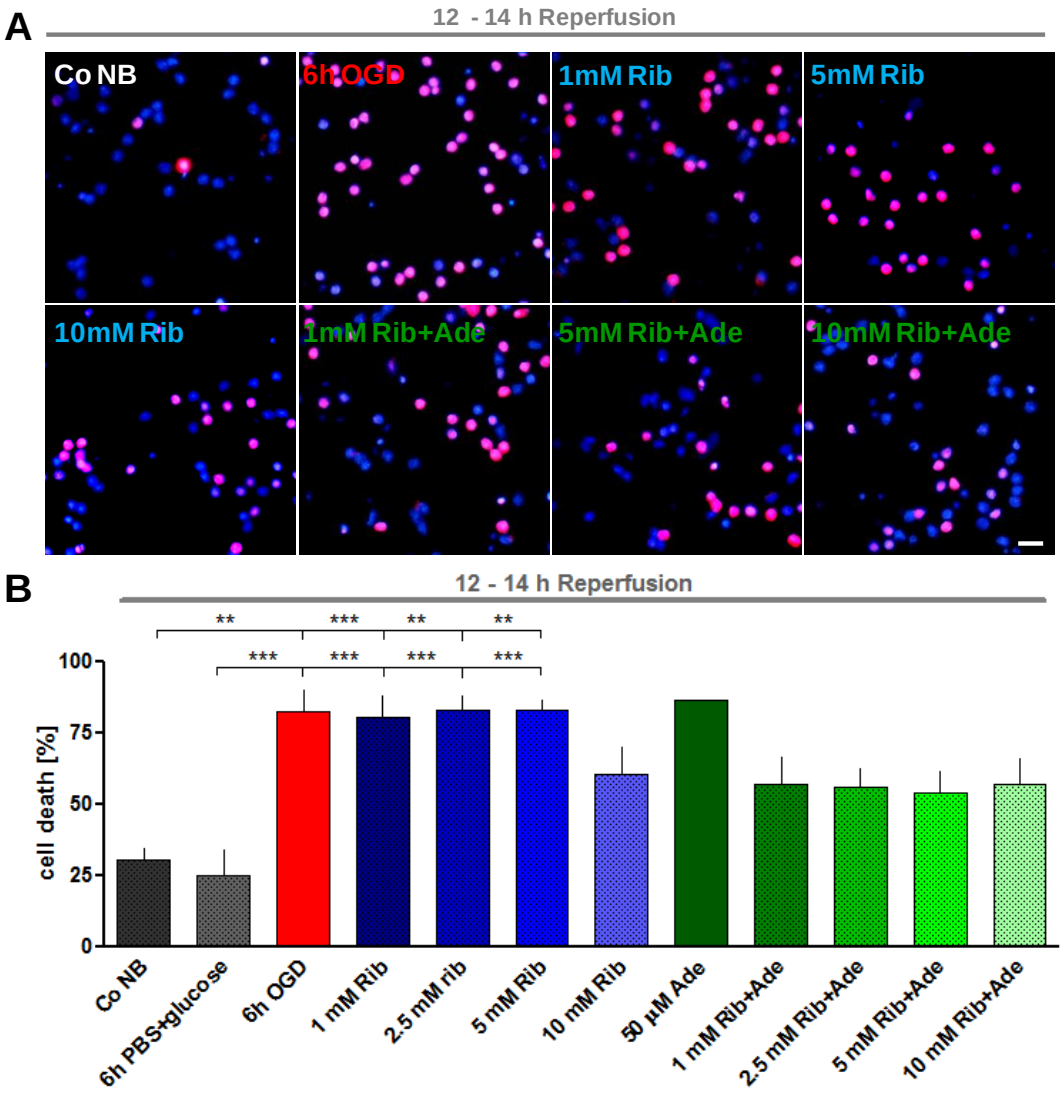

Figure 8.7: Cell death after 6 h OGD and 12 - 14 h reperfusion in cells that were treated with/without D-ribose (Rib) and/or adenine (Ade) after the ischemic insult. *CGC were exposed to 6 h OGD an 12 – 14 h reperfusion in Neurobasal medium supplemented with/without Rib and/or Ade.* ***A*** *Cell death was analysed by Hoechst (blue, all cells) and propidium iodide (red, dead cells) staining after a 12 – 14 h reperfusion period. All pink cells are dead cells. Scale bar refers to 20µm.* ***B*** *The percentage of cell death calculated: ((propidium iodide positive cells x 100)/ Hoechst positive cells). All values are expressed as mean ± S.E.M; N = 2 - 6; (***) p < 0.001, (**) p < 0.01, (*) p < 0.05, one way ANOVA with Bonferroni's multiple comparison test.*

Holly Baum, a project student in the lab under my supervision, used the XTT assay and was able to detect a significant decrease in cell viability after 3 h OGD (at which time Hoechst/propidium iodide staining did not show an increased cell death, see Figure 8.3), which correlates with previous results showing that following 3 h OGD, there was an appreciable reduction in the total adenine nucleotide pool (Figure 8.5 E). Therefore the results obtained from cell death assays with Hoechst/propidium iodide could be confirmed with this more sensitive way of assessing the cell viability. However, there was not enough time to finish these experiments.

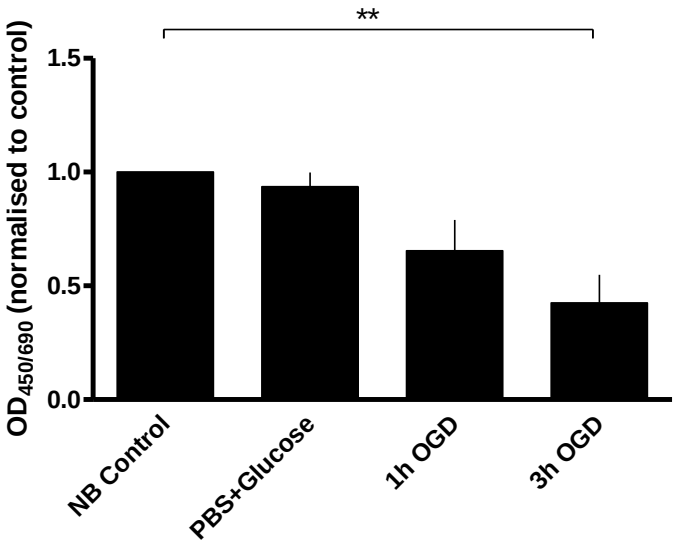

.

Figure 8.8: Exposing CGC to 3 h OGD results in a significant reduction of cell viability as assessed with the XTT cell viability assay. *After 7 - 8 days in culture, cells were incubated in PBS (supplemented with glutamine, Pen/Strep, KCl and B27 and equilibrated for 3 h with 95 % N_2/5 % CO_2) in an airtight chamber, equilibrated with 95 % N_2/5 % CO_2, for 1 or 3 h. Control (Co) cells were incubated in supplemented Neurobasal medium. Cells were then washed with PBS and exposed to PBS containing the XTT reagents for 4 h. Thereafter the optical density was measured on a plate reader at a wavelength of 450 nm with a reference wavelength of 690 nm. Values were normalised to the control values (fold of control) and are expressed as mean ± S.E.M. (**) $p < 0.01$, one way ANOVA with Bonferroni's multiple comparison test.*

8.3 Discussion

8.3.1 Effect of D-Ribose and Adenine on basal cell viability

Prolonged exposure of cells to Rib or Ade had no adverse effect on cell viability. Only at high Rib concentrations (50 mM) did I observe increased cell death. Treatment of quiescent human peripheral blood mononuclear cells with 50 mM Rib has also been shown to induce apoptosis after 2 days exposure (Barbieri et al., 1994). As explained above, this is likely due to osmotic stress and could have been confirmed upon 50 mM sucrose administration. However, the involvement of Rib in the production of advanced glycation end products (AGE) cannot be excluded. AGEs are formed by non-enzymatic reaction of reducing sugars with free aminogroups of lipids, proteins or nucleic acids with subsequent oxidation, fragmentation and cross-linking. AGEs are formed at a slow and constant rate in the body, but their generation is for example enhanced in diabetics (Peppa et al., 2003). Ribosylation of tau (Chen et al., 2009), α-synuclein (Chen et al., 2010a) and BSA (Wei et al., 2009) has been shown to induce misfolding into globular aggregates with high cytotoxic effects. However, in all these studies the pure protein was incubated with 1 M Rib over a prolonged incubation period (≥ 24 h) and the role of Rib in production of AGEs *in vivo* has not been studied yet. Oral administration of Rib (13 weeks, 15 g/kg bodyweight/day) to rats revealed no microscopic histopathology that could be attributed to Rib (Griffiths et al., 2007) and haematological and biochemical parameters in healthy human volunteers were not changed over a period of 2 weeks (Seifert et al., 2008). Furthermore Rib has been administered to patients over a prolonged period (several months - 1 year) without any toxic side effects (Salerno et al., 1999; Jurecka et al., 2008). Hence, Rib at concentrations as low as 1 mM is unlikely to negatively affect cell viability over prolonged incubation/treatment periods.

8.3.2 Effect of D-Ribose and Adenine on post-ischemic cell viability

Prophylactic administration of Rib for 3 h prior to the ischemic insult seemed to preserve cell viability in a concentration-dependent manner. However, analysis of the total adenine nucleotide content did not reveal better preservation of TAN levels or energetic parameters immediately after OGD. Nevertheless, Rib might help the cells to preserve the TAN levels for a longer period compared to control cells. Therefore further analysis of TAN levels after 1 or 3 h OGD (Figure 8.5 E) could clarify the mechanism by which Rib helps to improve cell survival.

The protective effect of prophylactic Rib administration may also be mediated by increasing glycogen stores in CGC. Rib can be converted to fructose-6-phosphate via metabolism in the non-oxidative branch of the pentose phosphate pathway (see Introduction). Indeed treatment of myocardial tissue with Rib under control conditions has been shown to increase glycogen stores and the tolerance to ischemic insults (Wallen et al., 2003). This might also explain why Rib in combination with Ade did not further improve cell viability compared to Rib alone.

Following 12 - 14 h reperfusion the percentage of dead cells increased to 80 %, showing that there is a further loss of neurons during reperfusion (White et al., 2000). Neither administration of 1 mM Rib nor administration of 50 µM Ade on its own for the duration of reperfusion seemed to improve cell viability. However, treatment of cells after OGD with the combination of Rib/Ade (1 mM/50 µM) was effective in preserving cell viability (~ 50 % cell death, ~ 37 % improved cell survival). It is reasonable to assume that this protective effect is linked to improved recovery of post-ischemic ATP levels, as has been shown in many times in myocardial tissue (Zimmer, 1992, 1998) and in hippocampal tissue in the previous chapter. These results are important as it provides evidence that Rib/Ade may be useful when given after a stroke. Additionally the fact that Rib/Ade has to be applied with allopurinol may further enhance this protective effect, since xanthine oxidase inhibition would increase salvage of accumulated hypoxanthine as well as reduce the generation of reactive oxygen radicals (Atlante et al., 1997).

As explained in the introduction (Chapter 1, section 1.1.1.1) the main current treatment for acute ischemic stroke patients target the restoration of the blood supply to the affected brain area. Despite this being important, it does not improve post-ischemic ATP levels, as seen in *in vivo* models of ischemia. Additionally the occurrence of peri-infarct depolarisations (see Chapter 1, section 1.3.2), further challenge hypoperfused brain areas energetically (Somjen, 2002; Dohmen et al., 2008; Doyle et al., 2008). Therefore addition of supplements such as Rib/Ade might be a usefull additional strategy to help the brain to restore the balance of its energy metabolism.

Therefore both strategies: delaying the degradation of ATP during ischemia, with creatine (see previous chapter) and improving the recovery of post-ischemic ATP levels with Rib/Ade are effective strategies for improving neuronal function and viability. In summary these results show that manipulating both, the decline and incomplete recovery of ATP during ischemia and reperfusion with substances that are known to be tolerated in humans exerts promising neuroprotective effects in *in vitro* models of cerebral ischemia. Therefore these results provide good evidence for the initiation of *in vivo* animal studies as well as small-scale, low risk clinical trials with Rib/Ade in patients having suffered stroke or head injury.

9 Future directions and possible translation into clinical trials

9.1 Future directions

In line with previous reports (Gerlach et al., 1971; Allsop and Watts, 1980; Mascia et al., 2000) my data show that the brain has a strong capacity through the purine salvage pathway, and especially APRT, to restore its ATP levels when supplied with the precursors Rib/Ade.

Another possibility to prove the importance of purine salvage in the brain for the restoration of post-ischemic ATP levels and cell viability would have been to inhibit HGPRT or purine nucleoside phosphorylase, both of which should reduce post-ischemic ATP recovery and exacerbate ischemic damage. However, difficulties in obtaining the inhibitor of purine nucleoside phosphorylase immucillin-H (Kicska et al., 2001) and the inhibitor of HGRPT carbocylcic GMP (Bennett et al., 1985), plus the fact that I wanted to restrict studies to chemicals already in use by patients, meant that I did not use these drugs.

The fact that Rib/Ade or high Rib concentrations improve cell viability after OGD strongly suggests that the approach of enhancing the purine salvage pathway after OGD is neuroprotective, providing hope that this could be effective in the injured human brain. Furthermore, I have shown that adenosine release during ischemic periods can be enhanced upon Rib/Ade and decreased upon creatine pre-treatment. These strategies open up new possibilities for manipulating adenosine release during various physiological or pathophysiological conditions, where it is known to play a major role. For example during epileptic seizures, enhanced adenosine release and subsequent A_1 receptor activation might shorten the seizure duration and intensity (Etherington and Frenguelli, 2004).

Therefore there are two future directions that can be pursued based on the results of my thesis:

- Epilepsy: It would be interesting to investigate whether boosting cellular ATP levels by Rib/Ade would inhibit *in vitro* seizure activity, duration or intensity

via enhanced release of the anticonvulsant adenosine (see Discussion, chapter 6).

- Stroke: My results provide good evidence for studying the effects of Rib/Ade administration in *in vivo* animal models of stroke and even for the initiation of a small-scale, low risk clinical trial. However, since so many clinical trials with neuroprotective agents failed to show a beneficial effect, care has to be taken by the translation of preclinical studies into clinical trials (Gladstone et al., 2002; Ginsberg, 2008).

9.2 Translation of *in vitro* and *in vivo* neuroprotection studies into clinical trials

As mentioned in the introduction, a major disadvantage of *in vitro* models is the lack of blood borne components, severed input and output connections as well as the lack of a behavioural output. Therefore *in vitro* studies, including this thesis, mainly help to dissect the biochemical and physiological mechanisms of neuroprotection in isolated brain tissue, but have to be put in context with pre-clinical *in vivo* studies and subsequently clinical trials.

It is however, encouraging that the effect of Rib has been first established in *in vitro* (Kalsi et al., 1998; Smolenski et al., 1998) and *in vivo* animal models of myocardial ischemia (Zimmer, 1982, 1983; Zimmer and Ibel, 1984; Mauser et al., 1985; St Cyr et al., 1989; Zimmer et al., 1989; Muller et al., 1998) and has then been successfully translated into clinical trials (Pliml et al., 1992; Omran et al., 2003; Perkowski et al., 2007; Maccarter et al., 2008). This shows, as reported before, that the effect of Rib is not species-specific (Zimmer et al., 1984) and that it is a metabolic substrate for ATP synthesis in rodents and in humans, which is also true for adenine (Ayvazian and Skupp, 1965). To date many reviews have been published on *"the benefits of D-Ribose in cardiovascular disease"* (Pauly and Pepine, 2000; Pauly et al., 2003; Omran et al., 2004; Parang et al., 2005; Shecterle et al., 2010). Considering the

similarity of the heart and the brain with respect to their dependence on the salvage pathway, the weak capacity of purine *de novo* synthesis and the beneficial effect of Rib/Ade on post-ischemic ATP recovery and cell viability, it is reasonable to assume that the post-ischemic human brain might equally benefit from Rib or Rib/Ade/allopurinol. Additionally Rib is commercially available as a dietary supplement and allopurinol is a widely used treatment for gout, hence there is relatively little cost associated with the production of these substances. Likewise adenine is available at a high purity, which can be used for human studies (see (Schulman et al., 1971; Benke et al., 1973)).

Nevertheless, *in vivo* stroke studies could clarify whether Rib/Ade/allopurinol is neuroprotective, in terms of reducing brain infarct size and improving behavioural outcome as well as help to determine the effective concentrations and drug administration regimes, and therefore provide additional support and evidence for the initiation of clinical stroke trials.

9.2.1 Effective concentration of Rib/Ade/allopurinol administration

From my *in vitro* studies the exact plasma concentration of Rib/Ade needed to increase brain levels to ~ 1 mM/~ 50 µM, respectively, cannot be predicted. For that purpose *in vivo* animal studies would be useful in order to establish a dose-response curve to determine the minimal effective concentration upon intravenous infusion and/or oral supplementation. This is important for the translation into clinical trials, since it has been suggested that drug doses chosen in clinical trials may not be sufficiently high to increase CNS levels of the neuroprotectant used (Dorman and Sandercock, 1996; Ginsberg, 2008).

Serum Rib concentrations in humans can be increased up to 5.5 mM upon intravenous administration of 222 mg/kg/h Rib over 5 hours, and this concentration has been shown to be well tolerated (Gross et al., 1989). In rats adenine can be given in combination with 10 mg/kg/day allopurinol at a dose of 70 mg/kg/day without formation of kidney stones and oral administration of 60 mg/kg/day Ade in combination with 10 mg/kg/day allopurinol was well tolerated for 8 months

(Schulman et al., 1971). However, the corresponding blood Ade/allopurinol concentrations have not been reported, hence it is difficult to estimate whether this concentration is sufficiently high to increase brain Ade levels. At a lower dose of 10 mg adenine/kg/day only little orally administered adenine may reach the brain, since it is converted to AMP in the intestines (Benke et al., 1973). Nevertheless, these studies provide a good starting point for the choice of Rib/Ade/allopurinol concentrations for *in vivo* studies and potential clinical trials.

9.2.2 Therapeutic window of Rib/Ade/allopurinol administration

Most *in vivo* and *in vitro* studies, including my work, tested the neuroprotective effects of drug administration either in advance or soon after the ischemic insult. However, the therapeutic window for acute stroke patients is longer and much more variable, since they are often hospitalised several hours after onset of stroke. Accordingly it has been suggested that another pitfall in the translation of preclinical animal studies into clinical trials, is the time window at which the drug is applied (median time to treatment in clinical trials is ~ 14 h in studies published between 1995 and 1999) (Gladstone et al., 2002). Therefore it would be interesting to study whether Rib/Ade would still be neuroprotective *in vitro* and *in vivo* models if added several hours after the ischemic insult.

9.2.3 Optimal Duration of Rib/Ade/allopurinol administration

Another disadvantage of *in vitro* models is the limited time scale for which they can be used. Therefore the optimal duration of Rib/Ade/allopurinol administration (days, weeks, months?) can only be established in *in vivo* models. It is however encouraging that long term administration of Rib (> 12 month) (Salerno et al., 1999; Jurecka et al., 2008) as well as Ade/allopurinol (> 8 month) (Schulman et al., 1971) is well tolerated by humans.

9.2.4 Patient selection

Another important criteria for the translation of preclinical studies (based on a homogenous population) into clinical trials (dealing with a heterogenous population) is the appropriate patient selection.

Since neuroprotective strategies target the penumbra, patients with no evidence of penumbral tissue (as determined by PET or MRI scans) should not be included in the clinical trials or posthoc analysis (Gladstone et al., 2002; Muir, 2002). Therefore a better selection of patient eligibility might not only reduce the sample sizes needed but also reveal a neuroprotective effect of the substances tested, in those who have tissue left to salvage.

Additionally, preclinical studies mainly use one *in vivo* stroke model, such as middle cerebral artery occlusion, whereas clinical trials allow the entry of many different stroke types, such as haemorrhagic and ischemic strokes. The population heterogeneity alone with accordingly too small sample sizes may be sufficient to explain the negative results of neuroprotective trials (Dorman and Sandercock, 1996; Muir, 2002).

In that respect one advantage of Rib/Ade/allopurinol is that it is a metabolic intervention that does not, unlike other neuroprotective strategies, target a specific receptor or pathway which may play distinct roles in the different types and severities of stroke. Instead it addresses the energetic state of the tissue, which is generally challenged by ischemia. In fact the incomplete recovery of ATP has been shown to occur after transient ischemia, induced by uni- or bilateral cerebral artery occlusion (Kobayashi et al., 1977; Levy and Duffy, 1977; Welsh et al., 1982; Onodera et al., 1986; Hashimoto et al., 1992; Phillis et al., 1996; Folbergrova et al., 1997) as well as after cardiac arrest (Kleihues et al., 1974; Kleihues et al., 1975; Hoxworth et al., 1999) in rats, gerbils, cats and monkeys, showing that this is common to different types of strokes in different species. Hence the improved recovery of ATP by Rib/Ade/allopurinol suplementation is a metabolic intervention that might prove beneficial for different types of stroke.

10 Appendix 1

10.1 Solutions for cerebellar granule cell culture

10 x Krebssolution	*250 ml*	
pH was adjusted with 5 M NaOH to pH 7,4	**NaCl**	**18.13 g**
	KCl	**1.00 g**
	$NaH_2PO_4H_2O$	**0.35 g**
The solution was steril filtered and stored at 4°C	**D-Glucose**	**6.50 g**
	Phenol-Red	**0.025 g**
	HEPES	**14.85 g**
	H_2O	**250 ml**

3,82 % $MgSO_4$	**H_2O**	**100 ml**
Steril filtered, stored at RT	**$MgSO_4$**	**3,82 g**
1,2 % $CaCl_2$	**H_2O**	**100 ml**
Steril filtered, stored at RT	**$CaCl_2$**	**1,2 g**
DNase	**10 mg/ml H_2O**	
Aliquots stored at - 20°C		
Trypsin Inhibitor	**31 mg in 600 µl Solution 1 oder PBS**	
Aliquots stored at - 20°C		
1 M KCl	**0.7 g/in 10 ml Neurobasal medium or PBS**	

1 x Krebs solution	*100 ml*	
Steril filtered and used within 2 weeks	**10 x Krebssolution**	**10 ml**
	BSA	**0,3 g**
	3,82 % $MgSO_4$	**800 µl**
	H_2O	**90 ml**

Solution 3	*10 ml*	
Freshly prepared	**1 x Krebs solution**	**10 ml**
	DNAseI	**100 µl**
	Trypsin Inhibitor	**100 µl**
	3,82 % $MgSO_4$	**100 µl**

Solution 5	*10 ml*	
Freshly prepared	**1 x Krebs solution**	**10 ml**
	1,2 % $CaCl_2$	**12 µl**
	3,82 % $MgSO_4$	**83 µl**

Neurobasal medium		***20 ml***
Stored at 4°C and used within 2 weeks	**Neurobasal**	**20 ml**
	Glutamine	**200 µl**
	Pen/Strep	**20 µl**
	B-27 Supplement	**400 µl**
*Not added for pre-plating step	**1 M KCl***	**20 µl**

Supplemented PBS		***20 ml***
Stored at 4°C and used within 2 weeks	**PBS**	**20 ml**
	D-Glucose	**90 mg**
	Glutamine	**200 µl**
	Pen/Strep	**20 µl**
	B-27 Supplement	**400 µl**
* made up in PBS	**1 M KCl***	**20 µl**

10.2 Solutions for acute hippocampal brain slices

10 x aCSF		***1 L***
Stored at 4°C	**NaCl**	**72.5 g**
	$NaHCO_3$	**21.8 g**
	$NaH_2PO_4 2H_2O$	**1.92 g**
	KCl	**2.2 g**
	H_2O	**1 L**

1 x aCSF		***1 L***
Freshly prepared; $CaCl_2$ was added after 10 min bubbling with 95% O_2/5% CO_2	**10 x aCSF**	**100 ml**
	D-Glucose	**1.8 g**
	1M $CaCl_2$	**2 ml**
	1M $MgSO_4$	**1 ml**
	H_2O	**900 ml**

OGD aCSF	*500 ml*	
Freshly prepared; $CaCl_2$ was added after 10 min bubbling with 95% N_2/5% CO_2	**10 x aCSF**	**50 ml**
	Sucrose	**1.71 g**
	1M $CaCl_2$	**1 ml**
	1M $MgSO_4$	**0.5 ml**
	H_2O	**450 ml**

10.3 Solutions for High performance liquid chromatography

1 M HPLC phosphate buffer	*500 ml*	
Stored at 4°C	**K_2HPO_4**	**52.254 g**
	KH_2PO_4	**27.218 g**

10.3.1 Solutions for ion-pairing HPLC

Buffer A	*500 ml*	
Freshly prepared/ Stored at 4°C for < 2 days, filtered before use	**10 x HPLC phosphate buffer**	**24.382 ml**
	TBAHS	**0.5085 g**
	H_2O	**350.61 ml**

Buffer B	*250 ml*	
Freshly prepared/ Stored at 4°C for < 2 days, filtered before use	**10 x HPLC phosphate buffer**	**16.25 ml**
	H_2O	**171.25 ml**
	HPLC grade Methanol	**62.5 ml**

10.3.2 Solutions for reverse phase HPLC with fluorescence detection

Buffer A	*500 ml*	
Freshly prepared/ Stored at 4°C for < 2 days, filtered before use	**10 x HPLC phosphate buffer**	**10 ml**
	H_2O	**490 ml**

Buffer B	***500 ml***	
Freshly prepared/ Stored at 4°C for < 2 days, filtered before use	**10 x HPLC phosphate buffer**	**10 ml**
	H_2O	**365 ml**
	HPLC grade Methanol	**125 ml**

10.4 Solutions for cell viability assays

Propidium iodide solution	***50 ml***	
Stored at 4°C and used at 100 µl/ml	**Propidium iodide**	**2.5 mg**
	Sodium citrate	**50 mg**
	H_2O	**50 ml**
Hoechst		
Aliquots stored at -20°C, diluted 1:10 in PBS and used at 10 µl/ml	**8 mM in PBS or Solution 1**	

XTT assay	***10 ml***	
Freshly prepared	**XTT**	**10 mg**
	1.25 mM PMS in PBS	**0.2 ml**
	Supplemented PBS	**10 ml**

10.5 Chemicals and stock solutions

Cell culture chemicals	**Supplier**	**Storage**
B27	Invitrogen	Lightsensitive, -20°C
DNAse	Roche	-20°C
Glutamine	From media prep	-20°C
Pen/Strep	From media prep	-20°C
Phenolred	Sigma Aldrich	RT
Trypsin	From media prep	-20°C
Trypsin Inhibitor (Soy bean)	Invitrogen	-20°C
Neurobasal medium	Invitrogen; Cat No.: 21103	4°C
Phenol Red	Sigma	RT

HPLC chemicals	Supplier	Storage
1,1,2-Trichloro-1,2,2-trifluoro-ethane CHROMASOLV®	Sigma Aldrich	4°C
Dipotassium hydrogen phosphate	Fisher Scientific	RT
HPLC grade Acetonitril	Sigma Aldrich	RT
HPLC grade Methanol	Sigma Aldrich	RT
Orthophosphoric acid	Fisher Scientific	RT
Perchloric acid 70%	Fisher Scientific	RT/light sensitive
Potassium dihydrogen phosphate	Fisher Scientific	RT
Tetrabutylammonium hydrogen sulphate (TBAHS)	Sigma Aldrich	RT
Tetrahydrofuran	Sigma Aldrich	RT
Tri-*n*-octylamine	Sigma Aldrich	RT

Drugs	Supplier	Stock solutions
8-CPT	Sigma Aldrich	10 mM in 1N NaOH/ 1 mM in H_2O
Adenine	Sigma Aldrich	100 mM in 1N NaOH
Adenosine	Sigma Aldrich	1 mM/10 mM in H_2O
ADP	Sigma Aldrich	10 mM in H_2O
Allopurinol	Sigma Aldrich	100 mM in 1N NaoH
AMP	Sigma Aldrich	1 mM in H_2O/10 mM in 1N NaOH
ATP	Sigma Aldrich	10 mM/1 mM in H_2O
Creatine	Sigma Aldrich	Endconcentration in aCSF
D-Ribose	Sigma Aldrich	1 M in aCSF/ Neurobasal
Forskolin	Acent	10 mM in DMSO
GDP	Sigma Aldrich	1 mM in H_2O
GMP	Sigma Aldrich	10 mM in H_2O
GTP	Sigma Aldrich	1 mM in H_2O
Guanosine	Sigma Aldrich	10 mM in 1N NaOH
Hypoxanthine	Sigma Aldrich	100 mM in 1N NaOH
IMP	Sigma Aldrich	10 mM in H_2O
Inosine	Sigma Aldrich	10 mM in H_2O
NADH	Sigma Aldrich	10 mM in H_2O
PPADS	Tocris	10 mM in H_2O
Rotenone	Sigma Aldrich	10 mM in DMSO
Serotonin	Sigma Aldrich	10 mM in H_2O
Xanthine	Sigma Aldrich	100 mM in 1N NaOH
Hoechst	Sigma Aldrich	80 mM in PBS

11 Appendix 2

11.1 Factors that determine the separation process in reverse phase HPLC

There are numerous parameters that influence the separation of sample compounds in reverse phase HPLC, some of which are shown in Table 11.1. Commonly used terms to describe the properties of a HPLC method are the:

- retention times of analytes (T_R), which describes the time from injection of the sample to the appearance of the peak maximum in the detector
- selectivity (separation factor) describes the relative T_R of two compounds with respect to each other (T_{R2}/T_{R1})
- resolution of peaks (R_S) takes the width of peaks into account and describes the degree of separation of two peak maxima ($R_S = T_{R1} - T_{R2}$ / average peak width)
- column efficiency is expressed as the number of theoretical plates (N, dimensionless) and determines the sharpness of the peaks and hence the R_S, which increases with increasing N.

Although changes to both phases will affect most parameters, they exert these effects via different mechanisms, as summarised in Table 11.1.

Chromatographic conditions	**Mechanism**
Temperature	Viscosity of mobile phase decreases with increasing temperature, resulting in improved mass transfer analytes between mobile and stationary phase
Flow rate	Determines the longitudinal diffusion of analytes, which affects the ability of the reverse phase medium to absorb sample compounds
Mobile phase	**Mechanism**
pH	The ionisation of acidic and basic residues depends on the pH. pH should be adjusted to suppress ionisation in order to allow sufficient interaction with the stationary phase
Type and percentage of organic modifier	The lower the polarity of the mobile phase the higher its elutive capacity, with water being the most polar eluent (water>methanol>acetonitrile>tetrahydrofuran).
Gradient/Isocratic elution	The gradient profile and/or the parameters of an isocratic elution affect the elution time of compounds
Ionic strength	Higher salt concentrations of the buffer can help to reduce residual silanol (SiOH) and sample ionisation as well as electrostatic repulsion between them, however high buffer concentrations lead to salt precipitates in the HPLC system
Ion pairing agents	Improves retention of charged analytes
Stationary phase	**Mechanism**
Column length	Increasing column length will increase the number of theoretical plates (N), however so will the runtime and the backpressure
Alkyl chain length	Longer alkyl chains will increase the hydrophobic properties of the stationary phase (C_{18}>C_8>C_4>C_3)
Particle size	Efficiency increases with increasing particle size, however so will the runtime and the backpressure

Table 11.1: Factors of a reverse phase HPLC system, that determine the separation process.

Table 11.2 summarises all the changes to the mobile and stationary phases of the reverse phase system, which I have tried to improve the separation of purine/pyrimidine metabolites. However, none of these parameters resulted in a sufficient resolution of ATP/GMP and/or IMP as well as AMP/hypoxanthine/xanthine.

Mobile phase	**Coeluting compounds**	**Gradient profile**
pH 7 20 mM phosphate buffer	HX/X/AMP ATP/IMP/GMP	Linear gradient to 25 % MetOH
pH 6.5 20 mM phosphate buffer	X/AMP GMP/ATP	
pH 6 20 mM phosphate buffer	HX/X ATP/IMP/GMP	Gradient profile does not improve resolution
pH 5.5 20 mM acetate buffer	HX/X/AMP	
pH 5 20 mM acetate buffer	HX/X/AMP IMP/GMP	Gradient profile does not improve resolution
Stationary phase factor	**Comments**	
Two C_8, 5 µm, 150 mm columns in series	Increased T_R but no sufficiently improved R_S or selectivity	
$C_{18,}$ 3 µm, 150 mm	Improved efficiency, increased T_R, but no sufficiently improved R_S or selectivity	

Table 11.2: Effect of changing several mobile phase and/or stationary phase parameters on the separation of standard compounds: *The resolution of ATP/IMP and/or GMP as well as AMP/ xanthine (X) and/or hypoxanthine (HX) could not be improved by various adjustments of the mobile phase (pH and buffer) or stationary phase (column).*

12 Appendix 3

The following tables summarise reported adenine nucleotide levels of *in vivo* rat brain (Table 12.1) or *in vitro* brain slices (Table 12.2). Since not all of the reported values are given in concentrations per mg protein, values reported per mg wet weight and or mg dry weight were converted to mg protein, following a wet weight to protein ratio of 1: 10 obtained from my own data and published reports (Whittingham and Lipton, 1981) and a wwt/dwt ratio of 1:5 (Xu et al., 2006).

species	Age/weight	Detection	Brain region	ATP	ADP	AMP	EC	TAN [nmol/mg protein] (estimated)	Reference
SD	E18	In situ freezing Fluorimetric/enzymatic [nmol/mg dwt]	Cortex	20.5±3.4					(Pundik et al., 2006)
			Hippocampus	18.4±3.3					
			Cerebellum	19.1±2.4					
Wistar	P7	Whole animal freezing Fluorimetric/enzymatic [µmol/g wwt]	Whole brain	2.4±0.08	0.27±0.03	0.03±0.02		27	(Vannucci et al., 1996)
SD	145-160 g	Microwave irradiation HPLC [µmol/g wwt]	Cortex	2.49±0.07	0.82±0.045	0.176±0.011	0.835±0.006	34.86	(Phillis et al., 1996)
SD	145-155 g	Microwave irradiation HPLC [µmol/g wwt]	Cortex	2.92±0.045	0.78±0.017	0.14±0.009	0.86±0.004	38.4	(Phillis et al., 1995)
Wistar	140-160 g	Whole animal freezing HPLC [nmol/mg protein]	Striatum	23.6±2.2	3.1±0.4	3.4±0.4	0.83±0.08	30.1	(Milusheva et al., 1996)*
SD	140-170 g	Microwave irradiation HPLC [nmol/mg protein]	Whole brain	28.8±2.4	13.5±0.5	2.2±0.3	0.80±0.1	44.5	(Delaney and Geiger, 1996)*
Wistar	220-270 g	In situ freezing HPLC/fluorimetric [µmol/g wwt]	forebrain	2.79±0.07	0.29±0.02	0.024±0.003	0.945±0.003	31.04	(Onodera et al., 1986)
Wistar	240-320 g	In situ freezing Fluorimetric/enzymatic [µmol/g wwt]	Cortex	3.01±0.09	0.36±0.03	0.026±0.010	0.94±0.006	33.96	(Yoshida et al., 1982)
Wistar	270-330 g	In situ freezing Fluorimetric/enzymatic [µmol/g wwt]	Hippocampus	2.67±0.07	0.31±0.01	0.06±0.01	0.93±0.01	30.4	(Folbergrova et al., 1997)
Wistar	290-400 g	In situ freezing HPLC[µmol/g wwt]	Cortex	2.83±0.07	0.158±0.008	0.008±0.002	0.971±0.002	29.96	(Chapman et al., 1981)

species	Age/weight	Detection	Brain region	ATP	ADP	AMP	EC	TAN [nmol/mg protein] (estimated)	Reference
rats		Reeze-blowing technique Spectrophotometrically [nmol/g wwt]	Whole brain	2.75±0.10	0.377±0.022	0.038±0.007	0.934±0.003	31.65	(Winn et al., 1979)
rats	275-425 g	In situ freezing Fluorimetric/enzymatic [µmol/g wwt]	Whole brain	3.06±0.07	0.27±0.007	0.03±0.001	0.951±0.001	33.6	(Ljunggren et al., 1974)
Wistar	250-300 g	In situ freezing Enzymatic [nmol/mg dwt]	Cortex	14.4±2.0				nd	(Xu et al., 2006)
			Hippocampus	15.5±2.1					
			Brain stem	10.9±2.1					
Wistar	300 g	Urethane/ Microwave irradiation Fluorimetric/enzymatic [nmol/mg protein]	Cerebral cortex	23.7±1.0				nd	(Kobayashi et al., 1998)
			Superioror colliculus	20.9±0.8					
			Hippocampus	26.5±1.0					
			Cerebellum	26.1±0.6					
SD	304-403 g	In situ freezing HPLC [µmol/g wwt]	Cortex	2.47	0.4	0.06	0.91	29.3	(Verhaegen et al., 1995)
Wistar	300-365 g	In situ freezing Fluorimetric/enzymatic [µmol/g wwt]	Cortex	2.8±0.05	0.3±0.006	0.043±0.002	0.938±0.002	31.43	(Folbergrova et al., 1981)
			Hippocampus	2.93±0.02	0.3±0.018	0.044±0.006	0.941±0.002	32.74	
			Cerebellum	2.61±0.03	0.24±0.01	0.039±0.002	0.945±0.002	28.89	
SD	330-450 g	In situ freezing HPLC [µmol/g dwt]	Cortex	11.4±0.6	1.4±0.1	0.18±0.03	0.94±0.01		(Marklund et al., 2006)

species	Age/weight	Detection	Brain region	ATP	ADP	AMP	EC	TAN [nmol/mg protein] (estimated)	Reference
Han:Wist	1 year	In situ freezing Fluorimetric/enzymatic [µmol/g wwt]	Cortex	2.68±0.15	0.27±0.03		0.937±0.009	nd	h and Hoyer, 1991)
Wistar	1 year (490 g)	In situ freezing HPLC [µmol/g wwt]	Cortex	2.74±0.11	0.40±0.02			nd	(Hoyer and Lannert, 2008)
			Hippocampus	2.49±0.22	0.44±0.03			nd	
Wistar	15-20 weeks	Microwave irradiation/ HPLC [nmol/mg protein]	Cortex	27.4±3.3	8.6±1.0	2.5±0.6		38.5	(Yamada et al., 1988)
			Hypothalamus	22.3±5.1	5.8±0.9	3.2±0.5		31.3	
			Hippocampus	28.1±1.8	9.0±1.8	3.2±1.4		40.3	
			Striatum	30.1±3.2	9.4±0.8	2.8±1.0		42.3	
			Cerebellum	24.7±3.0	6.0±0.9	1.6±0.3		32.3	

Table 12.1: Reported in vivo adenine nucleotide concentrations in rat brain. *wwt wet weight ; dwt dry weight; EC energy charge (ATP+0.5xADP/TAN); SD Sprague Dawley; All total adenine nucleotide values (TAN = [ATP] + [ADP] + [AMP]) are expressed as nmol/mg protein on a wwt/protein ratio of 1:10 obtained from our own data and published reports (Whittingham and Lipton, 1981) and a wwt/dwt ratio of 1:5 (Xu et al., 2006). All rats older than p7 were male; all animals were under anesthesia, apart from references signed with an asterix (*). Data is presented in ascending age of the animals.*

species	Age/weight	Preparation	Detection	Brain region	Incubation conditions	ATP	ADP	AMP	TAN	EC	Reference
Wistar	140-160 g	Dopamine incubation	Freezing HPLC [nmol/mg protein]	Striatum 400 µm (tissue chopper)	90 min	11.82±1.48	4.82±2.24	2.72±1.37	19.36±4.15	0.73±0.04	(Milusheva et al., 1996)
SD	180-240 g	nd	Freezing HPLC [nmol/mg protein]	Hippocampus, 400 µm (tissue chopper)	interface	8.3	1.1	0.2		0.9	(Fredholm et al., 1984)
SD	250 – 300 g	Anesthesia/ ice cold aCSF Kynurenic ascorbic acid	Freezing Bioluminescence [nmol/mg protein]	Hippocampus, 300 µm (Vibratome)	Interface?	13.3±1.1					(Galeffi et al., 2000)
Holtzman	110-130 days	3°C aCSF	Freezing Enzymatic/fluorimetric [nmol/mg protein]	Hippocampus ~500 µm (free hand)	37°C, 60 min submerged	13.4±0.4			19.0±0.6	0.85±0.01	(Kass and Lipton, 1982)
Wistar	350-450 g	Anesthesia aCSF	Freezing Enzymatic/fluorimetric [nmol/mg protein]	Hippocampus 400 µm (tissue chopper)	36.5°C, 60 min/ 5h submerged	12.78±1.03	3.38±0.22	0.95±0.18	17.10±1.18	0.84±0.012	(Whittingham et al., 1989)
Fisher	2-3 month	Anesthesia	Freezing HPLC [nmol/mg protein]	Hippocampus 400 µm (tissue slicer)	aCSF+amino acids submerged	31°C 9.4±0.5 34°C 13.4±1.4 37°C 10.1±0.8					(Paschen and Djuricic, 1995)

Table 12.2: Reported adenine nucleotide concentrations in rat brain slices. *EC energy charge; TAN total adenine nucleotides [nmol/mg protein]; all animals were male.*

13 Appendix 4

13.1 Stability of total adenine nucleotides over a 9 h incubation period

In order to establish the metabolic integrity of brain slices over a prolonged incubation period I measured the total adenine nucleotide (TAN) levels of brain slices incubated in standard aCSF (green dots), 10 mM Sucrose (black dots, osmotic control), 10 mM Glucose (blue dots) as well as 10 mM Ribose (red dots) after 3 h (N = 4 - 14), 5 h (N = 3 - 7) and after 9 h (N = 2) incubation at 34°C (Figure 13.1 A). There was a ~ 20 % drop in the TAN levels after 9 h and a rise in IMP levels (Figure 13.1 B) in all slices. Interestingly Ribose-treated slices always had higher IMP levels, potentially due to increased purine salvage or *de novo* synthesis. Due to the drop of TAN levels after 9 h incubation I tried to keep the experimental window at ≤ 8 h since the metabolic integrity of hippocampal brain slices has been shown to be stable over that incubation period (Whittingham et al., 1984b).

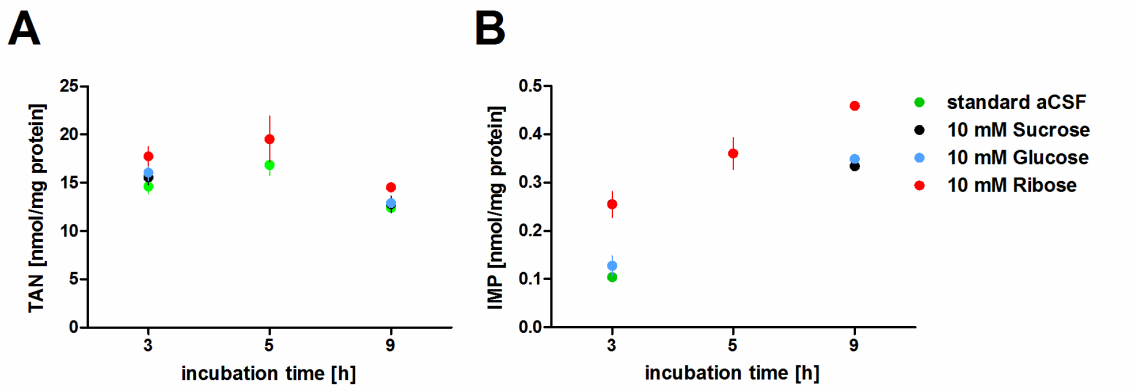

Figure 13.1: *Stability of* ***A*** *the total adenine nucleotide (TAN) pool and* ***B*** *IMP levels, over a prolonged incubation period in brain slices incubated in standard aCSF (green dots), 10 mM Sucrose (black dots, osmotic control), 10 mM Glucose (blue dots) as well as 10 mM Ribose (red dots). There was a 20 % reduction of the TAN pool after a 9 h incubation period (N = 2). IMP levels increased over that incubation time and interestingly IMP levels in Ribose treated slices were consistenly elevated, suggesting increased purine salvage or purine de novo synthesis.*

13.2 Time course of Xanthine Oxidase inhibition by Allopurinol

Adenosine biosensors contain all of the enzymes, including xanthine oxidase, required to convert adenosine to hydrogen peroxide, which oxidises on a polarised platinum wire and produces a current proportional to the adenosine concentration. The xanthine oxidase inhibitor allopurinol is converted to the active inhibitor oxypurinol by xanthine oxidase itself, thereby producing hydrogen peroxide. Therefore adenosine biosensors were used to determine the effectiveness of allopurinol to inhibit the adenosine signal, by incubating them with allopurinol for up to 3 h and measuring the response to adenosine applied in the continuous presence of allopurinol (Figure 13.2 A).

These experiments were performed by Holly Baum, a project student under my supervision. The initial response to 10 µM adenosine was similar to the response to 10 µM allopurinol (Figure 13.2 B). The initial response to adenosine was depressed by 32 % after 10 min incubation with allopurinol (N = 3), by 61 % after 1 h incubation (N = 3) and by 78 % after 2 h incubation (N = 3). After 3 hours incubation with allopurinol, the response to 10 µM adenosine was nearly abolished (96% depression of the original signal, N = 2, Figure 13.2 C). This suggests that allopurinol is effectively inhibiting xanthine oxidase and that a 3 hr incubation period is needed for a nearly complete inhibition.

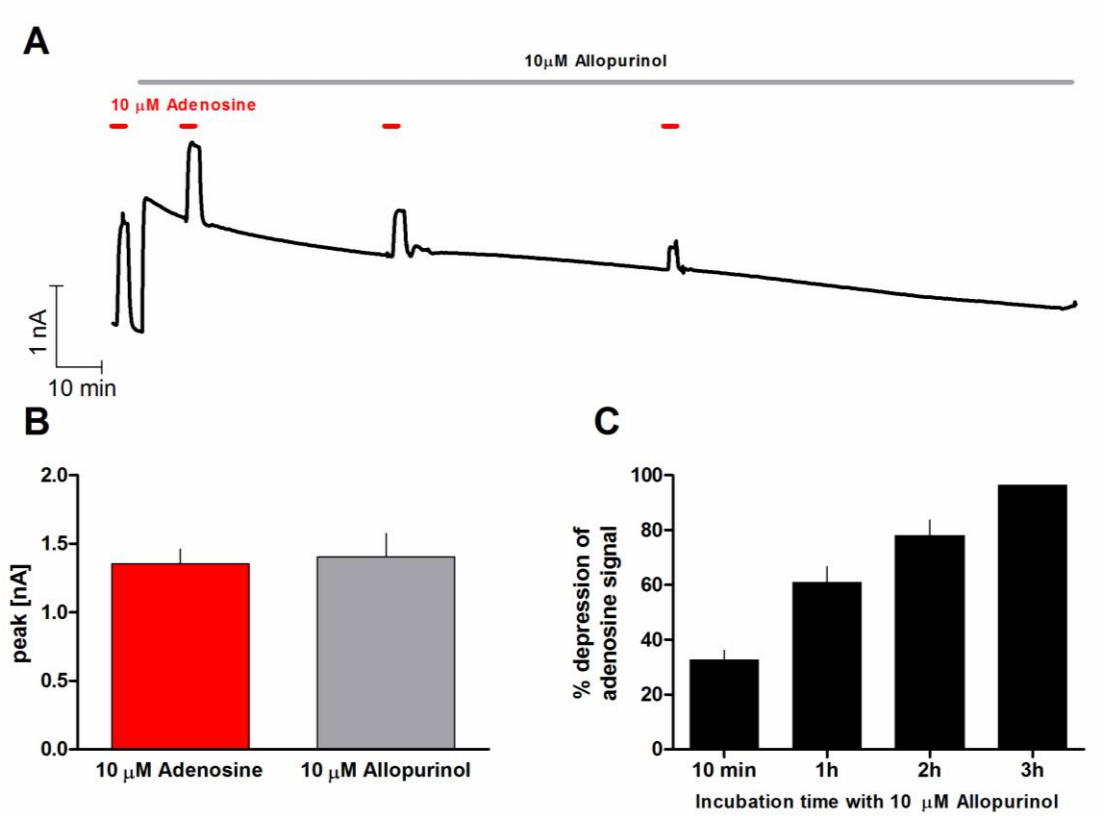

Figure 13.2: Allopurinol inhibits the adenosine signal on adenosine biosensors: A *Representative adenosine sensor trace showing the time-dependent inhibition by allopurinol on the adenosine response. Sensors were exposed to 10 µM adenosine alone and after 10 min, 1 h or 2 h incubation (see red horizontal lines) with 10 µM allopurinol (as indicated by the grey line).* ***B*** *The maximum initial current detected in response to stimulation with 10 µM adenosine or 10 µM allopurinol was the same.* ***C*** *The percentage depression of the adenosine signal detected in the continuous presence of allopurinol was calculated relative to that with adenosine alone for each experiment. All values are presented as mean ± S.E.M.*

13.3 Effect of high Ribose and Glucose on adenine nucleotide levels

To study the effect of Glucose and Ribose (Rib) on pre- and post-ischemic TAN levels, slices were incubated with 10 mM sucrose (osmotic control), Rib, or an additional 10 mM glucose (total glucose concentration in the aCSF was 20 mM) for 3 h, before being exposed to oxygen/glucose deprivation (OGD). Thereafter slices were transferred back to sucrose-, Rib- or glucose-supplemented aCSF for various reperfusion times (Figure 13.3). Although there were no significant differences between slices incubated with the different sugars, the TAN and ATP levels in glucose- and especially Rib-treated slices were consistently higher after OGD than TAN levels in sucrose-treated slices (Figure 13.3 A and D). The reason for the better recovery in glucose-treated slices might lie in the fact that there was still some glucose surrounding the tissue during OGD, which might explain the higher energy charge (EC) in glucose-treated slices during 5 min OGD (EC = 0.73 ± 0.02 compared to 0.55 ± 0.07 in ribose and 0.53 ± 0.06 in sucrose treated slices, data not shown). However, the beneficial effect of Rib on TAN levels after the ischemic insult might be due to enhanced purine salvage during OGD, as seen in the significantly higher IMP levels (Figure 13.3 C), the product of the hypoxanthine guanine phosphoribosyltransferase (HGPRT) catalysed reaction (hypoxanthine + PRPP → IMP). Furthermore AMP levels were not significantly elevate in Rib-treated slices (Figure 13.3 B) compared to glucose- and sucrose-treated slices, further suggesting that the increased IMP levels are unlikely to be derived from increased degradation of AMP.

However upon 10 min OGD and reperfusion there was no complete recovery of pre-ischemic TAN and ATP levels in either condition. In fact the TAN levels decreased further upon 6 h reperfusion, which might be due to a complete disturbance of the energy metabolism. However, in control slices incubated for 9 h (time control, see Figure 13.1 A) I also observed a reduction of the TAN pool by 20 %, suggesting a slow degradation of the tissue during the incubation period.

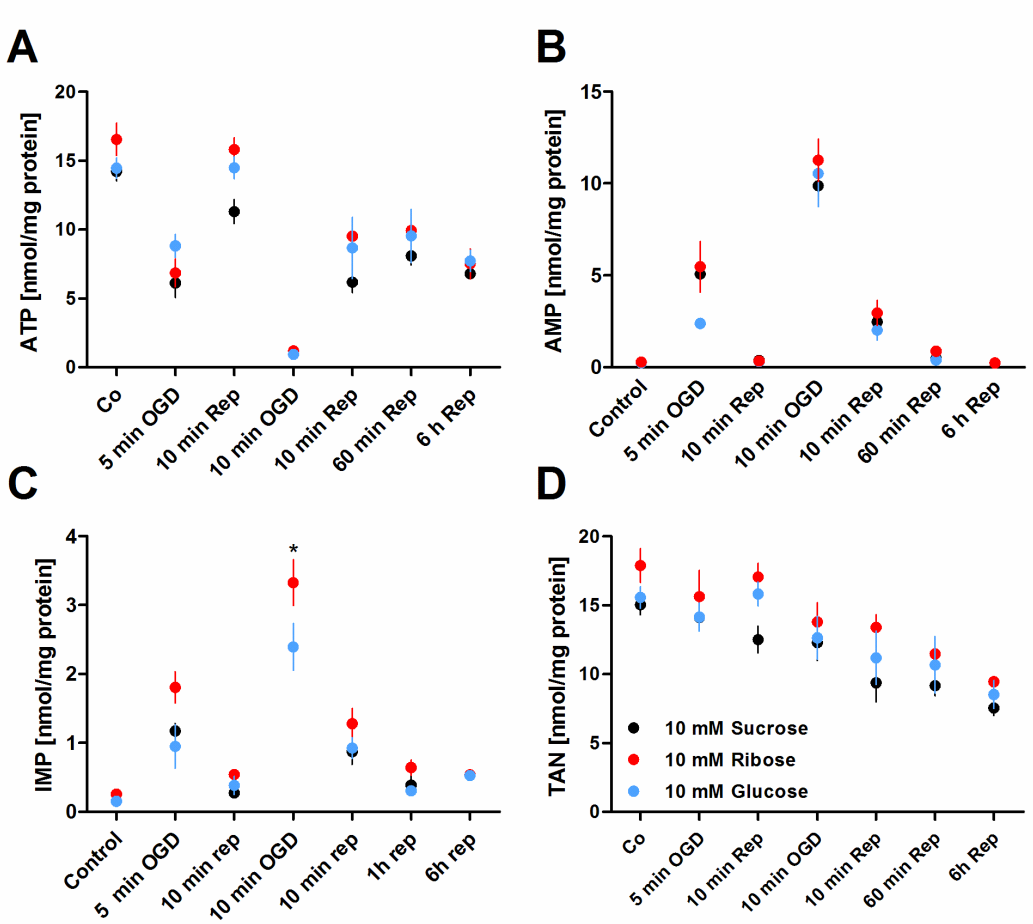

Figure 13.3: *Effect of sucrose, D-ribose and glucose on pre- and post-ischemic* ***A*** *ATP,* ***B*** *AMP,* ***C*** *IMP and* ***D*** *total adenine nucleotide (TAN) levels. Slices were incubated for 3 h with 10 mM sucrose, ribose or glucose before they were washed in aCSF (to remove residual glucose), exposed to oxygen/glucose deprivation (OGD) and transferred back into sucrose, glucose or ribose supplemented aCSF for various reperfusion (rep) time points. All values are expressed as mean ± S.E.M; N = 3 - 6; (*) p < 0.05, one way ANOVA with Bonferroni's multiple comparison test.*

13.4 Effect of 8-CPT on the recovery of synaptic transmission in Rib/Ade treated slices after OGD

In order to test whether the incomplete recovery of synaptic transmission after OGD in Rib/Ade treated slices was due to increased levels of extracellular adenosine I applied 1 µM 8-CPT to the slices after 1 h reperfusion (Figure 13.4). The fEPSP traces increased by 250 % in one experiment and by 28 % in the two other experiments, suggesting that the extracellular adenosine levels were close to the pre-ischemic adenosine levels in control slices (21 % increase in control slices, Chapter 6).

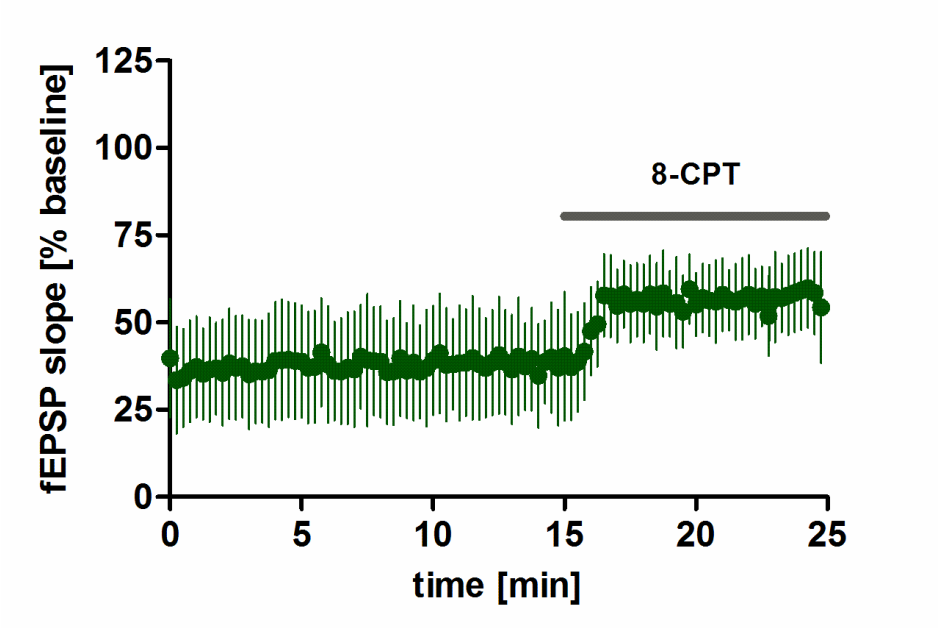

Figure 13.4: *Effect of the A_1 receptor antagonist 8-CPT (1 µM) on the recovery of synaptic transmission after 1 h reperfusion in Rib/Ade treated slices (N = 3). The fEPSP traces increased by 250 % in one experiment and by 28 % in the two other experiments, showing that the extracellular adenosine levels were close to the pre-ischemic adenosine levels in control slices (21 % increase).*

13.5 Effect of 5 mM Creatine on the decline and recovery of synaptic transmission during OGD

In order to test whether higher creatine concentrations resulted in further delayed decline of synaptic transmission during OGD or improved recovery after OGD, I treated 2 slices with 5 mM creatine and compared the results to the ones observed for 1 mM creatine (Figure 13.5). The decline in synaptic transmission was similar between the two (Figure 13.5 A), and anoxic depolarisation occurred after 12 and 14.5 min in the two slices, which is slightly longer than the mean time to AD in 1 mM creatine treated slices (13.5 ± 0.9 min, see Chapter 7). The recovery of synaptic transmission seemed to be slightly delayed in 5 mM Creatine treated slices (Figure 13.5 B).

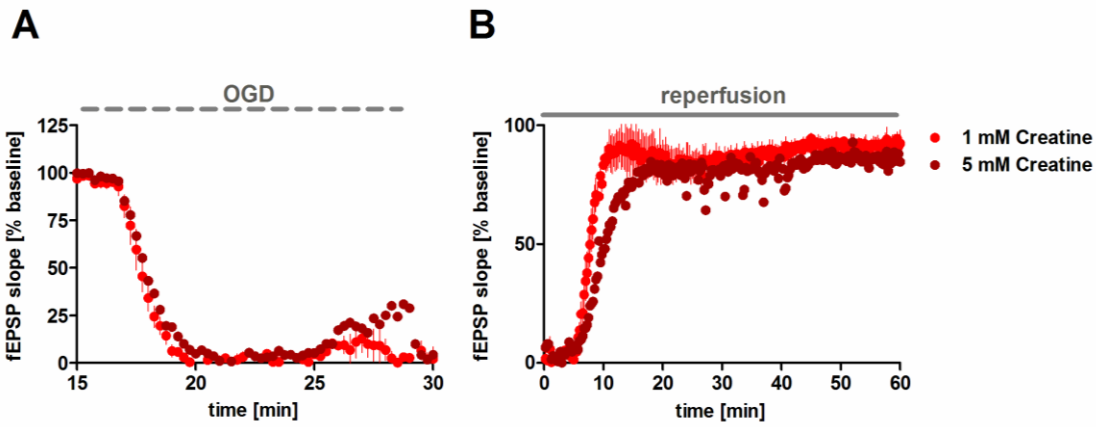

Figure 13.5: *Effect of 5 mM creatine on decline and recovery of synaptic transmission. 2 slices were treated with 5 mM creatine for ≥ 3 h and exposed to OGD until anoxic depolarisation (AD) occurred and perfused again with 5 mM creatine.* ***A*** *There was no difference in the decline of synaptic transmission between 5 and 1 mM creatine treated slices. The increase in fEPSPs during OGD marks the epileptiform activity, after which the AD occurred. The dashed grey line refers to the duration of OGD, which was 12 and 14.5 min in the two slices treated with 5 mM creatine (time until AD).* ***B*** *The recovery of synaptic transmission in 5 mM creatine seemed to be slightly delayed compared to 1 mM creatine.*

13.6 Addition of Rib/Ade and creatine after the ischemic insult

In additional sets of experiments, I tested the effect of Rib/Ade or creatine on the recovery of synaptic transmission if added after the ischemic insult (OGD till AD) during a 150 min reperfusion period. However as seen in Figure 13.6, the results were very variable and have to be repeated. I did not observe a clear effect of either of the treatments, although a trend towards improved synaptic transmission could be seen in creatine treated slices, which is potentially linked to its radical scavenging properties (Lawler et al., 2002; Sestili et al., 2006).

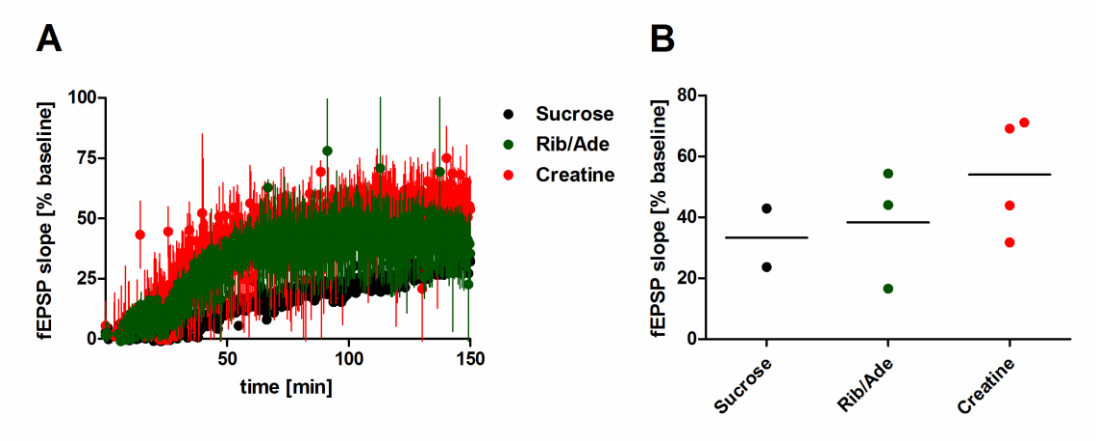

Figure 13.6: Effect of Rib/Ade or creatine application on the recovery of synaptic transmission if added after the ischemic insult. *Slices were exposed to OGD until the AD occurred and perfused with sucrose (osmotic control, 1 mM, N = 2), Rib/Ade (1 mM/ 50 µM, N = 3) or creatine (1 mM, N = 4).* ***A*** *fEPSP traces and* ***B*** *scatter plot showing the amount of recovery after 150 min reperfusion for all experiments.*

13.7 Manipulations of intracellular tissue ATP levels affect the adenosine release during OGD

Figure 13.7 shows the full time course of adenosine release and fEPSP decline and recovery upon exposure to 5 min OGD in control slices and slices pre-treated with Rib/Ade, creatine or Rib/Ade + creatine. Rib/Ade treatment results in significantly higher adenosine release, but does not affect the pattern of release whereas creatine, which significantly reduces adenosine release also changes the pattern of release. Likewise Rib/Ade + creatine pre-treatment reduces the adenosine release, suggesting that despite the increased ATP levels the buffer capacity of phosphocreatine is still sufficient to delay the degradation of ATP.

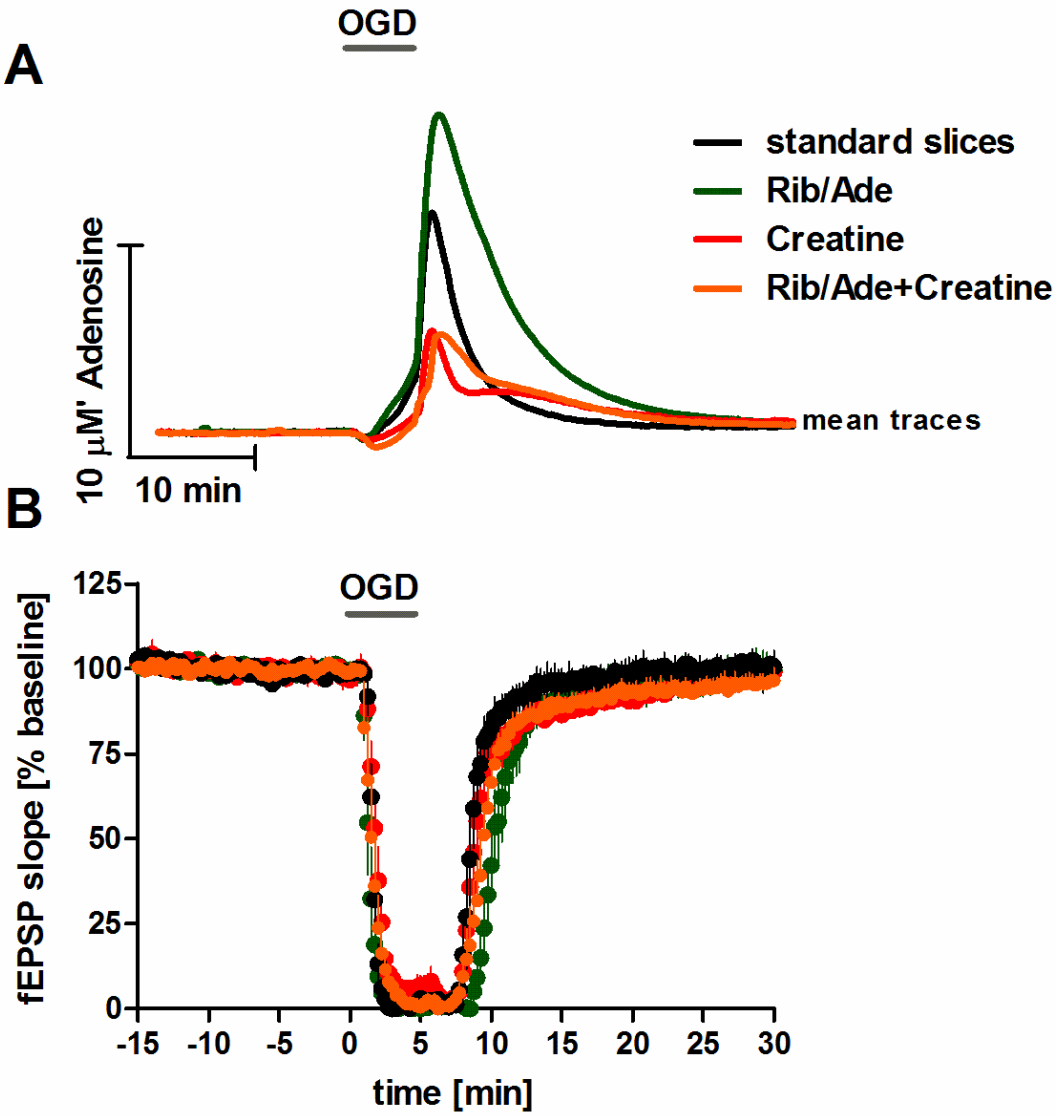

Figure 13.7: Modulation of intracellular adenine nucleotides influences adenosine release during OGD: A *mean traces for adenosine sensor recordings and* ***B*** *fEPSPs of control slices (black trace, N = 4), slices pre-treated with Rib/Ade (1 mM/ 50 µM, N = 4), Creatine (red trace,1 mM, N = 3) or Rib/Ade + Creatine (N = 3) and exposed to 5 min oxygen/glucose deprivation (OGD) and subsequent 30 min reperfusion.*

13.8 Subsequent ischemic periods

In order to test whether Rib/Ade could be used to replenish the reduced adenosine release upon subsequent ischemic periods, I tried to establish a protocol that would allow for a reduced recovery after the first ischemic insult and a faster recovery after the second as shown before (Pearson et al., 2001). However, 5 min was too short since all slices nearly completely recovered. 6.25 min, as suggested before, resulted in variable responses, as shown in Figure 13.8. Some slices recovered completely and underwent anoxic depolarisation during the second ischemic period (see red trace) and some slices recovered completely after both ischemic insults (see black trace). If the AD occurred during the first ischemic period (after about 7 min) there was a complete loss of synaptic transmission during the second ischemic period. Therefore, I did not pursue these experiments.

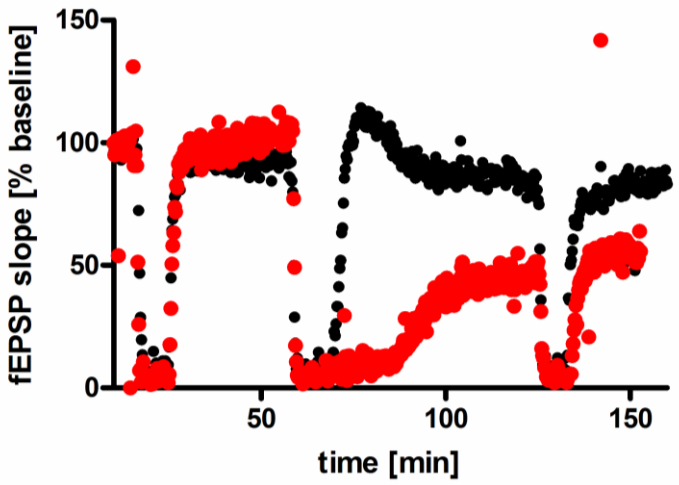

Figure 13.8: Effect of three subsequent ischemic periods on the recovery of synaptic transmission. *Slices were exposed to 6.25 min OGD, allowed to recover for 45 min and exposed to 6.25 min OGD, allowed to recover for 60 min and exposed to 6.25 min OGD again. Sometimes the anoxic depolarisation occurred during the second ischemic period (see red trace) resulting in an incomplete recovery of synaptic transmission. If AD did not occur there was a complete recovery of synaptic transmission as seen in the black trace.*

References

Abbracchio M. P., Burnstock G., Verkhratsky A., Zimmermann H. (2009) Purinergic signalling in the nervous system: an overview. *Trends Neurosci.* **32**:19-29.

Abraham W. C., Williams J. M. (2003) Properties and mechanisms of LTP maintenance. *Neuroscientist* **9**:463-474.

Adams A., Harkness R. A. (1976) Developmental changes in purine phosphoribosyltransferases in human and rat tissues. *Biochem. J.* **160**:565-576.

Adams H. P., Jr., Adams R. J., Brott T., del Zoppo G. J., Furlan A., Goldstein L. B., Grubb R. L., Higashida R., Kidwell C., Kwiatkowski T. G., Marler J. R., Hademenos G. J. (2003) Guidelines for the Early Management of Patients With Ischemic Stroke: A Scientific Statement From the Stroke Council of the American Stroke Association. *Stroke* **34**:1056-1083.

Adams H. P., Jr., del Zoppo G., Alberts M. J., Bhatt D. L., Brass L., Furlan A., Grubb R. L., Higashida R. T., Jauch E. C., Kidwell C., Lyden P. D., Morgenstern L. B., Qureshi A. I., Rosenwasser R. H., Scott P. A., Wijdicks E. F. M. (2007) Guidelines for the Early Management of Adults With Ischemic Stroke: A Guideline From the American Heart Association/ American Stroke Association Stroke Council, Clinical Cardiology Council, Cardiovascular Radiology and Intervention Council, and the Atherosclerotic Peripheral Vascular Disease and Quality of Care Outcomes in Research Interdisciplinary Working Groups: The American Academy of Neurology affirms the value of this guideline as an educational tool for neurologists. *Stroke* **38**:1655-1711.

Aden U., Halldner L., Lagercrantz H., Dalmau I., Ledent C., Fredholm B. B. (2003) Aggravated Brain Damage After Hypoxic Ischemia in Immature Adenosine A2A Knockout Mice. *Stroke* **34**:739-744.

Agnew W. F., Crone C. (1967) Permeability of Brain Capillaries to Hexoses and Pentoses in the Rabbit. *Acta Physiol. Scan.* **70**:168-175.

Aitken P. G., Breese G. R., Dudek F. F., Edwards F., Espanol M. T., Larkman P. M., Lipton P., Newman G. C., Nowak T. S., Jr., Panizzon K. L., et al. (1995) Preparative methods for brain slices: a discussion. *J. Neurosci. Methods* **59**:139-149.

Allsop J., Watts R. W. E. (1980) Activities of amidophosphoribosyltransferase (EC 2.4.2.14) and the purine phosphoribosyltransferases (EC 2.4.2.7 and 2.4.2.8), and the phosphoribosylpyrophosphate content of rat central nervous system at different stages of development: Their possible relationship to the neurological dysfunction in the Lesch-Nyhan syndrome. *J. Neurol. Sci.* **46**:221-232.

Almeida T., Rodrigues R. J., de Mendonça A., Ribeiro J. A., Cunha R. A. (2003) Purinergic P2 receptors trigger adenosine release leading to adenosine A2A receptor activation and facilitation of long-term potentiation in rat hippocampal slices. *Neuroscience* **122**:111-121.

Ames A., 3rd (2000) CNS energy metabolism as related to function. *Brain Res. Brain Res. Rev.* **34**:42-68.

An S., Kumar R., Sheets E. D., Benkovic S. J. (2008) Reversible Compartmentalization of de Novo Purine Biosynthetic Complexes in Living Cells. *Science* **320**:103-106.

Andersen P., Morris R., Amaral D., Bliss T., O'Keefe J. (2006) The hippocampus book, 1 Editior. Oxford University Press, USA.

Andres R. H., Ducray A. D., Schlattner U., Wallimann T., Widmer H. R. (2008) Functions and effects of creatine in the central nervous system. *Brain Res. Bull.* **76**:329-343.

Arai A., Lynch G. (1992) Factors regulating the magnitude of long-term potentiation induced by theta pattern stimulation. *Brain. Res.* **598**:173-184.

Atkinson D. E. (1968) The energy charge of the adenylate pool as a regulatory parameter. Interaction with feedback modifiers. *Biochemistry* **7**:4030-4034.

Atlante A., Gagliardi S., Minervini G. M., Ciotti M. T., Marra E., Calissano P. (1997) Glutamate neurotoxicity in rat cerebellar granule cells: a major role for xanthine oxidase in oxygen radical formation. *J. Neurochem.* **68**:2038-2045.

Attwell D., Laughlin S. B. (2001) An energy budget for signaling in the grey matter of the brain. *J. Cereb. Blood Flow Metab.* **21**:1133-1145.

Au J. L., Su M. H., Wientjes M. G. (1989) Extraction of intracellular nucleosides and nucleotides with acetonitrile. *Clin Chem* **35**:48-51.

Ayvazian J. H., Skupp S. (1965) The Study of Purine Utilization and Excretion in a Xanthinuric Man. *J. Clin. Invest.* **44**:1248-1260.

Baldwin S. A., Beal P. R., Yao S. Y., King A. E., Cass C. E., Young J. D. (2004) The equilibrative nucleoside transporter family, SLC29. *Pflugers Arch.* **447**:735-743.

Balestrino M., Rebaudo R., Lunardi G. (1999) Exogenous creatine delays anoxic depolarization and protects from hypoxic damage: dose-effect relationship. *Brain Res* **816**, pp 124-130.

Balestrino M., Lensman M., Parodi M., Perasso L., Rebaudo R., Melani R., Polenov S., Cupello A. (2002) Role of creatine and phosphocreatine in neuronal protection from anoxic and ischemic damage. *Amino Acids* **23**:221-229.

Barbieri D., Grassilli E., Monti D., Salvioli S., Franceschini M. G., Franchini A., Bellesia E., Salomoni P., Negro P., Capri M., et al. (1994) D-ribose and deoxy-D-ribose induce apoptosis in human quiescent peripheral blood mononuclear cells. *Biochem. Biophys. Res. Commun.* **201**:1109-1116.

Barsotti C., Ipata P. L. (2002) Pathways for alpha-D-ribose utilization for nucleobase salvage and 5-fluorouracil activation in rat brain. *Biochem. Pharmacol.* **63**:117-122.

Barsotti C., Ipata P. L. (2004) Metabolic regulation of ATP breakdown and of adenosine production in rat brain extracts. *Int J Biochem Cell Biol* **36**:2214-2225.

Bender E., Buist A., Jurzak M., Langlois X., Baggerman G., Verhasselt P., Ercken M., Guo H. Q., Wintmolders C., Van den Wyngaert I., Van Oers I., Schoofs L., Luyten W. (2002) Characterization of an orphan G protein-coupled receptor localized in the dorsal root ganglia reveals adenine as a signaling molecule. *Proc. Natl Acad. Sci. U S A* **99**:8573-8578.

Bendich A., Brown G. B., Philips F. S., Thiersch J. B. (1950) The direct oxidation of adenine in vivo. *J. Biol. Chem.* **183**:267-277.

Benke P. J., Herrick N., Smitten L., Aradine C., Laessig R., Wolcott G. J. (1973) Adenine and folic acid in the Lesch-Nyhan syndrome. *Pediatr. Res.* **7**:729-738.

Bennett L. L., Brockman R. W., Rose L. M., Allan P. W., Shaddix S. C., Shealy Y. F., Clayton J. D. (1985) Inhibition of utilization of hypoxanthine and guanine in cells treated with the carbocyclic analog of adenosine. Phosphates of carbocyclic nucleoside analogs as inhibitors of hypoxanthine (guanine) phosphoribosyltransferase. *Mol. Pharm.* **27**:666-675.

Benowitz L. I., Carmichael S. T. (2010) Promoting axonal rewiring to improve outcome after stroke. *Neurobiol. Dis.* **37**:259-266.

Berger R., Middelanis J., Vaihinger H.-M., Mies G., Wilken B., Jensen A. (2004) Creatine Protects the Immature Brain From Hypoxic-Ischemic Injury. *J. Soc. for Gyn. Invest.* **11**:9-15.

Betz A. L. (1985) Identification of hypoxanthine transport and xanthine oxidase activity in brain capillaries. *J. Neurochem.* **44**:574-579.

Betz A. L., Drewes L. R., Gilboe D. D. (1975) Inhibition of glucose transport into brain by phlorizin, phloretin and glucose analogues. *Biochim. Biophys. Acta* **406**:505-515.

Boison D. (2006) Adenosine kinase, epilepsy and stroke: mechanisms and therapies. *Trends Pharm. Sci.* **27**:652-658.

Boison D., Stewart K. A. (2009) Therapeutic epilepsy research: from pharmacological rationale to focal adenosine augmentation. *Biochem. Pharmacol.* **78**:1428-1437.

Brosh S., Zoref-Shani E., Danziger E., Bromberg Y., Sperling O., Sidi Y. (1996) Adenine nucleotide metabolism in primary rat neuronal cultures. *Int. J. Biochem. & Cell Biol.* **28**:319-328.

Broughton B. R. S., Reutens D. C., Sobey C. G. (2009) Apoptotic Mechanisms After Cerebral Ischemia. *Stroke* **40**:e331-339.

Brown A. K., Raeside D. L., Bowditch J., Dow J. W. (1985) Metabolism and salvage of adenine and hypoxanthine by myocytes isolated from mature rat heart. *Biochim. Biophys. Acta* **845**:469-476.

Brown A. M. (2004) Brain glycogen re-awakened. *J. Neurochem.* **89**:537-552.

Brown A. M., Ransom B. R. (2007) Astrocyte glycogen and brain energy metabolism. *Glia* **55**:1263-1271.

Brown E. G., Newton R. P., Shaw N. M. (1982) Analysis of the free nucloetide pools of mammalian tissue by high-pressure liquid chromatography. *Anal. Biochem.* **123**:378-388.

Brundege J. M., Diao L., Proctor W. R., Dunwiddie T. V. (1997) The Role of Cyclic AMP as a Precursor of Extracellular Adenosine in the Rat Hippocampus. *Neuropharmacol.* **36**:1201-1210.

Burnstock G. (1971) Neural nomenclature. *Nature* **229**:282-283.

Burnstock G. (1993) Physiological and pathological roles of purines: an update. *Drug Dev. Res* **28**:195-206.

Burnstock G. (2006) Purinergic signalling. *Br. J. Pharmacol.* **147 Suppl 1**:S172-181.

Burnstock G., Campbell G., Satchell D., Smythe A. (1970) Evidence that adenosine triphosphate or a related nucleotide is the transmitter substance released by non-adrenergic inhibitory nerves in the gut. *Br. J. Pharmacol.* **40**:668-688.

Cameron J. S., Moro F., Simmonds H. A. (1993) Gout, uric acid and purine metabolism in paediatric nephrology. *Pediatr. Nephrol.* **7**:105-118.

Camilo O., Goldstein L. B. (2004) Seizures and epilepsy after ischemic stroke. *Stroke* **35**:1769-1775.

Cappeln G., Nielsen J., Jessen F. (1999) Synthesis and degradation of adenosine triphosphate in cod (Gadus morhua) at subzero temperatures. *J. Sci. of Food and Agri.* **79**:1099-1104.

Caretti A., Bianciardi P., Sala G., Terruzzi C., Lucchina F., Samaja M. (2010) Supplementation of creatine and ribose prevents apoptosis in ischemic cardiomyocytes. *Cell Physiol. Biochem.* **26**:831-838.

Carter A. J., Müller R. E., Pschorn U., Stransky W. (1995) Preincubation with Creatine Enhances Levels of Creatine Phosphate and Prevents Anoxic Damage in Rat Hippocampal Slices. *J. Neurochem.* **64**:2691-2699.

Chan P. H. (2001) Reactive Oxygen Radicals in Signaling and Damage in the Ischemic Brain. *J. Cereb. Blood Flow Metab.* **21**:2-14.

Chapman A. G., Atkinson D. E. (1973) Stabilization of adenylate energy charge by the adenylate deaminase reaction. *J. Biol. Chem.* **248**:8309-8312.

Chapman A. G., Westerberg E., Siesjo B. K. (1981) The metabolism of purine and pyrimidine nucleotides in rat cortex during insulin-induced hypoglycemia and recovery. *J. Neurochem.* **36**:179-189.

Chen J.-F., Huang Z., Ma J., Zhu J., Moratalla R., Standaert D., Moskowitz M. A., Fink J. S., Schwarzschild M. A. (1999) A2A Adenosine Receptor Deficiency Attenuates Brain Injury Induced by Transient Focal Ischemia in Mice. *J. Neurosci.* **19**:9192-9200.

Chen L., Wei Y., Wang X., He R. (2009) D-Ribosylated Tau forms globular aggregates with high cytotoxicity. *Cell. Mol. Life Sci.* **66**:2559-2571.

Chen L., Wei Y., Wang X., He R. (2010a) Ribosylation rapidly induces alpha-synuclein to form highly cytotoxic molten globules of advanced glycation end products. *PLoS One* **5**:e9052.

Chen L. Y., Rex C. S., Sanaiha Y., Lynch G., Gall C. M. (2010b) Learning induces neurotrophin signaling at hippocampal synapses. *Proc. Natl Acad. Sci. U S A* **107**:7030-7035.

Chen P., Goldberg D. E., Kolb B., Lanser M., Benowitz L. I. (2002) Inosine induces axonal rewiring and improves behavioral outcome after stroke. *Proc. Natl Acad. Sci. U S A* **99**:9031-9036.

Contestabile A. (2002) Cerebellar granule cells as a model to study mechanisms of neuronal apoptosis or survival in vivo and in vitro. *The Cerebellum* **1**:41-55.

Cornford E. M., Oldendorf W. H. (1975) Independent blood-brain barrier transport systems for nucleic acid precursors. *Biochim. Biophys. Acta* **394**:211-219.

Costenla A. R., Lopes L. V., de Mendonca A., Ribeiro J. A. (2001) A functional role for adenosine A3 receptors: modulation of synaptic plasticity in the rat hippocampus. *Neurosci. Lett.* **302**:53-57.

Cunha R. A. (2001) Adenosine as a neuromodulator and as a homeostatic regulator in the nervous system: different roles, different sources and different receptors. *Neurochem. Int.* **38**:107-125.

Cunha R. A., Vizi E. S., Ribeiro J. A., Sebastiao A. M. (1996) Preferential release of ATP and its extracellular catabolism as a source of adenosine upon high- but not low-frequency stimulation of rat hippocampal slices. *J. Neurochem.* **67**:2180-2187.

Dale N., Frenguelli B. G. (2009) Release of adenosine and ATP during ischemia and epilepsy. *Curr. Neuropharmacol.* **7**:160-179.

Dale N., Pearson T., Frenguelli B. G. (2000) Direct measurement of adenosine release during hypoxia in the CA1 region of the rat hippocampal slice. *J Physiol* **526 Pt 1**:143-155.

Das D. K., Engelman R. M., Clement R., Otani H., Prasad M. R., Rao P. S. (1987) Role of xanthine oxidase inhibitor as free radical scavenger: a novel mechanism of action of allopurinol and oxypurinol in myocardial salvage. *Biochem. Biophys. Res. Commun.* **148**:314-319.

de Mendonca A., Ribeiro J. A. (1994) Endogenous adenosine modulates long-term potentiation in the hippocampus. *Neuroscience* **62**:385-390.

de Mendonca A., Ribeiro J. A. (1997) Adenosine and neuronal plasticity. *Life Sci.* **60**:245-251.

de Mendonca A., Ribeiro J. A. (2000) Long-term potentiation observed upon blockade of adenosine A1 receptors in rat hippocampus is N-methyl-D-aspartate receptor-dependent. *Neurosci. Lett.* **291**:81-84.

de Mendonca A., Sebastiao A. M., Ribeiro J. A. (2000) Adenosine: does it have a neuroprotective role after all? *Brain Res. Brain Res. Rev.* **33**:258-274.

Dechent P., Pouwels P. J. W., Wilken B., Hanefeld F., Frahm J. (1999) Increase of total creatine in human brain after oral supplementation of creatine-monohydrate. *Am. J. of Physio. - Regulatory , Integrative and Comparative Physio.* **277**:R698-R704.

Delaney S. M., Geiger J. D. (1996) Brain regional levels of adenosine and adenosine nucleotides in rats killed by high-energy focused microwave irradiation. *J. Neurosci. Methods* **64**:151-156.

Della Ragione F., CartenÃ¬-Farina M., Gragnaniello V., Schettino M. I., Zappia V. (1986) Purification and characterization of 5'-deoxy-5'-

methylthioadenosine phosphorylase from human placenta. *J. Biol. Chem.* **261**:12324-12329.

Desmond D. W., Moroney J. T., Sano M., Stern Y., Merino J. G. (2002) Incidence of Dementia After Ischemic Stroke: Results of a Longitudinal Study * Editorial Comment. *Stroke* **33**:2254-2262.

DiGeronimo R. J., Gegg C. A., Zuckerman S. L. (1998) Adenosine depletion alters postictal hypoxic cerebral vasodilation in the newborn pig. *Am. J. of Phys. - Heart and Circulatory Phys.* **274**:H1495-H1501.

Dirnagl U., Iadecola C., Moskowitz M. A. (1999) Pathobiology of ischaemic stroke: an integrated view. *Trends Neurosci.* **22**:391-397.

Dohmen C., Sakowitz O. W., Fabricius M., Bosche B., Reithmeier T., Ernestus R.-I., Brinker G., Dreier J. P., Woitzik J., Strong A. J., Graf R. (2008) Spreading depolarizations occur in human ischemic stroke with high incidence. *Annals of Neurol.* **63**:720-728.

Dorman P. J., Sandercock P. A. G. (1996) Considerations in the Design of Clinical Trials of Neuroprotective Therapy in Acute Stroke. *Stroke* **27**:1507-1515.

Doyle K. P., Simon R. P., Stenzel-Poore M. P. (2008) Mechanisms of ischemic brain damage. *Neuropharmacol.* **55**:310-318.

Drury A. N., Szent-Gyorgyi A. (1929) The physiological activity of adenine compounds with especial reference to their action upon the mammalian heart. *J. Physiol.* **68**:213-237.

Du F., Zhu X. H., Zhang Y., Friedman M., Zhang N., Ugurbil K., Chen W. (2008) Tightly coupled brain activity and cerebral ATP metabolic rate. *Proc. Natl Acad. Sci. U S A* **105**:6409-6414.

Dunwiddie T. V., Diao L. (1994) Extracellular adenosine concentrations in hippocampal brain slices and the tonic inhibitory modulation of evoked excitatory responses. *J. Pharm. and Exp. Ther.* **268**:537-545.

Dunwiddie T. V., Masino S. A. (2001) The role and regulation of adenosine in the central nervous system. *Annu. Rev. Neurosci.* **24**:31-55.

Dunwiddie T. V., Diao L., Kim H. O., Jiang J. L., Jacobson K. A. (1997) Activation of hippocampal adenosine A3 receptors produces a desensitization of A1 receptor-mediated responses in rat hippocampus. *J. Neurosci.* **17**:607-614.

Dux E., Fastbom J., Ungerstedt U., Rudolphi K., Fredholm B. B. (1990) Protective effect of adenosine and a novel xanthine derivative propentofylline on the cell damage after bilateral carotid occlusion in the gerbil hippocampus. *Brain. Res.* **516**:248-256.

Dzeja P. P., Terzic A. (2003) Phosphotransfer networks and cellular energetics. *J. Exp. Biol.* **206**:2039-2047.

Edwards F. A., Konnerth A., Sakmann B., Takahashi T. (1989) A thin slice preparation for patch clamp recordings from neurones of the mammalian central nervous system. *Pflugers Arch.* **414**:600-612.

Erecinska M., Silver I. A. (1994) Ions and energy in mammalian brain. *Prog. Neurobiol.* **43**:37-71.

Etherington L. A., Frenguelli B. G. (2004) Endogenous adenosine modulates epileptiform activity in rat hippocampus in a receptor subtype-dependent manner. *Eur. J. Neurosci.* **19**:2539-2550.

Etherington L. A., Patterson G. E., Meechan L., Boison D., Irving A. J., Dale N., Frenguelli B. G. (2009) Astrocytic adenosine kinase regulates basal synaptic adenosine levels and seizure activity but not activity-dependent adenosine release in the hippocampus. *Neuropharmacol.* **56**:429-437.

Feig S., Lipton P. (1990) N-methyl-D-aspartate receptor activation and Ca2+ account for poor pyramidal cell structure in hippocampal slices. *J. Neurochem.* **55**:473-483.

Feigin V. L., Lawes C. M., Bennett D. A., Anderson C. S. (2003) Stroke epidemiology: a review of population-based studies of incidence, prevalence, and case-fatality in the late 20th century. *Lancet Neurol.* **2**:43-53.

Fenton R. A., Dobson J. G., Jr. (1992) Fluorometric quantitation of adenosine concentration in small samples of extracellular fluid. *Anal. Biochem.* **207**:134-141.

Fields R. D., Burnstock G. (2006) Purinergic signalling in neuron-glia interactions. *Nat. Rev. Neurosci.* **7**:423-436.

Fiske C. H., Subbarow Y. (1929) Phosphorus compounds of muscle and liver. *Science* **70**:381-382.

Flynn R. W. V., MacWalter R. S. M., Doney A. S. F. (2008) The cost of cerebral ischaemia. *Neuropharmacol.* **55**:250-256.

Folbergrova J., Ingvar M., Siesjo B. K. (1981) Metabolic changes in cerebral cortex, hippocampus, and cerebellum during sustained bicuculline-induced seizures. *J. Neurochem.* **37**:1228-1238.

Folbergrova J., Li P. A., Uchino H., Smith M. L., Siesjo B. K. (1997) Changes in the bioenergetic state of rat hippocampus during 2.5 min of ischemia, and prevention of cell damage by cyclosporin A in hyperglycemic subjects. *Exp. Brain Res.* **114**:44-50.

Forghani R., Krnjevic K. (1995) Adenosine antagonists have differential effects on induction of long-term potentiation in hippocampal slices. *Hippocampus* **5**:71-77.

Fredholm B. B., Dunwiddie T. V., Bergman B., Lindstrom K. (1984) Levels of adenosine and adenine nucleotides in slices of rat hippocampus. *Brain. Res.* **295**:127-136.

Fredholm B. B., Chen J. F., Masino S. A., Vaugeois J. M. (2005) Actions of adenosine at its receptors in the CNS: insights from knockouts and drugs. *Annu. Rev. Pharmacol. Toxicol.* **45**:385-412.

Fredholm B. B., AP I. J., Jacobson K. A., Klotz K. N., Linden J. (2001) International Union of Pharmacology. XXV. Nomenclature and classification of adenosine receptors. *Pharmacol Rev* **53**:527-552.

Fredholm B. B., Abbracchio M. P., Burnstock G., Daly J. W., Harden T. K., Jacobson K. A., Leff P., Williams M. (1994) Nomenclature and classification of purinoceptors. *Pharmacol Rev* **46**:143-156.

Frenguelli B. G. (1997) The effects of metabolic stress on glutamate receptor-mediated depolarizations in the in vitro rat hippocampal slice. *Neuropharmacol.* **36**:981-991.

Frenguelli B. G., Llaudet E., Dale N. (2003) High-resolution real-time recording with microelectrode biosensors reveals novel aspects of adenosine release during hypoxia in rat hippocampal slices. *J. Neurochem.* **86**:1506-1515.

Frenguelli B. G., Wigmore G., Llaudet E., Dale N. (2007) Temporal and mechanistic dissociation of ATP and adenosine release during ischaemia in the mammalian hippocampus. *J. Neurochem.* **101**:1400-1413.

Fujii S., Kuroda Y., Ito K., Kaneko K., Kato H. (1999) Effects of adenosine receptors on the synaptic and EPSP-spike components of long-term potentiation and depotentiation in the guinea-pig hippocampus. *J. Physiol.* **521 Pt 2**:451-466.

Fujii S., Kato H., Ito K., Itoh S., Yamazaki Y., Sasaki H., Kuroda Y. (2000) Effects of A1 and A2 adenosine receptor antagonists on the induction and reversal of long-term potentiation in guinea pig hippocampal slices of CA1 neurons. *Cell Mol. Neurobiol.* **20**:331-350.

Gadalla A. E., Pearson T., Currie A. J., Dale N., Hawley S. A., Sheehan M., Hirst W., Michel A. D., Randall A., Hardie D. G., Frenguelli B. G. (2004) AICA riboside both activates AMP-activated protein kinase and competes with adenosine for the nucleoside transporter in the CA1 region of the rat hippocampus. *J. Neurochem.* **88**:1272-1282.

Gaitonde M. K., Evans G. M. (1982) The effect of inhibition of hexosemonophosphate shunt on the metabolism of glucose and function in rat brain in vivo. *Neurochem. Res.* **7**:1163-1179.

Gaitonde M. K., Evison E., Evans G. M. (1983) The Rate of Utilization of Glucose Via Hexosemonophosphate Shunt in Brain. *J. Neurochem.* **41**:1253-1260.

Galeffi F., Sinnar S., Schwartz-Bloom R. D. (2000) Diazepam promotes ATP recovery and prevents cytochrome c release in hippocampal slices after in vitro ischemia. *J. Neurochem.* **75**:1242-1249.

Gallo V., Kingsbury A., Balazs R., Jorgensen O. S. (1987) The role of depolarization in the survival and differentiation of cerebellar granule cells in culture. *J. Neurosci.* **7**:2203-2213.

Gallo V., Ciotti M. T., Coletti A., Aloisi F., Levi G. (1982) Selective release of glutamate from cerebellar granule cells differentiating in culture. *PNAS* **79**:7919-7923.

Gebhart B., Jorgenson J. A. (2004) Benefit of ribose in a patient with fibromyalgia. *Pharmacotherapy* **24**:1646-1648.

Gerlach E., Marko P., Zimmer H. G., Pechan I., Trendelenburg C. (1971) Different response of adenine nucleotide synthesis de novo in kidney and brain during aerobic recovery from anoxia and ischemia. *Experientia* **27**:876-878.

Giannecchini M., Matteucci M., Pesi R., Sgarrella F., Tozzi M. G., Camici M. (2005) Uptake and utilization of nucleosides for energy repletion. *Int. J. Biochem. Cell Biol.* **37**:797-808.

Gidday J. M., Fitzgibbons J. C., Shah A. R., Kraujalis M. J., Park T. S. (1995) Reduction in cerebral ischemic injury in the newborn rat by potentiation of endogenous adenosine. *Pediatr. Res.* **38**:306-311.

Ginsberg M. D. (2008) Neuroprotection for ischemic stroke: past, present and future. *Neuropharmacol.* **55**:363-389.

Gladstone D. J., Black S. E., Hakim A. M. (2002) Toward Wisdom From Failure: Lessons From Neuroprotective Stroke Trials and New Therapeutic Directions. *Stroke* **33**:2123-2136.

Gray J., Owen R., Giacomini K. (2004) The concentrative nucleoside transporter family, SLC28. *Pflügers Arch. Eur. J. Phys.* **447**:728-734.

Greenwood M. C., Dillon M. J., Simmonds H. A., Barratt T. M., Pincott J. R., Metreweli C. (1982) Renal failure due to 2,8-dihydroxyadenine urolithiasis. *Eur. J. Pediatr.* **138**:346-349.

Griffiths J. C., Borzelleca J. F., St Cyr J. (2007) Sub-chronic (13-week) oral toxicity study with D-ribose in Wistar rats. *Food Chem. Toxicol.* **45**:144-152.

Gross M., Zollner N. (1991) Serum levels of glucose, insulin, and C-peptide during long-term D-ribose administration in man. *Klin. Wochenschr.* **69**:31-36.

Gross M., Reiter S., Zollner N. (1989) Metabolism of D-ribose administered continuously to healthy persons and to patients with myoadenylate deaminase deficiency. *Klin. Wochenschr.* **67**:1205-1213.

Gualano B., Artioli G., Poortmans J., Lancha Junior A. (2011) Exploring the therapeutic role of creatine supplementation. *Amino Acids* **38**:31-44.

Gutensohn W. (1973) Purification and characterization of a neural hypoxanthine-guanine-phosphoribosyltransferase (HGPRT). *Adv. Exp. Med. Biol.* **41**:19-22.

Hack N., Hidaka H., Wakefield M. J., Balazs R. (1993) Promotion of granule cell survival by high K+ or excitatory amino acid treatment and Ca2+/calmodulin-dependent protein kinase activity. *Neuroscience* **57**:9-20.

Hardie D. G. (2007) AMP-activated/SNF1 protein kinases: conserved guardians of cellular energy. *Nat. Rev. Mol. Cell Biol.* **8**:774-785.

Hardie D. G., Hawley S. A. (2001) AMP-activated protein kinase: the energy charge hypothesis revisited. *Bioessays* **23**:1112-1119.

Hardie D. G., Pan D. A. (2002) Regulation of fatty acid synthesis and oxidation by the AMP-activated protein kinase. *Biochem. Soc. Trans.* **30**:1064-1070.

Hardie D. G., Frenguelli B. G. (2007) A neural protection racket: AMPK and the GABA(B) receptor. *Neuron* **53**:159-162.

Hardie D. G., Salt I. P., Davies S. P. (2000) Analysis of the role of the AMP-activated protein kinase in the response to cellular stress. *Methods Mol. Biol.* **99**:63-74.

Hardie D. G., Hawley S. A., Scott J. W. (2006) AMP-activated protein kinase--development of the energy sensor concept. *J. Physiol.* **574**:7-15.

Hashimoto K., Kikuchi H., Ishikawa M., Kobayashi S. (1992) Changes in cerebral energy metabolism and calcium levels in relation to delayed neuronal death after ischemia. *Neurosci. Lett.* **137**:165-168.

Hata R., Maeda K., Hermann D., Mies G., Hossmann K.-A. (2000a) Evolution of Brain Infarction After Transient Focal Cerebral Ischemia in Mice. *J. Cereb. Blood Flow Metab.* **20**:937-946.

Hata R., Maeda K., Hermann D., Mies G., Hossmann K. A. (2000b) Evolution of brain infarction after transient focal cerebral ischemia in mice. *J Cereb Blood Flow Metab* **20**:937-946.

Hawley S. A., Boudeau J., Reid J. L., Mustard K. J., Udd L., Makela T. P., Alessi D. R., Hardie D. G. (2003) Complexes between the LKB1 tumor suppressor, STRAD alpha/beta and MO25 alpha/beta are upstream kinases in the AMP-activated protein kinase cascade. *J. Biol.* **2**:28.

Heiss W.-D., Thiel A., Grond M., Graf R. (1999) Which Targets Are Relevant for Therapy of Acute Ischemic Stroke? *Stroke* **30**:1486-1489.

Hermann D. M., Kilic E., Hata R., Hossmann K. A., Mies G. (2001) Relationship between metabolic dysfunctions, gene responses and delayed cell death after mild focal cerebral ischemia in mice. *Neuroscience* **104**:947-955.

Hertz L. (2008) Bioenergetics of cerebral ischemia: A cellular perspective. *Neuropharmacol.* **55**:289-309.

Hesse G. W., Shashoua V. E. (1990) Protein synthesis as a function of depth in slices of rat hippocampus. *Neurosci. Lett.* **109**:186-190.

Hillered L., Hallstrom A., Segersvard S., Persson L., Ungerstedt U. (1989) Dynamics of extracellular metabolites in the striatum after middle cerebral artery occlusion in the rat monitored by intracerebral microdialysis. *J. Cereb. Blood Flow Metab.* **9**:607-616.

Ho O. H., Delgado J. Y., O'Dell T. J. (2004) Phosphorylation of proteins involved in activity-dependent forms of synaptic plasticity is altered in hippocampal slices maintained in vitro. *J. Neurochem.* **91**:1344-1357.

Hossmann K. A. (2008) Cerebral ischemia: models, methods and outcomes. *Neuropharmacol.* **55**:257-270.

Howard M., Sen H. A., Capoor S., Herfel R., Crooks P. A., Jacobson M. K. (1998) Measurement of adenosine concentration in aqueous and vitreous. *Invest. Ophthalmol. Vis. Sci.* **39**:1942-1946.

Hoxworth J. M., Xu K., Zhou Y., Lust W. D., LaManna J. C. (1999) Cerebral metabolic profile, selective neuron loss, and survival of acute and chronic hyperglycemic rats following cardiac arrest and resuscitation. *Brain. Res.* **821**:467-479.

Hoyer S., Lannert H. (2008) Long-term effects of corticosterone on behavior, oxidative and energy metabolism of parietotemporal cerebral cortex and hippocampus of rats: comparison to intracerebroventricular streptozotocin. *J. Neural Transm.*

Inouye S., Yamada Y., Miura K., Suzuki H., Kawata K., Shinoda K., Nakazawa A. (1999) Distribution and developmental changes of adenylate kinase isozymes in the rat brain: localization of adenylate kinase 1 in the olfactory bulb. *Biochem. Biophys. Res. Commun.* **254**:618-622.

Ipata P. L., Camici M., Micheli V., Tozz M. G. (2011) Metabolic network of nucleosides in the brain. *Curr. Top. Med. Chem.* **11**:909-922.

Isakovic A. J., Dencic S. M., Segal M. B., Redzic Z. B. (2008) Transport of [14C]hypoxanthine by sheep choroid plexus epithelium as a monolayer in primary culture: Na+-dependent and Na+-independent uptake by the apical membrane and rapid intracellular metabolic conversion to nucleotides. *Neurosci. Lett.* **431**:135-140.

Itoh R., Oka J., Ozasa H. (1986) Regulation of rat heart cytosol 5'-nucleotidase by adenylate energy charge. *Biochem. J.* **235**:847-851.

Jaeken J., Wadman S. K., Duran M., van Sprang F. J., Beemer F. A., Holl R. A., Theunissen P. M., de Cock P., van den Bergh F., Vincent M. F., et al. (1988) Adenylosuccinase deficiency: an inborn error of purine nucleotide synthesis. *Eur. J. Pediatr.* **148**:126-131.

Jordan D. O. (1952) Nucleic acids, purines, and pyrimidines. *Annu. Rev. Biochem.* **21**:209-244.

Jurecka A., Tylki-Szymanska A., Zikanova M., Krijt J., Kmoch S. (2008) D: -Ribose therapy in four Polish patients with adenylosuccinate lyase deficiency: Absence of positive effect. *J. Inherit. Metab. Dis.*

Jurkowitz M. S., Litsky M. L., Browning M. J., Hohl C. M. (1998) Adenosine, inosine, and guanosine protect glial cells during glucose deprivation and mitochondrial inhibition: correlation between protection and ATP preservation. *J. Neurochem.* **71**:535-548.

Kadam S. D., White A. M., Staley K. J., Dudek F. E. (2010) Continuous electroencephalographic monitoring with radio-telemetry in a rat model of perinatal hypoxia-ischemia reveals progressive post-stroke epilepsy. *J. Neurosci.* **30**:404-415.

Kalsi K. K., Smolenski R. T., Yacoub M. H. (1998) Effects of nucleoside transport inhibitors and adenine/ribose on ATP concentration and adenosine production in cardiac myocytes. *Adv. Exp. Med. Biol.* **431**:95-98.

Kammermeier H. (1993) Meaning of energetic parameters. *Basic Res. Cardiol.* **88**:380-384.

Kanemitsu H., Tamura A., Kirino T., Karasawa S., Sano K., Iwamoto T., Yoshiura M., Iriyama K. (1988) Xanthine and uric acid levels in rat brain following focal ischemia. *J. Neurochem.* **51**:1882-1885.

Kass I. S., Lipton P. (1982) Mechanisms involved in irreversible anoxic damage to the in vitro rat hippocampal slice. *J. Physiol.* **332**:459-472.

Katayama M., Matsuda Y., Shimokawa K., Tanabe S., Kaneko S., Hara I., Sato H. (2001) Simultaneous determination of six adenyl purines in human plasma by high-performance liquid chromatography with fluorescence derivatization. *J. Chromatogr. B Biomed. Sci. Appl.* **760**:159-163.

Kauffman F. C., Brown J. G., Passonneau J. V., Lowry O. H. (1969) Effects of changes in brain metabolism on levels of pentose phosphate pathway intermediates. *J. Biol. Chem.* **244**:3647-3653.

Kawamura M., Jr., Ruskin D. N., Masino S. A. (2010) Metabolic autocrine regulation of neurons involves cooperation among pannexin hemichannels, adenosine receptors, and KATP channels. *J. Neurosci.* **30**:3886-3895.

Kelly-Hayes P. M., Robertson J. T., Broderick J. P., Duncan P. W., Hershey L. A., Roth E. J., Thies W. H., Trombly C. A. (1998) The American Heart Association Stroke Outcome Classification. *Stroke* **29**:1274-1280.

Kessey K., Mogul D. J. (1998) Adenosine A2 receptors modulate hippocampal synaptic transmission via a cyclic-AMP-dependent pathway. *Neuroscience* **84**:59-69.

Khym J. X. (1975) An analytical system for rapid separation of tissue nucleotides at low pressures on conventional anion exchangers. *Clin. Chem.* **21**:1245-1252.

Kicska G. A., Long L., HÃ¶rig H., Fairchild C., Tyler P. C., Furneaux R. H., Schramm V. L., Kaufman H. L. (2001) Immucillin H, a powerful transition-state analog inhibitor of purine nucleoside phosphorylase, selectively inhibits human T lymphocytes. *PNAS* **98**:4593-4598.

Kim H., Kim C., Carpentier A., Poortmans J. (2011) Studies on the safety of creatine supplementation. *Amino Acids*:1-10.

Kleihues P., Kobayashi K., Hossmann K. A. (1974) Purine nucleotide metabolism in the cat brain after one hour of complete ischemia. *J. Neurochem.* **23**:417-425.

Kleihues P., Hossmann K. A., Pegg A. E., Kobayashi K., Zimmermann V. (1975) Resuscitation of the monkey brain after one hour complete ischemia. III. Indications of metabolic recovery. *Brain. Res.* **95**:61-73.

Kleindorfer D., Kissela B., Schneider A., Woo D., Khoury J., Miller R., Alwell K., Gebel J., Szaflarski J., Pancioli A., Jauch E., Moomaw C., Shukla R., Broderick J. P., for The Neuroscience I. (2004) Eligibility for Recombinant Tissue Plasminogen Activator in Acute Ischemic Stroke: A Population-Based Study. *Stroke* **35**:e27-29.

Kobayashi M., Lust W. D., Passonneau J. V. (1977) Concentrations of energy metabolites and cyclic nucleotides during and after bilateral ischemia in the gerbil cerebral cortex. *J. Neurochem.* **29**:53-59.

Kobayashi T., Yamada T., Okada Y. (1998) The levels of adenosine and its metabolites in the guinea pig and rat brain during complete ischemia-in vivo study. *Brain. Res.* **787**:211-219.

Kochanowski N., Blanchard F., Cacan R., Chirat F., Guedon E., Marc A., Goergen J. L. (2006) Intracellular nucleotide and nucleotide sugar contents of cultured CHO cells determined by a fast, sensitive, and high-resolution ion-pair RP-HPLC. *Anal. Biochem.* **348**:243-251.

Kost A., Ivanov M. (1980) Etheno derivatives of adenine and cytosine (review). *Chem. of Heterocyc. Comp.* **16**:209-221.

Kreisman N. R., Soliman S., Gozal D. (2000) Regional differences in hypoxic depolarization and swelling in hippocampal slices. *J. Neurophysiol.* **83**:1031-1038.

Krnjevic K. (2008) Electrophysiology of cerebral ischemia. *Neuropharmacol.* **55**:319-333.

Kuramoto N., Wilkins M. E., Fairfax B. P., Revilla-Sanchez R., Terunuma M., Tamaki K., Iemata M., Warren N., Couve A., Calver A., Horvath Z., Freeman K., Carling D., Huang L., Gonzales C., Cooper E., Smart T. G., Pangalos M. N., Moss S. J. (2007) Phospho-dependent functional modulation of GABA(B) receptors by the metabolic sensor AMP-dependent protein kinase. *Neuron* **53**:233-247.

Laghi Pasini F., Guideri F., Picano E., Parenti G., Petersen C., Varga A., Di Perri T. (2000) Increase in plasma adenosine during brain ischemia in man: a study during transient ischemic attacks, and stroke. *Brain Res. Bull.* **51**:327-330.

Lakhan S. E., Kirchgessner A., Hofer M. (2009) Inflammatory mechanisms in ischemic stroke: therapeutic approaches. *J. Transl. Med.* **7**:97.

Lamberts R. R., Caldenhoven E., Lansink M., Witte G., Vaessen R. J., St Cyr J. A., Stienen G. J. M. (2007) Preservation of diastolic function in monocrotaline-induced right ventricular hypertrophy in rats. *Am. J. of Phys. - Heart and Circulatory Phys.* **293**:H1869-H1876.

Larson J., Wong D., Lynch G. (1986) Patterned stimulation at the theta frequency is optimal for the induction of hippocampal long-term potentiation. *Brain. Res.* **368**:347-350.

Latini S., Pedata F. (2001) Adenosine in the central nervous system: release mechanisms and extracellular concentrations. *J. Neurochem.* **79**:463-484.

Latini S., Corsi C., Pedata F., Pepeu G. (1996) The source of brain adenosine outflow during ischemia and electrical stimulation. *Neurochem. Int.* **28**:113-118.

Lawler J. M., Barnes W. S., Wu G., Song W., Demaree S. (2002) Direct antioxidant properties of creatine. *Biochem. Biophys. Res. Commun.* **290**:47-52.

Levitt B., Head R. J., Westfall D. P. (1984) High-pressure liquid chromatographic-fluorometric detection of adenosine and adenine nucleotides: application to endogenous content and electrically induced release of adenyl purines in guinea pig vas deferens. *Anal. Biochem.* **137**:93-100.

Levy D. E., Duffy T. E. (1977) Cerebral energy metabolism during transient ischemia and recovery in the gerbil 1. *J. Neurochem.* **28**:63-70.

Li H., Yan Z., Zhu J., Yang J., He J. (2010) Neuroprotective effects of resveratrol on ischemic injury mediated by improving brain energy metabolism and alleviating oxidative stress in rats. *Neuropharmacol.* **60**:252-258.

Lin W., Seela F., Eickmeier H., Reuter H. (2004) 1,N6-Etheno derivative of 7-deaza-2,8-diazaadenosine. *Acta Crystallogr, C* **60**:o566-568.

Lin Y., Phillis J. W. (1991) Oxypurinol reduces focal ischemic brain injury in the rat. *Neurosci. Lett.* **126**:187-190.

Lin Y., Phillis J. W. (1992) Deoxycoformycin and oxypurinol: protection against focal ischemic brain injury in the rat. *Brain. Res.* **571**:272-280.

Lipmann F. (2006) Metabolic Generation and Utilization of Phosphate Bond Energy. John Wiley & Sons, Inc.

Lipton P. (1999) Ischemic cell death in brain neurons. *Physiol. Rev.* **79**:1431-1568.

Lipton P., Whittingham T. S. (1982) Reduced ATP concentration as a basis for synaptic transmission failure during hypoxia in the in vitro guinea-pig hippocampus. *J. Physiol.* **325**:51-65.

Lipton P., Aitken P. G., Dudek F. E., Eskessen K., Espanol M. T., Ferchmin P. A., Kelly J. B., Kreisman N. R., Landfield P. W., Larkman P. M., et al. (1995) Making the best of brain slices: comparing preparative methods. *J. Neurosci. Methods* **59**:151-156.

Litsky M. L., Hohl C. M., Lucas J. H., Jurkowitz M. S. (1999) Inosine and guanosine preserve neuronal and glial cell viability in mouse spinal cord cultures during chemical hypoxia. *Brain. Res.* **821**:426-432.

Ljunggren B., Ratcheson R. A., Siesjo B. K. (1974) Cerebral metabolic state following complete compression ischemia. *Brain. Res.* **73**:291-307.

Lloyd H. G., Lindstrom K., Fredholm B. B. (1993) Intracellular formation and release of adenosine from rat hippocampal slices evoked by electrical stimulation or energy depletion. *Neurochem. Int.* **23**:173-185.

Lohmann K. (1929) Über die Pyrophosphatfraktion im Muskel. *Naturwissenschaften* **17**:624-625.

Lopes L. V., Cunha R. A., Kull B., Fredholm B. B., Ribeiro J. A. (2002) Adenosine A(2A) receptor facilitation of hippocampal synaptic transmission is dependent on tonic A(1) receptor inhibition. *Neuroscience* **112**:319-329.

Lopes L. V., Rebola N., Costenla A. R., Halldner L., Jacobson M. A., Oliveira C. R., Richardson P. J., Fredholm B. B., Ribeiro J. A., Cunha R. A. (2003) Adenosine A3 receptors in the rat hippocampus: Lack of interaction with A1 receptors. *Drug Dev. Res.* **58**:428-438.

Lu Q., Wang J. (2008) Single molecule conformational dynamics of adenylate kinase: energy landscape, structural correlations, and transition state ensembles. *J. Am. Chem. Soc.* **130**:4772-4783.

Lust W. D., Taylor C., Pundik S., Selman W. R., Ratcheson R. A. (2002) Ischemic cell death: dynamics of delayed secondary energy failure during reperfusion following focal ischemia. *Metab. Brain Dis.* **17**:113-121.

Lynch J. J., 3rd, Alexander K. M., Jarvis M. F., Kowaluk E. A. (1998) Inhibition of adenosine kinase during oxygen-glucose deprivation in rat cortical neuronal cultures. *Neurosci. Lett.* **252**:207-210.

Lyoo I. K., Kong S. W., Sung S. M., Hirashima F., Parow A., Hennen J., Cohen B. M., Renshaw P. F. (2003) Multinuclear magnetic resonance spectroscopy of high-energy phosphate metabolites in human brain following oral supplementation of creatine-monohydrate. *Psychiatry Res.* **123**:87-100.

Lythgoe B., Todd A. R. (1945) Structure of Adenosine Di- and Tri-Phosphate. *Nature* **155**:695-696.

Maccarter D., Vijay N., Washam M., Shecterle L., Sierminski H., St Cyr J. A. (2008) D-ribose aids advanced ischemic heart failure patients. *Int. J. Cardiol.*

Madry C., HaglerÃ¸d C., Attwell D. (2010) The role of pannexin hemichannels in the anoxic depolarization of hippocampal pyramidal cells. *Brain* **133**:3755-3763.

Makino K. (1935) Ueber die Konstitution der Adenosintriphosphosaeure. *Biochemische Zeitschrift* **278**:161-163.

Manfredi G., Yang L., Gajewski C. D., Mattiazzi M. (2002) Measurements of ATP in mammalian cells. *Methods* **26**:317-326.

Manfredi J. P., Holmes E. W. (1985) Purine salvage pathways in myocardium. *Annu. Rev. Physiol.* **47**:691-705.

Manzoni O. J., Manabe T., Nicoll R. A. (1994) Release of adenosine by activation of NMDA receptors in the hippocampus. *Science* **265**:2098-2101.

Marklund N., Salci K., Ronquist G., Hillered L. (2006) Energy metabolic changes in the early post-injury period following traumatic brain injury in rats. *Neurochem. Res.* **31**:1085-1093.

Marques A. F., Teixeira N. A., Gambaretto C., Sillero A., Sillero M. A. (1998) IMP-GMP 5'-nucleotidase from rat brain: activation by polyphosphates. *J. Neurochem.* **71**:1241-1250.

Marro P. J., Mishra O. P., Delivoria-Papadopoulos M. (2006) Effect of allopurinol on brain adenosine levels during hypoxia in newborn piglets. *Brain. Res.* **1073-1074**:444-450.

Maruyama K. (1991) The discovery of adenosine triphosphate and the establishment of its structure. *J. History of Bio.* **24**:145-154.

Mascia L., Cappiello M., Cherri S., Ipata P. L. (2000) In vitro recycling of alpha-D-ribose 1-phosphate for the salvage of purine bases. *Biochim. Biophys. Acta* **1474**:70-74.

Masino S. A., Geiger J. D. (2008) Are purines mediators of the anticonvulsant/neuroprotective effects of ketogenic diets? *Trends Neurosci.* **31**:273-278.

Matthews E. A., Dickenson A. H. (2004) Effects of spinally administered adenine on dorsal horn neuronal responses in a rat model of inflammation. *Neurosci. Lett.* **356**:211-214.

Mauser M., Hoffmeister H. M., Nienaber C., Schaper W. (1985) Influence of ribose, adenosine, and "AICAR" on the rate of myocardial adenosine triphosphate synthesis during reperfusion after coronary artery occlusion in the dog. *Circ. Res.* **56**:220-230.

McIlwain H. (1951) Metabolic response in vitro to electrical stimulation of sections of mammalian brain. *Biochem. J.* **49**:382-393.

McIlwain H. (1952) Phosphates of brain during in vitro metabolism: effects of oxygen, glucose, glutamate, glutamine, and calcium and potassium salts. *Biochem. J.* **52**:289-295.

McIlwain H., Buchel L., Cheshire J. D. (1951) The inorganic phosphate and phosphocreatine of Brain especially during metabolism in vitro. *Biochem. J.* **48**:12-20.

Mergenthaler P., Dirnagl U., Meisel A. (2004) Pathophysiology of stroke: lessons from animal models. *Metab. Brain Dis.* **19**:151-167.

Milusheva E. A., Doda M., Baranyi M., Vizi E. S. (1996) Effect of hypoxia and glucose deprivation on ATP level, adenylate energy charge and [Ca2+]o-dependent and independent release of [3H]dopamine in rat striatal slices. *Neurochem. Int.* **28**:501-507.

Mitani A., Takeyasu S., Yanase H., Nakamura Y., Kataoka K. (1994) Changes in intracellular Ca2+ and energy levels during in vitro ischemia in the gerbil hippocampal slice. *J. Neurochem.* **62**:626-634.

Mitchell J. B., Lupica C. R., Dunwiddie T. V. (1993) Activity-dependent release of endogenous adenosine modulates synaptic responses in the rat hippocampus. *J. Neurosci.* **13**:3439-3447.

Miyoshi K., Akazawa Y., Horiguchi T., Noma T. (2009) Localization of adenylate kinase 4 in mouse tissues. *Acta Histochem. Cytochem.* **42**:55-64.

Moustafa R. R., Baron J. C. (2008) Pathophysiology of ischaemic stroke: insights from imaging, and implications for therapy and drug discovery. *Br. J. Pharmacol.* **153 Suppl 1**:S44-54.

Muir K. W. (2002) Heterogeneity of Stroke Pathophysiology and Neuroprotective Clinical Trial Design. *Stroke* **33**:1545-1550.

Muller C., Zimmer H., Gross M., Gresser U., Brotsack I., Wehling M., Pliml W. (1998) Effect of ribose on cardiac adenine nucleotides in a donor model for heart transplantation. *Eur. J. Med. Res.* **3**:554-558.

Müller C. E., Iqbal J., Baqi Y., Zimmermann H., Röllich A., Stephan H. (2006) Polyoxometalates--a new class of potent ecto-nucleoside triphosphate diphosphohydrolase (NTPDase) inhibitors. *Bioorganic & Med. Chem. Letters* **16**:5943-5947.

Murray A. W. (1966) Purine-phosphoribosyltransferase activities in rat and mouse tissues and in Ehrlich ascites-tumour cells. *Biochem. J.* **100**:664-670.

Murray A. W. (1971) The biological significance of purine salvage. *Annu. Rev. Biochem.* **40**:811-826.

Newman G. C., Hospod F. E., Trowbridge S. D., Motwani S., Liu Y. (1998) Restoring adenine nucleotides in a brain slice model of cerebral reperfusion. *J. Cereb. Blood Flow Metab.* **18**:675-685.

Nicholls D. G., Ferguson S. J. (1992) Bioenergetics 2, 2 Editior. Academic Press.

Nishiyama J., Ueki M., Asaga T., Chujo K., Maekawa N. (2009) Protective action of D-ribose against renal injury caused by ischemia and reperfusion in rats with transient hyperglycemia. *Tohoku J. Exp. Med.* **219**:215-222.

Nitatori T., Sato N., Waguri S., Karasawa Y., Araki H., Shibanai K., Kominami E., Uchiyama Y. (1995) Delayed neuronal death in the CA1 pyramidal cell layer of the gerbil hippocampus following transient ischemia is apoptosis. *J. Neurosci.* **15**:1001-1011.

Noma T. (2005) Dynamics of nucleotide metabolism as a supporter of life phenomena. *J. Med. Invest.* **52**:127-136.

Nowak T. S., Jr., Fried R. L., Lust W. D., Passonneau J. V. (1985) Changes in brain energy metabolism and protein synthesis following transient bilateral ischemia in the gerbil. *J. Neurochem.* **44**:487-494.

Nyhan W. L. (2005) Disorders of purine and pyrimidine metabolism. *Mol. Genet. Metab.* **86**:25-33.

Olsson T., Cronberg T., Rytter A., Asztély F., Fredholm B. B., Smith M.-L., Wieloch T. (2004) Deletion of the adenosine A1 receptor gene does not alter neuronal damage following ischaemia in vivo or in vitro. *Eur. J. of Neurosci.* **20**:1197-1204.

Omran H., McCarter D., St Cyr J., Luderitz B. (2004) D-ribose aids congestive heart failure patients. *Exp. Clin. Cardiol.* **9**:117-118.

Omran H., Illien S., MacCarter D., St Cyr J., Luderitz B. (2003) D-Ribose improves diastolic function and quality of life in congestive heart failure patients: a prospective feasibility study. *Eur. J. Heart Fail.* **5**:615-619.

Onodera H., Iijima K., Kogure K. (1986) Mononucleotide metabolism in the rat brain after transient ischemia. *J. Neurochem.* **46**:1704-1710.

Orrego F., Lipmann F. (1967) Protein synthesis in brain slices. Effects of electrical stimulation and acidic amino acids. *J. Biol. Chem.* **242**:665-671.

Pacher P. l., Nivorozhkin A., SzabÃ³ C. (2006) Therapeutic Effects of Xanthine Oxidase Inhibitors: Renaissance Half a Century after the Discovery of Allopurinol. *Pharm. Rev.* **58**:87-114.

Palmer C., Towfighi J., Roberts R. L., Heitjan D. F. (1993) Allopurinol administered after inducing hypoxia-ischemia reduces brain injury in 7-day-old rats. *Pediatr. Res.* **33**:405-411.

Pankratov Y., Lalo U., Krishtal O. A., Verkhratsky A. (2009) P2X receptors and synaptic plasticity. *Neuroscience* **158**:137-148.

Pankratov Y. V., Lalo U. V., Krishtal O. A. (2002) Role for P2X receptors in long-term potentiation. *J. Neurosci.* **22**:8363-8369.

Parang P., Singh B., Arora R. (2005) Metabolic modulators for chronic cardiac ischemia. *J. Cardiovasc. Pharmacol. Ther.* **10**:217-223.

Pardridge W. M., Oldendorf W. H. (1977) Transport of metabolic substrates through the bloo-brain barrier 1. *J. Neurochem.* **28**:5-12.

Park C. R., Johnson L. H., Wright J. H., Jr., Batsel H. (1957) Effect of insulin on transport of several hexoses and pentoses into cells of muscle and brain. *Am. J. Physiol.* **191**:13-18.

Park J., van Koeverden P., Singh B., Gupta R. S. (2007) Identification and characterization of human ribokinase and comparison of its properties with E. coli ribokinase and human adenosine kinase. *FEBS letters* **581**:3211-3216.

Parkinson F. E., Sinclair C. J., Othman T., Haughey N. J., Geiger J. D. (2002) Differences between rat primary cortical neurons and astrocytes in purine release evoked by ischemic conditions. *Neuropharmacol.* **43**:836-846.

Paschen W., Djuricic B. (1995) Comparison of in vitro ischemia-induced disturbances in energy metabolism and protein synthesis in the hippocampus of rats and gerbils. *J. Neurochem.* **65**:1692-1697.

Pascoe M. C., Crewther S. G., Carey L. M., Crewther D. P. (2011) Inflammation and depression: why poststroke depression may be the norm and not the exception. *Int. J. Stroke* **6**:128-135.

Pascual O., Casper K. B., Kubera C., Zhang J., Revilla-Sanchez R., Sul J.-Y., Takano H., Moss S. J., McCarthy K., Haydon P. G. (2005) Astrocytic Purinergic Signaling Coordinates Synaptic Networks. *Science* **310**:113-116.

Pasque M. K., Wechsler A. S. (1984) Metabolic intervention to affect myocardial recovery following ischemia. *Ann. Surg.* **200**:1-12.

Pauly D. F., Pepine C. J. (2000) D-Ribose as a supplement for cardiac energy metabolism. *J. Cardiovasc. Pharmacol. Ther.* **5**:249-258.

Pauly D. F., Johnson C., St Cyr J. A. (2003) The benefits of ribose in cardiovascular disease. *Med. Hypotheses* **60**:149-151.

Pea F. (2005) Pharmacology of drugs for hyperuricemia. Mechanisms, kinetics and interactions. *Contrib. Nephrol.* **147**:35-46.

Pearson T., Damian K., Lynas R. E., Frenguelli B. G. (2006) Sustained elevation of extracellular adenosine and activation of A1 receptors underlie the post-ischaemic

inhibition of neuronal function in rat hippocampus in vitro. *J. Neurochem.* **97**:1357-1368.

Pearson T., Nuritova F., Caldwell D., Dale N., Frenguelli B. G. (2001) A depletable pool of adenosine in area CA1 of the rat hippocampus. *J. Neurosci.* **21**:2298-2307.

Pearson T., Currie A. J., Etherington L. A., Gadalla A. E., Damian K., Llaudet E., Dale N., Frenguelli B. G. (2003) Plasticity of purine release during cerebral ischemia: clinical implications? *J. Cell. Mol. Med.* **7**:362-375.

Pedata F., Melani A., Pugliese A. M., Coppi E., Cipriani S., Traini C. (2007) The role of ATP and adenosine in the brain under normoxic and ischemic conditions. *Purinergic Signal.* **3**:299-310.

Pellerin L., Magistretti P. J. (1994) Glutamate uptake into astrocytes stimulates aerobic glycolysis: a mechanism coupling neuronal activity to glucose utilization. *PNAS* **91**:10625-10629.

Peppa M., Uribarri J., Vlassara H. (2003) Glucose, Advanced Glycation End Products, and Diabetes Complications: What Is New and What Works. *Clin. Diab.* **21**:186-187.

Perasso L., Cupello A., Lunardi G. L., Principato C., Gandolfo C., Balestrino M. (2003) Kinetics of creatine in blood and brain after intraperitoneal injection in the rat. *Brain Res.* **974**:37-42.

Perasso L., Adriano E., Ruggeri P., Burov S. V., Gandolfo C., Balestrino M. (2009) In vivo neuroprotection by a creatine-derived compound: Phosphocreatine-Mg-complex acetate. *Brain Res.* **1285**:158-163.

Perkowski D., Wagner S., St Cyr J. A. (2007) D-ribose benefits "off" pump coronary artery bypass revascularization. *J. Card. Surg.* **22**:370-371.

Phillips R. A. (2008) A review of therapeutic strategies for risk reduction of recurrent stroke. *Prog. Cardiovasc. Dis.* **50**:264-273.

Phillis J. W. (1989) Adenosine in the control of the cerebral circulation. *Cerebrovasc. Brain Metab. Rev.* **1**:26-54.

Phillis J. W., O'Regan M. H. (1989) Deoxycoformycin antagonizes ischemia-induced neuronal degeneration. *Brain Res. Bull.* **22**:537-540.

Phillis J. W., Sen S. (1993) Oxypurinol attenuates hydroxyl radical production during ischemia/reperfusion injury of the rat cerebral cortex: an ESR study. *Brain Res.* **628**:309-312.

Phillis J. W., DeLong R. E., Towner J. K. (1985) Adenosine deaminase inhibitors enhance cerebral anoxic hyperemia in the rat. *J. Cereb. Blood Flow Metab.* **5**:295-299.

Phillis J. W., Walter G. A., Simpson R. E. (1991) Brain adenosine and transmitter amino acid release from the ischemic rat cerebral cortex: effects of the adenosine deaminase inhibitor deoxycoformycin. *J. Neurochem.* **56**:644-650.

Phillis J. W., Perkins L. M., Smith-Barbour M., O'Regan M. H. (1995) Oxypurinol-enhanced postischemic recovery of the rat brain involves preservation of adenine nucleotides. *J. Neurochem.* **64**:2177-2184.

Phillis J. W., O'Regan M. H., Estevez A. Y., Song D., VanderHeide S. J. (1996) Cerebral energy metabolism during severe ischemia of varying duration and following reperfusion. *J. Neurochem.* **67**:1525-1531.

Piccinin S., Di Angelantonio S., Piccioni A., Volpini R., Cristalli G., Fredholm B. B., Limatola C., Eusebi F., Ragozzino D. (2010) CX3CL1-induced modulation at CA1 synapses reveals multiple mechanisms of EPSC modulation involving adenosine receptor subtypes. *J. Neuroimmun.* **224**:85-92.

Pliml W., von Arnim T., Stablein A., Hofmann H., Zimmer H. G., Erdmann E. (1992) Effects of ribose on exercise-induced ischaemia in stable coronary artery disease. *Lancet* **340**:507-510.

Podgorska M., Kocbuch K., Pawelczyk T. (2005) Recent advances in studies on biochemical and structural properties of equilibrative and concentrative nucleoside transporters. *Acta. Biochim. Pol.* **52**:749-758.

Pogolotti A. L., Jr., Santi D. V. (1982) High-pressure liquid chromatography--ultraviolet analysis of intracellular nucleotides. *Anal. Biochem.* **126**:335-345.

Prass K., Royl G., Lindauer U., Freyer D., Megow D., Dirnagl U., Stockler-Ipsiroglu G., Wallimann T., Priller J. (2007) Improved reperfusion and neuroprotection by creatine in a mouse model of stroke. *J. Cereb. Blood Flow Metab.* **27**:452-459.

Prather J. W., Wright E. M. (1970) Molecular and kinetic parameters of sugar transport across the frog choroid plexus. *J. Mem. Bio.* **2**:150-172.

Pundik S., Robinson S., Lust W. D., Zechel J., Buczek M., Selman W. R. (2006) Regional metabolic status of the E-18 rat fetal brain following transient hypoxia/ischemia. *Metab. Brain Dis.* **21**:309-317.

Ramos-Salazar A., Baines A. D. (1985) Fluorometric determination of adenine nucleotides and adenosine by ion-paired, reverse-phase, high-performance liquid chromatography. *Anal. Biochem.* **145**:9-13.

Rathbone M. P., Middlemiss P. J., Gysbers J. W., Andrew C., Herman M. A., Reed J. K., Ciccarelli R., Di Iorio P., Caciagli F. (1999) Trophic effects of purines in neurons and glial cells. *Prog. Neurobiol.* **59**:663-690.

Rebaudo R., Melani R., Carità F., Rosi L., Picchio V., Ruggeri P., Izvarina N., Balestrino M. (2000) Increase of Cerebral Phosphocreatine in Normal Rats after Intracerebroventricular Administration of Creatine. *Neurochem. Res.* **25**:1493-1495.

Redondo R. L., Okuno H., Spooner P. A., Frenguelli B. G., Bito H., Morris R. G. (2010) Synaptic tagging and capture: differential role of distinct calcium/calmodulin kinases in protein synthesis-dependent long-term potentiation. *J. Neurosci.* **30**:4981-4989.

Redzic Z. B., Segal M. B., Gasic J. M., Markovic I. D., Vojvodic V. P., Isakovic A., Thomas S. A., Rakic L. M. (2001) The characteristics of nucleobase transport and metabolism by the perfused sheep choroid plexus. *Brain. Res.* **888**:66-74.

Rex C. S., Kramar E. A., Colgin L. L., Lin B., Gall C. M., Lynch G. (2005) Long-term potentiation is impaired in middle-aged rats: regional specificity and reversal by adenosine receptor antagonists. *J. Neurosci.* **25**:5956-5966.

Ribeiro J. A., Sebastiao A. M., de Mendonca A. (2002) Adenosine receptors in the nervous system: pathophysiological implications. *Prog Neurobiol* **68**:377-392.

Ribeiro J. A., Sebastiao A. M., de Mendonca A. (2003) Participation of adenosine receptors in neuroprotection. *Drug News Perspect.* **16**:80-86.

Rodrigues R. J., Almeida T., Richardson P. J., Oliveira C. R., Cunha R. A. (2005) Dual Presynaptic Control by ATP of Glutamate Release via Facilitatory P2X1, P2X2/3, and P2X3 and Inhibitory P2Y1, P2Y2, and/or P2Y4 Receptors in the Rat Hippocampus. *J. Neurosci.* **25**:6286-6295.

Rudolphi K. A., Schubert P., Parkinson F. E., Fredholm B. B. (1992) Neuroprotective role of adenosine in cerebral ischaemia. *Trends Pharm. Sci.* **13**:439-445.

Sacerdote M. G., Szostak J. W. (2005) Semipermeable lipid bilayers exhibit diastereoselectivity favoring ribose. *Proc. Natl Acad. Sci. U S A* **102**:6004-6008.

Sahasranaman S., Howard D., Roy S. (2008) Clinical pharmacology and pharmacogenetics of thiopurines. *Eur. J. of Clin. Pharm.* **64**:753-767.

Saito H., Nishimura M., Shinano H., Makita H., Tsujino I., Shibuya E., Sato F., Miyamoto K., Kawakami Y. (1999) Plasma concentration of adenosine during normoxia and moderate hypoxia in humans. *Am. J. Respir. Crit. Care Med.* **159**:1014-1018.

Sajikumar S., Frey J. U. (2004) Late-associativity, synaptic tagging, and the role of dopamine during LTP and LTD. *Neurobiol. Learn. Mem.* **82**:12-25.

Sajikumar S., Navakkode S., Frey J. U. (2005) Protein synthesis-dependent long-term functional plasticity: methods and techniques. *Curr. Opin. Neurobiol.* **15**:607-613.

Sala-Newby G. B., Freeman N. V. E., Skladanowski A. C., Newby A. C. (2000) Distinct Roles for Recombinant Cytosolic 5'-Nucleotidase-I and -II in AMP and IMP Catabolism in COS-7 and H9c2 Rat Myoblast Cell Lines. *J. Biol. Chem.* **275**:11666-11671.

Salerno C., D'Eufemia P., Finocchiaro R., Celli M., Spalice A., Iannetti P., Crifo C., Giardini O. (1999) Effect of D-ribose on purine synthesis and neurological symptoms in a patient with adenylosuccinase deficiency. *Biochim. Biophys. Acta* **1453**:135-140.

Sanders M. J., Grondin P. O., Hegarty B. D., Snowden M. A., Carling D. (2007) Investigating the mechanism for AMP activation of the AMP-activated protein kinase cascade. *Biochem. J.* **403**:139-148.

Sato H., Ueki M., Asaga T., Chujo K., Maekawa N. (2009) D-ribose attenuates ischemia/reperfusion-induced renal injury by reducing neutrophil activation in rats. *Tohoku J. Exp. Med.* **218**:35-40.

Saver J. L. (2006) Time Is Brain--Quantified. *Stroke* **37**:263-266.

Schaller B., Graf R. (2004) Cerebral ischemia and reperfusion: the pathophysiologic concept as a basis for clinical therapy. *J. Cereb. Blood Flow Metab.* **24**:351-371.

Schmidley J. W. (1990) Free radicals in central nervous system ischemia. *Stroke* **21**:1086-1090.

Schmidt A. P., Bohmer A. E., Antunes C., Schallenberger C., Porciuncula L. O., Elisabetsky E., Lara D. R., Souza D. O. (2009) Anti-nociceptive properties of the xanthine oxidase inhibitor allopurinol in mice: role of A1 adenosine receptors. *Br. J. Pharmacol.* **156**:163-172.

Schneider H. J., Rossner S., Pfeiffer D., Hagendorff A. (2007) d-ribose improves cardiac contractility and hemodynamics, and reduces expression of c-fos in the hippocampus during sustained slow ventricular tachycardia in rats. *Int. J. Cardiol.*

Schulman J. D., Greene M. L., Fujimoto W. Y., Seegmiller J. E. (1971) Adenine Therapy for Lesch-Nyhan Syndrome. *Pediatric Res.* **5**:77-82.

Schurr A., Rigor B. M. (1989) Cerebral ischemia revisited: new insights as revealed using in vitro brain slice preparations. *Experientia* **45**:684-695.

Schurr A., West C. A., Rigor B. M. (1988) Lactate-supported synaptic function in the rat hippocampal slice preparation. *Science* **240**:1326-1328.

Schurr A., West C. A., Rigor B. M. (1989) Electrophysiology of energy metabolism and neuronal function in the hippocampal slice preparation. *J. Neurosci. Methods* **28**:7-13.

Schurr A., Payne R. S., Miller J. J., Rigor B. M. (1999) Study of cerebral energy metabolism using the rat hippocampal slice preparation. *Methods* **18**:117-126.

Sciotti V. M., Park T. S., Berne R. M., Van Wylen D. G. (1993) Changes in extracellular adenosine during chemical or electrical brain stimulation. *Brain. Res.* **613**:16-20.

Segal S., Foley J. (1958) The metabolism of D-ribose in man. *J. Clin. Invest.* **37**:719-735.

Seifert J., Frelich A., Shecterle L., St Cyr J. (2008) Assessment of Hematological and Biochemical parameters with extended D-Ribose ingestion. *J. Int. Soc. Sports Nutr.* **5**:13.

Sestili P., Martinelli C., Bravi G., Piccoli G., Curci R., Battistelli M., Falcieri E., Agostini D., Gioacchini A. M., Stocchi V. (2006) Creatine supplementation affords cytoprotection in oxidatively injured cultured mammalian cells via direct antioxidant activity. *Free Radical Biol. and Med.* **40**:837-849.

Shecterle L. M., Terry K. R., St Cyr J. A. (2010) The patented uses of D-ribose in cardiovascular diseases. *Recent Pat. Cardiovasc. Drug Discov.* **5**:138-142.

Shen H., Chen G.-J., Harvey B. K., Bickford P. C., Wang Y. (2005) Inosine Reduces Ischemic Brain Injury in Rats. *Stroke* **36**:654-659.

Sheng X. R., Li X., Pan X. M. (1999) An iso-random Bi Bi mechanism for adenylate kinase. *J. Biol. Chem.* **274**:22238-22242.

Shryock J. C., Rubio R., Berne R. M. (1986) Extraction of adenine nucleotides from cultured endothelial cells. *Anal Biochem* **159**:73-81.

Shulman R. G., Rothman D. L., Behar K. L., Hyder F. (2004) Energetic basis of brain activity: implications for neuroimaging. *Trends Neurosci.* **27**:489-495.

Siesjo B. K. (1981) Cell damage in the brain: a speculative synthesis. *J Cereb Blood Flow Metab* **1**:155-185.

Siklos L., Kuhnt U., Parducz A., Szerdahelyi P. (1997) Intracellular calcium redistribution accompanies changes in total tissue Na+, K+ and water during the first two hours of in vitro incubation of hippocampal slices. *Neuroscience* **79**:1013-1022.

Simmonds H. A. (1986) 2,8-Dihydroxyadenine lithiasis--epidemiology, pathogenesis and therapy. *Verh. Dtsch. Ges. Inn. Med.* **92**:503-508.

Sims N. R., Zaidan E. (1995) Biochemical changes associated with selective neuronal death following short-term cerebral ischaemia. *Int. J. Biochem. Cell Biol.* **27**:531-550.

Sinha S. C., Smith J. L. (2001) The PRT protein family. *Curr. Op. in Struct. Bio.* **11**:733-739.

Smalley R. V., Guaspari A., Haase-Statz S., Anderson S. A., Cederberg D., Hohneker J. A. (2000) Allopurinol: intravenous use for prevention and treatment of hyperuricemia. *J. Clin. Oncol.* **18**:1758-1763.

Smith W. S., Sung G., Saver J., Budzik R., Duckwiler G., Liebeskind D. S., Lutsep H. L., Rymer M. M., Higashida R. T., Starkman S., Gobin Y. P., for the Multi M. I. (2008) Mechanical Thrombectomy for Acute Ischemic Stroke: Final Results of the Multi MERCI Trial. *Stroke* **39**:1205-1212.

Smolenski R. T., Kalsi K. K., Zych M., Kochan Z., Yacoub M. H. (1998) Adenine/ribose supply increases adenosine production and protects ATP pool in adenosine kinase-inhibited cardiac cells. *J. Mol. Cell Cardiol.* **30**:673-683.

Somjen G. G. (2002) Ion Regulation in the Brain: Implications for Pathophysiology. *The Neuroscientist* **8**:254-267.

Sonoki S., Tanaka Y., Hisamatsu S., Kobayashi T. (1989) High-performance liquid chromatographic analysis of fluorescent derivatives of adenine and adenosine and its nucleotides : Optimization of derivatization with chloroacetaldehyde and chromatographic procedures. *J. Chrom. A* **475**:311-319.

Soricelli A., Postiglione A., Cuocolo A., De Chiara S., Ruocco A., Brunetti A., Salvatore M., Ell P. J. (1995) Effect of Adenosine on Cerebral Blood Flow as Evaluated by Single-Photon Emission Computed Tomography in Normal Subjects and in Patients With Occlusive Carotid Disease : A Comparison With Acetazolamide. *Stroke* **26**:1572-1576.

Spector R. (1987) Hypoxanthine transport through the blood-brain barrier. *Neurochem. Res.* **12**:791-796.

Spector R. (1989) Micronutrient homeostasis in mammalian brain and cerebrospinal fluid. *J. Neurochem.* **53**:1667-1674.

Sperlagh B., Szabo G., Erdelyi F., Baranyi M., Vizi E. S. (2003) Homo- and heteroexchange of adenine nucleotides and nucleosides in rat hippocampal slices by the nucleoside transport system. *Br. J. Pharmacol.* **139**:623-633.

St Cyr J. A., Bianco R. W., Schneider J. R., Mahoney J. R., Jr., Tveter K., Einzig S., Foker J. E. (1989) Enhanced high energy phosphate recovery with ribose infusion after global myocardial ischemia in a canine model. *J. Surg. Res.* **46**:157-162.

Stocchi V., Cucchiarini L., Canestrari F., Piacentini M. P., Fornaini G. (1987) A very fast ion-pair reversed-phase HPLC method for the separation of the most significant nucleotides and their degradation products in human red blood cells. *Anal. Biochem.* **167**:181-190.

Stover J. F., Lowitzsch K., Kempski O. S. (1997) Cerebrospinal fluid hypoxanthine, xanthine and uric acid levels may reflect glutamate-mediated excitotoxicity in different neurological diseases. *Neurosci. Lett.* **238**:25-28.

Strbian D., Durukan A., Pitkonen M., Marinkovic I., Tatlisumak E., Pedrono E., Abo-Ramadan U., Tatlisumak T. (2008) The blood-brain barrier is continuously open for several weeks following transient focal cerebral ischemia. *Neuroscience* **153**:175-181.

Stryer L., Berg J. M., Tymoczko J. L. (1995) Biochemistry 4Editior. W.H. Freeman & Company.

Terkeltaub R. A. (2003) Clinical practice. Gout. *N. Engl. J. Med.* **349**:1647-1655.

Thangnipon W., Kingsbury A., Webb M., Balazs R. (1983) Observations on rat cerebellar cells in vitro: influence of substratum, potassium concentration and relationship between neurones and astrocytes. *Brain. Res.* **313**:177-189.

Thomas J. (1957) The composition of isolated cerebral tissue; purines. *Biochem. J.* **66**:655-658.

Tomaselli B., Nedden S. Z., Podhraski V., Baier-Bitterlich G. (2008) p42/44 MAPK is an essential effector for purine nucleoside-mediated neuroprotection of hypoxic PC12 cells and primary cerebellar granule neurons. *Mol. Cell Neurosci.* **38**:559-568.

Tomiya N., Ailor E., Lawrence S. M., Betenbaugh M. J., Lee Y. C. (2001) Determination of nucleotides and sugar nucleotides involved in protein glycosylation by high-performance anion-exchange chromatography: sugar nucleotide contents in cultured insect cells and mammalian cells. *Anal. Biochem.* **293**:129-137.

Tozzi M. G., Camici M., Mascia L., Sgarrella F., Ipata P. L. (2006) Pentose phosphates in nucleoside interconversion and catabolism. *Febs J.* **273**:1089-1101.

Tuerk R. D., Thali R. F., Auchli Y., Rechsteiner H., Brunisholz R. A., Schlattner U., Wallimann T., Neumann D. (2007) New candidate targets of AMP-activated protein kinase in murine brain revealed by a novel multidimensional substrate-screen for protein kinases. *J. Proteome Res.* **6**:3266-3277.

Turner C. P., Seli M., Ment L., Stewart W., Yan H., Johansson B. r., Fredholm B. B., Blackburn M., Rivkees S. A. (2003) A1 adenosine receptors mediate hypoxia-induced ventriculomegaly. *PNAS* **100**:11718-11722.

Vailaya A., Horváth C. (1998) Retention in reversed-phase chromatography: partition or adsorption? *J. Chrom. A* **829**:1-27.

Valtysson J., Persson L., Hillered L. (1998) Extracellular ischaemia markers in repeated global ischaemia and secondary hypoxaemia monitored by microdialysis in rat brain. *Acta Neurochir. (Wien)* **140**:387-395.

Van Acker K. J., Simmonds H. A., Potter C., Cameron J. S. (1977) Complete Deficiency of Adenine Phosphoribosyltransferase. *New England J. Med.* **297**:127-132.

Van den Berghe G., Bontemps F., Vincent M. F., Van den Bergh F. (1992) The purine nucleotide cycle and its molecular defects. *Prog. Neurobiol.* **39**:547-561.

Van Rompay A. R., Johansson M., Karlsson A. (1999) Identification of a novel human adenylate kinase. *Eur. J. of Biochem.* **261**:509-517.

Vannucci R. C., Brucklacher R. M., Vannucci S. J. (1996) The effect of hyperglycemia on cerebral metabolism during hypoxia-ischemia in the immature rat. *J. Cereb. Blood Flow Metab.* **16**:1026-1033.

Verhaegen M., Iaizzo P. A., Todd M. M. (1995) A comparison of the effects of hypothermia, pentobarbital, and isoflurane on cerebral energy stores at the time of ischemic depolarization. *Anesthesiology* **82**:1209-1215.

von Kugelgen I., Schiedel A. C., Hoffmann K., Alsdorf B. B., Abdelrahman A., Muller C. E. (2008) Cloning and functional expression of a novel Gi protein-coupled receptor for adenine from mouse brain. *Mol. Pharmacol.* **73**:469-477.

Wall M., Dale N. (2008) Activity-dependent release of adenosine: a critical re-evaluation of mechanism. *Curr. Neuropharmacol.* **6**:329-337.

Wall M., Eason R., Dale N. (2010) Biosensor measurement of purine release from cerebellar cultures and slices. *Purinergic Signal.* **6**:339-348.

Wall M. J., Wigmore G., Lopatar J., Frenguelli B. G., Dale N. (2008) The novel NTPDase inhibitor sodium polyoxotungstate (POM-1) inhibits ATP breakdown but also blocks central synaptic transmission, an action independent of NTPDase inhibition. *Neuropharmacol.* **55**:1251-1258.

Wallen W. J., Belanger M. P., Wittnich C. (2003) Preischemic administration of ribose to delay the onset of irreversible ischemic injury and improve function: studies in normal and hypertrophied hearts. *Can. J. Physiol. Pharmacol.* **81**:40-47.

Washington C. B., Giacomini K. M. (1995) Mechanisms of Nucleobase Transport in Rabbit Choroid Plexus. *J. Biol. Chem.* **270**:22816-22819.

Watts R. W., McKeran R. O., Brown E., Andrews T. M., Griffiths M. I. (1974) Clinical and biochemical studies on treatment of Lesch-Nyhan syndrome. *Arch. Dis. Child* **49**:693-702.

Watts R. W. E. (1983) Some regulatory and integrative aspects of purine nucleotide biosynthesis and its control: An overview. *Adv. in Enzyme Reg.* **21**:33-51.

Wei Y., Chen L., Chen J., Ge L., He R. Q. (2009) Rapid glycation with D-ribose induces globular amyloid-like aggregations of BSA with high cytotoxicity to SH-SY5Y cells. *BMC Cell Biol.* **10**:10.

Weigand M. A., Michel A., Eckstein H. H., Martin E., Bardenheuer H. J. (1999) Adenosine: a sensitive indicator of cerebral ischemia during carotid endarterectomy. *Anesthesiology* **91**:414-421.

Welsh F. A., O'Connor M. J., Marcy V. R., Spatacco A. J., Johns R. L. (1982) Factors limiting regeneration of ATP following temporary ischemia in cat brain. *Stroke* **13**:234-242.

White B. C., Sullivan J. M., DeGracia D. J., O'Neil B. J., Neumar R. W., Grossman L. I., Rafols J. A., Krause G. S. (2000) Brain ischemia and reperfusion: molecular mechanisms of neuronal injury. *J. Neurol. Sci.* **179**:1-33.

Whittingham T. S., Lipton P. (1981) Cerebral synaptic transmission during anoxia is protected by creatine. *J. Neurochem.* **37**:1618-1621.

Whittingham T. S., Lust W. D., Passonneau J. V. (1984a) An in vitro model of ischemia: metabolic and electrical alterations in the hippocampal slice. *J. Neurosci.* **4**:793-802.

Whittingham T. S., Lust W. D., Christakis D. A., Passonneau J. V. (1984b) Metabolic stability of hippocampal slice preparations during prolonged incubation. *J. Neurochem.* **43**:689-696.

Whittingham T. S., Warman E., Assaf H., Sick T. J., LaManna J. C. (1989) Manipulating the intracellular environment of hippocampal slices: pH and high-energy phosphates. *J. Neurosci. Methods* **28**:83-91.

Wiener S., Wiener R., Urivetzky M., Meilman E. (1974) Coprecipitation of ATP with potassium perchlorate: the effect of the firefly enzyme assay of ATP in tissue and blood. *Anal. Biochem.* **59**:489-500.

Wieraszko A., Ehrlich Y. H. (1994) On the role of extracellular ATP in the induction of long-term potentiation in the hippocampus. *J. Neurochem.* **63**:1731-1738.

Williams C., Forrester T. (1976) Loss of ATP in micromolar amounts after perchloric acid treatment. *Pflugers Arch.* **366**:281-283.

Williams M. H., Branch J. D. (1998) Creatine Supplementation and Exercise Performance: An Update. *J. Am. Coll. Nutr.* **17**:216-234.

Williams S. (2004) Ghost peaks in reversed-phase gradient HPLC: a review and update. *J. Chrom. A* **1052**:1-11.

Winn H. R., Rubio R., Berne R. M. (1979) Brain adenosine production in the rat during 60 seconds of ischemia. *Circ. Res.* **45**:486-492.

Wise-Faberowski L., Raizada M. K., Sumners C. (2001) Oxygen and Glucose Deprivation-Induced Neuronal Apoptosis is Attenuated by Halothane and Isoflurane. *Anesthesia & Analgesia* **93**:1281-1287.

Woodruff T. M., Thundyil J., Tang S. C., Sobey C. G., Taylor S. M., Arumugam T. V. (2011) Pathophysiology, treatment, and animal and cellular models of human ischemic stroke. *Mol. Neurodegener.* **6**:11.

Writing Group M. et al. (2010) Heart Disease and Stroke Statistics--2010 Update: A Report From the American Heart Association. *Circulation* **121**:e46-215.

Wyatt C. N., Mustard K. J., Pearson S. A., Dallas M. L., Atkinson L., Kumar P., Peers C., Hardie D. G., Evans A. M. (2007) AMP-activated protein kinase mediates carotid body excitation by hypoxia. *J. Biol. Chem.* **282**:8092-8098.

Xu K., Puchowicz M. A., Lust W. D., LaManna J. C. (2006) Adenosine treatment delays postischemic hippocampal CA1 loss after cardiac arrest and resuscitation in rats. *Brain. Res.* **1071**:208-217.

Yamada K., Uozumi T., Kawasaki T., Yamada K., Sogabe T., Ohta K. (1988) Regional changes in the cellular level of adenine nucleotides in ischemic rat brain subjected to single embolization. *J. Neurochem.* **51**:141-144.

Yamada Y., Goto H., Ogasawara N. (1980) Purification and properties of adenosine kinase from rat brain. *Biochim. et Biophys. Act. (BBA) - Enzymology* **616**:199-207.

Yatsu F. M., Lee L. W., Liao C. L. (1975) Energy metabolism during brain ischemia. Stability during reversible and irreversible damage. *Stroke* **6**:678-683.

Ying W. (2008) NAD+ and NADH in ischemic brain injury. *Front. Biosci.* **13**:1141-1151.

Yoshida S., Abe K., Busto R., Watson B. D., Kogure K., Ginsberg M. D. (1982) Influence of transient ischemia on lipid-soluble antioxidants, free fatty acids and energy metabolites in rat brain. *Brain. Res.* **245**:307-316.

Yoshimi Y., Watanabe S., Shinomiya T., Makino A., Toyoda M., Ikekita M. (2003) Nucleobase adenine as a trophic factor acting on Purkinje cells. *Brain. Res.* **991**:113-122.

Zakaria M., Brown P. R. (1981) High-performance liquid chromatography of nucleotides, nucleosides and bases. *J. Chromatogr.* **226**:267-290.

Zhu S., Li M., Figueroa B. E., Liu A., Stavrovskaya I. G., Pasinelli P., Beal M. F., Brown R. H., Kristal B. S., Ferrante R. J., Friedlander R. M. (2004) Prophylactic Creatine Administration Mediates Neuroprotection in Cerebral Ischemia in Mice. *J. Neurosci.* **24**:5909-5912.

Zimmer H. G. (1982) Ribose enhances the isoproterenol-elicited positive inotropic effect in rats in vivo. *J. Mol. Cell Cardiol.* **14**:479-482.

Zimmer H. G. (1983) Normalization of depressed heart function in rats by ribose. *Science* **220**:81-82.

Zimmer H. G. (1992) The oxidative pentose phosphate pathway in the heart: regulation, physiological significance, and clinical implications. *Basic Res. Cardiol.* **87**:303-316.

Zimmer H. G. (1996) Regulation of and intervention into the oxidative pentose phosphate pathway and adenine nucleotide metabolism in the heart. *Mol. Cell Biochem.* **160-161**:101-109.

Zimmer H. G. (1998) Significance of the 5-phosphoribosyl-1-pyrophosphate pool for cardiac purine and pyrimidine nucleotide synthesis: studies with ribose, adenine, inosine, and orotic acid in rats. *Cardiovasc. Drugs Ther.* **12 Suppl 2**:179-187.

Zimmer H. G., Gerlach E. (1978) Stimulation of myocardial adenine nucleotide biosynthesis by pentoses and pentitols. *Pflugers Arch.* **376**:223-227.

Zimmer H. G., Ibel H. (1984) Ribose accelerates the repletion of the ATP pool during recovery from reversible ischemia of the rat myocardium. *J. Mol. Cell. Cardiol.* **16**:863-866.

Zimmer H. G., Martius P. A., Marschner G. (1989) Myocardial infarction in rats: effects of metabolic and pharmacologic interventions. *Basic Res. Cardiol.* **84**:332-343.

Zimmer H. G., Ibel H., Suchner U., Schad H. (1984) Ribose intervention in the cardiac pentose phosphate pathway is not species-specific. *Science* **223**:712-714.

Zimmermann H. (1994) Signalling via ATP in the nervous system. *Trends in Neurosci.* **17**:420-426.

Zur Nedden S., Eason R., Doney A. S., Frenguelli B. G. (2009) An ion-pair reversed-phase HPLC method for determination of fresh tissue adenine nucleotides avoiding freeze-thaw degradation of ATP. *Anal. Biochem.* **388**:108-114.

Zur Nedden S., Hawley S., Pentland N., Hardie D. G., Doney A. S., Frenguelli B. G. (2011) Intracellular ATP Influences Synaptic Plasticity in Area CA1 of Rat Hippocampus via Metabolism to Adenosine and Activity-Dependent Activation of Adenosine A1 Receptors. *J. Neurosci.* **31**:6221-6234.

Publications

Cellular/Molecular

Intracellular ATP Influences Synaptic Plasticity in Area CA1 of Rat Hippocampus via Metabolism to Adenosine and Activity-Dependent Activation of Adenosine A_1 Receptors

Stephanie zur Nedden,[1] Simon Hawley,[2] Naomi Pentland,[2,3] D. Grahame Hardie,[2] Alexander S. Doney,[4] and Bruno G. Frenguelli[1,3]

[1]School of Life Sciences, University of Warwick, Coventry, CV4 7AL, United Kingdom, [2]Division of Molecular Physiology, College of Life Sciences, University of Dundee, Dundee, DD1 5EH, United Kingdom, and Departments of [3]Pharmacology and Neuroscience and [4]Medicine and Therapeutics, University of Dundee, Ninewells Hospital and Medical School, Dundee, DD1 9SY, United Kingdom

The extent to which brain slices reflect the energetic status of the *in vivo* brain has been a subject of debate. We addressed this issue to investigate the recovery of energetic parameters and adenine nucleotides in rat hippocampal slices and the influence this has on synaptic transmission and plasticity. We show that, although adenine nucleotide levels recover appreciably within 10 min of incubation, it takes 3 h for a full recovery of the energy charge (to ≥0.93) and that incubation of brain slices at 34°C results in a significantly higher ATP/AMP ratio and a threefold lower activity of AMP-activated protein kinase compared with slices incubated at room temperature. Supplementation of artificial CSF with D-ribose and adenine (Rib/Ade) increased the total adenine nucleotide pool of brain slices, which, when corrected for the influence of the dead cut edges, closely approached *in vivo* values. Rib/Ade did not affect basal synaptic transmission or paired-pulse facilitation but did inhibit long-term potentiation (LTP) induced by tetanic or weak theta-burst stimulation. This decrease in LTP was reversed by strong theta-burst stimulation or antagonizing the inhibitory adenosine A_1 receptor suggesting that the elevated tissue ATP levels had resulted in greater activity-dependent adenosine release during LTP induction. This was confirmed by direct measurement of adenosine release with adenosine biosensors. These observations provide new insight into the recovery of adenine nucleotides after slice preparation, the sources of loss of such compounds in brain slices, the means by which to restore them, and the functional consequences of doing so.

Introduction

The use of brain slices has revolutionized the study of the mammalian CNS, and they have now become a standard preparation in many laboratories and in many areas of neuroscience. Hippocampal brain slices are particularly widely used for studies into the fundamental properties of synaptic transmission and plasticity.

However, it is an unavoidable fact that their preparation is associated with ischemia (decapitation) and tissue trauma (dissection/slice cutting), which will affect metabolic status and result in departure from the *in vivo* state. Indeed, a substantially compromised energetic state of brain slices at the time of cutting has been demonstrated (Fredholm et al., 1984; Whittingham et al., 1984b), with high energy phosphate levels (ATP, phosphocreatine) in brain slices being as much as 50% lower than their *in situ* values (Thomas, 1957; Whittingham et al., 1984a; Schurr and Rigor, 1989). Accordingly, basal conditions in hippocampal slices have been described as reflecting a post-ischemic recovery state (Hossmann, 2008). However, as described as far back as the 1950s (McIlwain et al., 1951; McIlwain, 1952), brain slices do show remarkable metabolic recovery after preparation, and it is now common practice to allow a period of incubation (usually 1 h) before they are used for experiments.

Given the widespread use and importance of brain slices to neuroscience, the aims of our study were threefold: first, to assess the metabolic status of brain slices by studying the temperature-dependent recovery and stability of adenine nucleotide levels and energetic parameters, including the activity of AMP-activated protein kinase (AMPK), an enzyme involved in regulation of cellular energy homeostasis and exquisitely sensitive to the cellular ATP/AMP ratio; second, to investigate the potential causes for the reduced ATP content of brain slices compared with reported *in vivo* values and to evaluate whether the lower ATP levels are attributable to a lack of adenine nucleotide precursors by incubating slices with the free purine base adenine and the sugar precursor of adenylates, D-ribose; finally, to test whether elevated slice ATP levels change the electrophysiological properties of the tissue, such as the probability of transmitter release or the induction and expression of long-term potentiation (LTP).

Received Aug. 3, 2010; revised Feb. 18, 2011; accepted Feb. 24, 2011.

Author contributions: D.G.H., A.S.D., and B.G.F. designed research; S.z.N., S.H., and N.P. performed research; S.z.N., S.H., and B.G.F. analyzed data; S.z.N., S.H., D.G.H., A.S.D., and B.G.F. wrote the paper.

We thank Jan Lopatar, Abigail Perkins, and Dr. Rajen Mistry for help with slice preparation and adenosine biosensor experiments and Prof. Nicholas Dale for valuable input, including the derivation of the slice thickness equation and use of HPLC equipment. We are grateful to Research into Ageing for funding a studentship to S.z.N. S.H. was supported by EXGENESIS Integrated Project Grant LSHM-CT-2004-005272 from the European Commission.

Correspondence should be addressed to Prof. Bruno G. Frenguelli, School of Life Sciences, University of Warwick, Coventry CV4 7AL, UK. E-mail: b.g.frenguelli@warwick.ac.uk.

DOI:10.1523/JNEUROSCI.4039-10.2011

 0270-6474/11/316221-14$15.00/0

Our findings provide new insights into the energetic status of brain slices: they show that the loss of ATP precursors is responsible for the decreased ATP content of brain slices and that, by supplementing the artificial CSF (aCSF) with adenine and D-ribose, the recovery of tissue ATP levels can be improved. However, this has measurable consequences in terms of greater activity-dependent release of extracellular adenosine and, via activation of adenosine A_1 receptors (A_1Rs), the raising of the threshold for the induction of long-term potentiation.

Materials and Methods

Preparation of brain slices. Male Sprague Dawley rats (17–27 d old) were killed by cervical dislocation in accordance with Schedule 1 of the United Kingdom Government Animals (Scientific Procedures) Act 1986 and with local ethical review procedures. Sagittal brain slices (400 μm thick), composed of hippocampus and overlying neocortex, were prepared under standardized conditions in ice-cold aCSF containing 10 mM Mg^{2+}-using a Microm HM 650 V microtome as described previously (Dale et al., 2000; Frenguelli et al., 2007). Slices were either analyzed immediately during cutting for their purine nucleotide content or transferred to the recording chamber or an incubation chamber (50–100 ml) (Edwards et al., 1989) and submerged in continuously circulating, oxygenated standard aCSF at room temperature (22 ± 0.5°C) or 34 ± 1°C. The composition of the standard aCSF solution included the following (in mM): 124 NaCl, 3 KCl, 2 $CaCl_2$, 26 $NaHCO_3$, 1.25 NaH_2PO_4, 10 D-glucose, and 1 $MgSO_4$, pH 7.4 (with 95% O_2/5% CO_2).

In a separate set of experiments, nucleotide concentrations of (1) the intact hippocampus and cortex and (2) slices of varying thickness were analyzed. For this purpose, one hemisphere was used to dissect and separate hippocampus and cortex, and the other hemisphere was used to cut slices of varying thickness (200–3600 μm). Because with the microtome used no slices >1500 μm could be cut automatically, 3600 μm had to be measured with a guide. For these experiments, all nucleotide extractions were performed immediately after preparation (zur Nedden et al., 2009).

Nucleotide extraction. To determine the total adenine nucleotide (TAN) content of 400 μm brain slices, two slices for each time point [from time of cutting (time 0) to 5 h after cutting at 10 min, 30 min, 1 h, 2 h, 3 h, and 5 h] were transferred into ice cold aCSF to stop enzymatic activities. To minimize transfer of aCSF into the reaction mixture, slices were removed with a small spatula into a 1.5 ml microcentrifuge tube containing 1 ml of 5% perchloric acid (PCA). Nucleotide extraction was performed as described in detail previously (zur Nedden et al., 2009). Extracts were neutralized by a threefold organic extraction with 1 ml of tri-*n*-octylamine dissolved in 1,1,2-trichlorotrifluoroethane (1:1; v/v). The protein pellet was resuspended in 1 ml of 0.5 M NaOH, and the protein concentration was determined by Bradford assay, with bovine serum albumin (BSA) as standard.

For analysis of the TAN content of whole hippocampus and neocortex and 1200, 1500, and 3600 μm slices, the tissue was first homogenized in 500 μl of 5% PCA. The amount of this suspension containing 20 mg wet weight (equivalent to four 200 μm, two 400 μm, or one 800 μm slice) of the tissue was mixed with 5% PCA to a final volume of 1 ml and neutralized as described above.

We have shown previously that snap freezing in liquid N_2 and freeze thawing of brain tissue results in a degradation of adenine nucleotides and an underestimation of the energy charge (zur Nedden et al., 2009). For this reason, nucleotides were only extracted from fresh brain tissue and were analyzed on the same day.

Protein extraction. For each time point, two to three brain slices were placed in ice-cold aCSF to stop enzymatic activities. Slices were homogenized in 100 μl of protein lysis buffer with a Kontes pellet pestle motor (Sigma-Aldrich). The suspension was centrifuged (30 min, 4°C, 16,060 × *g*), and the supernatant was stored at −80°C for kinase assays and Western blot analysis. The composition of the protein lysis buffer was as follows: 50 mM Tris-HCl, pH 7.5, 0.1 mM EGTA, 1 mM EDTA, 1% Triton X-100, 1 mM sodium orthovanadate, 50 mM sodium fluoride, 5 mM sodium pyrophosphate, 270 mM sucrose, 0.1% β-mercaptoethanol, 0.02% sodium azide, and 1 protease inhibitor tablet for 16.6 ml of lysis buffer.

HPLC. For analysis of purine nucleotides and nucleosides, an ion pair reversed-phase HPLC method with tetrabutylammonium hydrogen sulfate (TBAHS) was used, as described previously (zur Nedden et al., 2009). Analytical separation was performed on a Supelcosil LC-18-T reversed-phase column (150 × 4.6 mm; inner diameter, 3 μm), with a gradient profile from 100% buffer A (65 mM potassium phosphate, pH 6.0, 4 mM TBAHS) to 100% buffer B (65 mM potassium phosphate, pH 6.0, 25% methanol) in 13 min. Peak identities were confirmed by comparison of the retention times of sample peaks with peaks of standard compounds, spiking the samples with individual standards and by comparison of the UV spectra with standard compounds. Concentrations were calculated by comparing the peak area of sample peaks with calibration curves for peak areas of each standard compound. All concentrations are expressed as nanomoles per milligram of protein.

Kinase assays. AMPK from extracts was immunoprecipitated with a mixture of α1 and α2 antibodies, and AMPK activity in the immunoprecipitates was determined using the AMARA peptide assay as described previously (Hardie et al., 2000; Gadalla et al., 2004).

Western blot analysis. The detection of dual-labeled Western blots by infrared imaging was performed as described previously (Hawley et al., 2003), except that, in the present study, the phosphorylation state of the native full-length protein was determined.

Electrophysiological recordings. Except for one series of experiments, slices (comprising hippocampus and overlying neocortex) were incubated for 3–8 h in standard aCSF or for 2 h in aCSF supplemented with 1 mM ribose/50 μM adenine (Rib/Ade) and 1–6 h in standard aCSF before being transferred to a recording chamber and fully submerged in aCSF at 33.4 ± 0.2°C and a flow rate of 6–7 ml/min. In the other series of experiments, slices were immediately transferred to the recording chamber during slice cutting to monitor the recovery of synaptic transmission in control and Rib/Ade-containing aCSF. A twisted bipolar Teflon-coated tungsten wire was placed to stimulate the Schaffer collateral/commissural pathway every 15 s, and field EPSP (fEPSPs) were recorded from stratum radiatum in area CA1 of the hippocampus with a glass microelectrode filled with aCSF (1 MΩ). The stimulus intensity was adjusted to 50–60% of that required to evoke a population spike. LTP was induced with tetanic stimulation (one train of 100 stimuli at 100 Hz) or with theta-burst (TBS) stimulation (0.5, 1, 2, or 3 × 10 trains of four stimuli at 100 Hz repeated at 200 ms intervals).

Adenosine biosensors. Adenosine and null microelectrode biosensors (50 μm diameter and 500 μm length) were purchased from Sarissa Biomedical Ltd. and were used to measure the real-time release of adenosine during LTP induction. The use of the sensors in hippocampal slices has been described previously (Frenguelli et al., 2003, 2007). The adenosine sensor relies on an enzyme cascade immobilized within a matrix on the surface of a platinum/iridium electrode to metabolize adenosine, thereby liberating H_2O_2, which is oxidized on the platinum/iridium electrode. This gives rise to an oxidation current proportional to the concentration of adenosine. The null sensor lacks enzymes and is used to establish the presence of any electroactive interferents. Both sensors were inserted into the stratum radiatum of the CA1 region of hippocampal slices between recording and stimulating electrodes. After insertion, slices were allowed to recover for 30–45 min before electrical stimulation for the recording of fEPSPs was started. After a stable fEPSP baseline of 15–20 min was collected, adenosine release was evoked with three TBS given 10 s apart. fEPSPs, adenosine and null sensor traces were recorded simultaneously. Thirty minutes after LTP induction, sensors were either taken out of the tissue or drugs were applied for 15–30 min before TBS was repeated. After each experiment, sensors were calibrated with 10 μM adenosine in the recording chamber. Because no nonspecific electroactive release could be detected on the null sensor, adenosine release was calculated without subtraction of the null trace, and the values are given as μM′ to reflect that the adenosine sensor measures adenosine and its metabolites (Frenguelli et al., 2007). To integrate the area under the curve of adenosine sensor traces, the baseline had to be set to 0, which was achieved by subtracting from the sensor trace a linear regression based on 5 min of baseline.

Statistical analysis. All values are expressed as mean ± SEM. For the electrophysiological and adenosine sensor measurements, *n* values refer

to the number of slices per experimental condition, which for most cases is also equal to the number of animals used. Slices were used in duplicate for nucleotide extraction and in triplicate for protein extraction. In these cases, *n* values represent the number of animals used. For statistical analysis of more than two groups, one-way ANOVA with Bonferroni's multiple comparison test was applied, whereas for comparisons between two independent groups, unpaired *t* tests were used. For comparison of the adenosine release before and after application of different drugs, a paired *t* test was applied. Calculations were performed with Prism 4; p values <0.05 were considered as statistically significant.

Chemicals. All HPLC standards, 1,1,2-trichloro-1,1,2-trifluoroethane (HPLC grade), EGTA, EDTA, sodium fluoride, sodium orthovanadate, sodium pyrophosphate, sodium azide, BSA, TBAHS, D-ribose, adenine, 8-cyclopentyltheophylline (8-CPT), nitrobenzylthioinosine (NBTI), dipyridamole (DIPY), N^6-cyclopentyladenosine (N^6-CPA), sodium polyoxotungstate (POM-1), and the Bradford reagent were obtained from Sigma-Aldrich. Protease inhibitor cocktail tablets and ATP were from Roche. HPLC-grade methanol, perchloric acid, orthophosphoric acid, tri-*n*-octylamine, Triton X-100, Tris base, and all salts used in the aCSF were obtained from Thermo Fisher Scientific. Protein G Sepharose was from GE Healthcare. Pyridoxalphosphate-6-azophenyl-2′,4′-disulfonic acid (PPADS) and forskolin were purchased from Ascent. Sheep antibodies against the α1 and α2 subunits of AMPK were described previously (Woods et al., 1996), and the antibody against the phosphorylated Thr-172 was from Cell Signaling Technologies.

Results

Metabolic recovery after slice cutting

Recovery of adenine nucleotides

To study the recovery of adenine nucleotides after slice preparation, HPLC analysis of slice extracts was performed on fresh slices immediately after cutting and after various incubation time points in aCSF (10 min to 5 h) at room temperature (22°C) and 34°C (Fig. 1*A*).

Immediately after cutting, ATP, ADP, and AMP were present in nearly equal amounts (6.0 ± 0.3, 4.0 ± 0.4, and 5.2 ± 0.8 nmol/mg protein, respectively; $n = 7$) (Fig. 1*B–D*) (supplemental Table 1, available at www.jneurosci.org as supplemental material). ATP levels significantly increased after only 10 min incubation (10.7 ± 1.0 and 11.0 ± 0.9 nmol/mg protein at 22°C and 34°C, respectively; $n = 7$; $p < 0.001$, one-way ANOVA) with a concomitant decrease of ADP (1.9 ± 0.3 and 1.5 ± 0.1 nmol/mg protein at 22°C and 34°C, respectively; $n = 7$; $p < 0.001$, one-way ANOVA) and AMP (1.1 ± 0.3 and 0.5 ± 0.1 nmol/mg protein at 22°C and 34°C respectively; $n = 7$; $p < 0.001$, one-way ANOVA) levels. ATP degradation metabolites (IMP, adenosine, inosine, hypoxanthine, and xanthine) were all elevated at the time of cutting and together accounted for ~5 nmol/mg protein (supplemental Table 2, available at www.jneurosci.org as supplemental material). The levels of these metabolites declined after slice cutting and stabilized after 10–60 min of incubation.

After the initial recovery, ATP, ADP, and AMP levels did not significantly change during the incubation time points tested (up to 5 h incubation), and there were no significant differences between adenine nucleotides of slices kept at 22°C and 34°C (Fig. 1*B–D*). As a consequence of these complementary changes in individual nucleotides, the total adenine nucleotide pool (TAN = [ATP] + [ADP] + [AMP]) (Fig. 1*E*) did not significantly change when slices were transferred from the ice-cold cutting solution (15.2 ± 1.1 nmol/mg protein; $n = 7$) into aCSF at 22°C (13.7 ± 1.4 nmol/mg protein; $n = 7$) or 34°C (13.0 ± 1.1 nmol/mg protein; $n = 7$), suggesting that most of the accumulated AMP is rephosphorylated to ATP rather than dephosphorylated to adenosine (via cytosolic 5′-nucleotidase, EC 3.1.3.5.) or deaminated to IMP (via AMP deaminase, EC 3.5.4.6.). The TAN pool remained stable over an incubation period of 5 h. Average TAN concentrations from all time points tested (10 min to 5 h) were 14.1 ± 0.3 nmol/mg protein in slices at 22°C and 15.4 ± 0.9 in slices at 34°C, with ATP accounting for ~85 and 89%, respectively.

Recovery of energetic parameters and AMPK activity

Two widely used measures of cellular energetic state are the adenylate energy charge, EC = ([ATP] + 0.5 [ADP])/[TAN] (Atkinson, 1968), which has a maximum value of 1 when all the adenine nucleotides are in the form of ATP and the ATP/AMP ratio.

Because of the nearly equal amounts of ATP, ADP, and AMP at the time of cutting, the EC was very low (0.54 ± 0.03; $n = 7$) (Fig. 2*A*) (supplemental Table 3, available at www.jneurosci.org as supplemental material) but recovered significantly after only 10 min incubation at 22°C (0.86 ± 0.019; $n = 7$; $p < 0.001$, one-way ANOVA) and 34°C (0.90 ± 0.007; $n = 7$; $p < 0.001$, one-way ANOVA). After 3 h the EC stabilized at 0.93 ± 0.003 for slices kept at 22°C and at 0.95 ± 0.002 for slices kept at 34°C, and, as for adenine nucleotides, there were no significant differences between slices at 22°C and 34°C.

The ATP/AMP ratio significantly recovered from time of cutting (1.4 ± 0.4; $n = 7$) (Fig. 2*B*) (supplemental Table 3, available at www.jneurosci.org as supplemental material) after only 10 min in slices at 34°C (22.9 ± 2.7; $n = 7$; $p < 0.001$, one-way ANOVA), whereas it took ~30 min to recover in slices incubated at 22°C (20.1 ± 1.8; $n = 6$; $p < 0.001$, one-way ANOVA). Similar to the EC, the ATP/AMP ratio stabilized after 3 h but with considerable differences between slices incubated at 22°C and at 34°C. At 22°C, the ATP/AMP ratio ranged between 35.2 and 38.0, whereas at 34°C, the ATP/AMP ratio was much higher between 63.5 and 64.2. The differences in the ATP/AMP ratio values between the two incubation temperatures became statistically significant after 30 min ($n = 6–8$; $p < 0.01$, one-way ANOVA) and remained statistically significant for the rest of the incubation period ($n = 5–8$; $p < 0.001$, one-way ANOVA).

The cellular ATP/AMP ratio is monitored by AMPK (EC 2.7.11.31), a key sensor and regulator of cellular energy metabolism (Hardie and Hawley, 2001; Hardie, 2007). AMPK is activated by phosphorylation of Thr172 by the upstream kinases LKB1 (Hawley et al., 2003) and calcium/calmodulin-dependent protein kinase kinase β (Hawley et al., 2005; Woods et al., 2005). In addition, an increase in cellular AMP provides both allosteric activation of the enzyme and protection of Thr172 from dephosphorylation, whereas both of these effects are antagonized by high intracellular ATP levels (Hardie et al., 2006; Sanders et al., 2007). Therefore, we investigated whether the lower ATP/AMP ratio in slices at 22°C was reflected by a higher AMPK activity.

AMPK activity (Fig. 2*C*) decreased from 0.066 ± 0.003 U/mg protein at time of cutting to 0.04 ± 0.001 U/mg protein after 30 min at 22°C (1.6-fold decrease; $n = 3$; $p < 0.001$, one-way ANOVA), by which time at 34°C AMPK activity had fallen 3.4-fold ($n = 2$). After 3 h, AMPK was three times more active in slices at 22°C (0.03 ± 0.003 U/mg protein; $n = 3$) than in slices at 34°C (0.01 ± 0.001 U/mg protein; $n = 3$; $p < 0.001$, one-way ANOVA). Western blots (Fig. 2*D*) showed that the ratio of phospho-AMPK/total AMPK decreased from 2.8 at time of cutting to 1.9 in slices at 22°C and to 1.1 in slices at 34°C after 3 h incubation ($n = 2$) (supplemental Fig. 1, available at www.jneurosci.org as supplemental material). Likewise, the phospho/total ratio of a substrate, acetyl-CoA carboxylase (ACC), decreased from 1.6 at time of cutting to 1.0 in slices at 22°C and to 0.5 in slices at 34°C after 3 h incubation (Fig. 2*D*) (supplemental Fig. 1, available at

www.jneurosci.org as supplemental material). These observations suggest that, despite similarities between TAN pools and EC values between slices incubated at room temperature and more physiological temperatures, the ATP/AMP ratio can influence the activity of key intracellular enzymes with potentially important consequences for neuronal and glial properties.

Basis of reduced TAN concentration in slices

EC values of brain slices reported here (Fig. 2*A*) (supplemental Table 3, available at www.jneurosci.org as supplemental material) are comparable with those reported *in vivo* (supplemental references, available at www.jneurosci.org as supplemental material). However, absolute TAN levels here (Fig. 1*E*) (supplemental Table 1, available at www.jneurosci.org as supplemental material) and in the *in vitro* literature (supplemental references, available at www.jneurosci.org as supplemental material) are ~40–60% lower than published *in vivo* values for rat brain, which are typically ~33.6 ± 4.7 nmol/mg protein (arithmetic mean ± SD of all *in vivo* published data in supplemental references, available at www.jneurosci.org as supplemental material) (Fig. 3*A*). In our study, the loss of adenine nucleotides occurred either before or during slice preparation, because TAN levels were already ~55% (~18.4 nmol/mg protein) lower at the time of cutting than published *in vivo* studies. We investigated several possible explanations for this observation.

The ischemic period leads to loss of diffusible ATP degradation products

The sum of ATP degradation metabolites (adenosine, inosine, hypoxanthine, xanthine, and IMP) at time of cutting was approximately ~5 nmol/mg protein (supplemental Table 2, available at www.jneurosci.org as supplemental material). Although, like ADP and AMP levels, these metabolites declined during the first 10–30 min of incubation, there was no corresponding rise in the TAN pool. Thus, they are likely to be lost from the tissue and thereby contribute to the reduced adenine nucleotide content of brain slices.

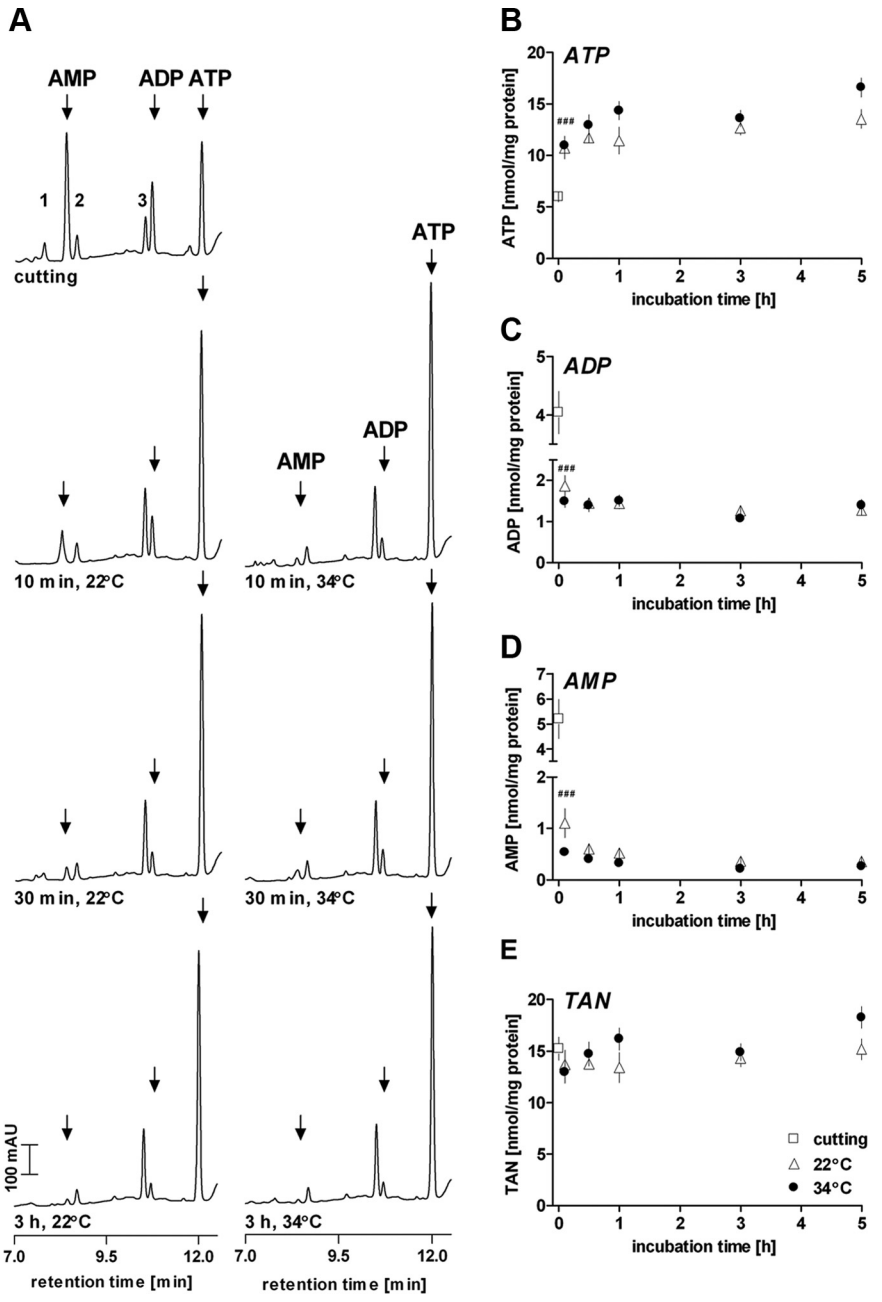

Figure 1. Rapid recovery of adenine nucleotides after slice preparation. ***A***, Representative HPLC traces obtained from brain slices after slice cutting and various incubation times in aCSF at room temperature (22°C; left traces) and 34°C (right traces). Note the consistently higher AMP levels in slices incubated at 22°C. Numbers on traces refer to the following compounds: 1, adenosine; 2, GDP; 3, GTP/UTP. Arrowheads indicate, from left to right, AMP, ADP, and ATP; mAU, milli absorbance units. ***B–E***, Recovery of ATP (***B***), ADP (***C***), AMP (***D***), and total adenine nucleotides (TAN = [ATP] + [ADP] + [AMP]) (***E***) from time of cutting (white squares, time 0) and various incubation times (0.1–5 h) in aCSF at 22°C (white triangles) or 34°C (black circles). Values are presented as mean ± SEM; $n = 5–8$. $^{###}p < 0.001$ for slices at 22°C and 34°C compared with time of cutting, one-way ANOVA with Bonferroni's multiple comparison test. When no error bars can be seen, they are smaller than the symbol.

The tissue suffers from physical damage causing additional loss of adenine nucleotides

To establish whether the dissection of tissue associated with slicing caused additional loss of adenine nucleotides, we determined the TAN content immediately after decapitation/dissection in entire hippocampus and cortex (because slices in this study were composed of hippocampus and overlaying neocortex). The TAN content of intact hippocampal and cortical tissue was higher than that in combined hippocampal/neocortical slices at 23.0 ± 2.1 and 28.9 ± 2.9 nmol/mg protein, respectively (Fig. 3*A*) ($n = 5$; $p > 0.05$ between hippocampal and cortical tissue, unpaired t test). The value for cortex is close to that reported *in vivo* (33.6 ± 4.7 nmol/mg protein) (Fig. 3*A*), but TAN levels in the hippocampus are lower than those reported *in vivo*. This suggests that the ischemic period during decapitation results in a loss of adenine nucleotides, especially in hippocampal tissue (~10 nmol/mg protein, ~29%), which additionally requires more physical and

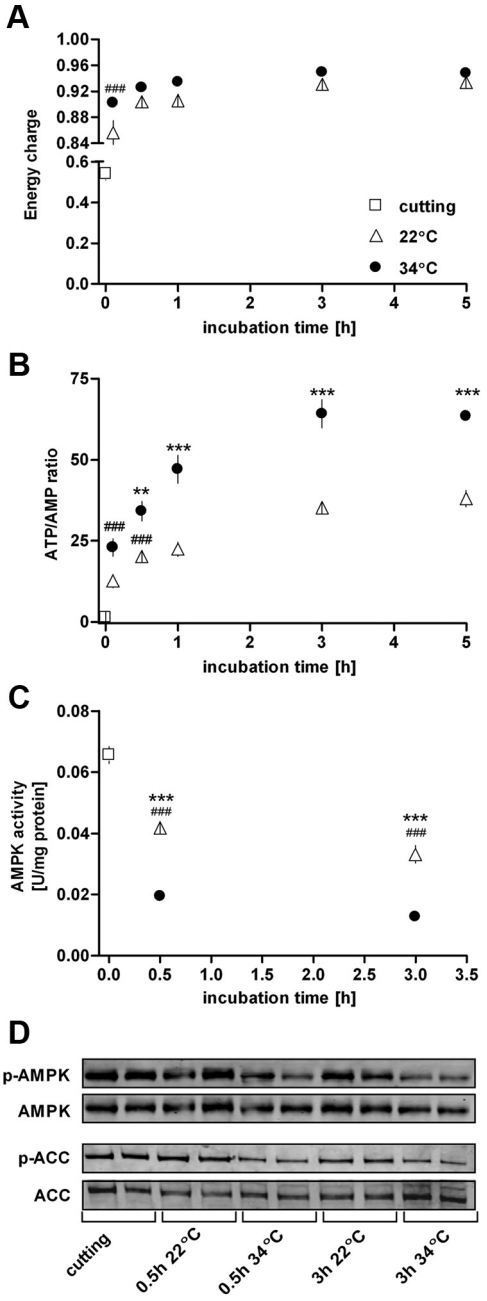

Figure 2. Differential influence of temperature on the recovery of energetic parameters and AMPK activity after slice cutting. Recovery of the tissue energy charge [(ATP + 0.5 ADP)/TAN] is not influenced by temperature (***A***), whereas the ATP/AMP ratio is significantly higher at elevated temperature ($n = 5–8$) (***B***). ***C***, Accordingly, AMPK activity in brain slices, as measured by pseudo-substrate phosphorylation, is lower at higher incubation temperature, reflecting the higher ATP/AMP ratio ($n = 3$ except for 0.5 h, 34°C, $n = 2$). White squares, Slices at time of cutting (time 0); white triangles, slices incubated in aCSF at room temperature (22°C); black circles, slices incubated in aCSF at 34°C. ***D***, Confirmation of increased AMPK activity through Western blot analysis of increased phosphorylation of AMPK (p-AMPK) and a downstream target, ACC (p-ACC). Also shown are total AMPK and ACC at different durations and temperature of incubation in two separate sets of slices. All values are presented as mean ± SEM. $^{\#\#\#}p < 0.001$ for slices at 22°C and 34°C compared with time of cutting; $^{**}p < 0.01$, $^{***}p < 0.001$ compared between slices at 22°C and 34°C, one-way ANOVA with Bonferroni's multiple comparison test. When no error bars can be seen, they are smaller than the symbol.

potentially traumatic dissection for removal. In contrast, neocortex may undergo more rapid cooling when the brain is dropped into ice-cold aCSF, which may better preserve adenine nucleotides.

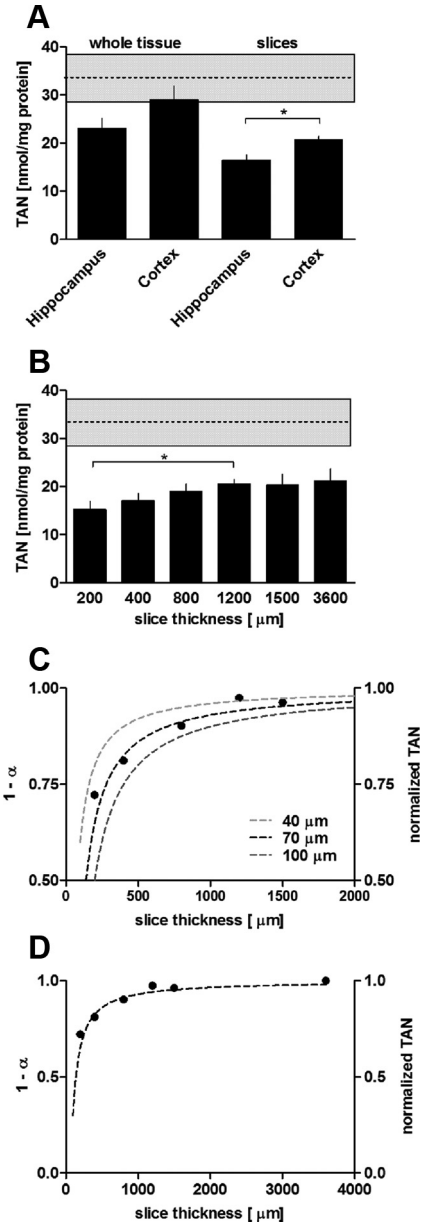

Figure 3. Tissue thickness and handling influences calculation of adenine nucleotide content of brain tissue. ***A***, TAN content of whole hippocampus ($n = 5$) and cortex ($n = 5$) immediately after dissection and hippocampal ($n = 3$) and neocortical slices ($n = 3$) immediately after cutting. Note that whole tissue TAN levels are lower than reported *in vivo* values (dotted black line represents the arithmetic mean ± SD as shown by the gray area for all reported values from supplemental references, available at www.jneurosci.org as supplemental material), possibly reflecting increased handling/trauma, with only whole cortex approaching *in vivo* values. ***B***, TAN levels of neocortical/hippocampal slices of varying thickness (200, 400, 800, 1200, 1500, and 3600 μm) immediately after cutting. All values in ***A*** and ***B*** are presented as mean ± SEM; $n = 3–8$. ***C***, Theoretical curves ($Y = 1 - \alpha$, where $\alpha = d/l$; dotted lines) to estimate the relative contribution of dead cut edges (d) to the total tissue thickness of slices (l, ranging from 100 to 2000 μm in 20 μm steps), assuming a total thickness for the two dead cut edges of 40 μm (light gray dotted line, 20 μm on each side of the slice), 70 μm (black dotted line, 35 μm on each side of the slice), or 100 μm (dark gray dotted line, 50 μm on each side of the slice). By normalizing the TAN levels obtained from slices at different thicknesses from ***B*** to the TAN values obtained for 3600 μm slices (plotted as black dots), we found that these normalized values fit the curve for a total dead cut edge layer of 70 μm (black dotted line). ***D***, Theoretical curve for the ratio of the thickness of cut dead edges (d; 70 μm) to the tissue thickness (l; ranging from 100 to 3600 μm in 20 μm steps), showing that, with increasing slice thickness, the relative contribution of the thickness of the cut edges decreases, approaching a value of 0.99 (black circles).

The difference in TAN levels between cortex and hippocampus can also be seen in slices (Fig. 3*A*). Hippocampal slices had significantly lower TAN levels than cortical slices (16.4 ± 1.1 and 20.7 ± 0.7 nmol/mg protein, respectively; $n = 3$; $p < 0.05$, unpaired *t* test). These values were ~28% lower than the respective whole tissue values reported above and ~38% (cortex) to 50% (hippocampus) lower than reported *in vivo* values (Fig. 3*A*).

The dead layer on slice surfaces distorts adenine nucleotide measurements

Empirical observations. To test whether the protein content of dead slice edges (typically 35–50 μm) (Feig and Lipton, 1990; Siklós et al., 1997; Frenguelli et al., 2003) results in an underestimate of ATP in the viable core of the slice, we prepared neocortical/hippocampal slices of different thickness, thereby changing the ratio of dead to viable tissue. Because there were no significant changes in the TAN levels between slice cutting and 5 h incubation (Fig. 1*E*) (supplemental Table 1, available at www.jneurosci.org as supplemental material) and to bypass the problem of a possible emerging nutrient-deprived core in very thick slices, the analysis was performed immediately after cutting.

The TAN content of slices, relative to the amount of protein, increased ~26% with increasing thickness from 15.2 ± 1.7 nmol/mg protein in a 200 μm slice to 20.6 ± 1.0 nmol/mg protein in a 1200 μm slice (Fig. 3*B*) ($n = 5–8$; $p < 0.05$, unpaired *t* test). There was no additional increase in the TAN levels in 1500 μm slices (20.3 ± 2.3 nmol/mg protein; $n = 4$), and we obtained a value of 21.1 ± 2.6 nmol/mg protein for 3600 μm slices ($n = 3$).

Theoretical predictions. To better understand the dependence of TAN content on slice thickness, we made the assumption that the TAN is proportional to the volume of the tissue (l^3) as defined by a unit of length *l*. If in a slice there is a layer of dead tissue of thickness *d* devoid of adenine nucleotides at either face of the slice, then the volume of tissue contributing to the TAN is $l^2(l - d)$. We further assumed that *d* is constant and does not depend on slice thickness and expressed *d* as a proportion of *l* ($d = \alpha l$). The volume of tissue contributing to the TAN is thus $l^3(1 - \alpha)$. If we consider a unit of volume (i.e., $l = 1$), then a plot of $1 - \alpha$ against the normalized TAN for different slice thicknesses, assuming constant *d*, should fit our observed data and provide a theoretical estimate of the dead layer of tissue at either face of the slice. In Figure 3*C*, we have plotted theoretical curves for the relative contribution of a dead tissue layer (*d*) of 20 μm (40 μm in total), 35 μm (70 μm in total), and 50 μm (100 μm in total) on both slice edges to the total tissue thickness (*l*, from 100 to 2000 μm slices in 20 μm steps). By normalizing the measured TAN values in Figure 3*B* to the TAN value obtained for 3600 μm slices (21.1 nmol/mg protein) and plotting it on the same graph, we observed a very good fit of our measured values to the theoretical curve obtained for an estimated total dead cut edge layers of 70 μm, or 35 μm for each edge (Fig. 3*C*,*D*, black dotted lines). We previously reported a value of 35 μm as an estimate of the dead slice layer based on histological assessment of 400 μm slices (Frenguelli et al., 2003), revealing a remarkable degree of consistency between our experimental observation and our theoretical model.

With this curve (ranging from 100 to 3600 μm in 20 μm steps) (Fig. 3*D*), an asymptotic value is approached at a tissue thickness of 3600 μm ($1 - \alpha = 0.980$), suggesting that the dead cut edges account for only 2% of the whole tissue thickness. Therefore, assuming a maximal TAN value of 21.1 nmol/mg protein (3600 μm slices) in slices, we might underestimate the TAN content of the viable core tissue in a 400 μm slice (17.1 ± 1.5 nmol/mg protein) by ~4 nmol/mg protein, ~19%. Nonetheless, when corrected for this amount, slice TAN levels in 400 μm neocortical/hippocampal slices remain ~37% (~12.5 nmol/mg protein) lower than reported *in vivo* values (33.6 ± 4.7 nmol/mg protein as shown by the gray area for the mean ± SD in Fig. 3*B*). Hence, this difference is likely attributable to the loss of adenine nucleotides and precursors during the ischemia and physical trauma associated with slice preparation.

Supplementation of aCSF with adenine nucleotide precursors improves cellular ATP levels

In vivo cerebral TAN or ATP levels recover after brief periods of ischemia (1–5 min) to pre-ischemic values after 60–90 min reperfusion (Ljunggren et al., 1974; Kobayashi et al., 1977; Nowak et al., 1985). However, there was no significant increase in TAN levels in slices over a 5 h incubation period (Fig. 1*E*). This might be attributable to a lack of purine precursor metabolites in the aCSF, which might otherwise be used to restore tissue ATP levels via purine salvage or *de novo* synthesis.

Because two key components of the purine salvage pathway, which is believed to predominate in brain (Gerlach et al., 1971; Mascia et al., 2000; Barsotti and Ipata, 2002), are adenine and D-ribose (Fig. 4*A*), we tested these compounds in brain slices. Incubating slices in 50 μM Ade and 1 mM Rib resulted in tissue levels of Ade reaching a maximum after 1 h incubation (0.92 ± 0.07 nmol/mg protein), with no additional increase after 3 h (0.95 ± 0.04 nmol/mg protein; $n = 3–5$) (data not shown). Interestingly, the uptake of Ade was facilitated by 1 mM Rib (0.56 ± 0.09 nmol/mg protein after 3 h incubation in 50 μM Ade alone compared with 0.95 ± 0.04 nmol/mg protein after 3 h incubation in 1 mM Rib/50 μM Ade; $p < 0.05$, one-way ANOVA), with no additional increase observed with higher Rib concentrations (0.83 ± 0.06 nmol/mg protein after 3 h incubation with 10 mM Rib/50 μM Ade, $n = 3$) (data not shown).

To test whether Ade and Rib could be used by the purine salvage pathway to restore adenine nucleotide levels in brain slices, we incubated freshly cut slices in aCSF supplemented with 1 mM Rib and 50 μM Ade (Fig. 4). The TAN content in slices incubated with Rib/Ade increased to 25.8 ± 0.7 nmol/mg protein after 3 h incubation (compared with 19.1 ± 1.2 nmol/mg protein in slices incubated in standard aCSF; $n = 3–5$; $p < 0.01$, one-way ANOVA) (Fig. 4*B*), with ATP accounting for ~92%. When corrected for the influence of the protein content of the dead slice edges (~4 nmol/mg protein) (Fig. 4*B*), these values (~30 nmol/mg protein) are close to the values reported for *in vivo* tissue (33.6 ± 4.7 nmol/mg) (Fig. 4*B*). The elevation of tissue TAN and ATP levels by Rib/Ade did not significantly impact on the EC, which stabilized at 0.96 ± 0.001, and the ATP/AMP ratio, which reached an asymptotic value after 3 h at 141.7 ± 17.5 compared with 94.9 ± 23.5 for slices incubated in standard aCSF ($n = 3–5$; $p > 0.05$, one-way ANOVA) (Fig. 4*C*).

Lower Rib concentrations (500 μM) were not as effective in increasing TAN levels and higher Rib concentrations (2.5–10 mM) did not further increase the TAN content of slices (data not shown). Furthermore, Ade (50 μM) on its own, as well as higher Rib concentrations (2.5 or 10 mM) on its own did not significantly increase the TAN content in slices (supplemental Table 4, available at www.jneurosci.org as supplemental material). This suggests that both metabolites are needed for effective conversion to adenine nucleotides during a 3 h incubation period.

To establish whether these elevated levels of TAN and ATP persisted when Rib/Ade was removed, we incubated slices in standard aCSF for 2 h after 3 h in Rib/Ade. During this time, tissue adenine content decreased back to baseline (0.1 ± 0.05

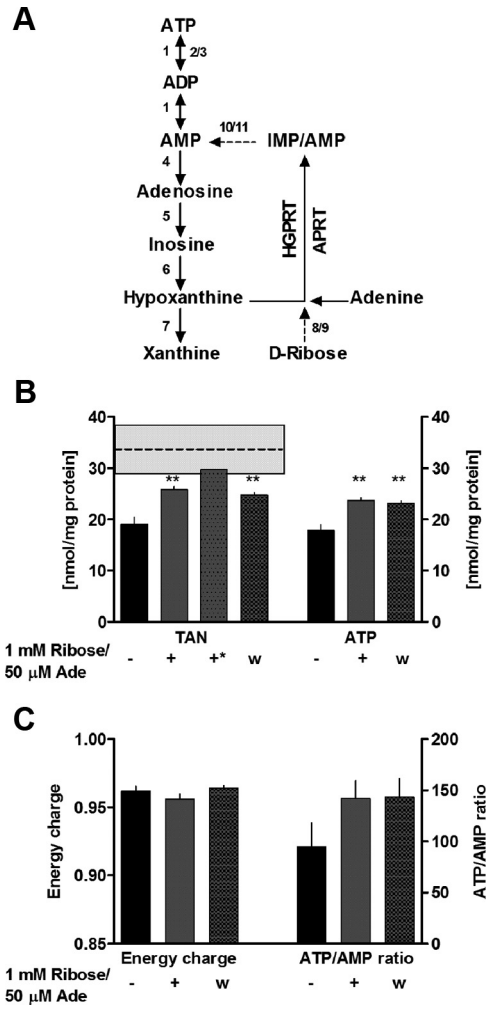

Figure 4. ***A***, Degradation of ATP and pathway for Ade and Rib utilization: 1, adenylate kinase; 2, ATPases; 3, ATP synthase; 4, 5′ nucleotidase; 5, adenosine deaminase; 6, purine nucleoside phosphorylase; 7, xanthine oxidase; 8, ribokinase; 9, phosphoribosylpyrophosphate synthetase; 10, adenylosuccinate synthetase; 11, adenylosuccinate lyase. APRT, Adenine phosphoribosyltransferase; HGPRT, hypoxanthine phosphoribosyltransferase. Solid lines indicate direct routes, and dashed lines indicate indirect routes. The reactions of the purine salvage pathway are catalyzed by HGPRT and APRT. ***B***, Improved recovery of TAN (left *y*-axis) and ATP (right *y*-axis) levels in slices after 3 h incubation in standard aCSF (−, black bars) or aCSF supplemented with 1 mM D-ribose/50 μM adenine (+, gray bars). Under these conditions and with the correction for dead tissue on the edge of slices (~4 nmol/mg protein), slice TAN levels (+*, dashed gray bar) are close to those reported *in vivo* (dotted black line represents the arithmetic mean ± SD as shown by the gray area for all reported values from supplemental references, available at www.jneurosci.org as supplemental material). Elevated TAN levels are maintained when ribose/adenine are washed out (w) of the tissue (hatched gray bars) by transferring the slices to standard aCSF for 2 h. ***C***, Energy charge (left *y*-axis) and ATP/AMP levels (right *y*-axis) are not significantly different in slices after 3 h incubation in standard aCSF (−, black bars), in aCSF supplemented with 1 mM D-ribose/50 μM adenine (+, gray bars) or after washout (w) of ribose/adenine (hatched gray bars) by transferring the slices to standard aCSF for 2 h. All values are presented as mean ± SEM; $n = 3$–5. $^{**}p < 0.01$ compared with slices incubated in standard aCSF, one-way ANOVA with Bonferroni's multiple comparison test. When no error bars can be seen, they are smaller than the symbol.

nmol/mg protein; $n = 3$) (data not shown). However, the higher TAN levels were maintained even when Rib and Ade were washed out of the slices (Fig. 4*B*) (supplemental Table 4, available at www.jneurosci.org as supplemental material) (24.9 ± 0.4 nmol/mg protein; $n = 3$; $p < 0.01$ compared with standard slices, one-way ANOVA), as were the energy charge and ATP/AMP ratio (Fig. 4*C*).

These data suggest that the full recovery of slice ATP levels is limited by the lack of ATP precursors in the aCSF. In addition, these data also indicate that providing ATP precursors in the form of Rib/Ade allows the viable core of brain slices to restore ATP levels to values close to those reported *in vivo*.

Electrophysiological properties of slices incubated in Rib/Ade

To establish whether the higher ATP and TAN levels in slices incubated in Rib/Ade would alter the electrophysiological properties of brain slices, we performed extracellular recordings from the CA1 region of hippocampal slices. Input–output curves, paired-pulse facilitation, and LTP were compared between slices incubated for 3–8 h in standard aCSF and slices incubated for 2 h in 1 mM Rib and 50 μM Ade then for 1–6 h in standard aCSF to wash these agents out of the tissue. A 2 h incubation period in Rib/Ade was chosen, because slice TAN levels reached an asymptotic value at that time (25.4 ± 2.3 nmol/mg protein), with no additional increase after 3 h (25.8 ± 0.6 nmol/mg protein; $n = 3$–5) (data not shown).

Basal synaptic transmission is normal in Rib/Ade-treated slices

The recovery of synaptic transmission after slice cutting was not different between standard and Rib/Ade-treated slices (supplemental Fig. 2, available at www.jneurosci.org as supplemental material). Furthermore, in a separate series of slices, there was no significant difference in input–output curves (Fig. 5*A*; $n = 15$–16) and paired-pulse ratios (Fig. 5*B*; $n = 18$–22) between the two set of slices ($p > 0.05$, one-way ANOVA). Likewise, 50 μM Ade on its own (Fig. 5*C*; $n = 4$) or in combination with 1 mM Rib (Fig. 5*D*; $n = 6$) did not change paired-pulse ratios when acutely applied to slices. This suggests that, under conditions of low-frequency stimulation of afferent fibers, the enhanced tissue ATP levels in Rib/Ade-treated slices is not being released to form adenosine in the extracellular space, which would, via inhibitory A_1Rs, inhibit glutamate release and raise the paired-pulse facilitation ratio. These negative results suggest that the activation A_1Rs and basal handling of adenosine is normal between standard and Rib/Ade-treated slices. To test this directly, we applied the selective A_1R agonist N^6-CPA (10 nM) (Gadalla et al., 2004) or the adenosine uptake inhibitors NBTI (5 μM)/DIPY (10 μM) (Frenguelli et al., 2007; Etherington et al., 2009) to both sets of slices (Fig. 5*E*,*F*). The concentrations chosen were submaximal for complete depression of the fEPSP to avoid a "floor effect" obscuring potential differences between the two sets of slices. Furthermore, we have shown previously that NBTI/DIPY causes a depression of the fEPSP that can be reversed with A_1R antagonists (Pearson et al., 2001) and have demonstrated the increase in extracellular adenosine directly with adenosine biosensors (Frenguelli et al., 2007; Etherington et al., 2009).

The rate and extent of fEPSP depression after a 15 min application of N^6-CPA was the same in control (50.0 ± 1.6%; $n = 5$) and Rib/Ade-treated (50.4 ± 1.6%; $n = 5$; $p > 0.05$, unpaired *t* test) slices (Fig. 5*E*). Likewise, the application NBTI/DIPY for 40 min resulted in the same rate and amount of depression in both sets of slices (40 ± 5.9% for standard slices; 43 ± 3.3% for Rib/Ade treated slices; $n = 4$; $p > 0.05$, unpaired *t* test) (Fig. 5*F*). These data suggest that Rib/Ade pretreatment does not influence the sensitivity of the A_1R to agonists, nor is the activity of equilibrative adenosine transporters affected.

Furthermore, the fact that acute application of Ade did not change paired-pulse ratios (Fig. 5*C*,*D*), shows that the recently described $G\alpha_i$-protein-coupled adenine receptor (Bender et al., 2002; von Kügelgen et al., 2008), if present in the hippocampus,

does not have any presynaptic effects on neurotransmitter release. However, to further exclude the possibility of differences in cAMP formation between Rib/Ade-treated slices and slices incubated in standard aCSF, we applied 50 μM forskolin to both sets of slices and compared the increase in fEPSP slopes (Fig. 5*G*,*H*). There was no significant difference in forskolin-induced potentiation between Rib/Ade-treated slices and slices incubated in standard aCSF (Fig. 5*G*) (147.4 ± 9.8% in standard slices and 159.1 ± 12.9% in Rib/Ade-treated slices; $n = 3–4$; $p < 0.05$ compared with baseline before application of forskolin, $p > 0.05$ between standard slices and Rib/Ade-treated slices at 20 min after application of forskolin, one-way ANOVA). Paired-pulse facilitation (50 ms interpulse interval) was similarly affected by forskolin in standard slices and Rib/Ade-treated slices (Fig. 5*H*) ($n = 3–4$; $p > 0.05$ between standard slices and Rib/Ade-treated slices, unpaired *t* test). This suggests that adenylyl cyclase activation and cAMP production is not impaired in Rib/Ade-treated slices.

Long-term potentiation is impaired in Rib/Ade-treated slices

Slices incubated in standard aCSF showed robust LTP 55–60 min after tetanic stimulation (one train of 100 shocks at 100 Hz; 135 ± 5.8% of baseline; $n = 9$; $p < 0.001$ compared with 5 min baseline before tetanic stimulation, one-way ANOVA) (Fig. 6*A*). However, LTP in slices incubated for 2 h in 1 mM Rib and 50 μM Ade decayed back to baseline 60 min after tetanic stimulation (108 ± 4.9% of baseline; $n = 11$; $p > 0.05$ compared with 5 min baseline before tetanic stimulation, one-way ANOVA) and was significantly lower in amplitude than LTP in control slices incubated in standard aCSF ($p < 0.001$ from 55 to 60 min after LTP induction, one-way ANOVA). Stable recordings could be achieved in Rib/Ade-treated slices over the same time period (94 ± 6.6% of baseline at 75 min; $n = 3$) (data not shown), which argues against baseline drift as being the cause for the observed decay in LTP. In contrast, acute application of Ade or Rib alone, or in combination, did not impair tetanus-induced LTP (133 ± 5% of baseline for standard slices, 131 ± 13% after acute application of 50 μM Ade, 140 ± 9% after acute application of 1 mM Rib, and 131 ± 8% after acute application of 1 mM Rib/50 μM Ade at 60 min after LTP induction; $n = 4–5$) (data not shown), implying a requirement for uptake and intracellular conversion to adenine nucleotides.

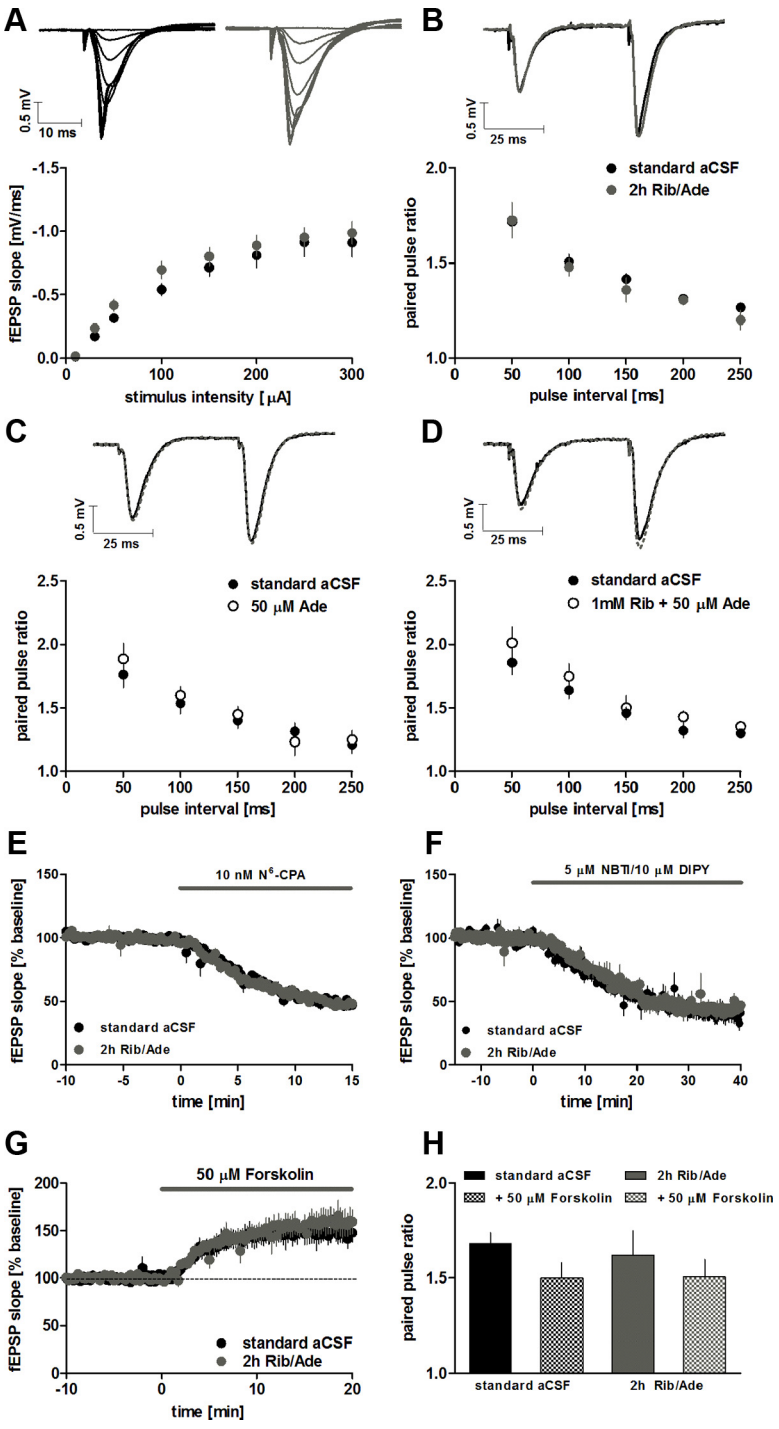

Figure 5. Basal synaptic transmission, adenosine A_1 receptor activation, and adenosine uptake are not different between slices incubated in standard aCSF and slices treated for 2 h in 1 mM Rib and 50 μM Ade. Input–output curves ($n = 15–16$) (***A***) and paired-pulse ratios ($n = 18–22$) (***B***) for slices incubated in standard aCSF (black circles) and slices treated for 2 h with Rib/Ade-supplemented aCSF (gray circles). Insets are representative fEPSPs from 10–300 μA (***A***) and at 50 ms interpulse interval (***B***) for controls and Rib/Ade-treated slices. ***C***, ***D***, Paired-pulse ratios for slices incubated in standard aCSF before (black circles) and after acute application of 50 μM Ade (***C***, white circles, $n = 4$) or 50 μM Ade and 1 mM Rib (***D***, white circles, $n = 6$). Insets are representative fEPSPs at 50 ms interpulse interval before (black traces) and after application of Ade or Rib/Ade (dotted gray traces). There was no difference in the rate or magnitude of fEPSP depression in response to the selective A_1R agonist N^6-CPA (10 nM; $n = 5$) (***E***) or the combination of the adenosine uptake inhibitors NBTI (5 μM)/DIPY (10 μM; $n = 4$) in standard slices or Rib/Ade-treated slices (***F***). ***G***, Forskolin-induced potentiation in standard slices (black circles) and Rib/Ade-treated slices (gray circles). Forskolin at 50 μM was applied to slices for 20 min and no differences were observed in the amount of potentiation (147.4 ± 9.8% in standard slices and 159.1 ± 12.9% in Rib/Ade treated slices; $n = 3–4$) or the decrease in paired-pulse facilitation ($n = 3–4$) (***H***). Recordings were performed at 33.4 ± 0.2°C at a flow rate of 7–8 ml/min after a ≥3 h recovery period from slice cutting. All values are presented as mean ± SEM. No significant differences observed between standard and Rib/Ade-treated slices with unpaired *t* tests or one-way ANOVA with Bonferroni's multiple comparison test. When no error bars can be seen, they are smaller than the symbol.

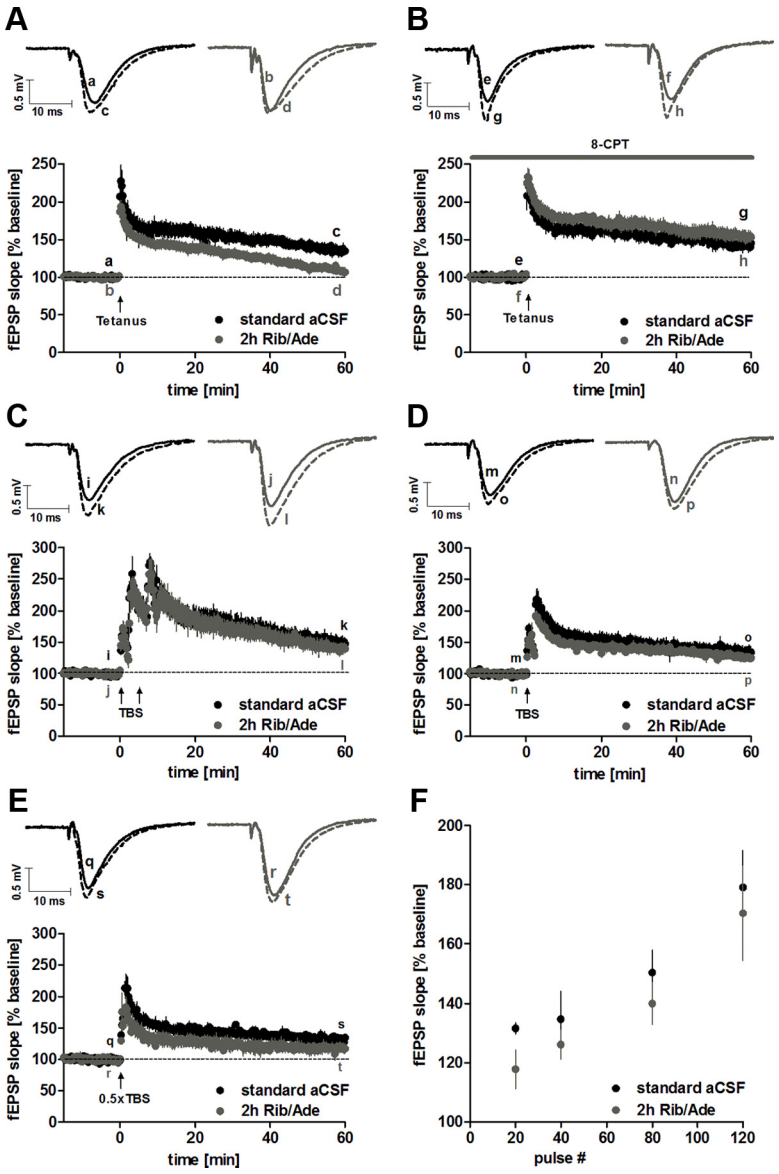

Figure 6. LTP induction with tetanic stimulation is impaired in slices treated for 2 h in 1 mM Rib and 50 μM Ade in an A_1R-dependent manner. ***A***, LTP after tetanic stimulation (1 × 100 stimuli at 100 Hz) in slices incubated for 2 h in Rib/Ade-supplemented aCSF (gray circles; $n = 11$) and slices incubated in standard aCSF (black circles; $n = 9$). ***B***, LTP after tetanic stimulation and in the presence of 8-CPT in slices incubated for 2 h in Rib/Ade-supplemented aCSF (gray circles; $n = 6$) and slices incubated in standard aCSF (black circles; $n = 5$). ***C***, ***D***, LTP is not different in slices incubated for 2 h in Rib/Ade-supplemented aCSF (gray circles) and standard aCSF (black circles) when either two (***C***; 5 min apart; 80 pulses; $n = 6–7$) or one (***D***; 40 pulses; $n = 6$ for both) TBS are delivered (TBS: 10 trains of 4 pulses at 100 Hz, 200 ms interval). ***E***, In contrast, a briefer TBS (5 trains, 20 pulses) resulted in significant LTP in standard slices 55–60 min after TBS (black circles; $n = 3$ from 2 animals) but not Rib/Ade-treated slices (gray circles; $n = 4$ from 3 animals). ***F***, Plot of pulse number versus magnitude of LTP 55–60 min (20, 40, 80 pulses) or 30 min (120 pulses) after induction in standard and Rib/Ade-treated slices. Note that, throughout the pulse number range, Rib/Ade-treated slices give rise to lower LTP, which falls below significant LTP induction threshold at 20 pulses. Data for 120 pulses from Figure 7 with 120 pulses delivered via 3 × 40 pulse theta trains at 10 s intervals with LTP measured after 30 min. All insets are representative of fEPSPs before (solid lines) and 60 min after the induction of LTP (dashed lines). Recordings were performed at 33.4 ± 0.2°C at a flow rate of 7–8 ml/min after a ≥3 h recovery period from slice cutting. All values are presented as mean ± SEM.

A potential reason for the impaired LTP stabilization in Rib/Ade-treated slices might be that, because of the higher TAN pool, enhanced synaptic activity during tetanic stimulation causes the activity-dependent release of ATP and/or its metabolite adenosine. To test this, we incubated slices in the ATP P_2 receptor antagonist PPADS (10 μM) and A_1R antagonist 8-CPT (1 μM) before the induction of LTP. Preincubation with PPADS did not prevent the decay of LTP in Rib/Ade-treated slices (108 ± 15% of baseline 60 min after LTP induction; $n = 4$) (data not shown). These observations suggest that, if ATP is being released during tetanic stimulation, it is not directly responsible via P_2 receptors for the impairment of LTP.

To test for a role for adenosine A_1 receptors, we applied 8-CPT (1 μM), a selective A_1R antagonist, to slices that had either been pretreated with Rib/Ade or incubated in standard aCSF. Ten minutes after acute application of 8-CPT, fEPSPs had increased to 121.4 ± 0.7% in standard slices ($n = 6$) (data not shown) and to 124.1 ± 0.5% in Rib/Ade-treated slices ($n = 8$) (data not shown) and was associated with a similar decrease in PPF in both (data not shown). Both these changes in synaptic transmission are indicative of the removal of a basal adenosine A_1R-dependent inhibitory tone. The fact that the changes were similar between the two conditions argues against the possibility of an increased basal adenosine tone in Rib/Ade-treated slices. This is consistent with the following observations: (1) similar tissue adenosine levels in both sets of slices after a 3 h incubation (standard slices, 0.05 ± 0.004 nmol/mg protein, $n = 3$; Rib/Ade-treated slices, 0.04 ± 0.002; $n = 3$; $p > 0.05$, unpaired t test) (data not shown), (2) normal basal transmission and paired-pulse facilitation in Rib/Ade-treated slices (Fig. 5*A–D*), (3) identical effects of A_1R activation and uptake inhibition (Fig. 5*E*,*F*), and (4) equal effects of forskolin (Fig. 5*G*,*H*).

Having established that the basal handling and effects of adenosine were similar in control and Rib/Ade-treated slices, we next examined the effect of the A_1R antagonist on tetanus-induced LTP with or without previous treatment with Rib/Ade. LTP was induced when a stable fEPSP baseline of 15 min was collected, ~30–40 min after application of 8-CPT. Both sets of slices showed robust LTP in the presence of 8-CPT 55–60 min after tetanic stimulation (Fig. 6*B*) (143 ± 6.0% in standard slices and 154 ± 6.7% in Rib/Ade-treated slices; $n = 5–6$; $p < 0.001$ compared with 5 min baseline before tetanic stimulation, $p > 0.05$ between standard slices and Rib/Ade-treated slices 55–60 min after tetanic stimulation, one-way ANOVA). This suggests that the activity-dependent release of adenosine contributes to the impairment of LTP induction in Rib/Ade-treated slices.

We hypothesized that this deficit in LTP induction represented a raising of the threshold for LTP by the activity-dependent accumulation of extracellular adenosine and activation of inhibitory A_1Rs. This hypothesis predicted that stronger activation of postsynaptic neurons should overcome

this threshold. Accordingly, we used a TBS LTP induction protocol (Larson et al., 1986), which is known to deliver sustained glutamatergic excitation while causing fatigue of GABA-mediated inhibition and hence greater activation of NMDA receptors (Chen et al., 2010).

Control and Rib/Ade-treated slices were stimulated with two TBS at 5 min intervals (2 × 10 trains of four pulses at 100 Hz with 200 ms intervals, i.e., 80 pulses in total). This protocol resulted in robust LTP in both standard and Rib/Ade-treated slices 55–60 min after TBS (Fig. 6*C*) (150.2 ± 7.6% in standard slices and 140.0 ± 7.1% in Rib/Ade-treated slices; $n = 6$–7; $p < 0.001$ compared with 5 min baseline before TBS, $p > 0.05$ between standard slices and Rib/Ade-treated slices at 55–60 min after TBS, one-way ANOVA). One TBS (40 pulses) resulted in smaller LTP 55–60 min after TBS and showed little difference between standard and Rib/Ade-treated slices (Fig. 6*D*) (137.7 ± 9.5% in standard slices and 126.2 ± 5.0% in Rib/Ade-treated slices; $n = 6$; $p < 0.01$ for standard slices and $p < 0.05$ for Rib/Ade-treated slices compared with 5 min baseline before TBS, $p > 0.05$ between standard slices and Rib/Ade-treated slices at 55–60 min after TBS, one-way ANOVA).

To confirm that TBS resulted in greater depolarization compared with tetanic stimulation, we measured the area associated with each pulse induced by tetanic stimulation (100 pulses) and TBS (40 pulses) in a manner similar to that described recently (Chen et al., 2010). A comparison of the normalized cumulative area evoked by each pulse in a tetanus and TBS (supplemental Fig. 3*A*, available at www.jneurosci.org as supplemental material) revealed a dramatic difference between the two: in a tetanus, most of the depolarization had occurred within the first 20 pulses, whereas during TBS, the depolarization increased almost linearly during the 40 pulse train.

Furthermore, during a tetanus, there was evidence of an influence of Rib/Ade in causing fatigue of transmission during the later stages of the train (>20 pulses) (supplemental Fig. 3*A*, available at www.jneurosci.org as supplemental material). This was prevented in slices treated with 8-CPT (supplemental Fig. 3*B*, available at www.jneurosci.org as supplemental material) and is consistent with a gradual synaptic accumulation of adenosine. Indeed, the apparent enhancement in 8-CPT/Rib/Ade-treated slices may reflect an action of adenosine on facilitatory adenosine A_2 (Kessey and Mogul, 1998; Fujii et al., 1999; Almeida et al., 2003) or A_3 (Costenla et al., 2001) receptors. In contrast, this Rib/Ade-induced fatigue was hardly present during one TBS (supplemental Fig. 3*A*, available at www.jneurosci.org as supplemental material), two TBS given 5 min apart (supplemental Fig. 3*C*, available at www.jneurosci.org as supplemental material), or three TBS given 10 s apart (supplemental Fig. 3*D*,*E*, available at www.jneurosci.org as supplemental material), suggesting rapid clearance of adenosine in the 200 ms between each 4 × 100 Hz stimuli.

An examination of the cumulative depolarization evoked by tetanic stimulation (supplemental Fig. 3*A*, available at www.jneurosci.org as supplemental material) predicted that ~20 pulses was the threshold for Rib/Ade to inhibit the induction of TBS LTP: this was the point at which cumulative tetanic depolarizations diverged when Rib/Ade was present and also equivalent to the number of TBS pulses required to evoke the maximal tetanic depolarization in Rib/Ade. Accordingly, delivery of 20 TBS pulses (5 × 4 pulses at 100 Hz, 200 ms apart) resulted in significant LTP in standard slices but not in Rib/Ade-treated slices 55–60 min after TBS (Fig. 6*E*) (131.6 ± 2% in standard slices and 117.8 ± 6.6% in Rib/Ade-treated slices; $n = 3$–4; $p < 0.01$ for standard slices and $p > 0.05$ for Rib/Ade-treated slices compared with 5 min baseline before TBS, one-way ANOVA). A comparison of the magnitude of LTP versus the number of TBS pulses (Fig. 6*F*) reveals a consistent inhibitory influence of Rib/Ade treatment on the magnitude of LTP.

These data point to the release of either ATP or adenosine during electrical stimulation, which, via adenosine A_1Rs, inhibits the induction of LTP in response to tetanic stimulation in Rib/Ade-treated slices. Importantly, this impairment can be overcome by additional stimulation, suggesting that the elevated levels of tissue ATP translate into raising the threshold for LTP induction.

Real-time measurement of adenosine release during LTP induction

To further test whether the higher TAN levels in Rib/Ade-treated slices resulted in a greater accumulation of adenosine during periods of electrical stimulation of afferent fibers, we used adenosine biosensors (Frenguelli et al., 2003) to measure the real-time release of adenosine during TBS and LTP induction. The sensors (adenosine and null sensors) were placed in stratum radiatum of the CA1 region of hippocampal slices between the recording and stimulating electrodes.

We could not detect any measurable release of adenosine during tetanic stimulation (100 Hz, 1 s) or consistently with one TBS (data not shown), presumably because the released adenosine is below the limit of detection for adenosine biosensors (50 nM) or because the released adenosine remained close to the site of release and was not available for detection by the sensor. For this reason, we used a more intense protocol that would be more likely to result in greater adenosine release and sufficient spillover of adenosine to be detected by the sensors. Accordingly, with a multiple TBS protocol (10 trains of four pulses at 100 Hz, 200 ms apart, repeated three times at 10 s intervals) (Fig. 7*A*), we were able to detect a rise in extracellular adenosine in slices incubated in standard aCSF and slices treated with Rib/Ade (Fig. 7*B*).

Rib/Ade-treated slices released significantly more adenosine during TBS as measured by integrating the area under the adenosine signal at the start of TBS to 5 min after stimulation (Fig. 7*B*) (0.64 ± 0.1 μM′*min in slices incubated in standard aCSF and 1.98 ± 0.1 μM′*min in Rib/Ade-treated slices; $n = 3$; $p < 0.01$, unpaired t test). Despite this greater release of adenosine, we could not observe any differences in LTP (Fig. 7*A*) between the two sets of slices as measured at 30 min after TBS. This is likely attributable to the fact that the strong stimulation protocol (Fig. 6*C*,*D*) overcame the inhibitory effects of A_1R.

These results suggest that higher intracellular TAN or ATP levels result in increased activity-dependent adenosine release during periods of strong electrical stimulation, which can modulate the induction threshold for LTP.

Mechanism of activity-dependent adenosine release

To establish whether the released adenosine arose from direct release of adenosine or from extracellular degradation of ATP, we used adenosine uptake inhibitors (NBTI/DIPY) and POM-1, a noncompetitive inhibitor of ectonucleotidases (Müller et al., 2006; Wall et al., 2008). To assess the effect of these drugs on adenosine release, TBS-induced adenosine release was evoked twice (45–60 min apart): the first TBS was in control aCSF (in either standard slices or Rib/Ade-treated slices), and the second was in the presence of NBTI (5 μM)/DIPY (10 μM) or POM-1 (100 μM), which were applied 30 min after the initial TBS. Repeating TBS twice within 45–60 min did not affect adenosine

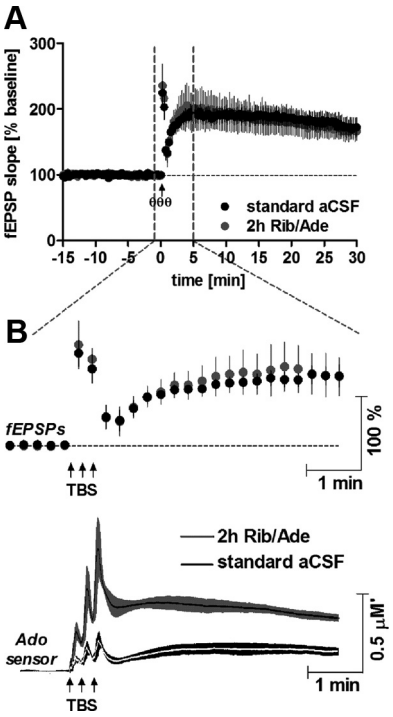

Figure 7. Real-time measurement of adenosine release during LTP induction reveals significantly higher adenosine release in slices treated for 2 h in 1 mM Rib and 50 μM Ade. ***A***, fEPSP slopes after LTP induction with TBS (10 trains of 4 pulses, at 100 Hz 200 ms apart, applied 3 times with 10 s intervals) are not different in slices incubated for 2 h in Rib/Ade-supplemented aCSF (gray circles; $n = 4$) and slices incubated in standard aCSF (black dots; $n = 5$). ***B***, fEPSP slopes and adenosine sensor traces from 1 min before and 5 min after TBS, as shown by the gray dotted lines in ***A***. Adenosine sensor traces show pooled traces of all experiments for standard slices (white line with black area for mean ± SEM, respectively; $n = 3$) and Rib/Ade-treated slices (black line with gray area for mean ± SEM, respectively; $n = 3$). Adenosine sensors placed between the recording and stimulating electrodes show significantly higher adenosine release in Rib/Ade-treated slices during LTP induction. All values are presented as mean ± SEM.

release (supplemental Fig. 4*A*, available at www.jneurosci.org as supplemental material). If adenosine was released directly, we would expect the transport inhibitors to reduce TBS-induced adenosine accumulation as they represent a major efflux pathway for adenosine into the extracellular space (Baldwin et al., 2004). If extracellular adenosine arose from the metabolism of ATP, POM-1 should reduce TBS-induced adenosine release.

The effectiveness of POM-1 to inhibit ATP breakdown in hippocampal brain slices was assessed by inserting adenosine biosensors into slices and measuring adenosine production after exogenous ATP application in the presence and absence of POM-1 (Wall et al., 2008). POM-1 caused a time-dependent inhibition of ATP breakdown: in the absence of POM-1, 50 μM ATP yielded 3.5 ± 0.2 μM′ adenosine. After application of POM-1 for 5 min, ATP breakdown was inhibited by 30 ± 3% (2.5 ± 0.1 μM′; $n = 3$; $p > 0.05$ compared with initial response, one-way ANOVA), whereas after 15 min, the metabolism of ATP was inhibited by 42 ± 2% (2 ± 0.2 μM′; $n = 3$; $p < 0.05$ compared with initial response, one-way ANOVA) (supplemental Fig. 4*B*,*C*, available at www.jneurosci.org as supplemental material). We therefore decided to wait 15 min after POM-1 application to study the effect of POM-1 on TBS-induced adenosine release.

In the presence of POM-1, TBS-induced adenosine release was variable but showed no evidence of inhibition of adenosine release. In fact, the reverse was observed: POM-1 seemed to increase TBS-induced adenosine release in both standard and Rib/Ade slices (supplemental Fig. 4*A*, available at www.jneurosci.org as supplemental material). This could represent an off-target effect, as we have suggested exist in the use of POM-1 (Wall et al., 2008), or could reflect a previously described ATP-mediated facilitation of adenosine release via the activation of ATP P_2 receptors (Almeida et al., 2003). To address this, we incubated Rib/Ade-treated slices with the P_2 antagonist PPADS (10 μM) for 10 min before TBS. PPADS had no significant effect on adenosine release in Rib/Ade-treated slices (2.0 ± 0.41 μM′*min for Rib/Ade-treated slices; $n = 10$; and 2.0 ± 0.61 μM′*min for Rib/Ade-treated slices in the presence of PPADS; $n = 3$; $p > 0.05$, unpaired *t* test,) and indeed did not affect the increased TBS-induced adenosine release in the presence of POM-1 (2.8 ± 0.45 μM′*min for Rib/Ade-treated slices after POM-1 application; $n = 4$; and 2.3 and 3.3 μM′*min in two Rib/Ade-treated slices in the presence of POM-1 and PPADS) (supplemental Fig. 4*A*, available at www.jneurosci.org as supplemental material). These negative results with the ectonucleotidase inhibitor POM-1 argue against an appreciable release of ATP and extracellular conversion to adenosine.

In contrast, application of NBTI/DIPY for 30 min resulted in a 50% reduction in TBS-induced adenosine release in both sets of slices (supplemental Fig. 4*A*, available at www.jneurosci.org as supplemental material) (50.3 ± 17.0% for control slices, $n = 4$, $p = 0.06$; 49.2 ± 11.0% for Rib/Ade-treated slices, $n = 3$, $p = 0.04$, paired *t* test), suggesting a role of equilibrative adenosine transporters in the release of adenosine in response to high-frequency stimulation of afferent fibers.

Discussion

Despite the importance and widespread use of brain slices as models of the mammalian CNS, criticisms remain regarding their metabolic integrity. Our aim was to address this issue to study (1) the energetic recovery of brain slices, (2) the reasons for reduced levels of ATP, (3) the possibility of improving cellular ATP, and (4) the functional consequences of raising tissue ATP levels.

Energetic recovery after slice preparation

In accordance with previous findings (Fredholm et al., 1984; Whittingham et al., 1984a,b), our results show that adenine nucleotide levels in brain slices recover quickly and remain stable for at least 5 h, independently of the incubation temperature. Likewise, the EC and ATP/AMP ratio show a rapid recovery after slice preparation, but it takes 3 h until they stabilize, well beyond the time conventionally allowed for slices to recover. Provided with an adequate supply of nutrients, it is likely that both interface and submerged slices will recover similarly in terms of adenine nucleotides and energetic parameters. Indeed, TAN and adenosine levels for interface hippocampal slices (~10.5 nmol/mg protein and 40 pmol/mg protein, respectively) (Fredholm et al., 1984) are not different from our results (~9.8 nmol/mg protein and 50 pmol/mg protein, respectively).

However, it is worth noting that other metabolites, such as cGMP and cAMP, lactate, or phosphocreatine, also require 1–3 h to achieve a steady state (Whittingham et al., 1984b). Likewise, the phosphorylation status of proteins involved in synaptic plasticity, such as GluA1, ERK2, and MEK1/2, changes during the first 3 h of incubation (Ho et al., 2004), whereas a recovery period of 4 h has been suggested for achieving stable long-term recordings of LTP in brain slices (Sajikumar and Frey, 2004; Sajikumar et al., 2005; Redondo et al., 2010).

Temperature dependence of the ATP/AMP ratio and AMPK activity

Our results indicate that slices maintained at 34°C have a significantly higher ATP/AMP ratio compared with slices at room temperature. This is likely attributable to the activity of adenylate kinase (EC 2.7.4.3; 2 ADP ↔ ATP + AMP), which is greater at temperatures above 32°C (Sheng et al., 1999; Lu and Wang, 2008). Accordingly, slices incubated at 22°C had a lower ATP/AMP ratio and showed a threefold higher AMPK activity than slices maintained at 34°C. This translated into increased phosphorylation of a downstream target, ACC, and suggests that other downstream targets are likely to be similarly affected.

Of the known AMPK targets relevant to synaptic physiology, AMPK phosphorylates $GABA_B$ receptors (Hardie and Frenguelli, 2007; Kuramoto et al., 2007) and calcium-activated potassium channels (Wyatt et al., 2007). Furthermore, a proteomic screen revealed 12 brain-specific downstream targets of AMPK, including synapsin I and PACSIN1, further suggesting a role for AMPK in regulating synaptic activity (Tuerk et al., 2007). Indeed, enhancing AMPK activity inhibits long-lasting LTP (Potter et al., 2010). Hence, incubating slices at elevated temperatures will more closely replicate metabolism *in vivo* with respect to the activity of enzymes and properties of synaptic transmission.

Basis of reduced tissue ATP content in brain slices

As seen in this and many other reports (McIlwain, 1952; Thomas, 1957; Kass and Lipton, 1982; Fredholm et al., 1984; Whittingham et al., 1989; Paschen and Djuricic, 1995; Milusheva et al., 1996), brain slices have ~40–60% lower ATP and TAN levels than the *in vivo* brain (Supplemental References). Our results suggest that this is attributable to the loss of adenine nucleotides and/or their metabolites, especially in hippocampal tissue, during slice preparation. However, incubation of slices in Rib/Ade-supplemented aCSF allowed the tissue to appreciably increase TAN levels. When corrected for the influence of the dead slice edges, which we could model accurately and which agreed with histological estimates we made previously (Frenguelli et al., 2003), TAN levels were within the range reported *in vivo*. This suggests that the recovery of ATP levels in brain slices is limited by the lack of precursors in the aCSF and does not necessarily reflect an intrinsic metabolic handicap.

Implications of improving the tissue ATP content in brain slices

Although Rib/Ade restored tissue nucleotide levels close to those observed *in vivo*, this did not have a bearing on basal synaptic transmission, paired-pulse facilitation, or the tonic handling and effects of extracellular adenosine. Instead, Rib/Ade inhibited LTP after tetanic stimulation and weak TBS. That the application of an A_1R antagonist reversed the fatigue of the fEPSP during the tetanus and prevented the decline of tetanus-induced LTP in Rib/Ade-treated slices suggests that the higher TAN levels resulted in greater activity-dependent adenosine release, thereby preventing the stable expression of LTP. This suggests that endogenous adenosine exerts an inhibitory influence on LTP induction (de Mendonça and Ribeiro, 1994; Forghani and Krnjević, 1995; Fujii et al., 2000; Rex et al., 2005), especially when used with weak stimulation protocols (Arai and Lynch, 1992; de Mendonça and Ribeiro, 2000). Interestingly, the threshold for adenosine-dependent regulation of TBS, based on the facilitatory actions of an A_1R antagonist, was 20 pulses (Arai and Lynch, 1992; de Mendonça and Ribeiro, 2000), consistent with our predictions based on tetanic and TBS cumulative depolarizations and experiments with Rib/Ade-treated slices. These observations and our own results point toward an adenosine A_1R-dependent regulation of LTP, which is influenced by the levels of intracellular adenine nucleotides.

However, our analysis of the TBS stimulus trains revealed no A_1R-dependent fatigue of the fEPSP. This may reflect the fact that the 200 ms burst spacing may allow time for the removal of extracellular adenosine between stimulus trains through metabolism, reuptake, or diffusion. Thus, to the two known actions of TBS that make it an effective and naturalistic stimulus for LTP induction, maximizing both postsynaptic depolarization and GABAergic fatigue, we may now potentially add a third: minimizing the intraburst synaptic accumulation of extracellular adenosine.

Using adenosine biosensors, we were able to detect in real time the release of adenosine during TBS. Rib/Ade-treated slices released significantly more adenosine, consistent with the availability of a greater precursor pool of ATP. To establish whether ATP or adenosine was released in response to high-frequency stimulation, we used the noncompetitive ectonucleotidase inhibitor POM-1 (Müller et al., 2006; Wall et al., 2008) and the equilibrative nucleoside transporter (ENT) inhibitors DIPY/NBTI (Frenguelli et al., 2007; Etherington et al., 2009). POM-1 failed to reduce, and indeed facilitated, TBS-induced adenosine release. This is unlikely to be attributable to ATP P_2 receptor-mediated facilitation of adenosine release reported by others (Almeida et al., 2003) because the facilitation was not affected by the P_2 antagonist PPADS. Instead, this facilitation may involve nonspecific actions of POM-1 (Wall et al., 2008) or could potentially involve ATP heteroexchange with adenosine (Sperlágh et al., 2003), which is insensitive to P_2 receptor antagonists but sensitive to ENT inhibition. Accordingly, DIPY/NBTI caused a 50% reduction in TBS-induced adenosine release, which is consistent with the direct release of adenosine during high-frequency stimulation (Wall and Dale, 2008; Klyuch et al., 2011).

In a wider context, the reduced tissue ATP levels observed after cerebral ischemia *in vivo* may, via reduced extracellular adenosine and reduced activation of the anticonvulsant A_1R (Boison and Stewart, 2009; Dale and Frenguelli, 2009), contribute to the development of post-ischemic epilepsy (Camilo and Goldstein, 2004; Kadam et al., 2010). Indeed, the influence of intracellular ATP on extracellular adenosine and neuronal excitability has been described recently (Kawamura et al., 2010) and may be the basis for the reduced incidence of seizures during a ketogenic diet (Masino and Geiger, 2008). Accordingly, elevation of tissue ATP levels with Rib/Ade may be of value in the post-ischemic brain. In fact, Rib has been used to improve post-ischemic cardiac function *in vitro*, *in vivo*, and in humans (Zimmer, 1998; Omran et al., 2003; Shecterle et al., 2010). Although Ade has to be administered with a xanthine oxidase inhibitor (Watts et al., 1974; Simmonds, 1986) to prevent its conversion to an insoluble metabolite, this may be beneficial (Phillis et al., 1995) because it would prevent the formation of nonsalvageable xanthine, thereby providing greater substrates for the purine salvage pathway in the post-ischemic brain. Thus, Rib/Ade may be of value in restoring ATP levels and adenosine release after brain injury.

In summary, the data presented address long-standing issues in the use of brain slices as *in vitro* models for the mammalian CNS. We confirm the long-held view that tissue adenine nucleotides are ~50% of the values reported *in vivo* but demonstrate that this is an underestimate (by ~20%) because of the contribution of damaged slice edges. Moreover, we show that slices have

an appreciable capacity, through the purine salvage pathway, to restore and maintain tissue ATP levels close to *in vivo* levels when presented with the ATP precursors Ade and Rib. The physiological consequences of elevated tissue ATP levels are in the greater activity-dependent release of adenosine and the raising of the threshold for the induction of LTP.

References

Almeida T, Rodrigues RJ, de Mendonça A, Ribeiro JA, Cunha RA (2003) Purinergic P2 receptors trigger adenosine release leading to adenosine A2A receptor activation and facilitation of long-term potentiation in rat hippocampal slices. Neuroscience 122:111–121.

Arai A, Lynch G (1992) Factors regulating the magnitude of long-term potentiation induced by theta pattern stimulation. Brain Res 598:173–184.

Atkinson DE (1968) The energy charge of the adenylate pool as a regulatory parameter. Interaction with feedback modifiers. Biochemistry 7:4030–4034.

Baldwin SA, Beal PR, Yao SY, King AE, Cass CE, Young JD (2004) The equilibrative nucleoside transporter family, SLC29. Pflugers Arch 447:735–743.

Barsotti C, Ipata PL (2002) Pathways for alpha-D-ribose utilization for nucleobase salvage and 5-fluorouracil activation in rat brain. Biochem Pharmacol 63:117–122.

Bender E, Buist A, Jurzak M, Langlois X, Baggerman G, Verhasselt P, Ercken M, Guo HQ, Wintmolders C, Van den Wyngaert I, Van Oers I, Schoofs L, Luyten W (2002) Characterization of an orphan G protein-coupled receptor localized in the dorsal root ganglia reveals adenine as a signaling molecule. Proc Natl Acad Sci U S A 99:8573–8578.

Boison D, Stewart KA (2009) Therapeutic epilepsy research: from pharmacological rationale to focal adenosine augmentation. Biochem Pharmacol 78:1428–1437.

Camilo O, Goldstein LB (2004) Seizures and epilepsy after ischemic stroke. Stroke 35:1769–1775.

Chen LY, Rex CS, Sanaiha Y, Lynch G, Gall CM (2010) Learning induces neurotrophin signaling at hippocampal synapses. Proc Natl Acad Sci U S A 107:7030–7035.

Costenla AR, Lopes LV, de Mendonça A, Ribeiro JA (2001) A functional role for adenosine A3 receptors: modulation of synaptic plasticity in the rat hippocampus. Neurosci Lett 302:53–57.

Dale N, Frenguelli BG (2009) Release of adenosine and ATP during ischemia and epilepsy. Curr Neuropharmacol 7:160–179.

Dale N, Pearson T, Frenguelli BG (2000) Direct measurement of adenosine release during hypoxia in the CA1 region of the rat hippocampal slice. J Physiol 526:143–155.

de Mendonça A, Ribeiro JA (1994) Endogenous adenosine modulates long-term potentiation in the hippocampus. Neuroscience 62:385–390.

de Mendonça A, Ribeiro JA (2000) Long-term potentiation observed upon blockade of adenosine A1 receptors in rat hippocampus is *N*-methyl-D-aspartate receptor-dependent. Neurosci Lett 291:81–84.

Edwards FA, Konnerth A, Sakmann B, Takahashi T (1989) A thin slice preparation for patch clamp recordings from neurones of the mammalian central nervous system. Pflugers Arch 414:600–612.

Etherington LA, Patterson GE, Meechan L, Boison D, Irving AJ, Dale N, Frenguelli BG (2009) Astrocytic adenosine kinase regulates basal synaptic adenosine levels and seizure activity but not activity-dependent adenosine release in the hippocampus. Neuropharmacology 56:429–437.

Feig S, Lipton P (1990) *N*-methyl-D-aspartate receptor activation and Ca2+ account for poor pyramidal cell structure in hippocampal slices. J Neurochem 55:473–483.

Forghani R, Krnjević K (1995) Adenosine antagonists have differential effects on induction of long-term potentiation in hippocampal slices. Hippocampus 5:71–77.

Fredholm BB, Dunwiddie TV, Bergman B, Lindström K (1984) Levels of adenosine and adenine nucleotides in slices of rat hippocampus. Brain Res 295:127–136.

Frenguelli BG, Llaudet E, Dale N (2003) High-resolution real-time recording with microelectrode biosensors reveals novel aspects of adenosine release during hypoxia in rat hippocampal slices. J Neurochem 86:1506–1515.

Frenguelli BG, Wigmore G, Llaudet E, Dale N (2007) Temporal and mechanistic dissociation of ATP and adenosine release during ischaemia in the mammalian hippocampus. J Neurochem 101:1400–1413.

Fujii S, Kuroda Y, Ito K, Kaneko K, Kato H (1999) Effects of adenosine receptors on the synaptic and EPSP-spike components of long-term potentiation and depotentiation in the guinea-pig hippocampus. J Physiol 521:451–466.

Fujii S, Kato H, Ito K, Itoh S, Yamazaki Y, Sasaki H, Kuroda Y (2000) Effects of A1 and A2 adenosine receptor antagonists on the induction and reversal of long-term potentiation in guinea pig hippocampal slices of CA1 neurons. Cell Mol Neurobiol 20:331–350.

Gadalla AE, Pearson T, Currie AJ, Dale N, Hawley SA, Sheehan M, Hirst W, Michel AD, Randall A, Hardie DG, Frenguelli BG (2004) AICA riboside both activates AMP-activated protein kinase and competes with adenosine for the nucleoside transporter in the CA1 region of the rat hippocampus. J Neurochem 88:1272–1282.

Gerlach E, Marko P, Zimmer HG, Pechan I, Trendelenburg C (1971) Different response of adenine nucleotide synthesis de novo in kidney and brain during aerobic recovery from anoxia and ischemia. Experientia 27:876–878.

Hardie DG (2007) AMP-activated/SNF1 protein kinases: conserved guardians of cellular energy. Nat Rev Mol Cell Biol 8:774–785.

Hardie DG, Frenguelli BG (2007) A neural protection racket: AMPK and the GABA(B) receptor. Neuron 53:159–162.

Hardie DG, Hawley SA (2001) AMP-activated protein kinase: the energy charge hypothesis revisited. Bioessays 23:1112–1119.

Hardie DG, Salt IP, Davies SP (2000) Analysis of the role of the AMP-activated protein kinase in the response to cellular stress. Methods Mol Biol 99:63–74.

Hardie DG, Hawley SA, Scott JW (2006) AMP-activated protein kinase–development of the energy sensor concept. J Physiol 574:7–15.

Hawley SA, Boudeau J, Reid JL, Mustard KJ, Udd L, Mäkelä TP, Alessi DR, Hardie DG (2003) Complexes between the LKB1 tumor suppressor, STRAD alpha/beta and MO25 alpha/beta are upstream kinases in the AMP-activated protein kinase cascade. J Biol 2:28.

Hawley SA, Pan DA, Mustard KJ, Ross L, Bain J, Edelman AM, Frenguelli BG, Hardie DG (2005) Calmodulin-dependent protein kinase kinase-beta is an alternative upstream kinase for AMP-activated protein kinase. Cell Metab 2:9–19.

Ho OH, Delgado JY, O'Dell TJ (2004) Phosphorylation of proteins involved in activity-dependent forms of synaptic plasticity is altered in hippocampal slices maintained in vitro. J Neurochem 91:1344–1357.

Hossmann KA (2008) Cerebral ischemia: models, methods and outcomes. Neuropharmacology 55:257–270.

Kadam SD, White AM, Staley KJ, Dudek FE (2010) Continuous electroencephalographic monitoring with radio-telemetry in a rat model of perinatal hypoxia-ischemia reveals progressive post-stroke epilepsy. J Neurosci 30:404–415.

Kass IS, Lipton P (1982) Mechanisms involved in irreversible anoxic damage to the in vitro rat hippocampal slice. J Physiol 332:459–472.

Kawamura M Jr, Ruskin DN, Masino SA (2010) Metabolic autocrine regulation of neurons involves cooperation among pannexin hemichannels, adenosine receptors, and KATP channels. J Neurosci 30:3886–3895.

Kessey K, Mogul DJ (1998) Adenosine A2 receptors modulate hippocampal synaptic transmission via a cyclic-AMP-dependent pathway. Neuroscience 84:59–69.

Klyuch BP, Richardson MJ, Dale N, Wall MJ (2011) The dynamics of single spike-evoked adenosine release in the cerebellum. J Physiol 589:283–295.

Kobayashi M, Lust WD, Passonneau JV (1977) Concentrations of energy metabolites and cyclic nucleotides during and after bilateral ischemia in the gerbil cerebral cortex. J Neurochem 29:53–59.

Kuramoto N, Wilkins ME, Fairfax BP, Revilla-Sanchez R, Terunuma M, Tamaki K, Iemata M, Warren N, Couve A, Calver A, Horvath Z, Freeman K, Carling D, Huang L, Gonzales C, Cooper E, Smart TG, Pangalos MN, Moss SJ (2007) Phospho-dependent functional modulation of GABA(B) receptors by the metabolic sensor AMP-dependent protein kinase. Neuron 53:233–247.

Larson J, Wong D, Lynch G (1986) Patterned stimulation at the theta frequency is optimal for the induction of hippocampal long-term potentiation. Brain Res 368:347–350.

Ljunggren B, Ratcheson RA, Siesjö BK (1974) Cerebral metabolic state following complete compression ischemia. Brain Res 73:291–307.

Lu Q, Wang J (2008) Single molecule conformational dynamics of adenylate kinase: energy landscape, structural correlations, and transition state ensembles. J Am Chem Soc 130:4772–4783.

Mascia L, Cappiello M, Cherri S, Ipata PL (2000) In vitro recycling of alpha-D-ribose 1-phosphate for the salvage of purine bases. Biochim Biophys Acta 1474:70–74.

Masino SA, Geiger JD (2008) Are purines mediators of the anticonvulsant/neuroprotective effects of ketogenic diets? Trends Neurosci 31:273–278.

McIlwain H (1952) Phosphates of brain during in vitro metabolism: effects of oxygen, glucose, glutamate, glutamine, and calcium and potassium salts. Biochem J 52:289–295.

McIlwain H, Buchel L, Cheshire JD (1951) The inorganic phosphate and phosphocreatine of Brain especially during metabolism in vitro. Biochem J 48:12–20.

Milusheva EA, Dóda M, Baranyi M, Vizi ES (1996) Effect of hypoxia and glucose deprivation on ATP level, adenylate energy charge and $[Ca^{2+}]$o-dependent and independent release of [^{3}H]dopamine in rat striatal slices. Neurochem Int 28:501–507.

Müller CE, Iqbal J, Baqi Y, Zimmermann H, Röllich A, Stephan H (2006) Polyoxometalates: a new class of potent ecto-nucleoside triphosphate diphosphohydrolase (NTPDase) inhibitors. Bioorg Med Chem Lett 16:5943–5947.

Nowak TS Jr, Fried RL, Lust WD, Passonneau JV (1985) Changes in brain energy metabolism and protein synthesis following transient bilateral ischemia in the gerbil. J Neurochem 44:487–494.

Omran H, Illien S, MacCarter D, St Cyr J, Lüderitz B (2003) D-Ribose improves diastolic function and quality of life in congestive heart failure patients: a prospective feasibility study. Eur J Heart Fail 5:615–619.

Paschen W, Djuricic B (1995) Comparison of in vitro ischemia-induced disturbances in energy metabolism and protein synthesis in the hippocampus of rats and gerbils. J Neurochem 65:1692–1697.

Pearson T, Nuritova F, Caldwell D, Dale N, Frenguelli BG (2001) A depletable pool of adenosine in area CA1 of the rat hippocampus. J Neurosci 21:2298–2307.

Phillis JW, Perkins LM, Smith-Barbour M, O'Regan MH (1995) Oxypurinol-enhanced postischemic recovery of the rat brain involves preservation of adenine nucleotides. J Neurochem 64:2177–2184.

Potter WB, O'Riordan KJ, Barnett D, Osting SM, Wagoner M, Burger C, Roopra A (2010) Metabolic regulation of neuronal plasticity by the energy sensor AMPK. PLoS One 5:e8996.

Redondo RL, Okuno H, Spooner PA, Frenguelli BG, Bito H, Morris RG (2010) Synaptic tagging and capture: differential role of distinct calcium/calmodulin kinases in protein synthesis-dependent long-term potentiation. J Neurosci 30:4981–4989.

Rex CS, Kramár EA, Colgin LL, Lin B, Gall CM, Lynch G (2005) Long-term potentiation is impaired in middle-aged rats: regional specificity and reversal by adenosine receptor antagonists. J Neurosci 25:5956–5966.

Sajikumar S, Frey JU (2004) Late-associativity, synaptic tagging, and the role of dopamine during LTP and LTD. Neurobiol Learn Mem 82:12–25.

Sajikumar S, Navakkode S, Frey JU (2005) Protein synthesis-dependent long-term functional plasticity: methods and techniques. Curr Opin Neurobiol 15:607–613.

Sanders MJ, Grondin PO, Hegarty BD, Snowden MA, Carling D (2007) Investigating the mechanism for AMP activation of the AMP-activated protein kinase cascade. Biochem J 403:139–148.

Schurr A, Rigor BM (1989) Cerebral ischemia revisited: new insights as revealed using in vitro brain slice preparations. Experientia 45:684–695.

Shecterle LM, Terry KR, St Cyr JA (2010) The patented uses of D-ribose in cardiovascular diseases. Recent Pat Cardiovasc Drug Discov 5:138–142.

Sheng XR, Li X, Pan XM (1999) An iso-random Bi Bi mechanism for adenylate kinase. J Biol Chem 274:22238–22242.

Siklós L, Kuhnt U, Párducz A, Szerdahelyi P (1997) Intracellular calcium redistribution accompanies changes in total tissue Na^+, K^+ and water during the first two hours of in vitro incubation of hippocampal slices. Neuroscience 79:1013–1022.

Simmonds HA (1986) 2,8-Dihydroxyadenine lithiasis–epidemiology, pathogenesis and therapy. Verh Dtsch Ges Inn Med 92:503–508.

Sperlágh B, Szabó G, Erdélyi F, Baranyi M, Vizi ES (2003) Homo- and heteroexchange of adenine nucleotides and nucleosides in rat hippocampal slices by the nucleoside transport system. Br J Pharmacol 139:623–633.

Thomas J (1957) The composition of isolated cerebral tissue; purines. Biochem J 66:655–658.

Tuerk RD, Thali RF, Auchli Y, Rechsteiner H, Brunisholz RA, Schlattner U, Wallimann T, Neumann D (2007) New candidate targets of AMP-activated protein kinase in murine brain revealed by a novel multidimensional substrate-screen for protein kinases. J Proteome Res 6:3266–3277.

von Kügelgen I, Schiedel AC, Hoffmann K, Alsdorf BB, Abdelrahman A, Müller CE (2008) Cloning and functional expression of a novel Gi protein-coupled receptor for adenine from mouse brain. Mol Pharmacol 73:469–477.

Wall M, Dale N (2008) Activity-dependent release of adenosine: a critical re-evaluation of mechanism. Curr Neuropharmacol 6:329–337.

Wall MJ, Wigmore G, Lopatár J, Frenguelli BG, Dale N (2008) The novel NTPDase inhibitor sodium polyoxotungstate (POM-1) inhibits ATP breakdown but also blocks central synaptic transmission, an action independent of NTPDase inhibition. Neuropharmacology 55:1251–1258.

Watts RW, McKeran RO, Brown E, Andrews TM, Griffiths MI (1974) Clinical and biochemical studies on treatment of Lesch-Nyhan syndrome. Arch Dis Child 49:693–702.

Whittingham TS, Lust WD, Passonneau JV (1984a) An in vitro model of ischemia: metabolic and electrical alterations in the hippocampal slice. J Neurosci 4:793–802.

Whittingham TS, Lust WD, Christakis DA, Passonneau JV (1984b) Metabolic stability of hippocampal slice preparations during prolonged incubation. J Neurochem 43:689–696.

Whittingham TS, Warman E, Assaf H, Sick TJ, LaManna JC (1989) Manipulating the intracellular environment of hippocampal slices: pH and high-energy phosphates. J Neurosci Methods 28:83–91.

Woods A, Salt I, Scott J, Hardie DG, Carling D (1996) The alpha1 and alpha2 isoforms of the AMP-activated protein kinase have similar activities in rat liver but exhibit differences in substrate specificity in vitro. FEBS Lett 397:347–351.

Woods A, Dickerson K, Heath R, Hong SP, Momcilovic M, Johnstone SR, Carlson M, Carling D (2005) Ca^{2+}/calmodulin-dependent protein kinase kinase-beta acts upstream of AMP-activated protein kinase in mammalian cells. Cell Metab 2:21–33.

Wyatt CN, Mustard KJ, Pearson SA, Dallas ML, Atkinson L, Kumar P, Peers C, Hardie DG, Evans AM (2007) AMP-activated protein kinase mediates carotid body excitation by hypoxia. J Biol Chem 282:8092–8098.

Zimmer HG (1998) Significance of the 5-phosphoribosyl-1-pyrophosphate pool for cardiac purine and pyrimidine nucleotide synthesis: studies with ribose, adenine, inosine, and orotic acid in rats. Cardiovasc Drugs Ther 12 [Suppl 2]:179–187.

zur Nedden S, Eason R, Doney AS, Frenguelli BG (2009) An ion-pair reversed-phase HPLC method for determination of fresh tissue adenine nucleotides avoiding freeze-thaw degradation of ATP. Anal Biochem 388:108–114.

Analytical Biochemistry 388 (2009) 108–114

Contents lists available at ScienceDirect

Analytical Biochemistry

journal homepage: www.elsevier.com/locate/yabio

An ion-pair reversed-phase HPLC method for determination of fresh tissue adenine nucleotides avoiding freeze–thaw degradation of ATP

Stephanie zur Nedden [a,*], Robert Eason [a], Alexander S. Doney [b], Bruno G. Frenguelli [a]

[a] Department of Biological Sciences, University of Warwick, Coventry CV4 7AL, UK
[b] Department of Medicine and Therapeutics, Ninewells Hospital and Medical School, Dundee DD1 9SY, UK

ARTICLE INFO

Article history:
Received 9 December 2008
Available online 20 February 2009

Keywords:
ATP
ADP
AMP
Energy charge
HPLC
Nucleotide extraction
Brain slice
Hippocampal

ABSTRACT

Knowledge of the energetic state of tissue is required in a wide range of experimental studies, particularly those investigating the decline and recovery of cellular metabolism after metabolic stress. Such information can be obtained from high-performance liquid chromatography (HPLC) determination of tissue levels of adenine nucleotides (ATP, ADP, and AMP) and their interrelationship in the tissue energy charge (EC). Accordingly, a large range of techniques with which to measure these molecules and their downstream metabolites have been reported. However, the accurate determination of the tissue EC also depends on the nucleotide extraction procedure given that changes in adenine nucleotide levels take place very quickly when ATPases are not inactivated immediately. In this article, we describe an ion-pair reversed-phase HPLC method by which separation of adenine nucleotides can be performed rapidly, allowing multiple analyses in 1 day, with both high sensitivity and extraction efficiency and using fresh samples, thereby avoiding freeze–thaw degradation of nucleotides. We applied this method to hippocampal brain slice extracts and show that same-day extraction and analysis results in a more accurate determination of the in situ energetic state than does the commonly used snap-freezing in liquid nitrogen.

The quantification of adenine nucleotides is frequently used for the assessment of the energetic state of tissues or cells because the relationship between the individual nucleotides in the total adenine nucleotide pool {[TAN] = $\sum$ ([ATP] + [ADP] + [AMP])}[1] reflects the energy supply-to-demand relationship [1]. Equations such as the adenylate energy charge {EC = ([ATP] + 0.5[ADP]/[TAN])} [2], which describes the ratio of charged adenylates (in terms of phosphoanhydride bonds) to the TAN pool, are commonly used to indicate the energy status of tissues. As such, accurate determinations of adenine nucleotide concentrations are required for many investigations into the energetic state of tissue.

There are several possible ways of measuring tissue adenylate levels, with bioluminescence assays and high-performance liquid chromatography (HPLC) methods being most commonly used [3]. Ultraviolet (UV)-based HPLC has the advantage of high sensitivity and allows the separation and quantification of a wide range of nucleotides/nucleosides and free bases in one run.

Because metabolic stress, such as ischemia, leads to further degradation of adenine nucleotides, resulting in formation of purine nucleosides (adenosine and inosine) as well as free purine bases (adenine, hypoxanthine, and xanthine), HPLC analysis can indicate a broad spectrum of metabolic changes. For the simultaneous measurement of purine nucleotides, nucleosides, and bases, ion-pair reversed-phase HPLC is most commonly used [4,5] because the separation of purine nucleotides is difficult with reverse-phase columns and purine nucleosides are only poorly retained in anion exchange HPLC [6].

We have developed a fast and sensitive ion-pair reversed-phase UV-based HPLC method that allows the analysis of at least 11 purine metabolites, including adenine nucleotides and their most important degradation metabolites (adenosine, inosine, hypoxanthine, xanthine, and IMP). This method is suitable for low-analyte concentrations, and its rapidity (13 min runtime) means that many fresh samples can be run in 1 day, avoiding degradation of adenine nucleotides in frozen tissue or on thawing [7]. Furthermore, keeping the separation runtime short also helps to reduce the cost of each analysis given that ion-pairing agents are expensive.

We describe how the analytical separation is obtained using a 3 μm Supelcosil LC-18-T column with a gradient elution at room temperature. We have used this method to determine the energetic state of hippocampal brain slices and, furthermore, to evaluate changes in adenine nucleotide levels caused by snap-freezing in liquid nitrogen.

* Corresponding author. Fax: +44 2476 523701.
E-mail address: s.zur-nedden@warwick.ac.uk (S. zur Nedden).

[1] *Abbreviations used:* TAN, total adenine nucleotides; EC, energy charge; HPLC, high-performance liquid chromatography; UV, ultraviolet; BSA, bovine serum albumin; TBAHS, tetrabutylammonium hydrogen sulfate; PCA, perchloric acid; aCSF, artificial cerebrospinal fluid; LOD, limit of detection; LOQ, limit of quantification; SEM, standard error of the mean.

0003-2697/$ - see front matter © 2009 Elsevier Inc. All rights reserved.
doi:10.1016/j.ab.2009.02.017

Materials and methods

Materials

HPLC standards, 1,1,2-trichloro-1,2,2-trifluoroethane, CHROMASOLV, bovine serum albumin (BSA), tetrahydrofuran, tetrabutylammonium hydrogen sulfate (TBAHS), and the Bradford reagent, used for protein determination, were obtained from Sigma–Aldrich (Poole, UK). ATP was obtained from Roche (Mannheim, Germany). Perchloric acid (PCA), orthophosphoric acid, tri-*n*-octylamine, HPLC-grade methanol, HPLC-grade acetonitrile, dipotassium hydrogen phosphate, potassium dihydrogen phosphate, and all salts used in the artificial cerebrospinal fluid (aCSF) were obtained from Fisher Scientific (Loughborough, UK).

HPLC apparatus

The HPLC system (Thermo Scientific, Hemel Hempstead, UK) consisted of a vacuum degasser (SCM 1000), Spectra System binary gradient pumps (P2000), an injector with a 20 μl injection valve, and a Spectra System photodiode array UV detector (UV 6000) equipped with a 10-μl flow cell. A Supelcosil LC-18-T reverse-phase column (150 × 4.6 mm i.d., 3 μm) protected with an HPLC Security Guard Cartridge (C8, 4 × 3.0 mm, Phenomenex, Macclesfield, UK) was used throughout the entire study. For peak analysis and quantification, ChromQuest software (version 4.2.34) was used. HPLC chromatograms were obtained at a wavelength of 254 nm. However, the UV spectrum from 220 to 360 nm was scanned for all runs and was used for spectral and purity analysis of sample and standard peaks.

HPLC method

The mobile phase consisted of buffer A (65 mM potassium phosphate buffer composed of 39 mM dipotassium hydrogen phosphate and 26 mM potassium dihydrogen phosphate, adjusted to pH 6 with orthophosphoric acid and 4 mM TBAHS) and buffer B (65 mM potassium phosphate buffer composed of 39 mM dipotassium hydrogen phosphate and 26 mM potassium dihydrogen phosphate, adjusted to pH 6 with orthophosphoric acid and 25% methanol). Both buffers were prepared in deionized water and filtered through a 0.4 μm filter before use. For each day of analysis, the column was equilibrated with 10 column volumes of buffer B and 30 column volumes of buffer A (flow rate of 1 ml/min). The retention times of standard compounds stabilized after two blank injections (gradient profile described below), and analytical separation could then be performed. The flow rate was 1 ml/min, and the gradient profile used was as follows: 1 min 100% buffer A, 3 min to 30% buffer B, 7.5 min to 80% buffer B, and 10 min to 100% buffer B. The run was kept at 100% buffer B for an additional 3 min before it was completed and the gradient was returned to 100% buffer A. The runtime for the elution of relevant compounds was 13 min. A 10-min reequilibration between runs was sufficient to restore initial conditions. Concentrations were calculated by comparing the peak area of sample peaks with calibration curves for peak areas of each standard compound. All concentrations are expressed as nanomoles per milligram (nmol/mg) protein. Standard solutions were prepared in deionized water as stock solutions at 1 and 10 mM concentrations and were stored at −20 °C.

Column protection

To keep the column performance at its best, special care was taken in column protection. The column was washed after each day with 25 column volumes of 25% methanol to remove any residual phosphate buffer. The guard cartridge was changed after 200 to 300 injections. When the peak shapes started to show broadening and the backpressure increased (250–350 injections), the column was regenerated by flushing it with 30 column volumes of water (40 °C), 100% methanol, 100% acetonitrile, 20 column volumes of 100% tetrahydrofuran, and 100% methanol in reverse-flow direction at a flow rate of 0.4 ml/min, as per the manufacturer's instructions.

Method validation

The lower limit of detection (LOD, signal-to-noise ratio > 3) and limit of quantification (LOQ, signal-to-noise ratio > 10) were measured for standard compounds dissolved in deionized water and standard compounds added to sample extracts at low concentrations. For the recovery of standard compounds after PCA extraction, two brain slices were homogenized in 1 ml of PCA. Half of the sample was spiked with various concentrations of a standard mixture (5–30 μM), and a similar amount of deionized water was added to the other half. Neutralization was performed as described below except that 500 μl (instead of 1 ml) of tri-*n*-octylamine in 1,1,2-trichlorotrifluoroethane (1:1, v/v) was used. The percentage recovery of standard compounds was calculated: (spiked sample peak area × 100)/(standard peak area + unspiked sample peak area). To estimate the intrasample variability in the peak area of individual sample peaks in both aliquots of the same brain slice extract, we prepared PCA homogenates of two brain slices, divided and neutralized them as described above, but analyzed both halves without adding additional standard compounds. The percentage difference of the peak area for individual compounds was calculated: (difference between two peak areas × 100)/average peak area for two peaks.

Preparation of brain slices

Hippocampal/neocortical brain slices (400 μm thick) were prepared from 19- to 24-day-old male Sprague–Dawley rats as described previously [8,9]. After slice cutting, slices were transferred to an incubation chamber and submerged within a beaker of continuously circulating, oxygenated standard aCSF [10] at 34 ± 0.5 °C for 3 h. The composition of the standard aCSF solution was as follows: 124 mM NaCl, 3 mM KCl, 2 mM $CaCl_2$, 26 mM $NaHCO_3$, 1.25 mM NaH_2PO_4, 10 mM D-glucose, and 1 mM $MgCl_2$ at pH 7.4 with 95% O_2/5% CO_2.

Nucleotide extraction

Two brain slices were placed in ice-cold standard aCSF to stop any enzymatic degradation. Slices were transferred into 1 ml of ice-cold 5% PCA with a small spatula to minimize fluid transfer and were immediately homogenized with a Kontes pellet pestle motor (Sigma–Aldrich). After centrifugation (2 min, 4 °C, 16,060*g*), the PCA was precipitated with 1 ml of tri-*n*-octylamine in 1,1,2-trichlorotrifluoroethane (1:1, v/v) [11]. The suspension was vortexed for 20 s and kept on ice for 10 min. After centrifugation (2 min, 12,100*g*), the organic extraction was repeated twice with the upper aqueous phase. Thereafter, the aqueous phase had a pH of 6 and contained water-soluble cell components such as purine nucleotides/nucleosides and bases. HPLC analysis of extracts was performed on the same day. The protein pellet was resuspended in 1 ml of 0.5 M NaOH, and protein concentration was determined by Bradford assay with BSA as standard. For determination of the effect of liquid nitrogen freezing, slices were transferred into ice-cold aCSF and dropped into liquid nitrogen with a small spatula. After 30 to 60 min in liquid nitrogen, slices were powdered under liquid nitrogen and homogenized in PCA. Extraction was performed as described above, and extracts were analyzed on the same day.

Statistical analysis

All values are expressed as means ± standard errors of the mean (SEM), and *n* values represent means of duplicate slices from *n* number of rats. For statistical analysis, an unpaired Student's *t* test was used. Calculations were carried out with Prism 4 software, and *P* values < 0.05 were considered as statistically significant.

Results

Chromatographic separation

Using the chromatographic procedure developed in this study, at least 12 different purine metabolite standards could be separated within 13 min, as shown in Fig. 1A (100 μM standard mixture, 2000 pmol). To keep the relative standard deviation of the retention times for each compound (Table 1) below ±2.5%, the reequilibration time after each run was kept at 10 min. Shorter reequilibration times (~5 min) led to unstable retention times of hypoxanthine and xanthine, whereas longer reequilibration times (~15 min) resulted in coelution of GMP and IMP at 5.5 min (data not shown). Although the retention times of CTP, GTP, ADP, and ATP were very stable even after a 5-min reequilibration time (Fig. 1B, 500 nM, 10 pmol), we chose to adopt a constant reequilibration time of 10 min because this allowed optimal and consistent separation of all compounds of interest. Furthermore, the retention times of all standard compounds did not change when the flow direction of the column was reversed, allowing us to use the column for a longer time.

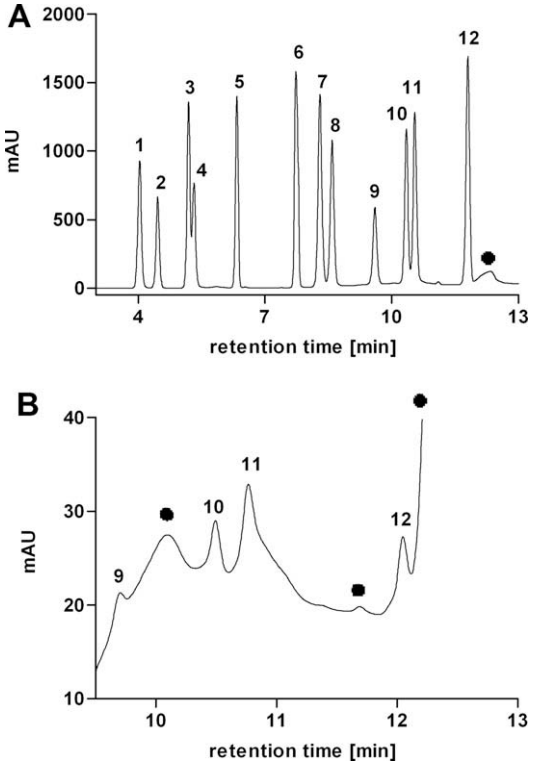

Fig. 1. HPLC chromatograms of purine standards. (A) A 100-μM standard mixture of 12 compounds. (B) A 500 nM mixture of CTP, GTP, ADP, and ATP injected after 5 min of reequilibration time. Numbers on traces refer to the following compounds: 1, hypoxanthine; 2, xanthine; 3, GMP; 4, IMP; 5, inosine; 6, adenosine; 7, AMP; 8, GDP; 9, CTP; 10, GTP; 11, ADP; 12, ATP. ●, baseline peak. mAU, milli-absorbance units.

At high gain, the baseline showed several small peaks eluting after 10 min and a larger ghost peak eluting after ATP (black dots in Fig. 1A and B) whose size increased and whose retention time decreased with the column life time. The nature of these peaks could not be clearly determined. They were not due to an impurity in any of the buffer components, to contamination of the injection valve, to the reequilibration time, or to the fact that the ion-pairing agent was used only in buffer A. A possible reason could be a precipitation of TBAHS during the gradient elution that can occur when using potassium phosphate buffers. However, because the ghost peak could be clearly distinguished from the ATP peak even at low concentrations of ATP, and to keep the runtime to a reasonable length, neither the gradient profile nor the buffer composition was changed.

UV absorbance spectra

The UV absorbance spectra (220–360 nm) for all standard and sample compounds were measured for all runs. Fig. 2A shows a contour graph and Fig. 2B shows the respective three-dimensional graphs of all standard compounds (100 μM, 2000 pmol). The two-dimensional UV absorbance spectra for trinucleotides, nucleosides, and free purine bases are shown in Fig. 2C and D, and the respective UV absorbance maxima are summarized in Table 1. Hypoxanthine, inosine, and IMP had the lowest UV absorbance maximum (247 nm), whereas xanthine (267 nm) and CTP (270 nm) had the highest absorbance maxima. The quantitative analysis was performed at a wavelength of 254 nm (black line in Fig. 2A). This was chosen to encompass the absorbance spectra of all separated compounds.

Limits of detection and quantification

The LOD (evaluated with a signal-to-noise ratio > 3) and LOQ (evaluated with a signal-to-noise ratio > 10) are summarized in Ta-

Table 1
HPLC method validation.

Compound	LOD	LOQ	Retention time (min)	UV absorbance maximum (nm)	Correlation coefficient (R^2)	% Recovery after PCA extraction
ATP	500 nM (10 pmol)	500 nM (10 pmol)	11.99	258	0.996	102.8 ± 4.0
ADP	500 nM (10 pmol)	500 nM (10 pmol)	10.60	259	0.996	109.3 ± 7.4
GTP	500 nM (10 pmol)	500 nM (10 pmol)	10.47	252	0.999	95.3 ± 5.7
CTP	100 nM (2 pmol)	500 nM (10 pmol)	9.68	270	0.999	90.9 ± 4.9
GDP	50 nM (1 pmol)	100 nM (2 pmol)	8.65	252	0.998	100.5 ± 2.4
AMP	50 nM (1 pmol)	100 nM (2 pmol)	8.30	259	0.997	99.4 ± 2.5
Adenosine	5 nM (0.1 pmol)	25 nM (0.5 pmol)	7.76	259	0.999	103.8 ± 2.5
Inosine	5 nM (0.1 pmol)	25 nM (0.5 pmol)	6.32	247	0.991	95.8 ± 2.6
IMP	10 nM (0.2 pmol)	100 nM (2 pmol)	5.47	247	0.999	98.1 ± 2.3
GMP	10 nM (0.2 pmol)	50 nM (1 pmol)	5.35	252	0.999	99.4 ± 1.7
Xanthine	10 nM (0.2 pmol)	50 nM (1 pmol)	4.48	267	0.994	103.7 ± 10.1
Hypoxanthine	10 nM (0.2 pmol)	50 nM (1 pmol)	3.90	250	0.999	102.2 ± 5.5

Note. The LOD of standard compounds dissolved in deionized water was classified as the concentration of the analyte 3 times the noise level. The LOQ was classified as the analyte concentration 10 times the noise level. At 10 min of reequilibration between runs, the retention times varied by ⩽± 2.5%. The R^2 value for each calibration curve (LOQ of 2000 pmol), measured at 254 nm, is also indicated. Recovery of standard compounds after PCA extraction was determined by spiking sample homogenates with various concentrations of standard compounds. All values are presented as means from three to nine determinations.

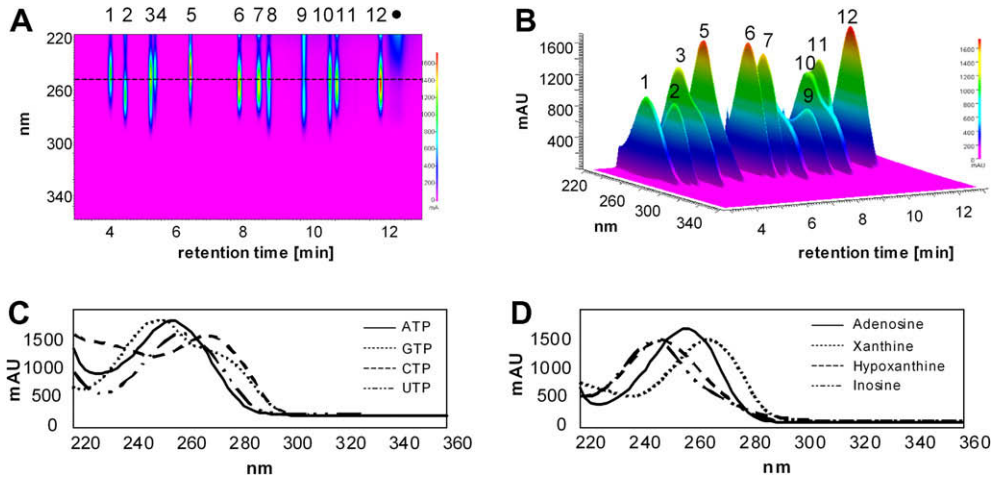

Fig. 2. Spectral view of HPLC chromatograms obtained from a 100-μM standard mixture. (A and B) Contour graph (A) and three-dimensional graph of all separated standard compounds. The *y* axis indicates the wavelength (220–360 nm). The *x* axis shows the retention time. The *z* axis shows the absorbance intensity in milli-absorbance units (mAU). The black dotted line in panel A indicates 254 nm, the wavelength that was used for quantitative analysis of standard and sample compounds. Compounds are numbered as in Fig. 1. (C and D) UV absorbance spectra (220–360 nm) for purine nucleotides (C) and purine nucleosides and free bases (D). UV absorbance maxima are summarized in Table 1.

ble 1 and shown for AMP in Fig. 3A. The LOD for standard compounds dissolved in deionized water ranged between 0.1 and 10 pmol, whereas the LOQ ranged between 0.5 and 10 pmol at 254 nm. The higher LOD and LOQ for GTP, ADP, and ATP were due to the baseline peaks shown in Fig. 1B, which merged with the standard peaks at concentrations below 500 nM (10 pmol), thereby making an accurate determination of the analyte peaks unreliable.

The LOQ estimated for sample peaks was among 1 pmol (hypoxanthine, xanthine, IMP, GMP, and inosine), 2 pmol (adenosine, AMP, and GDP), and 10 pmol (CTP, GTP, ADP, and ATP). The smallest amount of standards added to samples, which could be reliably detected by an increase in peak height, ranged between 1 and 2 pmol for hypoxanthine, xanthine, IMP, GMP, inosine, adenosine, AMP, and GDP. Due to the baseline peaks eluting after 10 min (see Fig. 1B), and due to the larger size of GTP and ATP peaks in samples (see Fig. 4A), the smallest amount of reliably detectable standards, determined by an increase in the peak area for CTP, GTP, ADP, and ATP, was 10 pmol.

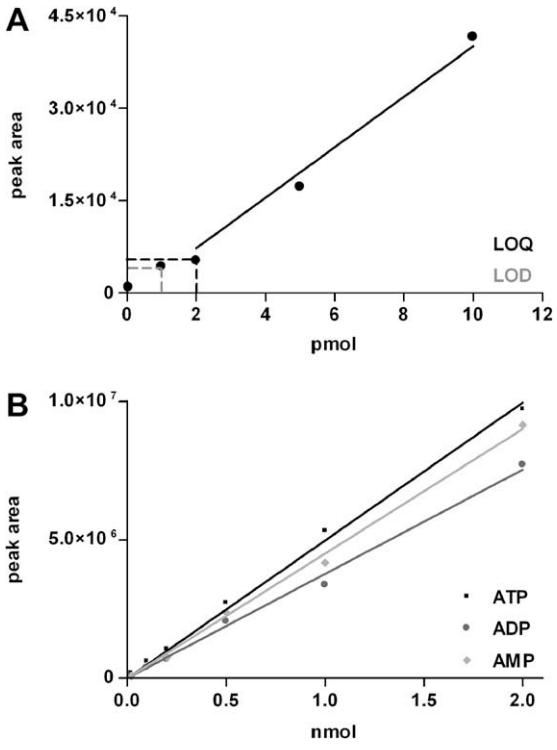

Fig. 3. Calibration curves for adenine nucleotides. (A) LOD (signal-to-noise ratio > 3) and LOQ (signal-to-noise ratio > 10) for AMP. (B) Calibration curves for ATP, ADP, and AMP (LOQ of 2000 pmol).

Linearity

A linear response, as indicated by correlation coefficients (R^2) in excess of 0.99, was observed for each compound ranging from the LOQ for standard compounds in water to at least 2000 pmol (100 μM). The calibration curves for ATP, ADP, and AMP are shown in Fig. 3B, and the respective R^2 values for all resolvable standard metabolites are summarized in Table 1. This linear range encapsulates the values observed for these compounds in brain tissue (see below).

Recovery of standard compounds after PCA extraction

PCA is commonly used to precipitate proteins of tissue samples and thereby to extract acid-soluble cell compounds, such as nucleotides, for subsequent analysis. However, during the neutralization process of PCA extracts, ATP can be adsorbed to the perchlorate precipitate [12,13]. To evaluate the extent to which PCA extraction influenced the yield of nucleotides and metabolites, standard compounds were added to half of a brain slice sample, whereas the other half had an equivalent volume of distilled water added. Both samples were subjected to PCA extraction and were subsequently neutralized to pH 6 by a threefold organic extraction with tri-*n*-octylamine/trichlorotrifluoroethane.

Because this protocol required the injection of two aliquots from the same brain sample (spiked and unspiked), we first needed to determine the intrasample variability of these two injections. For two unspiked aliquots of the same brain sample, as treated above, the differences between the two peak areas, expressed as percentages of the mean peak area, were 2.1 ± 0.9% (ATP), 6.8 ± 1.6% (ADP), and 14.4 ± 8.2% (AMP) (n = 4). These values likely overestimate any variability because the percentages do not take

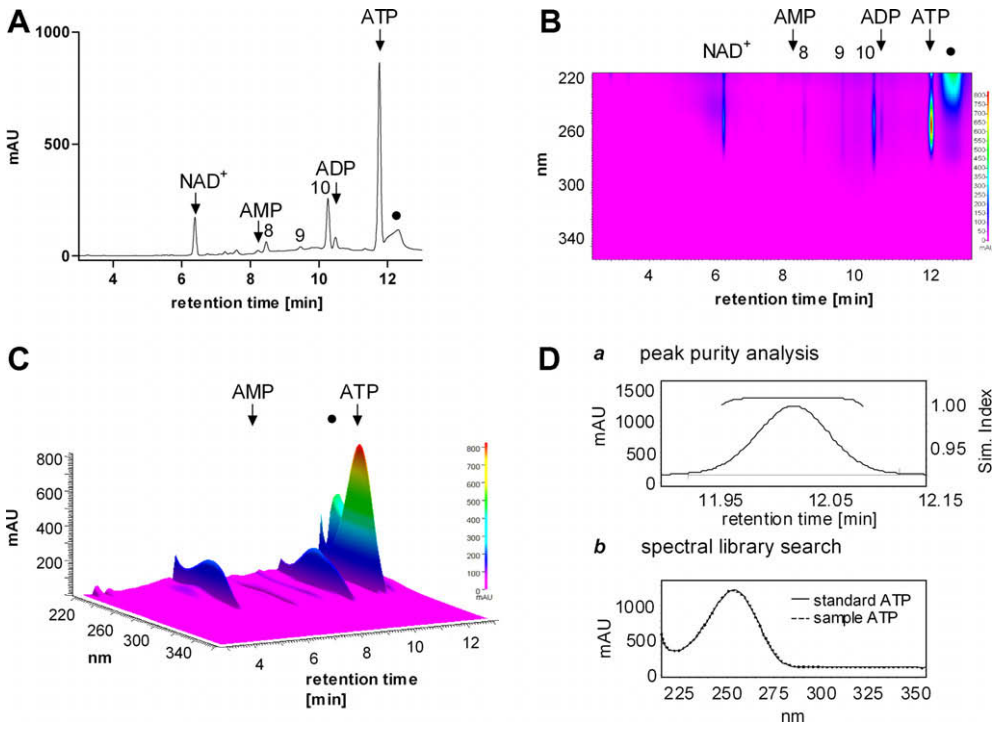

Fig. 4. Representative HPLC chromatogram from neutralized hippocampal brain slice extracts. Brain slices were incubated for 3 h in aCSF at 34 °C, and nucleotide extraction was performed on fresh tissue without prior freezing in liquid nitrogen. (A) Representative HPLC chromatogram obtained at 254 nm. (B and C) Contour graph (B) and three-dimensional graph (C) for separated compounds. Numbers on traces refer to the following compounds: 8, GDP; 9, CTP; 10, GTP/UTP. ●, ghost peak. mAU, milli-absorbance units. (D) Sample ATP peak verification by peak purity analysis (a) and spectral library search (b). Sim. Index, similarity index = 0.99. Sample ATP UV absorbance spectrum was 100% similar to standard ATP absorbance spectrum.

into account the size of the peak areas. Thus, for smaller peaks (e.g., AMP), subtle differences between aliquots would have a proportionately larger effect. This may also explain the reduction in apparent variability as the peaks become larger from ADP to ATP.

Nonetheless, to test whether these values reflected variability in the detection system, we injected sequential aliquots from solutions of standard compounds. This yielded much lower variability; the differences of the peak areas of subsequent injections of 20 μM (400 pmol) ATP, ADP, and AMP standards from the mean peak area were 1.3 ± 0.5%, 1.1 ± 0.4%, and 0.2 ± 0.1%, respectively ($n = 7$). Hence, the variability between the peak areas of two aliquots from the same brain slice is not due to poor precision of the system and more likely reflects subtle differences between the initial aliquots, which involved separating the homogenized tissue in two, a possible source of intrasample variability. This was performed only during these spiked sample experiments.

We observed that the recovery of all standard compounds in spiked brain samples was between 90% and 109% of the standard when dissolved in water (Table 1). Given the intrasample variability described above, we assumed a 100% recovery for all standard metabolites.

Analysis of brain slice extracts

To evaluate whether this HPLC method is suitable for studying the adenine nucleotide levels of biological tissue, we applied it to neutralized PCA extracts of hippocampal brain slices. A representative HPLC chromatogram is shown in Fig. 4A, and the contour and three-dimensional graphs of the absorbance spectra are shown in Fig. 4B and C. The identity of each sample peak was determined by comparison of the retention time with the respective standard compound, by spiking samples with standards, by comparison of the UV spectra with the particular standard compound, and by peak purity analysis, as shown for ATP in Fig. 4D. Peak purity analysis showed that sample adenine nucleotides were as pure as standard adenine nucleotides. However, the GTP peak was contaminated due to coelution with UTP. It is possible that these compounds could be resolved individually by appropriate changes to the buffer gradient profile, but because all adenine nucleotides were clearly separated, this was not pursued.

Effect of liquid nitrogen freezing on tissue adenylate levels

It is often convenient to snap-freeze tissue after the experiment for analysis at a later date. This may be the case when the analysis procedure or HPLC runtime is lengthy, thereby obviating the possibility of running several fresh samples on the day of the experiment. Given the known labile nature of adenine nucleotides, we sought to determine whether snap-freezing in liquid nitrogen and/or subsequent extraction results in a change of adenine nucleotide levels. For this purpose, brain slices were transferred into ice-cold aCSF. One set of slices was immediately homogenized in PCA, and another set of slices was frozen in liquid nitrogen for 30 to 60 min. Frozen slices were powdered under liquid nitrogen and subsequently homogenized in PCA. All neutralized extracts were analyzed on the same day of slice preparation.

Representative HPLC chromatograms, with adenine nucleotide and EC levels of fresh and liquid nitrogen frozen brain slices, are shown in Fig. 5. EC values from fresh tissue slices are very high (0.95 ± 0.003, $n = 4$), indicating that the slices are in good metabolic condition.

In contrast, snap-freezing in liquid nitrogen led to significantly higher ADP levels (1.1 ± 0.2 nmol/mg protein for fresh slices and 2.5 ± 0.3 nmol/mg protein for snap-frozen slices, $n = 4$, $P < 0.01$, un-

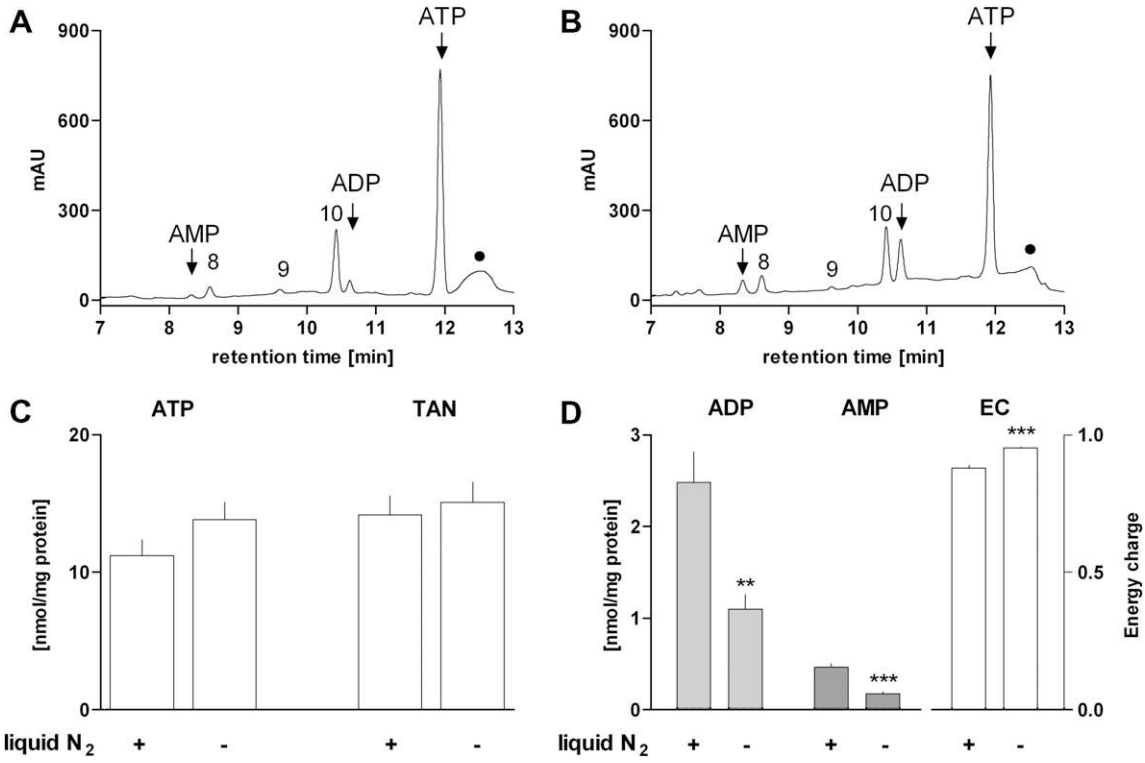

Fig. 5. Effect of liquid nitrogen freezing on adenine nucleotide levels. (A and B) HPLC chromatograms from unfrozen brain slices (A) and frozen brain slices (B). Numbers on traces refer to the following compounds: 8, GDP; 9, CTP; 10, GTP/UTP. ●, ghost peak. The rising baseline in panel B is due to a short reequilibration time between runs. (C and D) ATP and TAN levels (C) and ADP, AMP, and EC values (D) of fresh and liquid nitrogen frozen slices. Values are expressed as means ± SEM ($n = 4$). $^{**}P < 0.01$, $^{***}P < 0.001$ for AMP and EC (unpaired t test).

paired t test) and AMP levels (0.2 ± 0.02 nmol/mg protein for fresh slices and 0.5 ± 0.04 nmol/mg protein for snap-frozen slices, $n = 4$, $P < 0.001$, unpaired t test), indicating degradation of ATP during the freezing/extraction process. This results in significantly lower EC values (0.95 ± 0.003 for fresh slices and 0.88 ± 0.009 for snap-frozen slices, $n = 4$, $P < 0.001$, unpaired t test). However, there was no further degradation of adenine nucleotides in snap-frozen slices because the TAN pool was not significantly different between both groups (15.9 ± 1.4 nmol/mg protein for fresh slices and 14.2 ± 1.4 nmol/mg protein for snap-frozen slices, $n = 4$, $P > 0.05$, unpaired t test). This degradation of ATP is dependent on the presence of tissue given that freezing of standard ATP in liquid nitrogen did not lead to ATP breakdown (data not shown).

Discussion

The accurate determination of adenine nucleotides is critical in the study of energy metabolism. We therefore aimed to develop a fast, high-resolution, ion-pair reversed-phase HPLC method that allows the analysis of multiple fresh samples in 1 day, thereby avoiding freeze–thaw degradation of nucleotides. With the method described here, at least 11 different purine compounds can be separated within 13 min with a subsequent 10-min reequilibration time. This method is particularly useful for studying changes in the adenine nucleotide levels associated with experimental manipulations, extraction efficiency, or tissue storage. The short time of analysis and the accurate evaluation of the compounds make this method useful for routine and relatively high-throughput use.

The sensitivity, as determined by the LOQ, lies in the range of previously published UV-based HPLC methods [5,14], and calibration curves for standard compounds showed that they were linear over a wide concentration range (LOQ to 2000 pmol). As the signal of each standard compound increases linearly with increasing injection volume [5], injecting more than 20 µl on the column may result in even lower LOD and LOQ. Nonetheless, the absolute sensitivity is still lower than fluorescence-based HPLC analysis of adenine nucleotides [15]. However, for this method, purine compounds of sample extracts need to be etheno-derivatized with chloroacetaldehyde, a process that requires incubation at high temperatures (most commonly 80 °C) and limits the analysis to compounds containing an amino group in the purine or pyrimidine ring (e.g., adenine, cytosine). Furthermore, the derivatization efficiency of standard ATP is variable and never reaches 100% (see Supplemental Fig. 1A in the supplementary material). This precludes an accurate determination of the energetic state due to degradation of ATP during this process and thereby underestimates key parameters such as the energy charge. Therefore, UV-based HPLC analysis of adenine nucleotides (see Supplemental Fig. 1B), although less sensitive, results in a more reliable detection of the in situ energetic state.

To evaluate whether our method is suitable for the analysis of tissue samples, we analyzed hippocampal brain slices. Tissue nucleotides were extracted with PCA, and for neutralization a threefold organic extraction with tri-*n*-octylamine/trichlorotrifluoroethane was used. It is known that acid extraction and subsequent neutralization can lead to adsorption of ATP to the acid–salt precipitate [12,13], and the recovery of ATP has been reported to be between 45% and 96% [5,16–18], depending on the type of extraction and neutralization. In our hands, there was a complete recovery of standard compounds added to sample extracts. This may be due to our use of tri-*n*-octylamine/trichlorotrifluoroethane given that it has been reported that the removal of PCA with tri-*n*-octylamine/trichlorotrifluoroethane can result in a better recovery of nucleotides than, for example, precipitation as $KClO_4$ [19]. The

additional advantages of using tri-*n*-octylamine/trichlorotrifluoroethane for neutralization of acid extracts have been pointed out previously [20]. Most importantly this method does not introduce into the extracts additional salts that could interfere with HPLC separations. Furthermore, there is no possibility of making the solution too alkaline. In fact, the threefold organic extraction used in this study always resulted in a pH of 6, which allowed the best separation of all sample/standard compounds in the method described here given that the buffers used had the same pH.

HPLC chromatograms obtained from hippocampal brain slice extracts showed that all purine nucleotide compounds were clearly separated. Peak purity analysis and UV absorbance spectra comparisons further established the nature of the specific sample compounds. Including the time for slice preparation (30 min), slice incubation (3 h), extraction for tissue nucleotides (30 min), and washing of the column after use (50 min), at least 10 sample extracts could be analyzed in 1 day.

An interesting observation of this study is that freezing the brain tissue in liquid nitrogen and/or subsequent extraction can result in a significant change of adenine nucleotide levels. This has implications for the storage of tissue, especially if it is to be used for metabolic studies.

Due to the high activities of ATPases in fresh samples, changes in the adenine nucleotide levels take place very quickly when ATPase enzymes are not inactivated immediately. Snap-freezing of tissues in liquid nitrogen is a simple and widely used way to instantly stop any enzymatic activities and to store the sample for subsequent extraction. However, the maintenance of freezing conditions during the nucleotide extraction procedure is critical because thawing of the tissue will result in a recovery of enzymatic activities and potential degradation of ATP. Although samples in this study were kept and powdered in liquid nitrogen, there was a significant change in adenine nucleotide levels. This resulted in significantly lower EC values compared with fresh sample extracts. Freezing of standard ATP in liquid nitrogen did not lead to a degradation of ATP. Furthermore, it is unlikely that snap-freezing is not quick enough to stop enzymatic degradation of ATP or that enzymatic activities recover at such low temperatures. Because brain slices were powdered under liquid nitrogen, the degradation of ATP most likely occurs during the homogenization procedure. The tissue powder might thaw and, therefore, ATPase activities might recover before proteins are effectively precipitated with PCA.

Because tissue is frequently frozen in liquid nitrogen and stored at −80 to −20 °C for subsequent extraction and HPLC analysis, assumptions about the EC need to be made very carefully given that they might not reflect the in situ values. Hence, transferring tissue slices into ice-cold aCSF and performing the PCA extraction immediately lead to a more reliable evaluation of adenine nucleotide levels.

In summary, we have reported a method that is suitable for the detailed analysis of tissue adenine nucleotide levels and, due to its rapidity, allows within-day sample analysis. This helps to bypass the problem of freeze–thaw degradation of adenine nucleotides and results in an accurate determination of the tissue energy charge.

Acknowledgments

We are grateful to Professor Nicholas Dale for providing the HPLC system and for comments on the manuscript, and to Research into Ageing for funding a studentship to S.z.N.

Appendix A. Supplementary data

Supplementary data associated with this article can be found, in the online version, at doi:10.1016/j.ab.2009.02.017.

References

[1] H. Kammermeier, Meaning of energetic parameters, Basic Res. Cardiol. 88 (1993) 380–384.
[2] D.E. Atkinson, The energy charge of the adenylate pool as a regulatory parameter: interaction with feedback modifiers, Biochemistry 7 (1968) 4030–4034.
[3] G. Manfredi, L. Yang, C.D. Gajewski, M. Mattiazzi, Measurements of ATP in mammalian cells, Methods 26 (2002) 317–326.
[4] V. Stocchi, L. Cucchiarini, F. Canestrari, M.P. Piacentini, G. Fornaini, A very fast ion-pair reversed-phase HPLC method for the separation of the most significant nucleotides and their degradation products in human red blood cells, Anal. Biochem. 167 (1987) 181–190.
[5] N. Kochanowski, F. Blanchard, R. Cacan, F. Chirat, E. Guedon, A. Marc, J.L. Goergen, Intracellular nucleotide and nucleotide sugar contents of cultured CHO cells determined by a fast, sensitive, and high-resolution ion-pair RP-HPLC, Anal. Biochem. 348 (2006) 243–251.
[6] M. Zakaria, P.R. Brown, High-performance liquid chromatography of nucleotides, nucleosides, and bases, J. Chromatogr. 226 (1981) 267–290.
[7] G. Cappeln, J. Nielsen, F. Jessen, Synthesis and degradation of adenosine triphosphate in cod (*Gadus morhua*) at subzero temperatures, J. Sci. Food Agric. 79 (1999) 1099–1104.
[8] N. Dale, T. Pearson, B.G. Frenguelli, Direct measurement of adenosine release during hypoxia in the CA1 region of the rat hippocampal slice, J. Physiol. 526 (2000) 143–155.
[9] B.G. Frenguelli, G. Wigmore, E. Llaudet, N. Dale, Temporal and mechanistic dissociation of ATP and adenosine release during ischaemia in the mammalian hippocampus, J. Neurochem. 101 (2007) 1400–1413.
[10] F.A. Edwards, A. Konnerth, B. Sakmann, T. Takahashi, A thin slice preparation for patch clamp recordings from neurones of the mammalian central nervous system, Pflugers Arch. 414 (1989) 600–612.
[11] J.X. Khym, An analytical system for rapid separation of tissue nucleotides at low pressures on conventional anion exchangers, Clin. Chem. 21 (1975) 1245–1252.
[12] C. Williams, T. Forrester, Loss of ATP in micromolar amounts after perchloric acid treatment, Pflugers Arch. 366 (1976) 281–283.
[13] S. Wiener, R. Wiener, M. Urivetzky, E. Meilman, Coprecipitation of ATP with potassium perchlorate: the effect of the firefly enzyme assay of ATP in tissue and blood, Anal. Biochem. 59 (1974) 489–500.
[14] N. Tomiya, E. Ailor, S.M. Lawrence, M.J. Betenbaugh, Y.C. Lee, Determination of nucleotides and sugar nucleotides involved in protein glycosylation by high-performance anion-exchange chromatography: sugar nucleotide contents in cultured insect cells and mammalian cells, Anal. Biochem. 293 (2001) 129–137.
[15] M. Katayama, Y. Matsuda, K. Shimokawa, S. Tanabe, S. Kaneko, I. Hara, H. Sato, Simultaneous determination of six adenyl purines in human plasma by high-performance liquid chromatography with fluorescence derivatization, J. Chromatogr. B 760 (2001) 159–163.
[16] B. Levitt, R.J. Head, D.P. Westfall, High-pressure liquid chromatographic-fluorometric detection of adenosine and adenine nucleotides: application to endogenous content and electrically induced release of adenyl purines in guinea pig vas deferens, Anal. Biochem. 137 (1984) 93–100.
[17] J.C. Shryock, R. Rubio, R.M. Berne, Extraction of adenine nucleotides from cultured endothelial cells, Anal. Biochem. 159 (1986) 73–81.
[18] J.L. Au, M.H. Su, M.G. Wientjes, Extraction of intracellular nucleosides and nucleotides with acetonitrile, Clin. Chem. 35 (1989) 48–51.
[19] E.G. Brown, R.P. Newton, N.M. Shaw, Analysis of the free nucleotide pools of mammalian tissue by high-pressure liquid chromatography, Anal. Biochem. 123 (1982) 378–388.
[20] A.L. Pogolotti Jr., D.V. Santi, High-pressure liquid chromatography–ultraviolet analysis of intracellular nucleotides, Anal. Biochem. 126 (1982) 335–345.